



**Investigation and Development of Structural Composite  
Materials for Use as Electromagnetic Shielding Agents in the  
Current Aerospace Industry**

**Examiner's Copy**

**Denver Maharaj  
201298021**



**Investigation and Development of Structural Composite  
Materials for Use as Electromagnetic Shielding Agents in the  
Current Aerospace Industry**

Submitted in fulfilment of the requirements of the degree  
**Master of Science in Engineering**  
at the University of KwaZulu-Natal, Durban, South Africa

Submission Date: 09 January 2007

**Research Supervisor: Dr. CJ von Klemperer**

*This work is dedicated to my late Dad, Gregory Maharaj*

### **Author's Declaration**

I, Denver Maharaj, hereby declare that the following dissertation, and information presented herein, has been undertaken and completed in its entirety solely by myself except where due credit is given to relevant persons.

This report is submitted in fulfilment of the requirements of the degree, Master of Science in Engineering, at the University of KwaZulu-Natal, and has not been submitted previously to another tertiary institution.



**Denver Maharaj**

**Student Number: 201298021**

School of Mechanical Engineering

University of KwaZulu-Natal

Howard College Campus

King George V Avenue

Durban

KwaZulu-Natal

4041

South Africa

Date: 09 January 2007



## **Acknowledgments**

Firstly I would like to thank God and Jesus Christ constant help and for providing me with the ability to undertake this study.

I would like to express my sincerest gratitude to my supervisor, Dr. C von Klemperer, for allowing me to undertake this study and for assiduously overseeing the research progress over the past several months.

I would like to thank Prof. JW Odendaal (UP) who graciously aided UKZN with the electromagnetic shielding effectiveness testing at no cost.

I would like to thank the all of the industry professionals, most notably Ms. K Hall (AMT Composites), Dr. D Hoch (UKZN), Mr. B Burton (UKZN), Mr. G Vath (UKZN), Mr. G Kidson (DUT), Dr. S Adali (UKZN), Mr. N Sookay (UKZN), my fellow MSc colleague Mr. A Berghorst and Mr. A Harris (NCS Resins), for being most obliging and supportive when consulted.

I would like to thank the workshop staff at the School of Mechanical Engineering, UKZN, especially Mr. K Smith, Mr. S Govender and Mr. B Chander for their help. I would like to thank the administration staff at the School of Mechanical Engineering, UKZN – Mrs. O Chetty, Mrs. K Naicker and Ms. W Janssens for their help.

I would like to thank Mrs. M Sheth for providing me with useful advice when writing the report. Sincerest thanks to my dear friends, Mr. A Ramterath and Mr. P Padayachee, for their help with over the past few years. Finally, I would like to thank my family, my Mum, my brother Ardeane, and my sister Melanie, for their love and support during the course of my studies.

## **Abstract**

Due to the nature of today's competitive electronics market, the development of new electronic devices is constantly ongoing. Industry strives for devices that are lighter, smaller and able to operate at higher frequencies. In addition, more and more consumers are entering the market, and there is thus widespread use of devices that operate in the same frequency ranges causing electromagnetic interference (EMI).

Metals typically serve as excellent EMI shielding agents, but their high mass density, high cost and susceptibility to environmental degradation make them an undesired choice for current electronic devices. Conversely fibre composite materials are typically light weight, flexible and cheaper to produce, but typically lack the inherent EMI shielding capabilities that may be required.

The research work addresses the viability of composite materials for possible use as electromagnetic shielding agents, specifically in the aerospace industry. The study undertaken involved researching classical and contemporary approaches to this problem with the intention of determining which materials suffice the purpose of electromagnetic shielding.

The fundamental concepts behind electromagnetism and EMI are discussed. The study emphasises the various causes, and subsequent effects, of EMI. The mechanisms responsible for shielding against the negative effects of electromagnetic waves are explained.

A comparative study of various materials that were identified for possible use in the composite shielding in question was undertaken. The manufacturing processes that were identified as being most feasible for use in this work are explained. Studies to determine which materials and manufacturing processes yield results which were considered most promising were undertaken.

As the shielding materials in this work were not designed with a specific application in mind, a variety of tests were identified to determine the range of uses that shielding materials of this type could serve in practice. Testing that was identified as being significant included tensile, compressive and flexural regarding the mechanical properties; and electrical resistance and electromagnetic shielding regarding the electrical properties.

The electromagnetic shielding testing is of most importance in this work, and results indicating wave transmission, wave penetration and shielding effectiveness of the materials at frequencies between 750MHz and 5GHz are presented. The measured results were compared to that obtained by analytical means typically used in the industry, which are well-known to yield results which are unreliable, and the findings are addressed.

Comparative studies of cost vs. electromagnetic shielding, and mechanical strength vs. electromagnetic shielding were performed with the intention of suggesting the materials considered most suitable for possible use as electromagnetic shielding for use in the aerospace industry.

This research was conducted with support from Denel Aerospace Systems and Armscor in South Africa.

## **TABLE OF CONTENTS**

<b><u>Title</u></b>	<b><u>Page No.</u></b>
<b>1. INTRODUCTION</b>	<b>1</b>
<b>PART A: Literature on Electromagnetism</b>	<b>3</b>
<b>2. THEORY ON ELECTROMAGNETISM</b>	<b>4</b>
2.1 Fundamentals of Electromagnetism	4
2.2 Electromagnetic Waves	5
<b>3. THE AIRCRAFT ELECTROMAGNETIC ENVIRONMENT</b>	<b>9</b>
3.1 Lightning	10
3.1.1 Aircraft Initiated Lightning	11
3.1.2 Aircraft Intercepted Lightning	12
3.1.3 Lightning Zoning Diagrams	14
3.1.4 Direct Effects of Lightning Strike	16
3.1.5 Indirect Effects of Lightning Strike	16
3.2 Electromagnetic Pulses	17
3.3 High Intensity Radiated Environment	17
3.4 Precipitation Static	18
3.5 Electrostatic Discharge	19
<b>4. ELECTROMAGNETIC SHIELDING</b>	<b>20</b>
4.1 The Theory behind Electromagnetic Shielding	21
4.2 Calculations on EMI Shielding	24
4.2.1 General Shielding Effectiveness Calculations	24
4.2.2 Equations for Individual Shielding Mechanisms	25
4.2.2.1 Reflection	25
4.2.2.2 Absorption	26
4.2.2.3 Multiple Reflections	27
4.2.3 Additional Shielding Effectiveness Equations	27

4.2.4 Discussion on Shielding Effectiveness Calculations	29
4.3 Additional Calculations	29
<b>PART B: Composite Electromagnetic Shielding &amp; Material Selection</b>	<b>31</b>
<b>5. ANALYSIS OF COMPOSITE MATERIALS</b>	<b>32</b>
5.1 Background on Composites use in Aircraft	32
5.2 Discussion on Previous Composite Electromagnetic Shielding Material Research	38
<b>6. MATERIAL SELECTION STUDY</b>	<b>39</b>
6.1 Fabrics	39
6.1.1 Glass Fibre	39
6.1.2 Aramid Fibre	42
6.1.3 Carbon Fibre	43
6.1.3.1 Pan-based Carbon Fibre	44
6.1.3.2 Pitch-based Carbon Fibre	45
6.2 Resins	46
6.3 Filler Materials	50
6.3.1 Carbon Black	50
6.3.2 Nanotubes	51
6.3.3 Vapour Grown Carbon Fibre	54
6.3.4 Metal Filler Materials	55
6.3.4.1 Metal Powders	55
6.3.4.2 Metal Meshes	56
6.3.5 Discussion on Filler Materials	58
<b>PART C: Determination of Appropriate Manufacturing Methods and Test Methods for the Shielding Materials</b>	<b>60</b>
<b>7. MANUFACTURING PROCESSES</b>	<b>61</b>
7.1 Hand Lay-up Process	61
7.2 Vacuum-Assisted Resin Infusion Process	63

<b>8. APPROPRIATE TEST METHODS</b>	<b>65</b>
8.1 Mechanical Testing	65
8.1.1 Tensile Testing	65
8.1.2 Compressive Testing	68
8.1.3 Flexural Testing	70
8.1.4 Discussion on Mechanical Test Methods	73
8.2 Electrical Testing	74
8.2.1 Electromagnetic Shielding Effectiveness Testing	74
8.2.2 Electrical Resistance Testing	77
8.2.3 Discussion on Electrical Testing	78
<b>9. DETERMINATION OF APPROPRIATE MANUFACTURING PROCESSES</b>	<b>80</b>
9.1 Manufacture of Unidirectional E-glass Samples	81
9.2. Manufacture of 3K Woven Carbon Fibre Samples	88
9.3 Manufacture of Stitched Carbon Fibre Samples	90
9.4 Manufacture of Unidirectional Carbon Fibre Samples	93
9.5 Manufacture of 12K Woven Carbon Fibre Samples	95
9.6 Discussion on Manufacturing Processes	98
<b>PART D: Final Designs, Results and Discussions</b>	<b>101</b>
<b>10. COMPOSITE MATERIAL DESIGN AND ANALYSIS</b>	<b>102</b>
10.1 Discontinuous Filler Material Designs	103
10.1.1 Aluminium-doped Samples	103
10.1.1.1 Manufacture	103
10.1.1.2 Results and Discussion of Stitched Carbon Fibre Samples	107
10.1.1.3 Results and Discussion of 12K Woven Carbon Fibre Samples	112
10.1.1.4 Results and Discussion of Unidirectional Carbon Fibre Samples	116
10.1.2 Copper-doped Samples	121

10.1.2.1 Manufacture	121
10.1.2.2 Results and Discussion of Stitched Carbon Fibre Samples	124
10.1.2.3 Results and Discussion of 12K Woven Carbon Fibre Samples	128
10.1.2.4 Results and Discussion of Unidirectional Carbon Fibre Samples	132
10.1.3 Hybrid Powder-doped Samples	135
10.1.3.1 Manufacture	135
10.1.3.2 Results and Discussion of Stitched Carbon Fibre Samples	138
10.1.3.3 Results and Discussion of 12K Woven Carbon Fibre Samples	141
10.1.3.4 Results and Discussion of Unidirectional Carbon Fibre Samples	145
10.1.4 Discussion on Metal Powder Samples	148
10.2 Continuous Filler Material Designs	149
10.2.1 Manufacture	150
10.2.2 Results and Discussion of Stitched Carbon Fibre Samples	151
10.2.3 Results and Discussion of 12K Woven Carbon Fibre Samples	155
10.2.4 Results and Discussion of Unidirectional Carbon Fibre Samples	158
10.2.5 Discussion on Metal Mesh Samples	161
10.3 General Discussion on Test Results	163
<b>11. COST AND STRENGTH VS. SHIELDING ANALYSES</b>	<b>165</b>
11.1 Strength vs. Shielding Analysis	166
11.2 Cost vs. Shielding Analysis	168
11.3 Discussion on Strength vs. Shielding and Cost vs. Shielding	171
<b>12. FABRICATION OF COMPLEX-SHAPED LAMINATES</b>	<b>173</b>
12.1 Design of the Mould	173
12.2 Manufacture of the Box-Shaped Laminate	174

12.3 Concluding Remarks on Box-Shaped Laminates	175
<b>13. DISCUSSION ON RADAR CROSS SECTION</b>	<b>177</b>
13.1 Concepts of Radar Cross Section	177
13.2 Discussion on RCS	178
<b>14. CONCLUSION</b>	<b>180</b>
<b>APPENDICES</b>	<b>182</b>
APPENDIX A: METAL PROPERTIES	183
APPENDIX B: IMAGES OF ELECTROMAGNETIC SHIELDING MATERIALS	184
APPENDIX C: LAMINATE THICKNESS AND WEIGHT DATA	193
APPENDIX D: SAMPLE CALCULATIONS	199
APPENDIX E: THEORETICAL BARRIER IMPEDANCE AND SKIN DEPTH RESULTS	201
APPENDIX F: ACTUAL TESTING EMSE RESULTS	210
APPENDIX G: MECHANICAL FAILURE PICS	238
APPENDIX H: % DIFFERENCE IN SHIELDING RELATIVE TO ALUMINIUM ANALYTICAL DATA	242
APPENDIX I: COST ANALYSIS	248
APPENDIX J: BOX DESIGNS	249
APPENDIX K: RCS MEASUREMENT RESULTS	251
APPENDIX L: TECHNICAL PAPERS	265
<b>REFERENCES</b>	<b>291</b>

## **LIST OF FIGURES**

<b><u>Figure No.</u></b>	<b><u>Page No.</u></b>
Figure 2.1: The wave pattern of a perfect conductor	6
Figure 2.2: Electric Field Strength vs. Source Distance	7
Figure 2.3: Wave Impedance as a Function of Source Distance	8
Figure 3.1: A description of the propagation of EMI from a source to a victim	9
Figure 3.2: The altitude occurrence of lightning strike on aircraft	12
Figure 3.3: The possible distribution of P (+40 C), N (-40 C) and p (+10 C) charges in a typical South African thundercloud	13
Figure 3.4: Lightning Strike Density diagram for SA during the months of December 2005 to August 2006	14
Figure 3.5: The lightning strike zoning diagram of the A320 aircraft	15
Figure 4.1: A representation of the electromagnetic spectrum	20
Figure 4.2: The mechanisms of EMI shielding	22
Figure 4.3: Surface Impedance and Skin Depth of Various Metals vs. Radio Frequency	30
Figure 6.1: Diagram describing the functional structure of para-aramid	42
Figure 6.2: Functional unit of epoxy resin	47
Figure 6.3: A representation of a MWNT	52
Figure 6.4: The qualitative projected decrease in price of nanotubes by 2010	53
Figure 6.5: Illustration depicting the current-carrying capacity of various metals for unit cross-section and weight	58
Figure 7.1: A diagram describing a typical hand lay-up system	62
Figure 7.2: Vacuum-assisted resin infusion process	63
Figure 8.1: Tensile specimen as described in ASTM 638-02a	66
Figure 8.2: Comparison of compressive strengths obtained from different test methods	69
Figure 8.3: Compressive test specimen as detailed in ASTM 695-02a	70
Figure 8.4: Three-point bending loading scheme	71
Figure 8.5: The one-third and quarter-point four-point bending loading schemes as described in ASTM 6272-02	72
Figure 8.6: The Scientific Atlanta 5754 compact antenna range test set-up at UP	75
Figure 8.7: Schematic diagram of S-parameters of a two-ports network system	76
Figure 8.8: The RCL universal bridge circuit used to measure electrical resistance	78



Figure 9.1: The enclosed system prior to infusion	82
Figure 9.2: The laminates were visibly resin-starved in patches along the entire laminate	83
Figure 9.3: The system with two inlet pipes and the exit pipe along the midsection	84
Figure 9.4: The third laminate was similar in appearance to the previous two, aside from the region around the exit pipe	85
Figure 9.5: The hand lay-up E-glass fabric upon introducing vacuum pressure into the enclosed mould	86
Figure 9.6: Resin had embedded the fabric uniformly, and both laminates were similar in appearance	87
Figure 9.7: The resulting laminate from the vacuum-assisted resin infusion of E-glass with Prime 27 was uniform in appearance, and was free of visible inconsistencies	88
Figure 9.8: Resin flow had abruptly stopped at 70mins, and the resulting laminate contained an area of fabric that was completely resin-starved	89
Figure 9.9: Hand lay-up fabrication using 3K carbon fibre fabric and LR20 epoxy resin.	90
Figure 9.10: The area at the midsection of the laminate did not wet-out at all below the first ply	91
Figure 9.11: Hand lay-up laminate using stitched carbon fibre and LR20 resin	92
Figure 9.12: Stitched carbon fibre laminate manufactured using Prime 27 resin by means of vacuum-assisted resin infusion	93
Figure 9.13: Hand lay-up fabrication of unidirectional carbon fibre	94
Figure 9.14: Improperly infused unidirectional carbon fibre laminate fabricated using Prime 27 resin	95
Figure 9.15: Hand lay-up fabrication with 12K woven carbon fibre	96
Figure 9.16: An area of almost half of the 12K woven carbon fibre remained dry after infusion on both laminates	96
Figure 9.17: The materials only appeared completely wet after 50mins	97
Figure 9.18: The third 12K woven/Prime 27 composite	98
Figure 9.19: Optimising the manufacturing process involved temporarily joining two moulds together for the purpose of introducing appropriate pressure into each system	100
Figure 10.1: Aluminium powder under a microscope	104
Figure 10.2: The resin colour changed from being a transparent, light yellow colour to an opaque grey shade	105

Figure 10.3: An image depicting 100x and 200x magnification of 7.5% aluminium filler side by side	106
Figure 10.4: An image depicting 100x and 200x magnification of 15% aluminium loading samples	106
Figure 10.5: Comparative graph of EMSE (analytical) vs. Frequency for undoped stitched carbon fibre specimens	109
Figure 10.6: Comparative graph of EMSE (analytical) vs. Frequency for 7.5% aluminium-doped stitched carbon fibre specimens	110
Figure 10.7: Comparative graph of EMSE (analytical) vs. Frequency for 15% aluminium-doped stitched carbon fibre specimens	110
Figure 10.8: Actual EMSE vs. Frequency for undoped and aluminium-doped stitched carbon samples relative to an aluminium plate of the same size	111
Figure 10.9: Comparative graph of EMSE (analytical) vs. Frequency for undoped woven carbon fibre specimens	114
Figure 10.10: Comparative graph of EMSE (analytical) vs. Frequency for 7.5% aluminium-doped woven carbon fibre specimens	114
Figure 10.11: Comparative graph of EMSE (analytical) vs. Frequency for 15% aluminium-doped woven carbon fibre specimens	115
Figure 10.12: Actual EMSE vs. Frequency of the undoped and aluminium-doped woven samples relative to an aluminium plate of the same size	116
Figure 10.13: Comparative graph of EMSE (analytical) vs. Frequency for undoped unidirectional carbon fibre specimens	119
Figure 10.14: Comparative graph of EMSE (analytical) vs. Frequency for 7.5% aluminium-doped unidirectional carbon fibre specimens	119
Figure 10.15: Comparative graph of EMSE (analytical) vs. Frequency for 15% aluminium-doped unidirectional carbon fibre specimens	120
Figure 10.16: Actual EMSE vs. Frequency of the undoped and aluminium-doped unidirectional samples relative to an aluminium plate of the same size	121
Figure 10.17: Copper powder particles under a microscope	122
Figure 10.18: The resin colour changed from being a transparent, light yellow colour to an opaque reddish-brown shade	123
Figure 10.19: An image depicting 100x and 200x magnification of 7.5% copper filler side by side	123

Figure 10.20: An image depicting 100x and 200x magnification of 15% copper loading samples	124
Figure 10.21: Comparative graph of EMSE (analytical) vs. Frequency for 7.5% copper-doped stitched carbon fibre specimens	125
Figure 10.22: Comparative graph of EMSE (analytical) vs. Frequency for 15% copper-doped stitched carbon fibre specimens	126
Figure 10.23: Actual EMSE vs. Frequency of the undoped and copper-doped stitched carbon fibre specimens relative to an aluminium plate of the same size	127
Figure 10.24: Comparative graph of EMSE (analytical) vs. Frequency for 7.5% copper-doped woven carbon fibre specimens	130
Figure 10.25: Comparative graph of EMSE (analytical) vs. Frequency for 15% copper-doped woven carbon fibre specimens	130
Figure 10.26: Actual EMSE vs. Frequency of the undoped and copper-doped woven samples relative to an aluminium plate of the same size	131
Figure 10.27: Comparative graph of EMSE (analytical) vs. Frequency for 7.5% copper-doped unidirectional carbon fibre specimens	133
Figure 10.28: Comparative Graph of EMSE (analytical) vs. Frequency for 15% copper-doped unidirectional carbon fibre specimens	134
Figure 10.29: Actual EMSE vs. Frequency of the copper-filled unidirectional fibre samples relative to an aluminium plate of the same size	135
Figure 10.30: Hybrid powder consisting of aluminium and copper particles	136
Figure 10.31: The resin colour changed from being a transparent, light yellow colour to an opaque dull grey shade	136
Figure 10.32: An image depicting 100x and 200x magnification of a 7.5% hybrid powder-doped laminate side by side	137
Figure 10.33: An image depicting 100x and 200x magnification of 15% hybrid powder-doped samples	137
Figure 10.34: Comparative graph of EMSE (analytical) vs. Frequency for 7.5% hybrid powder-doped stitched carbon fibre specimens	139
Figure 10.35: Comparative graph of EMSE (analytical) vs. Frequency for 15% hybrid powder-doped stitched carbon fibre specimens	140

Figure 10.36: Actual EMSE vs. Frequency of the hybrid powder-doped stitched carbon samples relative to an aluminium plate	141
Figure 10.37: Comparative graph of EMSE (analytical) vs. Frequency for 7.5% hybrid powder-doped woven carbon fibre specimens	143
Figure 10.38: Comparative graph of EMSE (analytical) vs. Frequency for 15% hybrid powder-doped woven carbon fibre specimens	143
Figure 10.39: Actual EMSE vs. Frequency of the hybrid powder-doped woven carbon fibre specimens relative to an aluminium plate of the same size	144
Figure 10.40: Comparative graph of EMSE (analytical) vs. Frequency for 7.5% hybrid powder-doped unidirectional carbon fibre specimens	146
Figure 10.41: Comparative graph of EMSE (analytical) vs. Frequency for 15% hybrid powder-doped unidirectional carbon fibre specimens	147
Figure 10.42: Actual EMSE vs. Frequency of the hybrid-doped unidirectional samples relative to an aluminium plate of the same size	148
Figure 10.43: Alumesb 401 when viewed at 100x magnification	150
Figure 10.44: Comparative graph of EMSE (analytical) vs. Frequency for stitched carbon with one metal mesh layer	153
Figure 10.45: Comparative graph of EMSE (analytical) vs. Frequency for stitched carbon with two metal mesh layers	153
Figure 10.46: Actual EMSE vs. Frequency of the metal mesh/stitched samples relative to an aluminium plate	154
Figure 10.47: Comparative graph of EMSE (analytical) vs. Frequency for woven carbon fibre specimens with one metal mesh layer	156
Figure 10.48: Comparative graph of EMSE (analytical) vs. Frequency for woven carbon fibre specimens with two metal mesh layers	157
Figure 10.49: Actual EMSE vs. Frequency of the metal mesh/woven carbon fibre specimens relative to an aluminium plate of the same size	158
Figure 10.50: Comparative graph of EMSE (analytical) vs. Frequency for unidirectional carbon fibre specimens with one metal mesh layer	160
Figure 10.51: Comparative graph of EMSE (analytical) vs. Frequency for unidirectional carbon fibre specimens with two metal mesh layers	160

Figure 10.52: Actual EMSE vs. Frequency of the metal mesh/unidirectional carbon fibre samples relative to an aluminium plate of the same size	161
Figure 10.53: Theoretical EMSE results of a copper plate	163
Figure 10.54: Theoretical EMSE results of a copper plate (equations (4.6) and (4.18))	163
Figure 12.1: The open box-mould with the sides unclipped	174
Figure 12.2: The box-mould with the sides clipped in place	174
Figure 12.3: The laminate being removed from the mould	175
Figure 12.4: The final box-shaped laminate	176
Figure 13.1: RCS polar plot of the T-33 aircraft	179

## **LIST OF TABLES**

<b><u>Table No.</u></b>	<b><u>Page No.</u></b>
Table 3.1: Lightning Zone Diagram Key for the A320 Aircraft	15
Table 5.1: Advantages and Disadvantages of Utilising Composites in Aerospace Vehicles	33
Table 6.1: Comparative Study of the Properties found in Various Glass Types	41
Table 6.2: Properties of Kevlar 29 and Kevlar 49	42
Table 6.3: A Comparison between the Advantages and Disadvantages of using Carbon Fibre in Aircraft (circa 1990)	43
Table 6.4: Comparison of Various Properties found in Carbon Fibre	45
Table 6.5: Thermal and Electrical Properties of Epoxy Resins	48
Table 6.6: Selected Properties of LR20/LH281 Matrix Material	49
Table 6.7: Selected Properties of Prime 27/Prime 20 "Slow" Matrix Material	49
Table 8.1: List of Variables in Figure 8.1	67
Table 9.1: Fabric Thickness and Approximated Laminate Thicknesses for Various Fabrics	81
Table 10.1: Average Mechanical Properties of Aluminium-Doped Stitched Carbon Fibre Laminates	107
Table 10.2: Electrical Properties of Aluminium-doped Stitched Carbon Fibre Laminates	108
Table 10.3: Average Mechanical Properties of Aluminium-doped Woven Carbon Fibre Laminates	112
Table 10.4: Electrical Properties of Aluminium-doped Woven Carbon Fibre Laminates	113
Table 10.5: Average Mechanical Properties of Aluminium-doped Unidirectional Carbon Fibre Laminates	116
Table 10.6: Electrical Properties of Aluminium-doped Unidirectional Carbon Fibre Laminates	118
Table 10.7: Average Mechanical Properties of Copper-doped Stitched Carbon Fibre Laminates	124
Table 10.8: Electrical Properties of Copper-doped Stitched Carbon Fibre Laminates	125

Table 10.9: Average Mechanical Properties of Copper-doped Woven Carbon Fibre Laminates	128
Table 10.10: Electrical Properties of Copper-doped Woven Carbon Fibre Laminates	129
Table 10.11: Average Mechanical Properties of Copper-doped Unidirectional Carbon Fibre Laminates	132
Table 10.12: Electrical Properties of Copper-doped Unidirectional Carbon Fibre Laminates	133
Table 10.13: Average Mechanical Properties of Hybrid Powder-doped Stitched Carbon Fibre Laminates	138
Table 10.14: Electrical Properties of Hybrid Powder-doped Stitched Carbon Fibre Laminates	139
Table 10.15: Average Mechanical Properties of Hybrid Powder-doped Woven Carbon Fibre Laminates	141
Table 10.16: Electrical Properties of Hybrid Powder-doped Woven Carbon Fibre Laminates	142
Table 10.17: Average Mechanical Properties of Hybrid Powder-doped Unidirectional Carbon Fibre Laminates	145
Table 10.18: Electrical Properties of Hybrid Powder-doped Unidirectional Carbon Fibre Laminates	146
Table 10.19: Average Mechanical Properties of Mesh/Stitched Carbon Fibre Laminates	151
Table 10.20: Electrical Properties of Mesh/Stitched Carbon Fibre Laminates	152
Table 10.21: Average Mechanical Properties of Mesh/Woven Carbon Fibre Laminates	155
Table 10.22: Electrical Properties of Mesh/Woven Carbon Fibre Laminates	156
Table 10.23: Average Mechanical Properties of Mesh/Unidirectional Carbon Fibre Laminates	158
Table 10.24: Electrical Properties of Mesh/Unidirectional Carbon Fibre Laminates	159
Table 11.1 Mechanical Properties of Aluminium and its Alloys	166
Table 11.2: Differences in Tensile Strength, Yield Strength and Elastic Moduli between Composite Shielding Materials and Aluminium	167
Table 11.3: Comparative Cost Analysis of Composite Shielding	169
Table 11.4: Mass Densities, % Difference in Weight between Aluminium, and W/A Values	170

## **CHAPTER 1: INTRODUCTION**

The development of new and improved electronic devices is well-known to be a progressive field. For example, the first generation of cellular phones in the 1980's were quite bulky (about 300mm in length and 100mm in thickness), and one could basically just make and receive calls [1]. Today, a typical cellular phone is about 100mm in length and less than 20mm in thickness and can perform an array of functions one would not normally have associated with conventional telephones.

This is the type of rapid development that the industry strives for, and also what consumers have come to expect from the industry as the norm. The rapid advancement is not just restricted to cellular phones. The desire for lighter, smaller, faster multifunctional electronic devices is quite apparent in all facets of electronics, such as computers, calculators, mp3 players, televisions and video game systems. Apart from the onslaught of newer products constantly entering the market, which sophisticated consumers tend to purchase regularly, more and more first-time consumers are also beginning to use these electronic devices for communication, entertainment, computation and automation on a daily basis [2].

However, the constant integration of these devices into new roles brings forth a subsequent concern regarding electromagnetic interference (EMI). EMI, which is also commonly known as radio frequency interference (RFI), takes place when devices which are inadequately shielded from particular frequencies of electromagnetic radiation operate within close proximity of each other [3,4]. This is well-known, and many people have experienced EMI at some time without even knowing it. A common example is the result of one using a cellular phone in the vicinity of a typical FM radio - some severe static and interference is sometimes heard from the radio.

As electronic devices have become such an integral part in today's society, there is understandably a need for electromagnetic shielding structures in many facets of life today. However, each of these facets requires special attention, as shielding structures which are suitable in one application may not necessarily suffice the requirements of other applications. Electromagnetic shielding approaches are not generic in design, and consideration has to be given to factors such as mechanical strength, frequency ranges and cost prior to implementing the product in practice.



This work specifically pertains to the growing concern of EMI in aerospace applications. Aircraft of today are essentially “fly-by-wire” systems, which refers to the use of digital control systems opposed to the use of analogue control systems of older aircraft [4]. Additional to this, aircraft contain cockpit automation and digital navigation systems [4]. Due to the high amount of on-board electronic equipment, the concern regarding prevention of electromagnetic disturbances is not unfounded. Metals and their alloys have typically provided excellent electromagnetic shielding in aircraft, and are accepted as being the best shielding agents in practice [5,6,7]. However, despite the aerospace industry continually striving for higher-performance vehicles, comparatively little research has been undertaken regarding new electromagnetic shielding options in the past ten years [8]. Fibre composite materials have, however, been identified in recent years as being the desired choice for the replacement of metals in this regard. One of the chief obstacles preventing the substitution is the general inherent lack of electromagnetic shielding capabilities possessed in fibrous composite materials [9].

The undertaken study involved a thorough research of the phenomena responsible for potential EMI in airborne vehicles; investigating previous and current developments in the industry; researching and selecting appropriate composite materials for the application; refining manufacturing processes and developing appropriate mould surfaces for the composite laminates; identifying appropriate test methods and testing the properties of the composite laminates; and finally developing cost vs. shielding and strength vs. shielding models for the selected materials.

This work focuses specifically on the electromagnetic shielding aspects and mechanical strength only. Consideration is thus not given to radar stealth, thermal stability, thermal conductivity and environmental degradation of the shielding materials. The shielding materials were not designed for a single specific application in aircraft. Rather, the electromagnetic shielding materials were developed for the purpose of later integrating into aircraft applications should the criteria be met.

This research presents a wide range of topics regarding the physics, electrical engineering and mechanical engineering aspects associated with EMIs and electromagnetic shielding. It is hoped that the reader will knit the relevant information together to develop a thorough understanding of the principles behind successfully attaining electromagnetic shielding via fibre composite materials.

## **PART A: Literature on Electromagnetism**

## **CHAPTER 2: THEORY ON ELECTROMAGNETISM**

The primary concern of this research is electromagnetic shielding of aircraft structures. To adequately suggest a solution, it is imperative for one to understand the physics behind what occurs when electromagnetic radiation interacts with particular materials.

### **2.1 Fundamentals of Electromagnetism**

As the name suggests the phenomenon “electromagnetism” refers to the interaction between magnetic and electric fields. This interaction is best described by a well-known series of equations in engineering field theory referred to as “Maxwell’s equations” after James Clerk Maxwell. These equations show that either a time-varying magnetic or electric field acts as a source of the other [10]. It is well-understood that these equations form the basis of fundamental electromagnetic theory [10,11].

$$\oint \vec{E} \cdot d\vec{A} = \frac{Q_{encl}}{\epsilon_0} \quad (\text{Gauss's law for } \vec{E}) \quad (1.1) \quad [10]$$

$$\oint \vec{B} \cdot d\vec{A} = 0 \quad (\text{Gauss's law for } \vec{B}) \quad (1.2) \quad [10]$$

$$\oint \vec{B} \cdot d\vec{l} = \mu_0 (i_C + \epsilon_0 \frac{d\Phi_E}{dt})_{encl} \quad (\text{Ampere's law}) \quad (1.3) \quad [10]$$

$$\oint \vec{E} \cdot d\vec{l} = -\frac{d\Phi_B}{dt} \quad (\text{Faraday's law}) \quad (1.4) \quad [10]$$

Where:  $\vec{E}$  = electric field (N/C)

$\vec{A}$  = vector with area  $dA$

$Q_{encl}$  = enclosed charge (C)

$\epsilon_0$  = permittivity of free space ( $C^2/N.m^2$ )

$\vec{B}$  = magnetic field (T)

$d\vec{l}$  = vector with length  $dl$

$\mu_0$  = permeability of free space (Wb/A.m)

$i_c$  = conduction current (A)

$\Phi_E$  = electric flux (N.m<sup>2</sup>/C)

$\Phi_B$  = magnetic flux (Wb)

From equation (1.3), it is seen that a change in magnetic flux induces a current in a circuit, and “Faraday’s law of electromagnetic induction”, equation (1.5) below, shows that a change in magnetic flux also induces an electromotive force (emf) as well:

$$\varepsilon = -\frac{d\Phi_B}{dt} \quad (\text{Faraday's Law of Electromagnetic Induction}) \quad (1.5) \quad [10]$$

Where:  $\varepsilon$  = induced electromotive force (V)

From equation (1.5) it can be seen that electromagnetic induction leads to an emf. It can be said, using equations (1.1) to (1.5), that a conductive structure placed in the path of an electromagnetic wave will experience a current. If this particular structure is electrically non-conductive, there will not be a mechanism to promote adequate dissipation of the wave (electromagnetic shielding). However, in many cases, a high degree of electrical conductivity is not required for shielding [5,11]. It has been found that good shielding materials require resistivities of  $10 \Omega \cdot \text{cm}$  and less [5,12]. However, Dhawan *et al.* [13] also report that materials with resistivities less than  $10^2 \Omega \cdot \text{cm}$  will adequately suffice the purpose of electromagnetic shielding. Lee *et al.* [14] also report that a high degree of electrical conductivity contributes to improved shielding performance in materials as well. This provides some support regarding why electromagnetic shielding structures cannot be generic in design. Nonetheless, it is established that some electrical conductivity is required for adequate dissipation of the electromagnetic wave. Should the structure intended for shielding be electrically non-conductive, the wave will simply pass through the structure leading to possible interference. Such a phenomenon is referred to as “transmission” of the electromagnetic wave [15].

## **2.2 Electromagnetic Waves**

Electromagnetic waves are comprised of two components viz. an electric and magnetic field. The fields are perpendicular to each other, and the waves both propagate at right angles in relation the plane in which they are contained. The interaction is described in Figure 2.1.

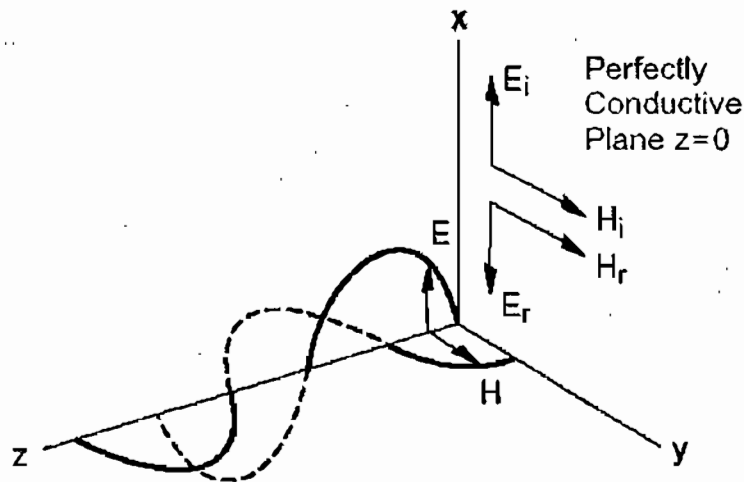


*Figure 2.1: The wave pattern of a perfect conductor [16]*

Maxwell's equations show that an accelerating point charge is required to produce electromagnetic waves. This charge does not emit waves equally in all directions [10]. The waves are strongest at  $90^\circ$  to the axis of motion of the charge, while there are no waves along the axis of motion of the charge [10]. The electric/magnetic disturbances spread out from its surface, and hence the term "electromagnetic radiation" is used interchangeably with "electromagnetic waves" [10]. Electromagnetic waves move in free space and air at the speed of light,  $2.998 \times 10^8$  m/s [10].

The relative magnitude between the electric and magnetic fields depend on the generating source of the wave, and the distance of the wave from the source [16]. The ratio between electric and magnetic fields is referred to as wave impedance, denoted by  $Z_w$ :

$$Z_w = \frac{E}{H} \quad (1.6) \quad [16]$$

Where:  $E$  = Electric field strength (V/m)

$H$  = Magnetic field strength (A/m)

$Z_w$  = Wave impedance ( $\Omega$ )

At distances close to the source, when  $R < \frac{\lambda}{2\pi}$ , equation (1.6) becomes:

$$\frac{E}{H} = \frac{377\lambda}{2\pi R} \quad (1.7) \quad [17]$$

At large distances from the source, when  $R > \frac{\lambda}{2\pi}$ , the equation becomes:

$$\frac{E}{H} = 377\Omega \quad (1.8) \quad [17]$$

Where: R = Distance from EMI emission source to material barrier (m)

$\lambda$  = Wavelength (m)

Wave impedance is a function of the impedance of the generating source of the electromagnetic wave [17]. Equation (1.7) is used when “near-field”, or high-impedance, conditions are met [17]. Equation (1.8) is used when “far-field”, or radiation field (plane waves), conditions are met [17]. The relationship between electric field and the source distance; and wave impedance and source distance is described in Figure 2.2 and Figure 2.3:

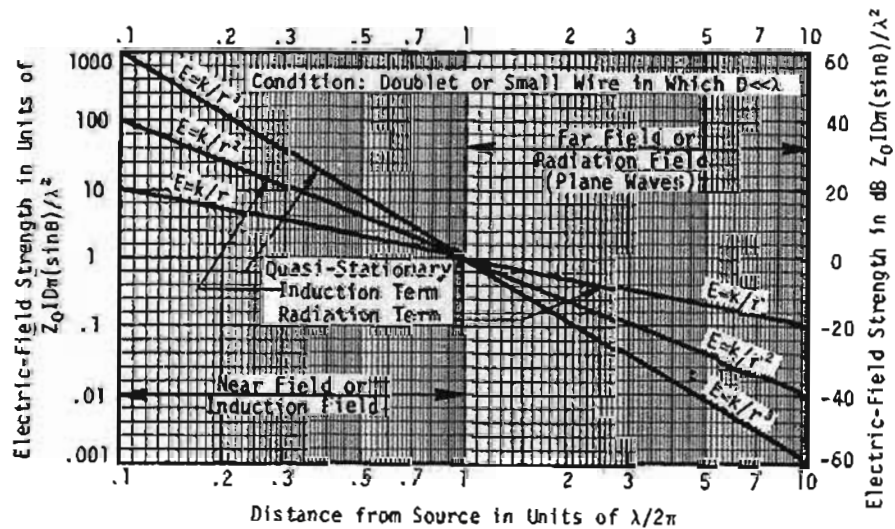


Figure 2.2: Electric Field Strength vs. Source Distance [17]

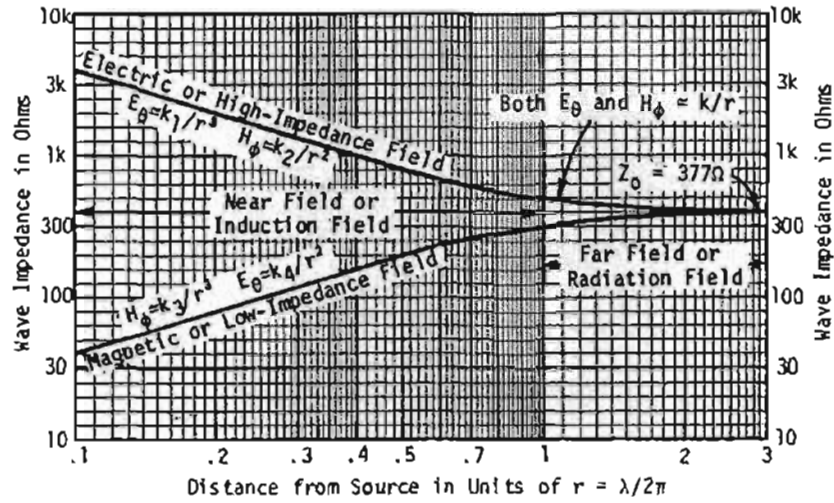


Figure 2.3: Wave Impedance as a Function of Source Distance [17]

As seen in Figures 2.2 and 2.3, an increase in frequency leads to  $r > \lambda/2\pi$  and thus the far-field region tends to be of importance. When shielding against the effects of electromagnetic waves, it is important to determine whether near-field or far-field conditions are expected. This will be explained in further detail in Chapter 4.

## CHAPTER 3: THE AIRCRAFT ELECTROMAGNETIC ENVIRONMENT

In practice there are several sources of electromagnetic radiation that could lead to interference in electronic devices and aircraft avionics. During a typical flight, aircraft are subject to a variety of disturbances that could lead to EMI. Some common types that fall under the all-encompassing term “EMI” include the effects of lightning strike; high intensity radiated fields (HIRF); and electrical and electronic system electromagnetic emissions; precipitation static (p-static) and electrostatic discharge (ESD) [3,18].

EMI may be classified into three sub-classes, which are: on-board systems, passenger carry-on devices, and externally generated EMI [4]. When on-board systems interfere with each other, it is referred to as electromagnetic compatibility [4]. Passenger carry-on devices include portable electronic devices that can transmit and receive frequencies, compact disc players and computers. Anyone who has flown on-board an aircraft has been cautioned against use of these devices during flight. Externally-generated EMI refers to disturbances caused by external sources such as lightning strike, HIRF and electromagnetic pulses (EMPs) [4].

In order for interference to take place, there needs to be three elements viz. an EMI source; a coupling path and a victim [19]. This situation is referred to as the “EMI triangle” [19]. This is described in Figure 3.1.

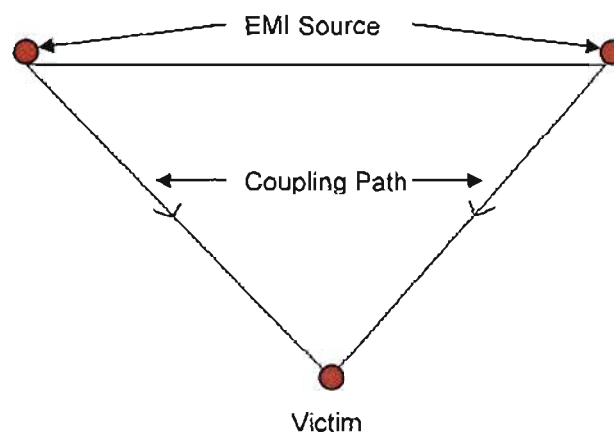


*Figure 3.1: A description of the propagation of EMI from a source to a victim*



As seen in Figure 3.1, a coupling path, which could result from lack of significant electrical conductivity on the surfaces of the victim, is necessary for transmission of the wave into the victim system.

### **3.1 Lightning**

Lightning is defined, by Uman [20], as a transient, high-current electric discharge whose path is generally measured in kilometres. Uman [20], goes on to say that lightning occurs when a region of the atmosphere attains a sufficiently large electric charge; and the electric field associated with this charge cause an electrical breakdown of the surrounding air.

Lightning is a naturally occurring phenomenon and, in the extent of this research, is taken as being impossible to prevent. Interaction between lightning and the surrounding environment is thus inevitable. It is therefore expected that lightning can, and does, directly interact with airborne vehicles.

In the infancy stages of air travel during the 1930's, lightning was not considered as being potentially destructive to airborne vehicles, and it was thought that a lightning strike would not result in any damage other than structural on aircraft [21]. However, upon reviewing possible causes for aircraft malfunction and disasters over the years at that time, it was found that lightning was often the most probable cause [21]. At the time, however, aircraft were not as dependant on electronic and avionic equipment to the extent at which they are today, and improvements in protection were focused on fuel tank designs, vent design and outlet location criteria, and flame suppression techniques [21].

Today, however, aircraft are almost fully-dependant on on-board electronic equipment, and could likely be rendered unable to fly in the event of electromagnetic disturbance [3,4]. Coupled with the increasing inclusion of composite materials, which are traditionally electrically non-conductive, effective EMI and lightning protection has become of increasing importance.

There are many research publications regarding the physics behind lightning strike, and thus a detailed account of different lightning strike types are not addressed in this work. Rather, an overview on the general cause and effect of lightning strikes, and how they influence airborne vehicles, is documented.

A single lightning stroke is made up of a series of flashes, and this on-off action causes the electromagnetic field surrounding the strike to expand and collapse [22]. This electromagnetic field motion can induce electrical currents into surrounding electronic equipment [22].

Lightning is generalised into two categories by aircraft pilots [23]. The first type is referred to as being “static discharge” and the second type is referred to as simply “lightning”, in aircraft pilot lingo [23]. Static discharges are the more common occurrence, and is characterised by radio static on the aircraft pilot’s earphone, followed by a corona discharge [23]. Corona discharge, or St. Elmo’s fire, is the luminous glow that is visible in darkness [23]. Static discharges are seemingly the cause of aircraft initiated lightning strike [23]. The other occurrence, simply referred to as lightning, involves aircraft intercepted lightning. Both types display similar effects to the aircraft upon inspection [23].

### **3.1.1 Aircraft Initiated Lightning**

Lightning strikes of this type are the most common in the aerospace industry, comprising a percentage total of 90% of lightning strike to aircraft [23]. Researchers have found that lightning strikes are most common on aircraft flying within clouds with temperatures between  $\pm 5^{\circ}\text{C}$  of freezing temperature ( $0^{\circ}\text{C}$ ) [23]. Globally, the majority of strikes are concentrated between altitudes of approximately 3–4 km, with South Africa (SA) having a maximum at approximately 3.8 km. The data shows that continental regions in which the freezing level is nearer to ground level experience strikes at a lower level than those with the freezing point at a higher altitude. Figure 3.2 illustrates these points.

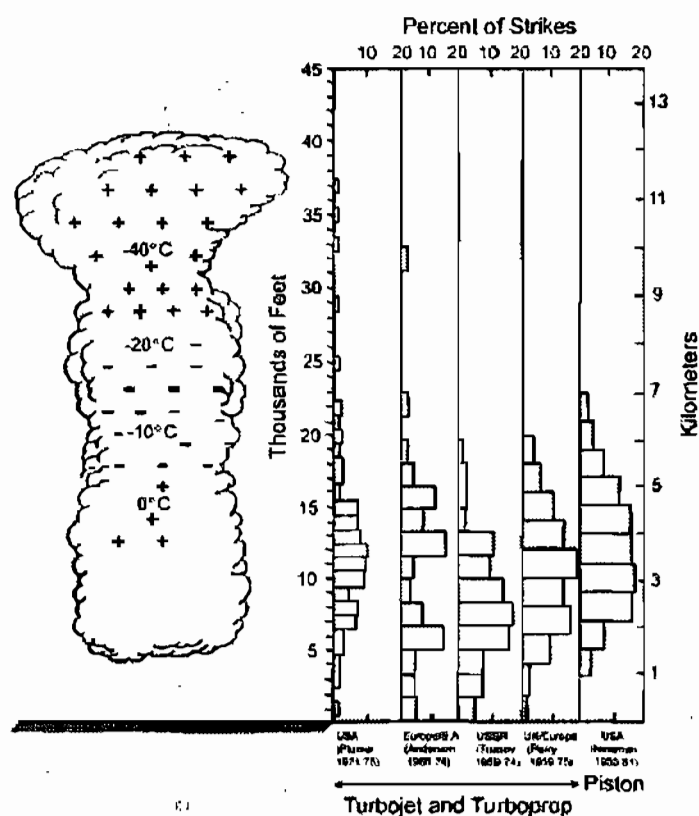
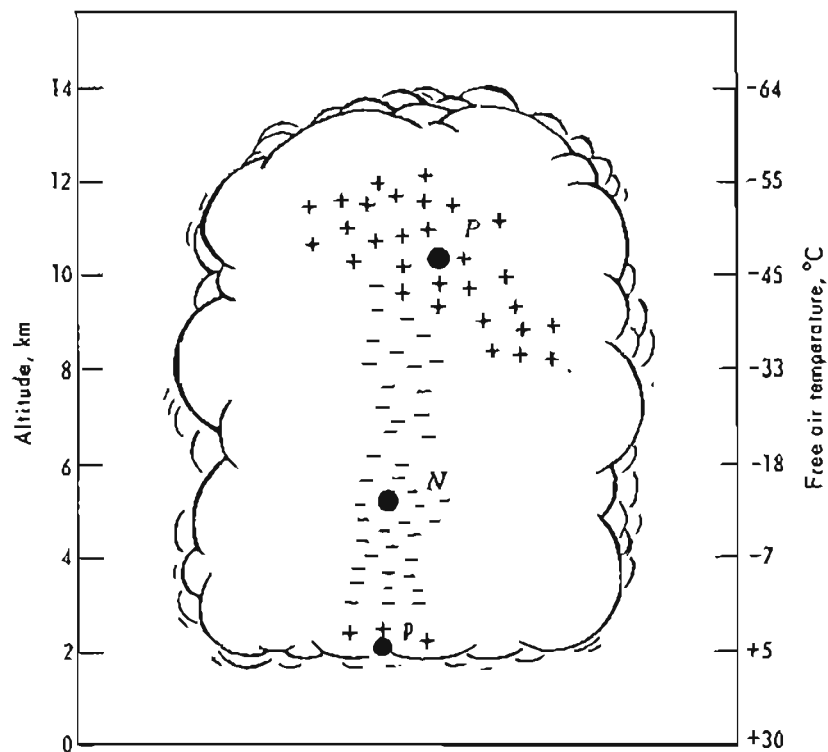


Figure 3.2: The altitude occurrence of lightning strike on aircraft [23]

It has been well documented that lightning will strike commercial aircraft at least once every year [21,23]. However, recent findings by the Boeing Company have shown that this figure is actually closer to twice per year [24].

### 3.1.2 Aircraft Intercepted Lightning

Natural lightning is commonly caused by atmospheric conditions such as thunderstorms, snowstorms and sandstorms, with the most common producer of lightning being the cumulonimbus thundercloud [20,21]. Thunderclouds are formed in the atmosphere when warm air at lower levels ascends, forming clouds, and the colder air at higher levels descends [20]. There tends to be a positive charge at the upper regions and a negative charge at lower regions of thunderclouds [20]. Figure 3.3 illustrates a typical South African thundercloud.



*Figure 3.3: The possible distribution of P (+40 C), N (-40 C) and p (+10 C) charges in a typical South African thundercloud [20]*

A typical lightning stroke begins with a weak predischARGE referred to as the “leader process” [20]. This is followed by a very luminous “return stroke”, which propagates from cloud to ground [20]. When a high negative potential lightning strike is near ground, the resulting electric field is sufficient to propagate upward-moving discharges from ground to the leader-tip [20]. Positive charged strokes are not as common as negative strokes, and are slower in speed and produce a larger charge transfer. Positive discharges are rarely composed of multiple strokes [20].

Figure 3.4 on page 14 shows lightning flash density in South Africa. This provides an indication on the frequency, and severity, of lightning strike in all regions in South Africa.

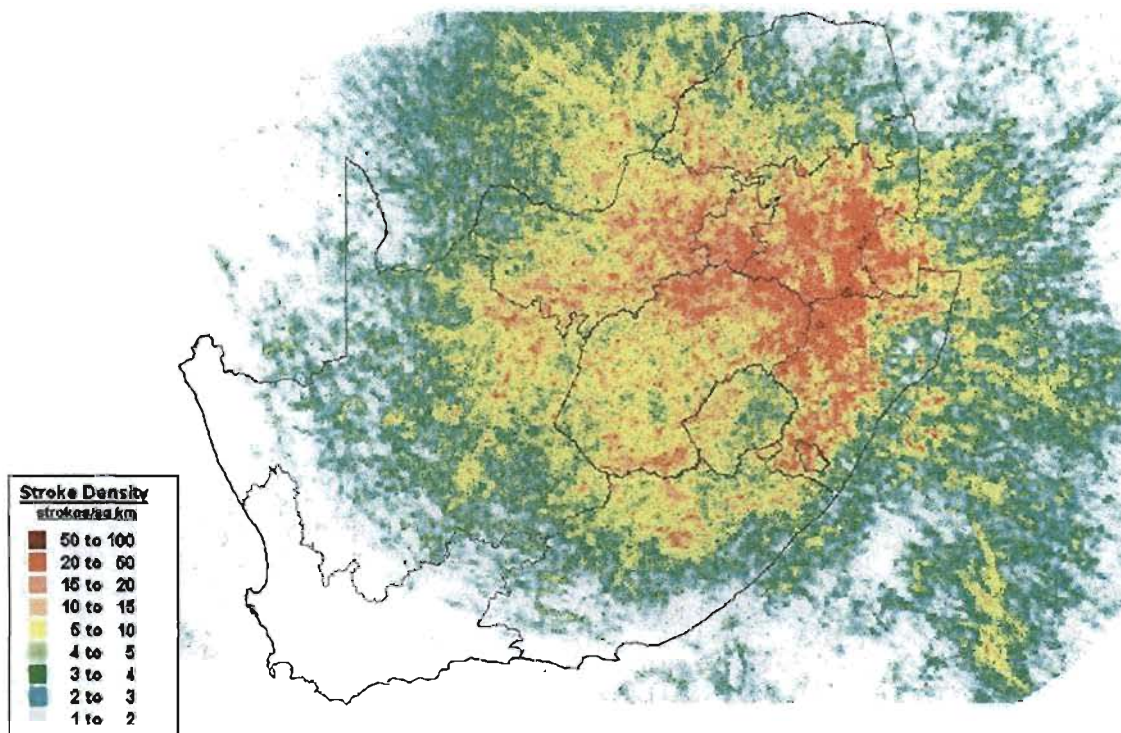


*Figure 3.4: Lightning Strike Density diagram for SA during the months of December 2005 to August 2006 [26]. As clearly seen, central areas of the country are subject to a high frequency of lightning strike, between 20-50 lightning strokes/sq km, in the recorded time.*

### **3.1.3 Lightning Zoning Diagrams**

There are many relevant design standards available that pertain to the specific disturbances. The design therefore involves researching currently implemented shielding devices used in industry; reviewing design standards; and reviewing any possible third party client requirements [25].

Although this work does not focus primarily on developing lightning strike protection structures, which require separate analysis, interaction between lightning and the external aircraft surfaces can occur. For this purpose it is imperative for designers to identify the regions which are most susceptible to lightning strike attachment. From this point, the designer can determine the type of protection the different aircraft locations require. Lightning zone diagrams are outlined in SAE ARP 5414A [27].

Industry design standards currently available describe typical lightning strike zones on aircraft. While the zoning diagrams tend to be specific to particular aircraft types, they can serve, in a general sense, to provide one with a clear indication of where to expect lightning strike to occur.

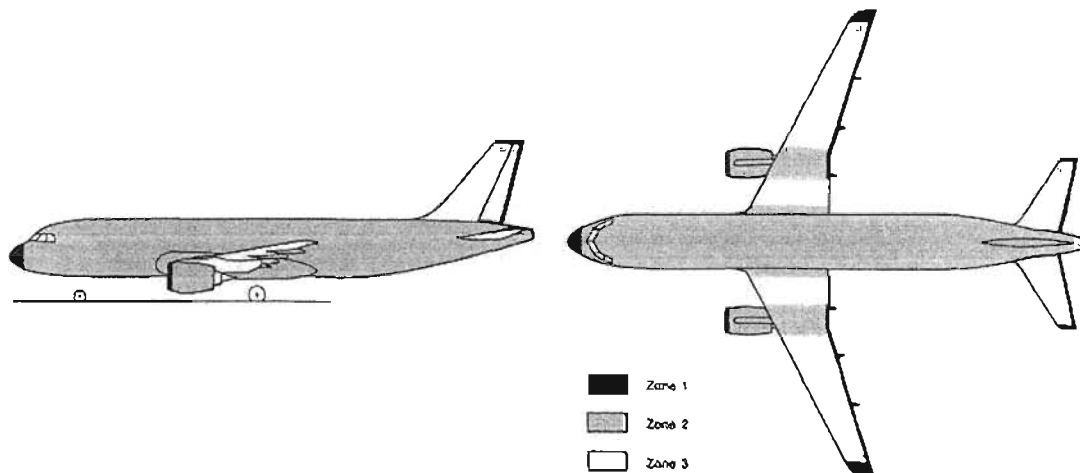


*Figure 3.5: The lightning strike zoning diagram of the A320 aircraft (Amended from [25])*

**Table 3.1: Lightning Zone Diagram Key for the A320 Aircraft [Amended from 25]**

ZONE	DIRECT EFFECTS	
1	Peak Current Action Integral Charge	200 kA $2 \times 10^6 A^2.S$ 200 C
2	Peak Current Action Integral Charge	100 kA $0.5 \times 10^6 - 1 \times 10^6 A^2.S$ 10 C
3	Peak Current Action Integral Charge	200 kA $0.5 \times 10^6 - 1 \times 10^6 A^2.S$ 10 C
	INDIRECT EFFECTS	
	Peak Current Rate of Current Rise	20 kA 200 kA/Ns

It was found, from studying lightning zone diagrams of various aircraft, that lightning typically attaches to extremities on aircraft, such as wing tips, and travel along the surface until reaching, and exiting from, the lower most extremity. Typically, pitting marks are seen on the surface that

lightning travelled along, and on occasion high current lightning strike burns through the material [21].

#### **3.1.4 Direct Effects of Lightning Strike**

When lightning strikes an aircraft, the direct effects include surface damage on bearings, hinges and outer skin (such as burn-through); and fuel ignition [21]. Until the 1970s, the chief concern regarding lightning strike was fuel ignition, and as explained, the electrically conductive nature of aluminium used in airframe skins was deemed as sufficient for protection against lightning strike [21].

However, with the recent inclusion of composite materials and fly-by-wire systems, protection against the effects of lightning has become an increasing concern [21,28]. It has been found that positive strokes are particularly hazardous to high-modulus fibre composite materials located in vulnerable lightning zones [28]. Due to its relatively high resistance compared with aluminium, carbon fibre has been found to explode in the event of a lightning strike [30]. This is due to electrical current converting to thermal energy [30]. The composite region which experiences direct lightning strike will generally have to be replaced prior to the next flight [29].

As clearly seen in the lightning strike zone diagrams, the extremities are particularly vulnerable to high current strike. The radome, however, cannot be shielded with the materials used to shield other areas. The radome houses an antenna and therefore has to be transparent to radar and communication signals [31]. Lightning diverter strips are typically used to provide an electrically conductive channel on the radome [31].

#### **3.1.5 Indirect Effects of Lightning Strike**

The indirect effects of lightning strike lead to electromagnetic disturbances in electronics and avionics. The effects range from minor radio static, to complete shut-down of on-board avionics [3].

Although, the protection of aircraft against EMI effects is the primary concern of this research, it was decided that it would be beneficial if the shielding material is sufficiently strong and contains sufficient electrical conductivity to allow safe landing of the airborne vessel upon lightning strike.

### **3.2 Electromagnetic Pulses**

Man-made sources, such as electromagnetic pulse (EMP) bombs, are deliberate attacks with the intention of causing harm. EMP is a transient wave that is produced by nuclear explosions occurring at lower altitudes [22].

Incidentally, interest in protection against EMI especially arose in the 1970's when scientists began studying the effects of EMPs produced by nuclear explosions [22]. An EMP is essentially described as being an electromagnetic shockwave [32]. Similar to conventional explosive devices producing shock waves of pressure in the surrounding atmosphere, an EMP will produce a shock wave that can propagate through any material that which allows the passage of radio waves [32]. The effects of EMP can be likened to that of a lightning strike, with anything from minor radio static, to complete shut down of on-board avionics being documented [32]. It was found that shorter pulses result in greater electromagnetic field intensity [32].

Akin to lightning, EMP generates large electromagnetic transient sources that can interact with electronic equipment on-board aircraft [22]. Newer solid state equipment is designed to operate on much lower current than older equipment, and currents induced by these surges can be sufficient to cause damage, if inadequately shielded [22].

### **3.3 High Intensity Radiated Environment**

The high intensity radiated field (HIRF) environment is of specific importance in the military field. HIRF encompasses damages induced by natural sources and man-made sources [4]. Much of the research undertaken with externally generated electromagnetic effects have been with lightning and EMP, but HIRF data been quite difficult to ascertain [4].

In his work for NASA, Shooman [4], has found that it is often easier to quantify HIRF in what it is not caused by. It is described as being an uncommon event, and HIRF is not caused by passenger cellular phones; interference from high frequency radio on a specific narrow body aircraft which is known to couple into the autopilot; not due to lightning effects; and is not due to effects of equipment failures [4].



In his work, Shooman [4], obtained anecdotes from various industry professionals ranging from managers to aircraft pilots, in order to build a knowledge base on HIRF. It was found that HIRF is generally kept classified by government for reasons such as military security [4]. However, some examples of HIRF in Shooman's [4] work include: commercial AM or short wave transmitters which disturbed the autopilot and engine controls; air traffic control, military and shipboard radar transmitters which affected communication and navigation equipment; countermeasures equipment on military aircraft which affect commercial aircraft in its vicinity, jammer equipment affected communication equipment; commercial FM transmitter affected navigation and communication equipment. It was therefore apparently found that communications and navigation equipment is the most susceptible in his study. There is also some suspicion that HIRF was the possible cause of the crash of TWA Flight 800, which apparently was flying in the proximity of several naval ships when it crashed [3].

Data pertaining to the HIRF in SA could not be obtained. Data was not provided by Armscor regarding this phenomenon either. It was, however, established through contact with industry professionals and Armscor that protection from frequencies ranging between 800 MHz and 3 GHz will be sufficient for the requirements of this work.

### **3.4 Precipitation Static**

As the name suggests, precipitation static (p-static) is catalysed by forms of precipitation [33]. When the aircraft is subject to precipitation, such as hail, dust and snow, there is a charge build-up on the dielectric surfaces [33]. The charging is due to friction between precipitation and the aircraft surfaces [33].

The resultant effects of p-static include severe noise generated in the communication/navigation range and overall degradation of sensitive avionic and electrical equipment [33-35]. Although p-static is sometimes encompassed in the EMI definition, separate protection devices, referred to as "static wick dischargers", are used in industry for this phenomenon [36]. These devices lower the discharge threshold of the structure to which they are attached thereby removing excess electrons before noise is generated [36].

### **3.5 Electrostatic Discharge**

Electrostatic discharge (ESD) is caused when two materials make contact and are subsequently separated [37]. This causes electrons to be stripped and transferred from one material to another. This causes a build-up of static charge in material [37].

ESD is of particular importance for semi-conductive and insulative materials [19]. Dhawan *et al.* [13] have found that materials with surface resistivities between  $10^4 - 10^8 \Omega \cdot \text{cm}$  will suffice antistatic applications. Conductive materials, which are required for electromagnetic shielding, typically have a low resistivity which is less than  $10^4 \Omega \cdot \text{cm}$ , and electrons should flow easily between the materials [37]. If the second surface is attached to a grounding point, as is the case with aircraft surfaces, the electrons will flow to ground and the excess charges will be neutralised [37].

## CHAPTER 4: ELECTROMAGNETIC SHIELDING

The sources for potential electromagnetic disturbances in aircraft have been established. It is apparent that structures that display electrical conductivity are required to provide the electromagnetic shielding, which is also known as electromagnetic “hardness”, for on-board electronic and avionic devices to prevent such disturbances from taking place.

As mentioned, EMI shields are not structures that follow generic designs in the sense that structures require specific shielding depending on operating conditions. To reinforce this statement with reference to the example of cellular phones given in Chapter 1, it was found that cellular phones transmit at frequencies between 824.04 and 848.97 MHz and receive at frequencies between 869.04 and 893.07 MHz [10]. It will therefore be essential to ensure electronic systems that are to operate without interference in the presence of cellular phones, be shielded within this range. This may not necessarily be the case for structures that are not meant to operate in the proximity of cellular phones.

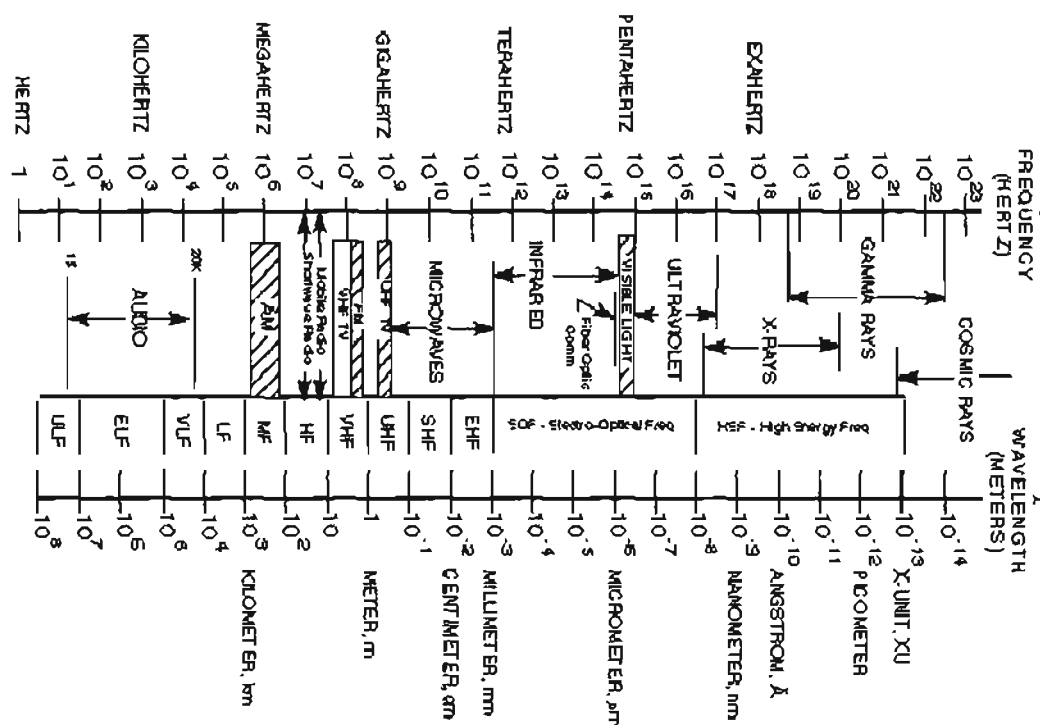


*Figure 4.1: A representation of the electromagnetic spectrum [38]. As can be seen, the frequency ranges that were explained in Chapter 3 to be of interest in this work are referred to as the high frequency (HF), very-high frequency (VHF) and ultra-high frequency (UHF) ranges i.e.  $10^6 - 10^9$  Hz range.*

#### **4.1 The Theory behind Electromagnetic Shielding**

Electromagnetic shielding materials can provide protection for enclosed surfaces from the effects of the external electromagnetic environment. The basis for lightning strike protection and this electromagnetic shielding comes from a structure referred to as a “Faraday Cage” [10,39]. This structure, which contains a conductive outer layer, provides the fundamental protection for electronic equipment that is to be protected from electric fields. The external electric field of the structure redistributes electrons such that the total electric field within the enclosure is zero [10]. In real terms, the Faraday cage effect can be seen in a typical automobile – it is long understood that one of the safest places to be in the event of lightning strike is inside a metal automobile.

The primary mechanism for shielding in electrically conductive structures, such as metals, is reflection [5,11]. Reflection relies on mobile charge carriers, such as electrons, being present within the material [5,11]. However, as mentioned previously, high electrical conductivity is not required as conductivity requires connectivity, whereas shielding does not [5,11]. However, shielding is enhanced by connectivity [5,11]. Reflection loss is a function of  $\sigma_r/\mu_r$ , and reflection loss decreases with increasing frequency [5,11]. ( $\sigma_r$  refers to the conductivity of a material relative to copper, and  $\mu_r$  refers to the permeability of a material relative to copper).

The secondary mechanism for shielding in these structures is absorption [5,11]. Significant absorption of the waves by the shield requires electric and/or magnetic dipoles within the shield material [5,11]. Absorption loss is a function of  $\sigma_r\mu_r$ , and absorption increases with increasing frequency [5,11]. Absorption loss is proportional to shield thickness [5,11].

The third mechanism for shielding is multiple reflections [5,11]. Multiple wave reflections take place at surfaces or interfaces within the shield [5,11]. This mechanism requires the presence of large surface areas or interfaces within the shield [5,11].

It is imperative that transmission of the wave through the shielding material is prevented. Figure 4.2 on page 22 describes the possible interactions of electromagnetic waves with a surface as described above.

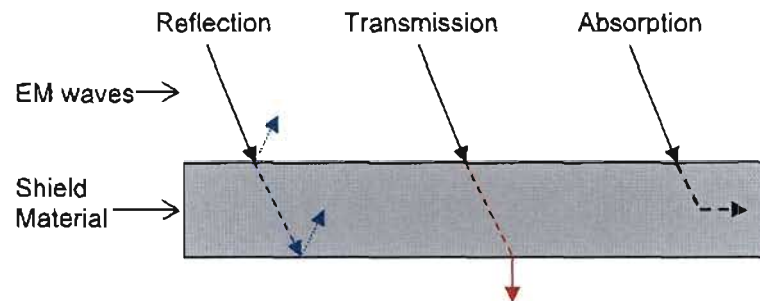


**Figure 4.2:** The mechanisms of EMI shielding. Reflection and Absorption clearly dissipate the wave before entry. Transmission must be prevented, as this allows electromagnetic waves into the system.

It has thus been established that exposure to electromagnetic waves results in current flow within the material in question. Table A1 in Appendix A presents the conductivity and permeability of various metals relative to copper.

From Ohm's law,  $I = V/R$ , it is seen that current flow is inversely proportional to electrical resistance. This shows that a small resistance is required for a high current flow. In most cases, resistance does not depend on current or voltage [10]. Resistance is directly proportional to resistivity and inversely proportional to electrical conductivity, as seen in the following equations:

$$R = \frac{\rho l}{A} = \frac{l}{\sigma A} \quad (4.1) \quad [10]$$

Where:  $\rho$  = electrical resistivity ( $\Omega \cdot \text{cm}$ )

$A$  = area ( $\text{cm}^2$ )

$l$  = length ( $\text{cm}$ )

$\sigma$  = electrical conductivity ( $\Omega^{-1} \cdot \text{cm}^{-1}$  or  $\text{S/cm}$ )

Current density through a particular material is given by:

$$J = \sigma \vec{E} = \frac{\vec{E}}{\rho} \quad (4.2) \quad [10]$$

Where:  $J$  = Current density ( $\text{A} \cdot \text{cm}^{-2}$ )

As can be seen from equations (4.1) and (4.2), a low electrical resistance is required for a high degree of electrical conductivity. It can also be said that electrical resistance is usually an intrinsic material property. In materials such as aluminium, it is expected that this resistance value remains constant (except at critical temperature,  $T_c$ , when dealing with superconductors [10]). In normal practice, materials are expected to have an electrical resistance value that exceeds zero, and therefore some wave penetration could be experienced.

Electromagnetic waves cannot propagate appreciable distances in electrically conductive materials due to the electric and magnetic field strengths that lead to current flow [10]. The electrical conductivities that these materials possess determine whether they will possess a mechanism for dissipating the wave. In ideal conductors the electric field strength is zero, and in such materials total reflectivity of the wave is possible [10]. This can be seen when substituting the relevant values into equations 4.1 and 4.2.

In practice, it is not possible to obtain a shielding material that provides total reflection as practical materials, including metals which are considered the best electromagnetic shielding agents, do not behave as ideal electrical conductors [10]. In other words, there will be some absorption associated with EMI shielding. The energy that is absorbed is converted into thermal energy as well, implying that the shielding material must display some degree of thermal conductivity as well. However, it has been found that materials that display good electrical conductivity generally have good thermal conductivity as well [10].

In theory, however, the electrical resistance of a material can be zero, as in materials referred to as “superconductors” [10]. In superconductors, electrical resistance is a function of temperature, and cooling the material below a certain temperature,  $T_c$ , results in a disappearance of electrical resistance [10]. In superconductors, the induced current will continue to flow even after the induced emf has disappeared [10].

In certain surfaces, the induced current will circulate throughout the volume of the material [10]. These are called eddy currents [10]. Eddy currents are the root cause of the “skin effect” [10]. The skin effect is the tendency of alternating currents to redistribute within a system such that the highest current density,  $J$ , is closer to the surface of the material [40,41]. Thus, the electric current tends to flow on the surface, or “skin”, of the material. The “skin depth” of a material is defined

as the surface thickness of a material at any frequency for which 63.2% of current is flowing therein [17]. Skin depth decreases with increasing frequency and with increasing conductivity [5].

## **4.2 Calculations on EMI Shielding**

There are many variables that could present an indication on the quality of shielding that materials possess. Such variables include transmission of the wave, reflection of the wave, absorption of the wave and extent of multiple reflections within the shielding material. These variables are all defined in terms of decibels (dB). However, the total electromagnetic shielding effectiveness (EMSE) is the term that presents the extent to which the shielding material offers protection, and encompasses the shielding contributions provided by the reflection, absorption and multiple reflection mechanisms [17]. This is often the term quoted when one speaks about the quality of shielding that materials possess.

It was found that many equations could be used in the computation of electromagnetic shielding variables. However, at the outset it must be stated that discrepancies between the results obtained from use of the various analytical approaches have been well-documented by previous researchers [40,42,43]. These discrepancies have been reported as being quite substantial, and in some cases have been greater than 100dB, especially around joints [40]. The computation of expected EMSE by use of theoretical equations is thus well-regarded as being a problem in the industry. In this study the various equations that have been identified as being suitable for the computation of analytical EMSE are reported.

### **4.2.1 General Shielding Effectiveness Calculations**

The figure-of-merit referred to as shielding effectiveness (SE) is defined by White [17] as a description of the performance of an electromagnetic shield material in reducing the electromagnetic energy either impinging upon a possible susceptible victim or exiting from an undesirable source. SE is typically quoted in the forms presented:

$$SE_{dB} = 10 \log_{10} \left( \frac{\text{incident power density}}{\text{transmitted power density}} \right) \quad (4.3) \quad [17]$$

The above equation can be written in terms of E and H, provided that they are measured in the same medium and have the same wave impedance:

$$SE_{dB} = 20 \log_{10} \left( \frac{E_b}{E_a} \right) \quad (4.4) \quad [17]$$

$$SE_{dB} = 20 \log_{10} \left( \frac{H_b}{H_a} \right) \quad (4.5) \quad [17]$$

Where: subscript “a” refers to E and H before the shield is installed, and subscript “b” refers to the E and H after the shield is installed.

SE is commonly provided in terms of a summation of the individual mechanisms responsible for contributing to shielding:

$$SE_{dB} = R_{dB} + A_{dB} + B_{dB} \quad (4.6) \quad [17]$$

Where:  $R_{dB}$  = Reflection loss (dB)

$A_{dB}$  = Absorption loss (dB)

$B_{dB}$  = Re-reflection loss (dB)

#### **4.2.2 Equations for Individual Shielding Mechanisms**

The calculation of the individual shielding mechanism terms for metals is explained by White [17]. The text was written prior to the wide-spread interest of composites in the aircraft industry, but equations presented in the text have been used by previous researchers in composite materials as well [5,6,11,13].

##### **4.2.2.1 Reflection**

There are three reflection equations presented by White in the document [17]. With respect to Figure 2.3, the different equations address the cases of high impedance (electric) fields, low impedance (magnetic) fields, and far-field conditions (plane waves) respectively.



Electric Fields:

$$R_{dB} \approx 141.7 - 10 \log_{10}(\mu_r f^3 r^2 / \sigma_r) \quad (4.7) \quad [17]$$

Magnetic Fields:

$$R_{dB} \approx 74.6 - 10 \log_{10}(\mu_r / f \sigma_r r) \quad (4.8) \quad [17]$$

Far-field Conditions:

$$R_{dB} \approx 108.1 - 10 \log_{10}(\mu_r f / \sigma_r) \quad (4.9) \quad [17]$$

Where:  $f$  = Frequency (MHz)

$r$  = Distance from the source (m)

As can be seen from equations (4.7) and (4.8), use of the equation will yield an approximated answer. The extent to which one can confidently accept the answer obtained from computation using these equations is not explained in [17].

Addition to this, another far-field condition equation has been presented by Das *et al.* [6], which is similar, though not identical to equation (4.9). The equation given in their work is:

$$R_{dB} \approx 108 + \log_{10}(\sigma_r / \mu_r f) \quad (4.10) \quad [17]$$

As seen, the use of equation (4.10) equation will yield a larger value for  $R_{dB}$  as the second term (negative term) is not multiplied by 10. However, it was found that equation (4.9) is likely more correct as it is used by the Chomerics (one of the leading commercial electromagnetic shielding manufacturers) as well [16].

4.2.2.2 Absorption

The absorption term should be secondary in metallic structures. However, the equation presented in [17] indicates that resulting values for absorption loss will be rather high. This term is expected to be secondary in metallic structures, and should be very small, if not 0dB [44]. The graph depicting absorption loss for various materials presented in [17] for aluminium indicates a 5mm aluminium plate will contribute approximately 600dB via absorption at 1GHz, which appears

incorrect according to Prof. JW Odendaal [44]. Nonetheless, the equation for absorption loss is presented as being:

$$A_{dB} = 1314.3t \sqrt{f\sigma_r\mu_r} \quad (4.11) \quad [17]$$

Where:  $t$  = thickness of shielding material (cm)

The equation for absorption loss presented by Das *et al.* is of the exact form, but is reduced by a factor of  $10^3$ . This equation appears to be more plausible to the author, as absorption is generally the secondary mechanism in electrically conductive materials. The equation presented is:

$$A_{dB} = 1.32t \sqrt{f\sigma_r\mu_r} \quad (4.12) \quad [6]$$

This absorption loss equation is also used by Chomerics [16].

#### 4.2.2.3 Multiple Reflections

Multiple reflections are only a consideration when absorption loss is less than 6 dB. Above this value, multiple reflections may be ignored [16]. However, qualitative examination of equation (4.11) above shows that absorption loss will almost always be above this value for conductive materials at high frequencies.

$$B_{dB} = 20 \log_{10}(1 - e^{-2t\sqrt{\pi f \mu \sigma}} e^{-j2t\sqrt{\pi f \mu \sigma}}) \quad (4.13) \quad [17]$$

Where:  $f$  = frequency (Hz)

$\mu$  = magnetic permeability of the material (Wb/A.m)

$\sigma$  = electrical conductivity of the material (S/m)

#### 4.2.3 Additional Shielding Effectiveness Equations

Use of equation (4.11) could provide erroneous results in the order of  $10^2$  dB. For this reason, additional equations were identified to determine whether they will better suffice the purpose of computing a more reliable SE value.

The Simon formalism [11] presents a means of determining EMSE specifically for conductive composites. However, this equation is suitable for approximation only, as it completely ignores multiple reflections as a term in the equation [11]. The first two terms combined refers to the reflection loss, whilst the latter term refers to the absorption loss, in the shielding material [11].

#### Simon formalism

$$SE = 50 + 10 \log_{10}(\rho f)^{-1} + 1.7t(f/\rho)^{\frac{1}{2}} \quad (4.14) \quad [11]$$

Where:  $\rho$  = volume resistivity ( $\Omega \text{ cm}$ )

$f$  = frequency (MHz)

$t$  = shielding material thickness (cm)

Equation (4.15) presents the formula proposed by Colaneri and Shaklette [43] for materials obeying the “classical good conductor” approximation  $\sigma/2\pi f \epsilon_0 \gg 0$  for far-field conditions. It is apparently valid when frequencies are much greater than cross-over frequency [11].

$$SE = 10 \log \left( \frac{\sigma}{32\pi f \epsilon_0} \right) + 20 \frac{d}{\delta} \log(e) \quad (4.15) \quad [43,45]$$

Where:  $\sigma$  = bulk conductivity ( $\Omega / \text{cm}$ )

$f$  = frequency (MHz)

$\epsilon_0 = 8.854 \times 10^{-14} \text{ F/cm}$

$d$  = shielding material thickness (cm)

$$\delta = \sqrt{\frac{1}{\mu_0 \pi f \sigma}} \text{ (cm)} \quad (\text{known as skin depth, explained in section 4.1}) \quad (4.16) \quad [43,45]$$

$e = 2.718281828$

Colaneri and Shaklette [43] have also developed equations for electrically thin samples ( $d < \delta$ ) for both the near and far field:

#### Near-Field:

$$SE = 20 \log_{10} \left( \frac{c Z_0 \sigma d}{2 \omega r} \right) \quad (4.17) \quad [11,43]$$

Far-Field:

$$SE = 20\log\left(1 + \frac{Z_0\sigma d}{2}\right) \quad (4.18) \quad [11,43]$$

Where:  $c$  = speed of light  $2.998 \times 10^8$  m/s

$Z_0$  = impedance of free space  $377 \Omega$

$\sigma$  = electrical conductivity ( $\Omega$ /m)

$d$  = shielding material thickness (m)

$\omega$  = angular frequency (rad/s)

$r$  = shield-to-source distance (m)

As seen from equation (4.18), EMSE is independent of frequency for electrically thin samples, indicating that the value remains constant for all frequencies as long as the  $d < \delta$  condition is met. For electrically thick samples, when the condition is no longer valid, the EMSE value is expected to increase monotonically as frequency increases [45].

#### **4.2.4 Discussion on Shielding Effectiveness Calculations**

Various equations that are useful in analytically determining EMSE have been provided. The extent to which one can confidently accept the results obtained from use of any of the equations is, however, unknown. As explained earlier, the calculation of EMSE is a well-known problem, and discrepancies have been documented in previous works [5,6,11,13]. It has been found that theoretical absorption losses that are quite high result from use of equation (4.11), which may result in erroneous values of EMSE being obtained.

As it was decided that the frequency range of interest for this work was between 800 MHz and 3 GHz, far-field conditions were adopted. The near-field range encompasses frequencies below 1 MHz, whilst the far-field range encompasses frequencies above 100 MHz [46].

#### **4.3 Additional Calculations**

Additional calculations that provide potentially useful information include determining the material impedance and surface (barrier) impedance. The impedance variables could also provide an indication on the type of SE a material will possess, even if the actual SE value is unknown. A

lower impedance is desired as this indicates a higher electrical conductivity, implying that there is a mechanism to dissipate the electromagnetic wave in the material [47]. However, the equation provided by White [17] is seemingly only applicable for the case where  $t \gg \delta$ , and uses the assumption  $t > 3\delta$ . In other words, the equation may only be suitable for electrically thick samples.

Intrinsic impedance (when  $t \gg \delta$ ):

$$|Z_m| = \sqrt{2 \times 10^3} \sqrt{\pi \mu f / \sigma} \quad (4.19) [17]$$

Barrier (Surface) impedance (any thickness):

$$Z_B = 369 \sqrt{\mu_r f / \sigma_r} \left( 1 - e^{-\frac{t}{\delta}} \right)^{-1} \quad (4.20) [17]$$

The surface impedance of various metals can be seen in the figure below. Typically metals have impedance values in the order of milliohms.

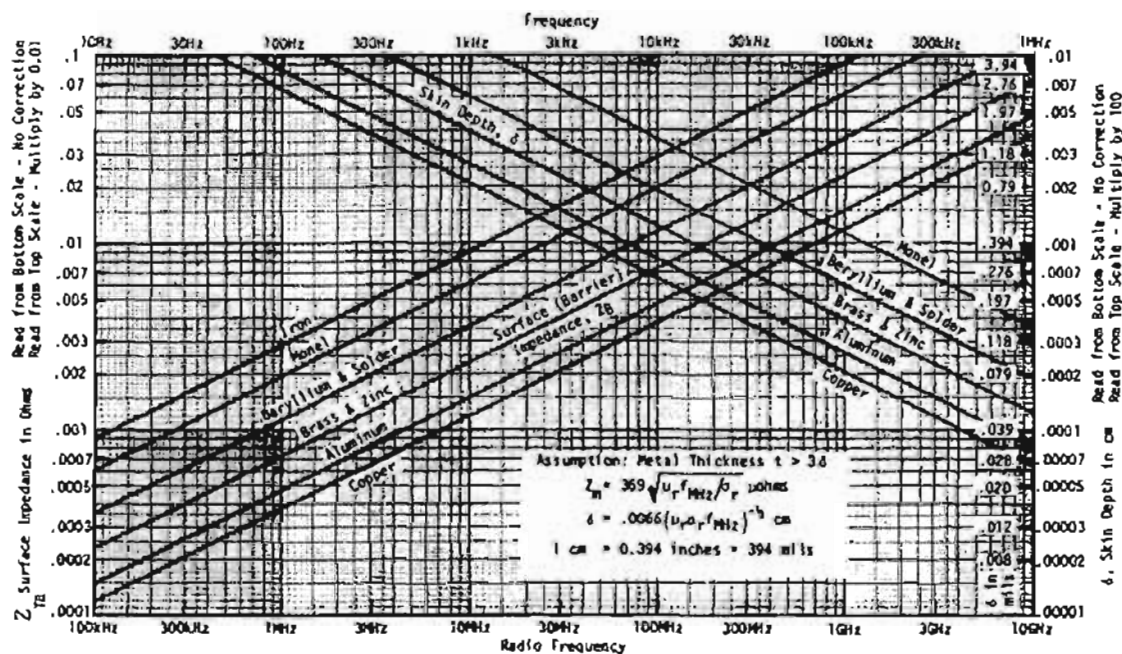


Figure 4.3: Surface Impedance and Skin Depth of Various Metals vs. Radio Frequency [17]

**PART B: Composite Electromagnetic Shielding &  
Material Selection**

## **CHAPTER 5: ANALYSIS OF COMPOSITE MATERIALS**

The phenomena responsible for electromagnetic disturbances in airborne vehicles have been established. It is apparent that materials which display electrical conductivity are necessary to effectively provide shielding of electromagnetic radiation in aircraft structures. A study on classical and current industry trends was undertaken to establish which materials are considered as being best suited for the required purpose by industry professionals. Studies of this nature will aid designers in selecting appropriate materials for their applications.

### **5.1 Background on Composites use in Aircraft**

The use of composite materials in aircraft structures is not globally groundbreaking by any means. In the early years of flight, aircraft were fabricated from composite materials, with wood, wire, and fabrics composing the structure [48]. During the 1930's engineers began investigating the possibility of integrating fibre composite materials into aircraft [48]. In the early stages, glass fibre and polyester matrix materials were investigated [48]. In 1943, a training aircraft was developed in the United States of America (USA) with a glass-fibre reinforced polyester laminate with a honey comb core fuselage [48]. This was apparently one of the first airborne machines to consist of fibre composites and flew successfully for the first time in March 1944 [48].

Polyester resins were later replaced in the post-war period with superior epoxies for structural applications [48]. Over the course of the next thirty years, composite materials were investigated with increasing interest, most notably to provide weight savings over the conventional metals that were used [48,49]. Electromagnetic effects were not primarily considered in the design criteria of these aircraft, as the metals used were deemed to provide sufficient protection [3]. There is no other evidence to substantiate that researchers were actively considering electromagnetic effects while developing fibre composites in aircraft.

The use of composite materials in aircraft opposed to orthodox metal materials provides a number of advantages, but also has associated disadvantages with their use. Table 5.1 presents some of these issues.

**Table 5.1 Advantages and Disadvantages of Utilising Composites in Aerospace Vehicles**  
**[Amended from 49]**

Advantages	Disadvantages
Higher specific strength and stiffness	Certification testing
Material design and tailorability	Systems integration
Reduced number of parts	Prototype tooling
No fatigue damage (Appears to be untrue)	Risk involved with new technology
No corrosion	Inefficient joints/cut-outs
Near zero coefficient of thermal expansion	Costly validation/certification
High resistance to shock and vibration	Sensitive to out-of-plane loads
	High coefficient of thermal expansion in the in-thickness direction

In terms of the global composites advancement in the aerospace field, the military has borne much of the financial expense, and accepted the associated risk that is customary with any new development [48]. This is presumably due to many of the raw materials used for composite manufacture being costly when development is in its infancy stages, and widespread use is thus not economically feasible in other sectors.

In the 1960's the Grumman Corporation began researching the use of composite materials in their aircraft [49]. When the F-14 military aircraft made its first flight in December 1970, the use of boron/epoxy composite material in the horizontal stabilizer (tail fins) yielded a weight saving of 18% when compared when metals were used [48,49]. However, the high cost of boron fibre has limited its use in commercial aircraft applications [48].

Boron/epoxy composite material was used in two other Grumman aircraft which flew in 1971, the F-111 and the F-15 [49]. However, the F-111 also utilised graphite/epoxy composite material on the underwing fairings as well, and this is apparently one of the first aircraft to utilise graphite/epoxy composite material [49]. In the 1960's, helicopter rotor blades, in helicopters such as the BK 107, were also being developed from carbon and glass fibre-reinforced epoxy composites for the first time [48].

By the mid-1970's aircraft such as the B-1 contained graphite/epoxy, boron/epoxy and glass/epoxy composite materials in the horizontal stabilizer, and this resulted in cost savings between 15-20% and a weight saving of 15% [49].



However, despite addressing concerns regarding weight and cost savings, composite materials at this time were apparently not considered as viable options for use as electromagnetic shielding and lightning strike dissipation agents. This is presumably the reason why metal was still utilised in the proximity of areas prone to lightning strike and electromagnetic disturbances.

Despite composite materials being introduced in these military aircraft, aircraft were manufactured predominantly from metals prior to the 1980's, most notably iron and aluminium alloys [48]. This was due to the excellent properties these materials intrinsically possess, such as strength and electrical and thermal conductivity. As explained previously, the chief disadvantages, weight and cost, became an increasing concern in more recent years and alternatives were required.

The 1980's saw the demand for high performance aircraft grow at a phenomenal rate, and a consequent demand for new materials to replace orthodox metals in the aerospace industry followed [48]. This led to further studies of composite materials as possible alternatives. The various advantages composite materials were identified as providing included low cost, weight reductions, corrosion resistance and easy processability [7,50-52]. By this time, electromagnetic effects were seemingly understood as being a cause for concern in aircraft, as protective measures were beginning to be investigated [48,49]. However, an obstacle preventing the expected substitution is the general lack of substantial electrical conductivity that fibre composites possess [6]. At the time, limited research appears to have been undertaken regarding electrically conductive composite materials, as there are few works to support it was.

Despite the apparent threat EMI presents, little advancement in electromagnetic shielding has been made in the last decade [53]. The possible reason is due to shielding providing no tangible value other than protection to the devices they shield [53]. This has been changing in recent years, and further demand for improved shielding options is expected to increase drastically in the coming years [53]. Electrically conductive additives that have been researched increasingly in recent years include conductive reinforcement materials, conductive resins and conductive fillers [5,6,52].

Work undertaken in the past few years has succeeded in providing novel solutions for electromagnetic shielding using composite materials. However, much of the work is still very much in its developmental phase, and production of newer electromagnetic shielding materials

using fibre composites is apparently not widespread as evidenced by the lack of composite electromagnetic shielding in industry.

Chung [5] explicitly states that continuous fibre polymer-matrix composites are particularly desired for today's aircraft electromagnetic shielding materials. It was known that strength was desired in the shielding material in this research, and thus materials that offer good structural support were researched with interest. Luo and Chung, [47], have also explained that continuous filler materials provide enhanced shielding and structural reinforcement opposed to discontinuous filler materials. Discontinuous fillers, such as powders, fibres and particles, could serve to degrade strength when increasing quantities are introduced into the matrix material [47]. As expected, this consequently results in a decrease of the filler-matrix bond as well [47].

It was known by the author prior to this work that carbon materials do contain a degree of electrical conductivity, high strength, and is known to be a light-weight material. Initially, it was thought by the author that introducing carbon flakes into the matrix system could present advantageous properties regarding EMSE. However, Chung [5], has proved that introduction of tiny carbon fibres (diameter  $< 1 \mu\text{m}$ ) in fact serves to degrade EMSE of the laminate.

A difference in coefficient of thermal expansions of the filler and matrix could also induce stress-strain forces at the interface of both components, which could subsequently lead to a degradation of the conducting route [54]. Krupa *et al.* [55] have found that higher stresses are induced at higher filler loadings. It appears that manipulation of electrical conductivity could result in degradation of mechanical properties. This may, however, be suitable if a balance between the two properties that is deemed acceptable is achieved. However, it will be quite difficult to quantify this value, and is quite specific to particular design requirements. Again, this reiterates the fact that electromagnetic shielding materials are not generic in design.

It was long understood that low surface impedance is a desired property in shielding materials [47]. This is beneficial to both electromagnetic shielding and lightning protection materials [47]. Polymer-matrix materials, which although are the preferred option in this work, were assumed to contain a high impedance, as they are generally insulative. It was thought by the author that producing electromagnetic shielding materials that contain electrically conductive matrix systems could alleviate the problems associated with discontinuous filler materials as they will inherently

possess lower impedance. Carbon-matrix systems could suffice this purpose, but are quite brittle, expensive, and extremely difficult to produce [56].

It was also thought that inherently conductive polymers could present advantageous results regarding electrical conductivity and EMSE. There has been great interest in the polymer polyaniline, which is an amorphous powder, which contains inherent electrical conductivity. However, reports on the degree of conductivity have been quite conflicting [14,15,57], but it is generally regarded as being moderately electrically conductive [13]. Addition to this, electrically conductive polymers such as polyaniline, despite possessing good processability, possess poor mechanical properties [5].

Hong *et al.* [2] have documented that electrically conductive polymer composite promote the shielding mechanism of absorption. Metals, which are typically used in aircraft for electromagnetic shielding, display reflection-dominant shielding characteristics [5,47]. Research work with polyaniline for example, has apparently focused on developing shielding materials displaying absorption as the dominant mechanism [13,15,57]. This is expected, as conductive polymers do promote absorption as the dominant characteristic [2].

Carbon black was originally suggested as being a suitable filler material, as composite materials containing the filler display excellent strength properties [58]. However, carbon black is also noted as being an excellent radar-absorptive material (RAM) [59], thereby implying absorption is the dominant shielding mechanism, and was likely unsuitable for the purpose of significant electrical conduction and more importantly electromagnetic shielding via reflection. The predominant disadvantage regarding absorptive materials is the inherent low reflection loss associated with them, as they promote absorption as the primary shielding mechanism. According to Cheng *et al.* [51], absorption-dominant shielding is generally desired for protection of home electronic devices. However these characteristics were quite unsuitable for electromagnetic shielding in this work.

Carbon and vapour-grown nanotubes were considered as possible filler materials, owing to the superior electrical and mechanical properties these filler materials possess [11,60]. Many researchers [11,60] have been working with nanotubes with the hopes of developing suitable electromagnetic shielding, but much of this work appears to have been purely research-based. It

would seem that the high cost of these materials make them undesirable for the current commercial applications.

The addition of metals into fibre composites was identified as being a likely option, as metals and their alloys do already serve as excellent reflection-dominant shielding agents in practice. The disadvantages regarding these likely inclusions, corrosion, weight and cost, are not as significant as the quantities in the composite could be much less than use of metal by itself. Jia *et al.* [61], states that the metal content used in aerospace applications for electrical conductivity can range between 60% - 90%. Metal-based fillers, such as nickel-coated carbon fibres in polymer composites have been found to already provide excellent EMSE [5].

A review into current industry designs pertaining to EMI and lightning strike protection has shown that wire meshes feature prominently in designs [9,24,51,52,62,63]. As wire meshes are continuous materials, they provide a constant electrically conductive path, and as shielding is enhanced by connectivity, it was believed that this will only result in a superior design. The new design for the Boeing 787, which is the first commercial carbon fibre plastic airframe, utilises a thin metal mesh in the outer layers of the composite structure [24]. The purpose for this is both to conduct currents from lightning strikes, and for electromagnetic shielding [24]. Gates [24] reports that Boeing is quite confident that this design will meet Federal Aviation Administration's (FAA) stringent flight requirements when their testing process is complete.

It is well known that composite manufacture using metals can be a tedious process [62,63]. Research has been ongoing with hybrid fibre/metal fabrics [9,51,52]. However, these fabrics are comparatively expensive to produce, as special knitting machines need to be manufactured, and currently these fabrics are seemingly being developed as a protective material for home electronics only [51]. Wire meshes may also require an additional manufacturing process to embed the fabric within the composite [63]. Recent developments have considered using a hot-melt adhesive or resin to pre-impregnate the metal fabric [63,64]. However, designers at Adam Aircraft use a copper mesh as the first ply with the rest of the laminate built upon it and it was found to be suitable [63].

Recent studies have also shown the viability of using metal-coated carbon non-woven material as a possible shielding alternative [62]. This generally is not a favoured approach as it can be costly [62]. Although the results have been promising; damage induced on the shield upon being struck

by lightning appears similar to that of metal-mesh composites [62]. This may likely prove to be more costly in terms of repairing the damaged component when compared with repair costs of metal-mesh composites, although this study has not apparently been undertaken at the time of writing.

## **5.2 Discussion on Previous Composite Electromagnetic Shielding Material Research**

Investigation of previous works was an extremely important step in determining which materials could best satisfy the current requirement. It was known that electrically conductive agents are required in some form to aid electrical conductivity in the final composite laminate. Continuous fabrics are generally required for structural applications, but materials such as glass and aramid fibre contain high electrical resistance and may thus be poor electromagnetic shielding materials. Carbon was desired as it provides high strength, and does contain some electrical conductivity. However, for greater shielding performance, filler materials even in carbon-fibre composites are inevitable. In order to improve electrical conductivity metals, or materials that possess the electrical conductivity of metals, are undeniably required to promote reflection. It was found that inherently electrically conductive composites promote absorption as the dominant shielding mechanism. There was also some concern that introduction of fillers may also result in the degradation of mechanical strength. However, this requires mechanical testing to ascertain whether the reduction is of a satisfactory level to those concerned. As stated before, shielding is not generic, and shielding materials with higher EMSE but lower strengths could be desired for certain applications whilst lower EMSE and higher strengths could be desired for other applications.

## **CHAPTER 6: MATERIAL SELECTION STUDY**

Presently composite materials are used in an array of applications in aircraft. However, one application that composite materials are known to have difficulty contending with, is dissipation of electromagnetic waves and electrical currents. It was found that composite materials that promote electromagnetic shielding and structural support are required in aircraft [5,47]. For structural applications such as this, materials such as continuous reinforcement fabrics are required. Possible continuous materials suitable for structural purposes may be glass fibre, carbon fibre and aramid fibre. Composite materials containing these materials are considered as being “high performance” [65], but composite materials containing the latter two are considered “high-tech” [49]. In order to determine the materials which would best suit both the structural and electromagnetic shielding requirements in this work, an in-depth study on the properties of potentially suitable materials was undertaken.

### **6.1 Fabrics**

#### **6.1.1 Glass Fibre**

Glass fibre tends to dominate the composites market in terms of global composites production, with the approximate percentage being documented at being 90% [66,67]. This is quite possibly due to the combination of comparatively lower cost of the raw material and good mechanical properties associated with glass-fibre composites. However, glass fibre composites generally offer no weight savings opposed to orthodox metals [48]. The cost saving when using these composites is obtained from the lower manufacturing costs [48,68].

The formation of glass fibre is the result of heating glass in a furnace at high temperature ( $>1000^{\circ}\text{C}$ ), and subsequently drawing the molten glass through bushings, which have between 100-200 holes, at high speed [48,69]. This results in between fifty to several thousand glass filaments with diameters ranging from  $5 - 24\mu\text{m}$  being produced [69]. The filaments are then stretched and reduced in diameter [69]. The filaments are then cooled, dried and baked [69]. Textile and “sizing” operations are then performed to obtain the required fabric type i.e. yarn, roving, chopped strands [69].

Although fibrous glass materials possess high strength, stiffness, chemical resistance and low specific gravity, they were originally developed for insulating applications [66]. The various types of glass fibre include A-glass, C-glass, D-glass, S-glass, and the most popular type, E-glass.

A-glass, which is now obsolete, was used for the manufacture of windows. When in production, use of A-glass resulted in a cheap composite that contained good acid resistance [48,70]. C-glass was developed to provide chemical resistance which is absent in E-glass [48,69,71]. D-glass was developed with improved electrical grade for modern radomes, electrical circuit boards and electromagnetic materials [48,69]. This glass contains very low electrical losses, and is thus transparent to electromagnetic waves [48,69]. S-glass, also known as R-glass in Europe and Asia, was developed to contain an improved strength and elastic modulus when compared with E-glass [48]. This glass is specifically required in the aerospace industry, as it meets requirements for fatigue, humidity and temperature resistance [69]. E-glass, which is the glass fibre that is produced on the largest scale, was specifically developed for radome applications [48]. As seen, development of glass fibres was, for the most part, focused on exploiting their excellent dielectric properties. They are known to be transparent to electromagnetic radiation, and are expected to be quite unsuitable for providing any significant electromagnetic shielding.

**Table 6.1: Comparative Study of the Properties found in Various Glass Types (Amended from [ 48,65,66,72,73])**

Property	Units	A	C	D	E	S	R
<b>Composition % of weight</b>	$SiO_2$	72.0	65.0	73.0	55.2	65.0	60.0
	$Al_2O_3$	2.5	4.0	* <sup>a</sup>	14.8	25.0	25.0
	$B_2O_3$	0.5	5.0	23	7.3	-	-
	$MgO$	0.9	3.0	*	3.3	10.0	6.0
	$CaO$	9.0	14.0	*	18.7	-	9.0
	$Na_2O$	12.5	8.5	*	0.3	-	-
	$K_2O$	1.5	-	*	0.2	-	-
	$Fe_2O_3$	0.5	0.5	-	0.3	-	-
	$F_2$	-	-	-	0.3	-	-
<b>Tensile Strength of Virgin Filament</b>	GPa	3.1	3.1	2.5	3.4	4.58	4.4
<b>Young's Modulus</b>	GPa	73	74	55	76-80	80-85	86
<b>Elongation</b>	%	3.6		4.5	3.9	4.6	5.2
<b>Density</b>	$g/cm^3$	-	-	2.14	2.60	2.49	2.53
<b>Dielectric Constant</b>		-	-	3.85	6.11	5.6	6.2
<b>Coefficient of Thermal Expansion</b>	$10^{-6}/^{\circ}C$	-	8	2-3	5	5	4

Note: <sup>a</sup> The sum of the \* = 4 percent

As D-glass is used in radome design, the use of the material for electromagnetic shielding is particularly ineffective. This material is apparently most suitable for use in structures which require penetration of electromagnetic radiation. C-glass seemingly only provides the benefit of chemical resistance, and this was not a consideration in this research. This material does not contain any properties that are beneficial to this work, such as lower electrical resistance, over the cheaper E-glass. S-glass provides improvements in strength when compared with E-glass, but with no improvements regarding stiffness or weight [67,69], and the much higher cost made this material an undesired choice for this work.



It was decided by the author that E-glass fibre should be used as the fabric for preliminary testing. This fabric, due to its comparatively low cost, was selected solely to test repeatability in manufacturing processes, and was not considered seriously as an option for actual electromagnetic shielding design. It was logically considered that the more insulative the structural material is, the more electrically conductive filler material will be required to promote electrical conductivity in the final laminate. The glass fabric purchased in September 2006 was 190g/m unidirectional E-glass from AMT Composites, Durban, SA, at a cost of R44.70/m excl.VAT.

### 6.1.2 Aramid Fibre

Aramid fibres are produced from an aromatic polyamide, poly (p-benzamide) [65]. The para-aramid grade with the highest modulus is of interest for most composites [48]; and use of the most popular para-aramid fibre, which is commonly referred to by its Dupont trade-name, Kevlar, was also considered as an alternative in this work. The two varieties of para-aramid fibre of interest are Kevlar 29 and Kevlar 49. Kevlar 49 has twice the elastic modulus of Kevlar 29, and is available in a special aerospace grade [65].

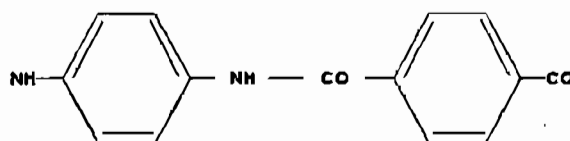


Figure 6.1: Diagram describing the functional structure of para-aramid (re-created from [48])

Table 6.2: Properties of Kevlar 29 and Kevlar 49 (Amended from [67,73,74,75])

Property	Units	Kevlar 29	Kevlar 49
Tensile Strength	GPa	3.45	3.62
Young's Modulus	GPa	58.6	124.0
Density	$\times 10^3 \text{ Kg.m}^{-3}$	1.44	1.44
Coefficient of Thermal Expansion	$10^{-6} / ^\circ \text{K}$	-2 (along axis)	-2 (along axis)
Resistivity <sup>a</sup>	$\Omega. \text{m}$	*	*

Note: <sup>a</sup> \* Data for resistivity was unavailable, but it is documented that volume resistivities for aramid fibres are high, and are retained at elevated temperatures [66].

Like glass fibre, Kevlar does not possess significant electrical conductivity [66]. It will likely prove to be a poor electromagnetic shielding material in a polymer-base. The high cost of Kevlar, despite the lack of advantageous electrical properties, was also a deciding factor in excluding this material from designs in this work.

### **6.1.3 Carbon Fibre**

Carbon fibre was selected as a possible alternative based both on its well-known excellent strength properties and its inherent electrically conductive nature. It is for these reasons military aircraft began to include carbon-fibre epoxies in their designs in the 1970's and 1980's. Extensive tests undertaken on military aircraft, such as the Harrier AV-8B/GR5 in the 1980's, conclusively proved that carbon-fibre epoxy composites provide the inherent electromagnetic shielding capabilities required by fighter aircraft [48]. The results obtained also indicated that this material contained shielding properties similar to that of the orthodox metals that were typically used previously [48]. The table below outlines some of the advantages and disadvantages associated with carbon fibre in aircraft designs.

**Table 6.3: A comparison between the advantages and disadvantages of using carbon fibre in aircraft (circa 1990) [ Amended from 48]**

<b>Advantages</b>	<b>Disadvantages</b>
1. Weight saving over aluminium alloys through high specific stiffness and specific strengths	1. Susceptibility to operational damage and impact
2. Tailored directional mechanical properties	2. Restricted environmental stability in terms of temperature and moisture absorbency
3. Reduced part counter over metallic equivalents	3. Excessive localised damage through lightning strikes
4. Modified radar response compared to metals	4. Uncertainties on repair techniques
5. Non-corroding in salt environments	5. Cost
6. Excellent fatigue resistance	
7. Dimensional stability	

Table 6.3 provides some insight into the benefits and limitations of carbon fibre. However, development over the last decade has resulted in improvements in some limitations such as cost reduction and new repair techniques [28,56].

Other designs include dielectrically shielded carbon fibre composites as skin panels, with aluminium trailing edges, such as the DC 10 Airliner [48]. This particular design reduced the metal content on the aircraft, but seemingly still utilised the aluminium as the electrically conductive channel, and the composite as merely a means for structural support. The Beechcraft Starship, which is widely regarded as being the world's first all-composite production aircraft, utilised carbon fibre in its airframe [48,76]. The studies performed on this aircraft displayed that carbon fibre epoxy is approximately one thousand times more electrically resistive than aluminium [76]. Despite this electrical resistance sufficing the electromagnetic shielding requirement, the electrical resistance required to adequately provide a channel for lightning current flow was found to be less than  $1\Omega$  [77]. It was considered unlikely that carbon fibre polymer composites can, on its own, provide this resistance, and suitable electrically conductive filler materials on regions prone to lightning strike were deemed necessary.

Carbon fibre does, however, possess the inherent conductive properties required for masking black boxes, and scattering radar signals at radar frequencies, and this was confirmed in tests performed on the Seeker II aircraft in SA [77].

Carbon fibre composites are now described as being the most significant of the various fibre composites in the current aerospace industry, with E-glass and aramid composites typically serving secondary roles [48]. While it is possible to produce carbon fibre from a variety of materials such as hydro-carbon gases and rayon, carbon fibre is commercially derived from one of two precursor materials – polyacrylonitrile (PAN) and pitch (from coal or oil) [48,66].

#### 6.1.3.1 Pan-based Carbon Fibre

The raw material of PAN is acrylonitrile (AN), which is a monomer used in the production of materials such as synthetic rubber and acrylonitrile butadiene styrene (ABS) resin [48,73,78]. In the first stage of PAN production, the AN undergoes a polymerisation process with a co-monomer and is spun under clean conditions [48,73,78]. The PAN precursor is then dissolved in a solvent to form a dope [48,73,78]. The material is then pumped through a spinnerette within a

coagulating bath which serves to remove the solvent, leaving behind solid PAN filaments [48]. This stage is also referred to as the “white fibre process”, denoting the colour of the fibre left behind [74]. The PAN polymer then undergoes an oxidation process [78,79]. This process is carried out between 200° C- 300° C [48,73,78,79]. This is then followed by carbonisation in nitrogen inert gas atmosphere between 1000° C- 1500° C and under longitudinal tension [48,73,78,79]. Increased heating in the 3000° C range in this stage, referred to as graphitisation, results in a higher fibre modulus [48,73,78,79]. The material then undergoes a surface treatment and “sizing”, and is subsequently wound into spools [48,78,79].

### 6.1.3.2 Pitch-based Carbon Fibre

The first stage in the production of pitch-based carbon fibre is the refining of oil or coal pitch for spinning [48,79]. The material then undergoes a molten spinning process to form pitch fibre [48,79]. The pitch fibre is then passed through air between 200° C- 300° C, followed by a carbonisation process as with PAN-based carbon fibre [79]. Increased heating will result in higher performance fibres [66]. It was first assumed that manufacturing carbon fibre using the by-product material from oil or coal would prove to be a cheaper alternative to the PAN-based variety [48]. However, cleaning and converting the pitch into a usable form in fact offset the cost of the raw material, such that the cost of the two fibre types is comparable [48]. The advantage of pitch-based carbon fibre is that it can display higher electrical conductivity and a higher elastic modulus [48,79]. However, pitch-based carbon fibre is considered as being structurally weaker than the PAN-based variety, and is not typically used when strength is a criterion [48,79].

**Table 6.4: Comparison of Various Properties found in Carbon Fibre [Amended from 48,78]**

Property	Units	PAN HTS	PAN HM	Pitch (Type P)	Pitch UHM
Young's modulus	GPa	210-230	380	340	690
Tensile strength	GPa	2.34	2.21	1.38	2.41
Density	$\times 10^3 \text{ Kg/m}^3$	1.74	1.86	1.99	2.05
Resistivity <sup>a</sup>	$\mu\Omega \cdot \text{m}$	18	10	7.5	2.5
Coefficient of Thermal Expansion	$10^{-6}/^\circ \text{C}$	-1.1	-1.1	-1.1	-1.1

Note: <sup>a</sup> These values of resistivity are approximated

Carbon fibre composites can provide a variety of advantages over glass-fibre composites and metals. Such advantages include possible weight savings over both glass fibre composites and metal with regards to high specific stiffness and specific strength; dimensional stability; and fatigue resistance [48]. There are disadvantages associated with carbon-fibre composites as well though. These include excessive damage due to lightning strike; susceptibility to operational damage and impact and uncertainties on repair techniques in some cases [48]. The most significant disadvantage in this work was that carbon-fibre composites cannot display the magnitude of electrical conductivity found in metals, without possibly including filler materials to enhance electrical conductivity.

However, carbon fibre did display many properties that were desired in this work; certainly more so than the other continuous reinforcement materials that were reviewed. Carbon fibre was therefore selected as being a possible material for the electromagnetic shielding composite material.

There were no specifics available to determine whether the carbon fibre available from AMT Composites, Durban, SA, was pitch-based or PAN-based; and whether their carbon was high strength, high modulus, etc. For this reason, three varieties of carbon fibre fabric were obtained viz. 400g/m  $\pm 45^\circ$  stitched cloth; 12K epoxy-fixed woven cloth; and 300g/m unidirectional cloth. It was thought that it be best if the properties possessed by these materials were obtained through testing.

The cost of these materials, as of September 2006, was: R230.00/m<sup>2</sup> for 12K woven carbon fabric; R244.00/m<sup>2</sup> for 400g/m  $\pm 45^\circ$  stitched carbon fabric; and R156/m for 300g/m unidirectional carbon fabric (All of these prices excluded VAT).

It was found that there are currently restrictions on carbon fibre procurement globally [80]. This was due to restrictions placed by Airbus and Boeing for their aircraft [80]. However, the use of these materials was necessary, and they were still quite affordable for this work as well.

## 6.2 Resins

The promising results that carbon-matrix materials provide were initially investigated, with the intention of possibly utilising the material in the electromagnetic shielding designs. However, it was soon found that carbon matrix materials could not be easily fabricated in SA [56]. Electrically conductive resins, manufactured by companies like Boyce Components LLC, were briefly considered, but rejected due to high cost and poor strength properties possessed by these materials [81], and readily available polymer-based matrix materials were investigated.

Thus “resin”, in the case of this research, is the term used to denote the polymer material which will serve as the composite matrix. There are many types of polymer resins, such as polyester, bismaleimide, polyamide and epoxy, each possessing unique inherent physical, mechanical and electrical properties [65]. The chemical composition of the resin determines the exact properties that it will possess [65]. The resin, or matrix material, will serve to protect the fibres, transfer the stress, enhance transverse properties and improve fracture and impact performance [65].

When fibre composites were first investigated for incorporation in aircraft in the 1930's, E-glass was considered as the structural agent, whilst polyester resin was considered as the matrix material [48]. The development of superior epoxy resins in the 1940's saw polyester resins being superseded by epoxies for most structural applications [48]. Polyester resins are not certified aircraft-grade by today's standards, and focus was thus placed on epoxy resin in this work [56].

Epoxy-based resins are the predominant resins for use with carbon fibre and high performance applications, due to their mechanical properties, low shrinkage, adhesion and environmental stability [66]. All epoxies contain two carbon atoms and one oxygen atom in the arrangement shown in Figure 6.2.

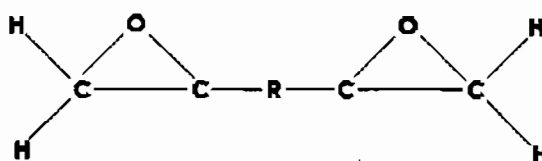


Figure 6.2: Functional unit of epoxy resin [re-created from 82]

Epoxyes are also noted as being the most widely used of the different matrix varieties and accounted for more than two thirds of the aerospace market in 1990 [48,66]. However, epoxyes are also noted for being used in the electronics industry, likely due, amongst other reasons, to its insulative properties [66].

The chemistry behind epoxyes will not be explained in this work, but it was noted that different epoxyes can contain diverse properties [65]. Through experience it was found that most epoxyes are generally applied in similar fashion to reinforcement fabrics when building composite materials. Prior to applying resin to the fabric, it is necessary to engage the use of a hardener to promote adhesion of the reinforcement fibre to the matrix [48]. There is usually a pre-determined ratio between resin and hardener that should be adopted when mixing these chemicals together. It was found by the author previously that failure to include hardener, or failure to include the recommended amount of hardener, will result in resin remaining viscous indefinitely. It may also become necessary to use an accelerator, or subsequently heat the constituents in order to promote gelling of the resin [66]. The appropriate use of the mentioned coupling agents, and post-curing processes, are apparent in the laminated material's final properties [66].

**Table 6.5: Thermal and Electrical Properties of Epoxy Resins (Amended from [66])**

	Units	Rigid, Unfilled	Rigid, Filled	Flexible, Unfilled	Flexible, Filled
<b>Coefficient of Thermal Expansion</b>	$10^{-6}/^{\circ}\text{C}$	55	30	100	70
<b>Dielectric Constant</b>		4.2	4.7	3.9	4.1
<b>Dielectric Strength</b>	$\times 10^6 \text{ V/m}$	17.7	17.7	13.8	14.2
<b>Arc Resistance</b>	s	85	150	120	130

A disadvantage of epoxyes includes epoxy's tendency to absorb moisture from their surroundings, and this can reduce strength and stiffness of the laminated material [48]. Also, the performance of epoxy matrix systems begins to rapidly deteriorate at elevated temperatures ( $T > 140^{\circ}\text{C}$ ) [48]. If structures are required to perform above this temperature, other matrix systems, such as a carbon matrix which is typically used in aerospace applications, may become necessary [47,48].

Research undertaken by Luo and Chung [47], however, displayed interesting results regarding the contribution of EMSE matrix materials provide to continuous carbon fibre. Lou and Chung [47] stated that carbon matrix materials theoretically enhance EMSE by an insignificant amount when compared with polymer matrix materials.

For this work, two epoxies were selected to the satisfaction of those concerned viz. LR20 epoxy resin (for use with LH281 hardener) and Prime 27 epoxy resin (for use with Prime 20 “slow” hardener). These items were purchased from AMT Composites, Durban, SA, during August 2006 for R66.00/kg (R110.00/kg for hardener) and R68.00/kg (R122.00/kg for hardener) respectively in August 2006. All of these prices excluded VAT. The properties of LR20 can be seen in Table 6.6 and the properties of Prime 27 can be seen in Table 6.7:

**Table 6.6: Selected Properties of LR20/LH281 Matrix Material |Amended from 82|**

<b>Heat Distortion Temperature (° C)</b>	70
<b>Final Hardness (MPa)</b>	85±3
<b>Compressive Strength (MPa)</b>	100±5
<b>Tensile Strength (MPa)</b>	53±5
<b>Flexural Strength (MPa)</b>	110±5
<b>Elongation at Break (%)</b>	3.3
<b>Demould Time at Room Temperature (hrs)</b>	24-38
<b>Time to Harden at Room Temperature (days)</b>	7
<b>Post-curing time at 65° C (hrs)</b>	16
<b>Viscosity at 25° C (mPa.s)</b>	800-1100
<b>Hardener viscosity at 25° C (mPa.s)</b>	650

**Table 6.7: Selected Properties of Prime 27/Prime 20 “Slow” Matrix Material |Amended from 83|**

<b>Heat Distortion Temperature (° C)</b>	70
<b>Barcol Hardness</b>	28
<b>Elastic Modulus (GPa)</b>	3.471±5
<b>Tensile Strength (MPa)</b>	73.3
<b>Elongation at Break (%)</b>	4.5
<b>Demould Time at Room Temperature (hrs)</b>	13.15
<b>Time to Harden at Room Temperature (days)</b>	7
<b>Post-curing time at 65° C (hrs)</b>	7
<b>Viscosity at 25° C (mPa.s)</b>	480-510
<b>Hardener viscosity at 25° C (mPa.s)</b>	160



### **6.3 Filler Materials**

It was established that continuous carbon materials could suffice for the application of electromagnetic shielding. However, to enhance shielding, other filler materials with superior electrical conductivity to that of carbon were investigated with the intention of yielding higher EMSE than that possessed by carbon-fibre epoxy composites without fillers.

The aim of this work was not to ascertain the exact percolation threshold (percolation threshold is characterised by the sharp drop of several orders of magnitude in electrical resistivity upon addition of fillers [60]) of fillers in matrix materials, but rather to determine whether a trend between electrical and mechanical properties was evident as filler content varied.

#### **6.3.1 Carbon Black**

Carbon black consists of tiny spheroids of carbon typically in the order of 20-50 nm in size, and is produced by the burning of carbonaceous materials [84,85]. It is therefore inexpensive and is widely used in applications that require tensile strength, stiffness, wear resistance and toughness [84,85].

Most notably, carbon black is used in the automotive industry for use in vehicle tires, but recent years have seen its use in more diverse applications [6, 59]. Such applications include EMI and ESD protective structures, and radar-absorptive materials [6,59 ].

However, when exploiting the properties carbon black can provide, trade-offs in other material properties were found to be evident [86]. When maximising the electrical conductivity of materials, significant reductions in flexural modulus and impact strength were seen [84]. This already indicates carbon black-filled composites will not satisfy the strength requirement of this work.

Properties of carbon black have been manipulated such that very high conductivity was achieved, but again, this resulted in low strength and stiffness [86]. Carbon black in glass-fibre epoxy composites (7% wt (0.6mm thickness) and 5% wt (1.9mm thickness)) has displayed good radar absorptive properties [59]. This suggests that laminates of this type will be unsuitable for

significant electrical conduction or electromagnetic protection, as reflection is not the primary shielding mechanism, which was desired.

As there were significant disadvantages regarding both shielding and strength properties, carbon black was rejected as a possible filler material in this work.

### **6.3.2 Nanotubes**

Since the discovery of fullerene fibres (nanotubes) in the 1980's, a widespread interest in the properties the materials possess has been generated [85]. They are 30-100 times stronger than steels, but weigh less than 20% of steels' mass [84]. Since their discovery, researchers have been exploiting the excellent strength, thermal, electrical and magnetic properties found in nanotubes, and new materials using nanotubes are in constant development [87]. This is seen by the high number of U.S patents for materials using nanotubes filed in the last decade [87-92].

In recent years, the term "nanotubes" is used interchangeably with "carbon nanotubes", as these are the type that excite the most interest and have arguably the most potential from a commercial point of view [85,93]. Nanotubes come in various types, notably single-walled nanotubes (SWNTs) and multi-walled nanotubes (MWNTs).

SWNTs are typically 1-2 nm in diameter and are single molecules. MWNTs are formed out a collection of SWNTs, in which weak Van der Waals forces hold the tubes together resembling a "Russian doll" structure [87,93]. MWNTs are significantly easier to produce, and are consequently cheaper to purchase [87,93].

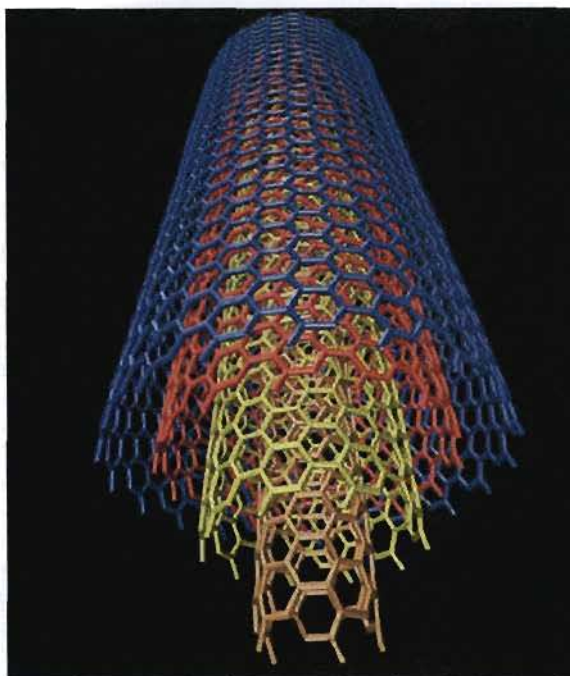


*Figure 6.3: A representation of a MWNT [93]. As clearly seen, the structure consists of many SWNTs.*

Nanotubes are many thousands of times longer than their diameter, meaning they have a very high aspect ratio [85]. The high aspect ratio of nanotubes means that they can impart the same electrical conductivity at a lower loading than other fillers such as carbon black and chopped carbon fibre, and the composite laminate containing this filler will likely be extremely strong [87,93]. The high aspect ratio also indicates that fewer flaws are present in the laminate [84].

Nanotubes are sharp and thin in physical structure, and their appearance resembles a lightning rod [94]. The electrical conductivity of the nanotube is proportional to its chirality (degree of twist), and it has been found that nanotubes have a resistivity less than that of metals [85,94]. This determines whether the nanotube behaves like a metal (conductor) or a semi-conductor. Summarizing, the physical and mechanical properties of the nanotube are determined by the chirality and aspect ratio.

Industry prices of nanotubes are dependant on the level of purity of the nanotube and range from being 40% pure to >95% pure, which is the most expensive type [94-96]. Current (2006) prices range from US\$2.00/g for MWNTs (>50nm diameter, 50  $\mu$ m long); to US\$2000.00/g for super purified SWNTs [96]. Also available are special grade nanotubes, which are designed for the specific purpose of EMI shielding [96].

Researchers have found that using nanotubes instead of carbon fibres as filler materials have resulted in up to 90% reduction in loading [84]. However, the limited supply and high cost of nanotubes prevent the integration of nanotubes into current designs. Due to the high cost of nanotubes, much of the development has seemingly been restricted to research only. Mass production and commercialisation of nanotubes has not been achieved as yet. This is expected to change drastically by 2010 as depicted by the qualitative illustration in Figure 6.4.

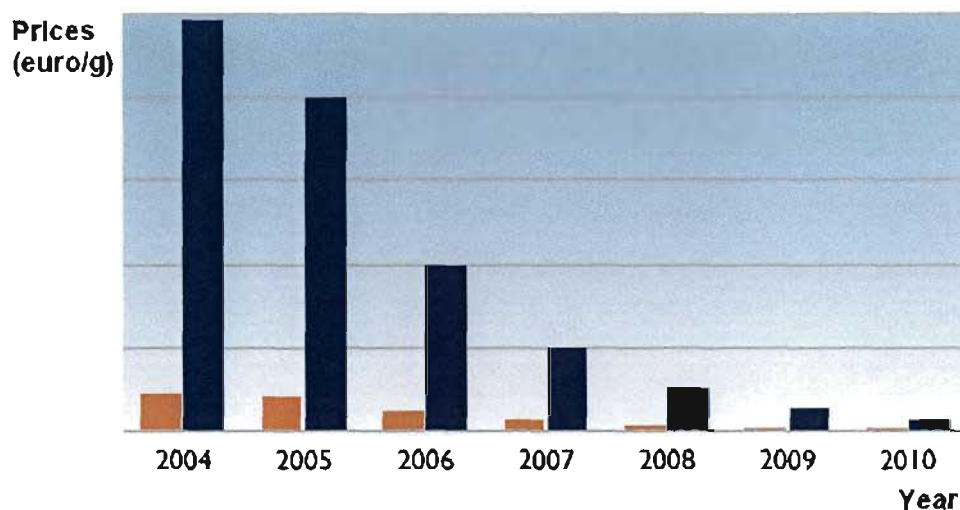


**Figure 6.4:** The qualitative projected decrease in price of nanotubes by 2010. Cost of the material is expected to be inversely proportional to production in coming years (Amended from [97]) – The orange bars represent price in Pound Sterling/g for the same product.

With the drastic cost reduction coupled with the production increase, it appears that long term possibilities using nanotubes are very promising. It was hoped that nanotubes could be purchased for use in the electromagnetic shielding materials in this research. However, consultation with international suppliers indicated that suitable grade products are at least \$500/g, and the products could not be readily exported to SA as of August 2006 [98]. It was not within the current project budget to obtain this material for test specimens, and was therefore not considered further. However, if the cost reduction follows the predicted trend, integration of suitable nanotubes in aerospace electromagnetic shielding materials may very well become a likely possibility in future years.

### **6.3.3 Vapour Grown Carbon Fibre**

Vapour-grown carbon fibres (VGCF) are filler materials that are similar to MWNTs, but are much larger, and have aspect ratios in the 100-500 range [87]. However, VGCF is much cheaper and readily available, making them an attractive option [87]. However, the disadvantage is that there are larger microstructural defects present compared with carbon nanotubes. Research has been undertaken on this filler material in recent years to determine its properties, and also to build a knowledge base that may be transferable to nanotubes [11,87].

It was found that VGCFs possess excellent strength, electrical and thermal properties. Yang *et al.* have found that VGCFs in a liquid crystal polymer (LCP) matrix display 41dB of EMSE [11]. However, these results were obtained at a frequency of 15 MHz and using 15 wt% of VGCF. Yang *et al.* also determined the percolation threshold of VGCF in the LCP matrix is 5 wt%. At this point, the resistivity dropped 11 orders of magnitude [11]. The bulk resistivity of the 15 wt% sample was the lowest, at 7  $\Omega \cdot \text{cm}$  [11].

Studies performed by Xu *et al.* [99] using vinyl ester composites displayed percolation behaviour, but at a lower loading of 2 – 3 wt%. Although the samples still contained a high resistivity, it was noted that the addition of VGCF resulted in a resistivity drop from the order of  $10^{10}$  to  $10^2$  in their work [99]. Also of interest is the unusual occurrence of two percolation threshold points for that particular sample [99] - (from previous experience, materials display one percolation threshold value). This displays the excellent electrically conductive properties found in VGCF. The relatively high resistivity value even after the second percolation threshold is possibly a result of the vinyl ester matrix, which is well-known to be insulating. It is assumed that a composite material with suitable conductivity could be obtained if matrix materials that contain lower electrical resistances are used.

Due to the expected lower cost when compared with nanotubes, and its excellent properties, it was hoped that similar experiments could be undertaken in this work. However, as of August 2006, VGCF was commercially available from one supplier in the USA [100,101]. It was found that this material is not readily exported to SA as well [101]. Research with VGCF therefore had to be rejected as a possibility in this work.

### **6.3.4 Metal Filler Materials**

#### **6.3.4.1 Metal Powders**

Due to some metals being intrinsically excellent electrical conductors, as well as possessing excellent strength properties, the use of metals in applications such as electromagnetic shielding is justly expected. Material availability and the isotropic nature of metals also present benefits absent in some other fillers.

It is known that metal fillers can be used with composites to form excellent shielding materials [5]. Chung [5] states that metal particles are more desirable as opposed to carbon as filler materials, due to their higher conductivity of metals. However, the disadvantages of metals as fillers are poor oxidation resistance and thermal instability [5]. Metal particles are also larger in size than carbon particles, and generally are not smaller than  $2\mu\text{m}$  when obtained by forming or casting [5]. With this in mind, it was suspected that even use of metal particles could possibly lead to significant weight increases depending on the amount used.

Chung has found that submicron metal particles can be attained by electroplating submicron carbon particles [5]. Such particles can be attained by electroplating carbon particles with a diameter of  $0.1\mu\text{m}$  with nickel to result in  $0.4\mu\text{m}$  diameter nickel filaments. Nickel was selected based on the fact that it is less susceptible to oxidation damage. The use of 7% by volume of these filaments with a polymer matrix composite resulted in 87 dB EMSE at a frequency of 1 GHz [5]. This shielding performance is far superior to that displayed by the same volume of carbon filaments in the same matrix [5].

Metals that are noted for excellent electrical conductivity are silver, gold, copper and aluminium. Silver and gold are two of the most electrically conductive metals, but seemingly cost, strength and relatively high density of the materials are prohibiting factors for implementing them into practical industry design. Copper is known to be susceptible to oxidation damage, but it was thought that the high electrical conductivity and lower cost could result in desirable shielding materials. As mentioned earlier, designers at Adam Aircraft [63] utilise copper in their lightning and electromagnetic protection structures, and have not reported any problems with this practice. Aluminium metal was traditionally used in aircraft for lightning protection, due to its high

electrical conductivity; strength; and light-weight, and is long understood as being an excellent electromagnetic shielding agent in practice.

Copper and aluminium powders were selected as the filler materials in this work due to their apparent excellent electrical conductivity and low weight. As fillers are typically introduced into the matrix material by percentage weight, materials with lower weight will be more beneficial as there will be more particles for the same volume than heavier materials. This fact will likely be more beneficial to EMSE in a general sense as it is enhanced by connectivity of the particles, and the likelihood of achieving connectivity is greater when more particles are present.

The copper and aluminium powders were obtained during August 2006 from AMT Composites in Durban, SA, at a cost of R63.00/kg and R44.00/kg respectively (These prices excluded VAT).

#### 6.3.4.2 Metal Meshes

Metal meshes have long been used to provide electrical conductivity in traditionally non-conductive materials [62,102]. In aircraft such as the Boeing 787 meshes are used to provide a constant electrically conductive channel for shielding [24]. In recent years, researchers have been trying to find methods of obtaining conductive fabrics by knitting metal wires into glass fabrics.

Cheng *et al.* have developed a feasible method of fabricating conductive knitted fabrics [7]. This was done by knitting copper wires and glass fibres using the uncommingled yarn technique. The results, as expected, showed that electrical conductivity of this fabric varied with copper content [7]. That is, a better EMSE was obtained as the amount of copper increased.

Chen *et al.* have developed a method of fabricating hybrid conductive fabrics using stainless steel and copper wires [52]. The reinforcement material used was polyamide filaments, and the matrix material was polypropylene. Again, the results show that EMSE is dependant on the metal content in the fabric [52].

Cheng *et al.* [9,51], have also successfully developed a hybrid fabric by knitting stainless steel and copper wires with carbon fibre using the uncommingled yarn technique. Their previous experiments used glass fibre, which is typically insulative and is not preferred for some structural applications. The improvement in this fabric seemingly comes from the use a carbon fibre, which

has excellent electrical conductivity and strength properties. However, their results indicate that the fabric is suitable for shielding home electronic equipment, and it was found that absorption dominant shielding characteristics are sought in that industry. This fabric may likely not suffice the shielding of aircraft electronics/avionics.

The results that these researchers have found agree on the fact that EMSE is directly proportional to the amount of conductive material used in the hybrid fabrics. The metal content can be quite substantial, however, with the optimal shielding point requiring over 50% of wire in some fabrics [51].

For this work, it was unfeasible to manufacture special equipment for the fabrication of metal fabrics. Hybrid fabrics were thus also discounted as a possibility, especially as these fabrics are evidenced to promote absorption-dominant electromagnetic shielding characteristics [51]. Metal coatings on fibre composites was also rejected, as these materials display the advantageous properties found in cheaper mesh-composites, and there are still many uncertainties regarding repair techniques in these coated-materials [62]. At this stage it appears that it is more costly to repair these electro-plated composites than it will be to repair mesh composites, in the event of damage.

Pre-manufactured metal fabrics were found to be available from AMT Composites, Durban, SA. The material found to best suit this project requirement was "Alumesh 401". The material is specifically suitable for use on external aircraft surfaces, and was purchased at a cost of R920.00/kg in September 2006. The material was also the lightest in weight ( $90\text{g/m}^2$ ) of the metal fabrics available, despite having one of the largest thicknesses [102]. The product data sheet [102] included some interesting properties regarding the current-carrying capacity for unit cross-section and weight of various metals relative to carbon, and these can be seen in Figure 6.5 on page 58.



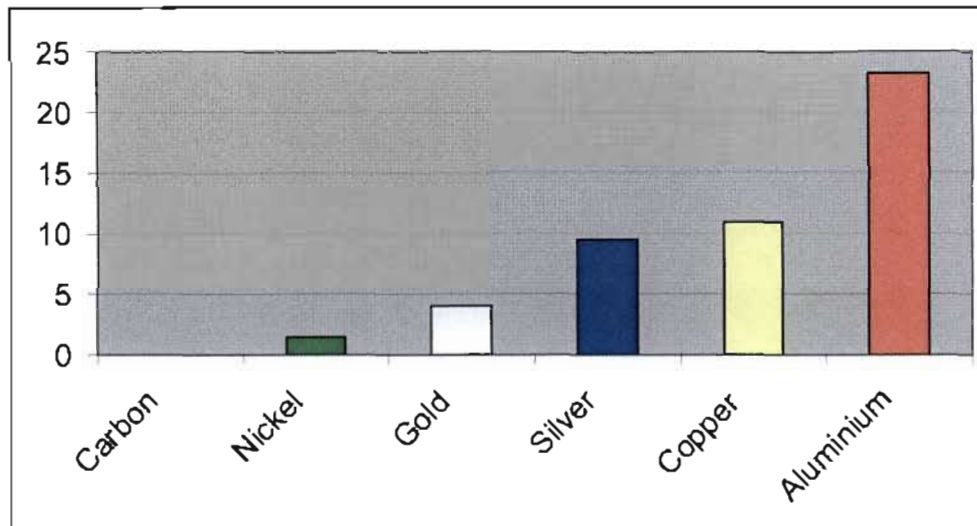


*Figure 6.5: The illustration, depicting the current-carrying capacity of various metals for unit cross-section and weight (units not provided), indicates the superiority of aluminium relative to the other materials in weight sensitive applications (Recreated from [102])*

### **6.3.5 Discussion on Filler Materials**

Various materials that could serve to increase electrical conductivity and enhance EMSE have been presented. However, there was difficulty, both in terms of project budget and import laws, in obtaining all of the materials that were originally desired for this work. In the early stages of carbon fibre development, prices were comparatively high [28], and upon significant cost reduction, carbon fibre composites have been used in increasing amounts in aircraft. This work is an indicative example of that.

For the time being, metal materials that provide excellent electrical conductivity and shielding were selected as being very suitable for the project requirements. A brief comparative study against the acceptable grade of nanotubes was undertaken, and it was found that nanotubes costs approximately R3250.00/g (using a conservative exchange rate of US\$1.00=R6.50, and excluding potential import duties), while copper powder costs approximately R0.06/g and aluminium powder costs approximately R0.04/g. Clearly, in terms of the size of a typical aircraft, it may very well be unlikely that costly materials such as nanotubes see development into practical design at least until costs significantly drop. In future years, should the predicted production rate increase and prices significantly decrease, the same developments that took place in aircraft with carbon fibre may likely occur with nanotubes as well. At this time, however, it was beyond the reach of

this work to seriously engage in researching a material which will unlikely see practical development in the near future.

**PART C: Determination of Appropriate Manufacturing  
Methods and Test Methods for the Shielding Materials**

## **CHAPTER 7: MANUFACTURING PROCESSES**

There is a variety of processes that are available for the manufacture of composite materials, ranging from the basic hand lay-up, to more complex processes such as the vacuum-assisted resin infusion process, resin transfer moulding, pultrusion and filament winding. The electromagnetic shielding material which will be constructed will primarily consist of flat shapes, and investigation of complex moulds and dies was not the focus in this work. For the purposes of this project, convenient fabrication methods, which could be implemented at University of KwaZulu-Natal (UKZN), had to be adopted. The preferable approaches that were identified for this purpose are hand lay-up and the vacuum-assisted resin infusion process.

### **7.1 Hand Lay-up Process**

The hand lay-up process is considered as being the oldest and simplest method of fabricating fibrous composites [65]. In this process, the fibre fabric cloth is laid upon, or within, a mould surface, and resin is introduced into the system via brushes or similar application tools. Layers of fabric are laid upon each other to provide the required composite material thickness. Depending on the type of resin used, different curing processes may be engaged to prepare the final composite laminate.

The advantages of this process are low cost and variable product size [65]. The disadvantages are possible emissions from resins which may cause health and safety concerns when working with epoxies, labour-intensive manufacture and possible poor product quality [65]. As resin is manually applied to the fabric, and the system is thus exposed to the atmosphere during manufacture, the process is referred to as being an “open-mould” process [65].

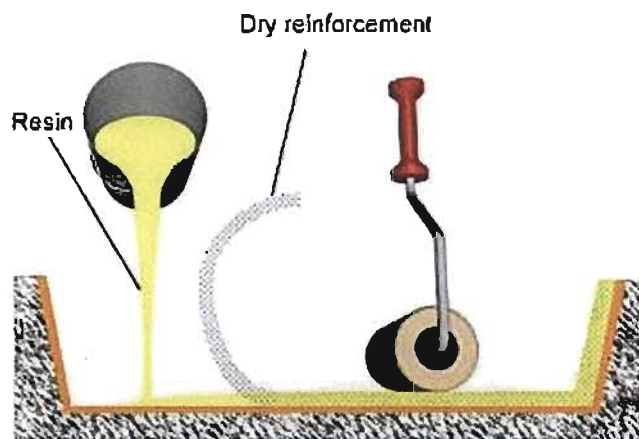


**Figure 7.1:** A diagram describing a typical hand lay-up system (Amended from [103])

However, the process may be the most viable method for the small batch production ( $< 10$  units) of laminated materials, especially when there is a possibility, as was the case in this research, that high-viscosity resins (resins including filler materials) may be required. In such an event, precautions will have to be implemented prior to fabrication to ensure the disadvantages associated with this manufacturing process are kept to a minimum. It is quite apparent that one has to ensure that the brushes or other application tools are free of contaminants when introducing resin into the system, as this could serve to degrade mechanical properties of the laminate.

Fabrications in which the materials are left to cure in the presence of the surrounding atmosphere are not favoured for the production of high-performance composite materials [65]. In many cases the wet composite materials are enclosed within a plastic bag and vacuum pressure is introduced in the enclosed system. Typically a layer of porous bleeder cloth material is placed upon the just-wet fabric; and a layer of breather cloth is placed over this. The purpose of the bleeder cloth is to allow excess resin to absorb through its fine holes; and the purpose of the breather cloth is to absorb this resin. This could result in laminates with better fibre-to-resin ratios, as the laminates will no longer be as resin-rich. This method is typically used when high-performance laminates are required [65]. The post-curing processes for composites fabricated by hand lay-up will be dependant on the type of resin used in their manufacture.

It was found by the author that it is best to ensure that there are no air bubbles between the breather cloth and wet-composite prior to introducing vacuum pressure, as the imprint of the

bubbles will reflect on the final laminate. Apart from being aesthetically displeasing, these surface defects could also degrade strength properties of the final laminate.

It was found that the shielding materials will be manufactured in small quantities (<5 units/annum), and hand lay-up manufacture with vacuum-bagging will thus be a very suitable process that will adequately suffice the application in industry.

## **7.2 Vacuum-Assisted Resin Infusion Process**

The vacuum-assisted resin infusion process is a manufacturing process in which resin is drawn into a system under the influence of vacuum pressure. The materials are laid dry upon the mould and tubing that serves as inlet and outlet channels are placed alongside these materials. The inlet tube is a means for resin to enter the system and the outlet tube is a means for excess resin to exit the system. The system is enclosed within a plastic bag and vacuum pressure is introduced. Resin is then fed into the system and embeds the material.

The process relies on the presence of a rigid lower mould, and a flexible upper mould which is sealed to the rigid mould by means of double sided tape, commonly referred to as “tacky tape”. The vacuum infusion process is described as being a “closed-mould” system, as the contents of the system are not exposed to the atmosphere during manufacture [65,104].



*Figure 7.2: Vacuum-assisted resin infusion process*

Within the system, additional spiral tubing may be included to aid the flow of resin to ensure a wet-out of the entire composite. Non-stick material such as “peel-ply” is used to ensure the laminate can be removed with ease upon curing. A layer of fabric that aids the flow of resin along

the system is required to ensure resin embeds the entire system. It was found by the author previously that resin flow may be hindered if there is inadequate material to aid resin flow.

Should a flow medium, such as shade cloth, be absent, there is a possibility that resin may not embed the entire contents of the system. This is particularly the case when dealing with long laminates. Bleeder fabric may also be required to absorb excess resin between the laminate and release film [65]. The remaining excess resin is exited through the outlet pipe and flows into a device referred to as a resin trap. The resin trap is essential in order to prevent exiting resin from entering the vacuum pump. Upon introducing resin into the system, and ensuring adequate coverage of the fabric, the laminate is ready for curing. Curing processes are again dependant on the type of resin used.

There are many advantages in using this process; namely lower tool costs when compared with other closed mould systems since an upper mould is not required, ideal for short production runs; improved fibre-to-resin ratio as excess resin is drawn out of the system; lower content of emissions in the working environment due to the closed mould nature of the process; and sufficient time to prepare materials as they are laid dry.

The disadvantages of the process can be quite significant as well. Due to the relatively complex nature of the process, there is a margin for error during fabrication [65]. The system has to be set in accordance with specific fabric configurations, and incorrect placement of tubing or other flow mediums could lead to damage of equipment.

The vacuum-assisted resin infusion process is also favoured in the small-batch production. However, the process is evidently more costly than hand lay-up fabrication as more raw materials are required when building composite laminates. Both processes were used to prepare the test samples in this research and the results are documented in Chapter 9.

## **CHAPTER 8: APPROPRIATE TEST METHODS**

A specific application was not defined for the composite electromagnetic shielding materials in this work. Rather, these shielding materials may be used in an array of aircraft applications when required. It will likely depend on the strength and shielding capabilities that particular shielding materials display that will determine their ultimate purpose. It has been stated that shielding materials are not usually designed generically, and this work is no different. However, the quality of shielding that particular regions of different aircraft require is unknown at this stage.

For the purpose of this work, it was best assumed that the same shield material could theoretically be in fact used for the housing of on-board avionics and also be used to provide shielding on the wing skins, should the relevant criteria be met by the shielding material. This had to be taken into consideration when developing appropriate test methods for the materials that were the focal point of this research.

It was determined through the primary customer that mechanical and EMSE testing was of predominant importance in this work. These included tensile testing, compressive testing, and flexural testing to determine the mechanical properties; and EMSE and electrical resistance testing to determine the electrical properties. It was decided that materials between 2-3mm in thickness are required for electromagnetic shielding, and therefore this was the specimen size that tests methods were identified for.

### **8.1 Mechanical Testing**

As the specific implementation of the shielding material was unknown, inspection of the mechanical properties can hopefully aid interested persons in selecting an appropriate application that optimises the materials' mechanical properties. Tensile and flexural testing were identified as being of most significance in this work, but compressive testing was investigated as well.

#### **8.1.1 Tensile Testing**

Uniaxial tensile testing is the most widespread and most studied mechanical test for fibrous composite materials [105]. The test method is preferred because of its simplicity to perform and due to the ease of interpreting the results obtained from the test itself [105]. The data that was



deemed essential for this research that is provided by tensile testing includes tensile stress, tensile strain, and tensile yield point.

Despite the simplicity of the test, there are some problems associated with tensile tests [105]. Such problems include establishing a uniform state of stress over the entire gauge length [105]; the mathematical system used to compute the results does not always correspond to the failure mode that has taken place [105]; and it has been found by the author that specimens could slide in the gripped surfaces when the test is underway. In order to develop a reliable means of comparison, each sample must be prepared, treated and handled in exactly the same way [106,107].

There are many standardised test methods for tensile testing that are available and are accepted internationally, but the two methods that were favoured by the author are described in ASTM D 638-02 [106] and ASTM D 3039M-00 [107]. The test procedure outlined in both methods is alike, but the specimen geometry differs.

In ASTM 638-02a [106] the composite specimen should either be prepared as-laminated in the desired geometry or prepared in the desired geometry by machining operations from laminated sheet material. The specimen, encompassed in the classification “reinforced composites” in [106], should be less than 7mm in thickness and should generally conform to the “dumbbell-shape” geometry described in Figure 8.1 below:

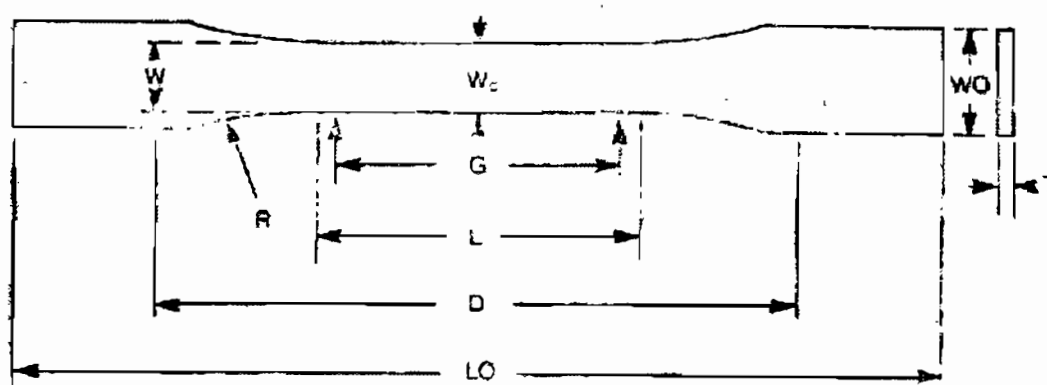


*Figure 8.1: Tensile specimen as described in ASTM 638-02a [106]*

**Table 8.1: List of Variables in Figure 8.1 [Amended from 106]**

<b>Description</b>	<b>Dimension (mm)</b>
Width – Width of narrow section	13
L- Length of narrow section	57
WO – Width overall	19
LO – Length overall	165
G – Gauge length	50
D – Distance between grips	115
R –Radius of fillet	76

In ASTM 3039M-00 [107] the specimen is recommended to be prepared in the “dumbbell” shape by means of tabbed surfaces that are bonded to a rectangular sample. Tabs are not required, but are recommended for their preparation, especially for highly unidirectional laminates [107]. The lack of tabs on the specimens may lead to damage of the sample when in the gripped surfaces, and may result in erroneous results being obtained. The method of fabricating specimens outlined in ASTM 3039M-00 has been found by the author in previous work to be more time consuming as it requires additional machining operations if one correctly prepares the tabbed surfaces. The tabbed surfaces are typically glass fibre, steel, or the same material as that being tested [107]. It was suggested that it is best to use the same material as that being tested, as the elastic modulus of both surfaces is alike [108]. The length of tabbed surfaces is determined by the general formula:

$$L_{\min} = \frac{F^{tu} h}{2F^{su}} \quad (8.1) \quad [107]$$

Where:  $L_{\min}$  = length of tabbed surface (mm)

$F^{tu}$  = ultimate tensile strength of specimen (MPa)

$h$  = thickness of specimen (mm)

$F^{su}$  = ultimate shear strength (lowest of bonding agent, tabbed surface, specimen) (MPa)

There are some disadvantages associated specifically with the approach outlined in ASTM 3039M-00. The tabbed surfaces can separate in the testing rig if the bond surfaces are not correctly prepared; the specimen could slip out of the gripped surfaces if the tabbed surfaces are not roughened; and the test results can be erroneous if the tabbed surfaces are not exactly parallel to the specimen [108]. It was found by the author that the best way to ensure the specimen is

parallel to the tabs is to bond large tabbed surfaces across the ends of large rectangular samples, and to subsequently cut the specimens from these pieces.

As there were only two tensile specimen moulds available for use at UKZN, only two specimens could be fabricated from a single source of resin. This could lead to erroneous results in any experiment, as the total set of specimens recommended for the tensile test (five specimens) would be fabricated from at least three different sources of resin. As composite materials with fillers were inevitable, it was decided that it be best if all the samples are prepared from a single source laminate. This will greater assure that all the specimens contain the same material composition.

Tensile tests are performed on an Instron 5500R universal testing machine at UKZN, and was adopted as the test machine for tensile testing in this work as well. Initially, it was hoped that specimens with bonded tabbed surfaces could be tested in this work. However, during preliminary tests, the bonded region sheared in the grip surfaces. Thus, dumbbell-shaped samples were machined from laminated sheet material for the final testing of the shielding materials in this work.

### **8.1.2 Compressive Testing**

Compression in fibre composite materials is a widespread form of testing; and failure of composite materials by compression is a common deformation in practice [105]. This method is also described as being relatively simple to perform [105]. Data provided by compressive test results that was identified as being interesting to this research was compressive strength.

As with tensile testing, there are a number of test methods that are globally accepted [105]. However, to maintain uniformity, ASTM guidelines were selected for this test as well. This was also preferred as it provides a more reliable means of comparison as both methods are issued by the same institution. Typically, test methods that are issued by different institutions, although accepted as being accurate, do differ in the approach and discrepancies between the results obtained by use of different methods have been documented, as seen in the figure on page 69.

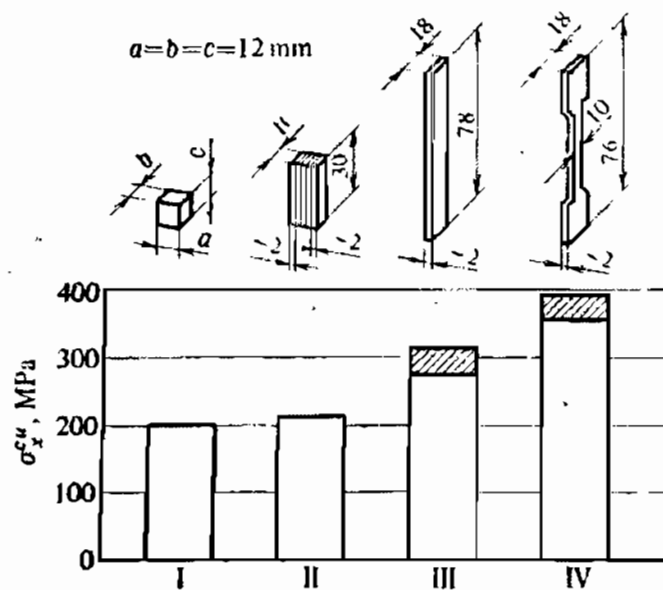
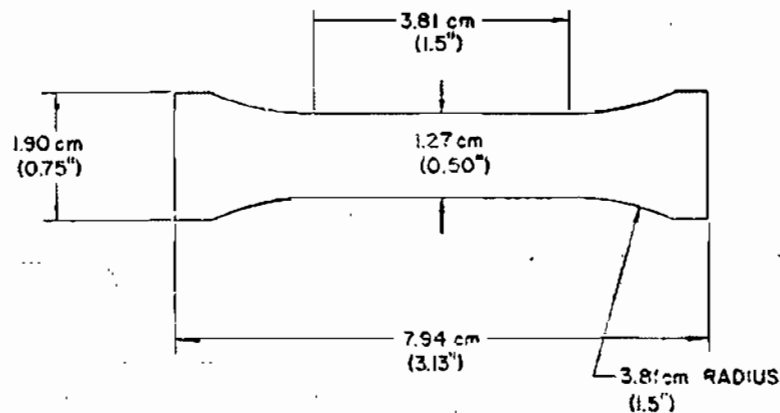


Figure 8.2: Comparison of compressive strengths obtained from different test methods [105]

There are two methods that describe the fabrication of compressive specimens of composite laminates, ASTM 695-02a [109] and ASTM D 3410 [110]. As with tensile testing, the ASTM 695-02a describes the fabrication of compressive specimens from laminated sheet material or from as-laminated manufacture [109]. ASTM D 3410 describes the manufacture of compressive test specimens using tabbed surfaces [110].

In ASTM 695-02a the recommended geometry for test specimens including and exceeding 3.2mm in thickness is a prism of width 12.7mm and length such that the slenderness ratio is between 11:1 and 16:1. "Slenderness ratio" is defined as the ratio of the length of a column of uniform cross section to its least radius of gyration [109]. The radius of gyration is obtained by 0.289 times the smaller cross-sectional dimension [109].

The recommended geometry for specimens less than 3.2mm in thickness is defined in the figure on page 70.



**Figure 8.3:** Compressive test specimen as detailed in ASTM 695-02a [109]

A supporting jig for thin specimens is recommended for this test, and the construction guidelines are presented in [109]. The purpose of this tool is to prevent buckling of the specimen during testing [105]. The tool does not hinder deformation in the plane direction of testing in any way [105].

The method described in ASTM 3410-87 [110] relies on the use of bonded tabbed surfaces parallel to the specimen. However, this method was not preferred by the author, as experience has shown that tabbed surfaces tend to shear during compressive testing using the testing instruments available at UKZN. This method was therefore not adopted in this work. It was decided that it would be best if the compressive test specimens were prepared from the same source material as the tensile test specimens. This will provide a good means of comparison as the specimens are identical in composition.

The appropriate tools for compressive testing conforming to ASTM 695-02a were unavailable at UKZN and testing was subsequently outsourced to the Durban University of Technology (DUT) to complete. The testing was undertaken on a Lloyds universal testing machine. However, the results obtained appear unreliable, and are dismissed in Chapter 10.

### **8.1.3 Flexural Testing**

The use of flexural (bending) tests of prismatic shapes has been widespread in engineering industry [105]. The preparation of bending specimens is considered the most straight-forward by the author, as they consist of simple rectangular sections, usually prepared from a single

laminated sheet material source. There are many different loading schemes that one could use with flexural tests, such as three-point, four-point, and five-point configurations [105]. The three-point and four-point configurations are generally used in practice, as there is indeterminacy regarding the fastening conditions of five-point bending [105]. For this work, the three-point and four-point configurations were investigated.

Three-point bending test methods are advised in ASTM D 790-02 [111]. The term “three-point” describes the loading conditions experienced by the specimen: specimen is placed upon two supports, and a load is exerted to the specimen at its midpoint. For isotropic materials, the use of three-point bending tests have been used almost exclusively [105]. The figure below describes this loading scheme:

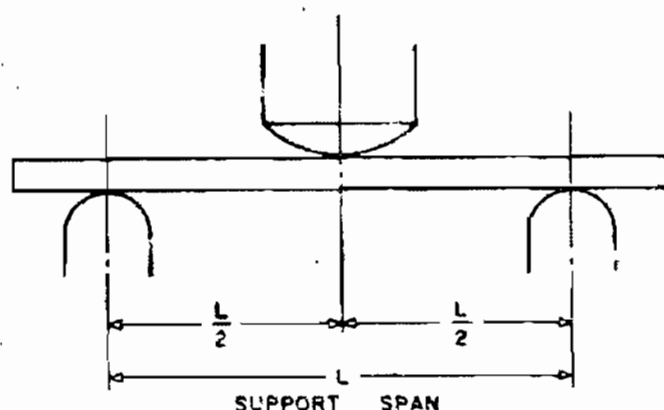


*Figure 8.4: Three-point bending loading scheme [111]*

The relevant specimen geometry was defined under “high-strength reinforced composites, including highly orthotropic laminates” in ASTM D 790-02, and specimen lengths that follow the support span-to-depth ratio of 16:1, 32:1 and 40:1 were recommended.

However, there are also associated shear forces at the midpoint of the specimen upon loading [105]. There have been problems documented in determining reliable results for high strength carbon-fibre composites with this method as shear forces influenced failure [105]. It was thought that there could likely be problems in accurately determining the elastic modulus of high-strength composite materials with this method due to the influence of shear forces. For this reason, the three-point bending test was not adopted in this work.

The four-point bending test described in ASTM 6272-02 [112] are used to determine bending stresses and to compute the elastic modulus of composite materials. Four-point bending is sometimes described as being a “pure-bending” loading scheme i.e. no shear forces introduced on the specimen during loading; although there are some shear forces in practice [112]. Generally, this test is accepted as being a pure-bending configuration in principle, and is considered more reliable than three-point bend tests in the computation of elastic modulus and pure bending stress [105].

The span-to-depth ratio for specimens in four-point bending is identical to that described for three-point bending in [111]. There are two four-point bending systems described in [112], as can be seen in Figure 8.5 below.

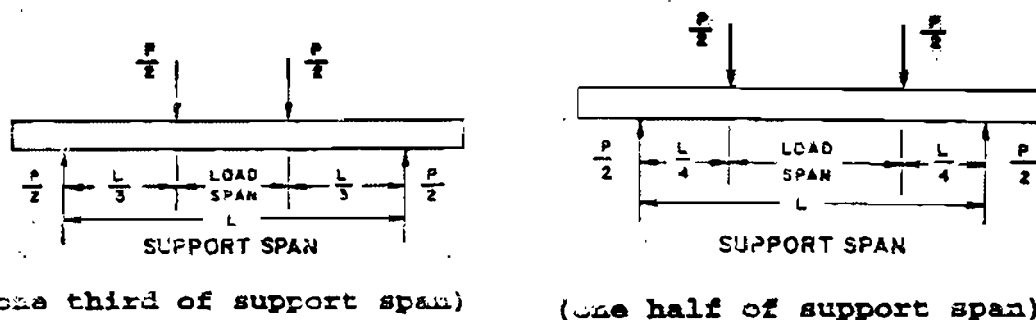


**Figure 8.5:** The one-third and quarter-point four-point bending loading schemes as described in ASTM 6272-02 [112]

It was found that the quarter-point load is preferred for higher modulus composites, such as graphite/epoxies and boron/epoxies, whilst the one third-point load system is preferred for lower modulus composites [113]. As carbon-fibre epoxy composites are the focus of this work, the quarter-point four-point bending test was adopted.

In order to accurately determine elastic modulus of the specimens with this test, mid-span deflections were taken at pre-determined load increments for all laminates. It was found that this is one of the simplest and most reliable means of obtaining elastic modulus. For determination of elastic modulus, equation (8.2) was employed.

$$E_x = \frac{Pcl^2}{8Iw_{max}} \quad (8.2) [105]$$

Where:  $Pc$  = bending moment (Nm)

$l$  = span length (m)

$I$  = moment of inertia ( $m^4$ )

$w_{max}$  = maximum midspan deflection (m)

#### **8.1.4 Discussion on Mechanical Test Methods**

The mechanical test method procedures explained were selected as a guide for testing the laminates fabricated in this research. The preference of fabricating the specimens for all the tests from a single laminated sheet material was due to the fact that uniformity in all the specimens is assured. The results obtained from the tests could be accepted with greater confidence as the specimens were fabricated from the same fabric and more importantly, the same matrix material. It was found that there could be discrepancies when comparing the results of similar test methods following methods prescribed by different institutions [105]. To ensure that these discrepancies are limited, ASTM guidelines were adhered to for all the mechanical tests.

The instrument identified for tensile and flexural testing was an Instron 5500R universal testing machine at UKZN, whilst a Lloyds universal testing machine was used for compressive testing at DUT.

It was hoped that physical testing to determine the fibre volume fraction of the specimens could be undertaken, but the high cost of these tests made this impossible in this work. It was hoped that the fibre volume fraction could be used to obtain the elastic modulus of the specimens in this work by use of the following “rule of mixtures” equation:

$$E_c = \eta_l \eta_o V_f E_f + V_m E_m \quad (8.3) [114]$$

Where:  $E_c$  = elastic modulus of the composite

$\eta_l$  = fibre length distribution factor

$\eta_o$  = fibre orientation distribution factor

$V_f$  = fibre volume fraction



$E_f$  = elastic modulus of the fibre

$V_m$  = matrix volume fraction ( $1 - V_f - V_v$ )

$V_v$  = void volume fraction

$E_m$  = elastic modulus of the matrix material

It was also considered that this equation would yield an approximate value as void volume fraction could not be determined with assurance due to uncertainties regarding the varying filler loadings in this work. The theoretical value for fibre orientation distribution factor would also have to be employed, and one cannot say with certainty that the fibres behave in this way in the practical orientation. In the light of this, the use of equation (8.2) was employed in the determination of elastic modulus, as this was considered to be the most reliable and cost-effective method for the purposes of this work. At least six deflection readings were taken in increments of 50N for all samples when required, and elastic moduli values were computed using equation (8.2).

## **8.2 Electrical Testing**

The electrical tests that were identified as being pertinent to this research were EMSE testing and electrical resistance testing. As the author has had little experience with testing of electrical properties of materials prior to this work, professionals noted for having a background in electromagnetism and electrical engineering were consulted to possibly aid with performing the tests.

### **8.2.1 Electromagnetic Shielding Effectiveness Testing**

EMSE testing was described as being a particularly complex procedure [115,116]. Using the relevant design equations can also be quite a tedious procedure, and does not always yield results which are reliable [40,116]. It was found that previous researchers have adopted ASTM D 4935-99 [117] for the EMSE testing of composite materials. This particular test involves use of a signal generator (source), spectrum analyser or field intensity meter (receiver), coaxial cables and connectors and attenuators [117]. In addition, a special brass specimen holder is required when testing. This test is sometimes referred to as the coaxial cable method in industry journals [52].

The standard pertains to the testing of electrically thin specimens, at frequencies between 30MHz and 1.5GHz. It was decided that this test may not suffice for the purpose of this work, as the frequency range required was between 800 MHz and 3 GHz.

The School of Electrical, Electronic and Computer Engineering at UKZN did not possess equipment of this nature, nor did any other potential test locations that were contacted in SA [118-127]. It was found that the University of Pretoria (UP) is apparently the only location in the southern hemisphere that possesses the relevant equipment for testing of this nature [128]. Prof. JW Odendaal from the Centre for Electromagnetism at UP was consulted, and he agreed to aid with the required testing.



*Figure 8.6: The Scientific Atlanta 5754 compact antenna range test set-up at UP [130]*

It was explained that specimens of a larger size provide a more accurate result when tested [129]. The preferred size was  $1\text{m}^2$  for each laminate. However, it was impractical, especially in terms of cost, to produce laminates of this size for each sample. Prof. JW Odendaal indicated that specimens of a smaller size,  $300\text{mm}^2$ , could be tested, but an aluminium sheet of similar thickness should be tested as a reference base to determine if there were any discrepancies with the results obtained from specimens of this size.

Shielding effectiveness testing at UP was undertaken on a Scientific Atlanta 5754 compact antenna range. This test equipment is very suitable for simulating far field range conditions, due to the large reflector present [131]. In addition, there is a Hewlett Packard 8510B network analyser installed in the test set-up. A set-up of this type is referred to as a “two-port network

system”, and variables referred to as “scattering parameters” (*S*-parameters) are obtained from testing [2].

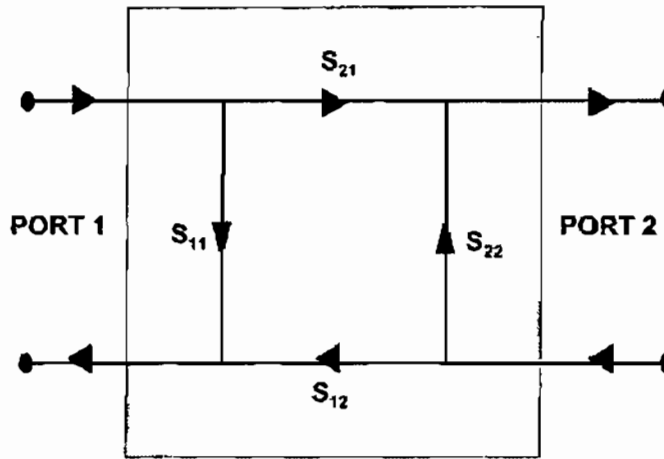


*Figure 8.7: Schematic diagram of S-parameters of a two-ports network system [2]*

The  $S_{12}$  ( $S_{21}$ ) and  $S_{11}$  ( $S_{22}$ ) parameters refer to the transmission and reflection coefficients respectively [2,129]. The analysis of *S*-parameters yield:

$$T = \left| \frac{E_T}{E_I} \right| = |S_{12}|^2 = |S_{21}|^2 \quad (8.4) \quad [2]$$

$$R = \left| \frac{E'_I}{E_I} \right|^2 = |S_{11}|^2 = |S_{22}|^2 \quad (8.5) \quad [2]$$

$$A + R + T = 1 \quad (8.6) \quad [2]$$

Where: A= linear absorption coefficient

R= linear reflection coefficient

T = linear transmission coefficient

The test for the  $S_{12}$  ( $S_{21}$ ) parameter yields a transmission value in dB, which can be used to determine EMSE by use of the following equations:

$$T_R = 10^{\frac{T_{dB}}{20}} \quad (8.7) \quad [129]$$

$$SE = \log \frac{1}{T_R} \quad (8.8) \quad [129]$$

Where:  $T_R$  = linear transmission value

As seen from equations (8.7) and (8.8), transmission is equal to SE in magnitude, but it is presented in the form of a gain, whilst SE is presented in the form of a loss.

Percentage penetration through the shielding material is given by:

$$\% \text{ Penetration} = 10^{\frac{T_{dB}}{20}} \times 100 \quad (8.9) \quad [129]$$

### **8.2.2 Electrical Resistance Testing**

It was decided that electrical resistance testing should be undertaken, to determine not only the electrical resistivity and electrical conductivity, but to also provide the required data for analytically computing EMSE and impedance values. However, the available standards that specifically pertain to the testing of plastics or composite were found to concern electrically insulating materials [132].

Many high-voltage electrical engineering and lightning protection companies in SA were consulted to possibly aid with testing [118-127]. Discussions found that testing of this type could apparently only be undertaken by the South African Bureau of Standards (SABS) in Johannesburg, SA [127]. However, the SABS could only determine electrical resistivity to a sensitivity of  $1 \text{ M}\Omega \text{ cm}$ . This was decided to be fruitless in terms of this research, as it was anticipated that the materials will be far less electrically resistive. The price quoted (R1020/specimen) was beyond the project budget as well.

Investigation of other standards pertaining to resistance testing of electrically conductive materials showed ASTM B193-02 [133] sufficed the project requirements. The method described pertains to the electrical resistance testing of electrical conductors, and it was assumed that the electromagnetic shielding materials developed will behave as electrical conductors.

The specimens defined in the test method are preferred to be 300mm, which is not conducive in terms of cost for this work. Upon consultation with Dr. Hoch at the School of Electrical, Electronic and Computer Engineering, UKZN [115], it was found that similar testing can be performed on specimens with 100mm by 100mm surface area, and will adequately suffice the purpose of this work. Similar approaches to obtain bulk resistivity have been used previously by Xu *et al.* [99] and by Tsotra and Friedrich [134].

The electrical resistance test specimens were prepared by means of cleaning and polishing to obtain good electrical contact with the test instrument. The electrical resistance measurements were performed using the Philips PM6303 RCL universal bridge circuit, shown in Figure 8.8, at UKZN.



*Figure 8.8: The RCL universal bridge circuit used to measure electrical resistance*

Upon determining the electrical resistance value, electrical resistivity and conductivity were obtained by use of equation (4.1).

### **8.2.3 Discussion on Electrical Testing**

Generally, upon determination of electrical resistivities and conductivities of potential shielding materials, the equations presented in Chapter 4 pertaining to electromagnetic shielding may be utilised to analytically obtain the desired EMSE and impedance variables. This was the process adopted in this research when the shielding materials were developed.

However, the electrical resistance values obtained from this machine appeared to be higher than expected. To determine if the machine was accurate, the electrical resistances of copper and aluminium plates of the same size as the composite specimens were measured on the same instrument. The copper plate was obtained from Non-Ferrous Metals, Durban, SA; and the aluminium plate was obtained from Aluminium City, Durban, SA. These too displayed higher resistances than expected, and thus to ensure a reliable means of comparison, the electrical conductivity of the copper plate was calculated using the resistance obtained from the same instrument, and relative conductivity was calculated using this value. It was found that this is an acceptable means of comparison in situations such as this [135]. However, the relative conductivity variable was only required for computation of equation (4.6), as the other equations used the conductivity variable.

The true value of EMSE that the shielding materials provide, however, is of the greatest importance in this work. It was stated that differences between theoretical and actual results of EMSE are common in industry, and the measured EMSE when in practice is the best indication of the true shielding performance of the materials. As the EMSE of an aluminium plate of the same size was measured at the same time as the specimens on the same instrument, a reliable means of comparison was obtained. These details are presented in detail in Chapter 10.

## **CHAPTER 9: DETERMINATION OF APPROPRIATE MANUFACTURING PROCESSES**

In most research work, results are most meaningful when they are compared with a comparable set of data. In terms of composite manufacture, there should generally be one variable at all times i.e. change of manufacturing process whilst all materials are kept constant; change of matrix material while manufacturing and structural materials are kept constant; or change structural materials whilst matrix material and manufacturing process are kept constant. When two or more variables are changed it becomes difficult to ascertain the cause of possible changes in material properties when comparing results.

In order to develop a reliable means of comparison in this work, it was decided that tests would be performed to establish which manufacturing method (from those described in Chapter 7) yielded results which were consistently repeatable for the materials purchased (as described in Chapter 6). This Chapter is replete with images of the laminates fabricated to provide a concise indication of what is being explained in the text to the reader.

At the outset, there was documented difficulty in the manufacture of unidirectional carbon fibre laminates when using Prime 27 epoxy resin and Prime 20 hardener [83]. In addition to this, it was found that Prime 27 epoxy is strictly suitable for use in fully closed mould systems [83]. It was decided that hand lay-up manufacture using this resin would thus not be investigated in this work.

The oven available at UKZN for post-curing composite laminates was fairly small in size; and the largest mould size that could comfortably fit inside was measured to be  $400\text{mm}^2$ . The 1.6mm thick aluminium sheet metal purchased for mould material was cut into  $400\text{mm}^2$  sections; and it was determined that the fabrics could be no larger than  $310\text{mm}^2$  to allow for Vac tacky tape and tubing along the sides of the moulds. However, the oven at UKZN only consisted of two levels; and thus twelve metal supports for the purpose of housing additional moulds in the oven were subsequently prepared by the author to provide curing space for six additional moulds.

As composite laminates with thicknesses between 2-3mm were required in this work, the expected sample sizes were approximated using the raw fabric thicknesses. The calculation is strictly suitable for approximation, and does not take into consideration the behaviour of the

materials when resin is introduced into the system or possible compaction when vacuum pressure is introduced into the system. The actual thickness was expected to vary, but this method provided an indication on the amount of fabric layers to use for other samples following these tests.

**Table 9.1: Fabric Thickness and Approximated Laminate Thicknesses for Various Fabrics**

<b>Fabric</b>	<b>Fabric Thickness (mm)</b>	<b>Approximated Number of Layers</b>	<b>Estimated Sample Thickness (mm)</b>
<b>Unidirectional E-glass (80/20)</b>	<b>0.3</b>	<b>9</b>	<b>2.7</b>
<b>Unidirectional Carbon Fibre</b>	<b>0.3</b>	<b>9</b>	<b>2.7</b>
<b>12K Woven Carbon Fibre</b>	<b>0.2</b>	<b>14</b>	<b>2.8</b>
<b>Stitched Carbon Fibre</b>	<b>0.4<sup>*</sup></b>	<b>7</b>	<b>2.8</b>

Note: <sup>\*</sup> There was some suspicion that this thickness was in actuality greater than 0.4mm, but it was confirmed by the supplier that 0.4mm is, in fact, the correct thickness [136]

### **9.1 Manufacture of Unidirectional E-glass Samples**

Due to the comparatively low-cost of unidirectional E-glass fabric when compared with carbon fabrics, it was decided that the preliminary test pieces would be fabricated using this fabric. It was already known that Prime 27 resin was suitable for fully closed mould processes, such as vacuum-assisted resin infusion, and was not suitable for open-mould systems such as hand lay-up. However, the suitability of LR20 epoxy resin in these processes was unknown. It was also known that the LR20 system has a substantially higher viscosity than the Prime 27 system, and there was some concern regarding its use in vacuum-assisted resin infusion.

It was assumed that nine layers of glass fabric would result in laminates between 2-3mm. The weight of 9 ply of 280mm<sup>2</sup> virgin fabric was 133g, and the quantities of resin and hardener used was 150g and 45g respectively. The enclosed system contained a resin inlet pipe on the upper region of the mould and a resin exit pipe on the lower region of the mould; and they were located such that they were not in direct contact with the E-glass fabric, but rather in contact with the shade cloth resin guides only. The E-glass itself was aligned such that the 80% fibre side was



perpendicular to the resin inlet pipe, so as to aid resin flow in the system. Figure 9.1 provides some clarity on what the enclosed lay-out looked like prior to infusion.



*Figure 9.1: The enclosed system prior to infusion*

Upon introduction into the enclosed system, the resin flowed rapidly, encapsulating approximately one third of the materials within a time of 20s. Upon reaching this point, resin continued to flow, but at a comparatively slower rate. The resin source was almost emptied out at 20mins into the process, and the inlet was sealed to prevent air from entering the system.

Resin visibly appeared to fully wet-out the materials at a time of 50mins into the process. This was thought to be quite a long time, as a vacuum pressure of 80kPa was introduced into the system. Investigation of the left-over resin in the source showed that an exothermic reaction had commenced and the resin had begun to gel. Resin in the piping appeared to retain a high degree of its initial viscosity. Resin exiting the system appeared to be flowing in the exit pipe in sporadic bursts; not quite reaching the resin trap each time it flowed up. This continued for a few minutes until some resin visibly appeared to flow into the trap. The sample was left to cure at lab temperature (20 °C) for a period of 30hrs.

Upon removal of the vacuum bag, inspection of the laminate inspection showed that it was unevenly infused; and resin encapsulation was visibly “patchy” along the exposed surface area of the material. The weight of the laminate was 214g, indicating that 81g of resin was present. The true thickness of the laminate was measured to be 1.65mm, indicating that the fabric compacted approximately 1mm.

A second test was undertaken, using the same materials, to determine if this result was an anomaly. The second infusion progressed in the exact manner, and the composite was left to cure for a period 30hrs. Upon removal, this laminate was quite similar in appearance to the previous one. This laminate was 218g in weight, implying that 85g of the laminate consisted of matrix material. The thickness of this laminate was 1.68mm. Figure 9.2 depicts the appearance of these two test pieces.



**Figure 9.2:** The laminates were visibly resin-starved in patches along the entire laminate. This was consistent along the entire laminate, from the surface in the closest proximity to the resin inlet pipe to the surface in the closest proximity with the resin exit pipe

The consistent appearance of these laminates indicates that resin flow, regardless of how irregular, was constant in this manner throughout the fabric during infusion. In previous experiments performed by the author, viscous resin tended to adequately encapsulate the region it was initially in contact with, but stopped flowing before the entire composite was fully embedded. This was due to the resin gelling, and thus becoming even more viscous, before the materials were fully wet. This type of problem was found to be alleviated in some instances by relocation of the piping in the system.

This experiment, however, proves that resin did not encapsulate the section of materials it was initially in contact with more than the latter regions, despite complete infusion only being visible after the remaining resin had gelled in the source. The problem was therefore not with the location of piping within the mould enclosure, but rather with the resin itself. Early suspicions were that the resin itself was unsuitable for the vacuum-assisted resin infusion of this material.

To confirm this, the placement of the fabric and piping was modified. A layer of shade cloth was used at the bottom surface; a layer of peel-ply cloth was placed above this; and thereafter the initial materials were laid as before. This was to aid the flow of resin on the underside, although there was no particular indication that this side was more resin-starved than other parts of the laminate. Nonetheless, this configuration provided greater assurance that the fabrics were fully encapsulated in resin. The exit pipe was placed along the midsection of the materials, and two inlet pipes were placed on the extreme ends of the materials in the mould. Placement of piping along the composite fabric was not preferred by the author, as it results in an imprint being visible on the final laminate, and could also lead to stress concentrations in the laminate. As expected, the time to visibly embed the materials was now 25mins, as there were two inlets introducing resin into the system simultaneously. Figure 9.3 below shows infusion in this system.



*Figure 9.3: The system with two inlet pipes and the exit pipe along the midsection. Although not visible, a layer of shade cloth and peel-ply is located on the base of the mould surface as well.*

The laminate was left to cure for 30hrs; and the vacuum bag was removed. Inspection of the laminate showed a similar appearance to that of the previous two. The visible difference in this laminate was a small section along the exit pipe that appeared visibly embedded in resin; but this was quite possibly to resin stagnating along the exterior surface of the exit pipe, as is quite common in this process. The region on the laminate that the exit pipe was directly upon appeared visibly resin-starved; more so than the rest of the laminate. Figure 9.4 depicts these findings.

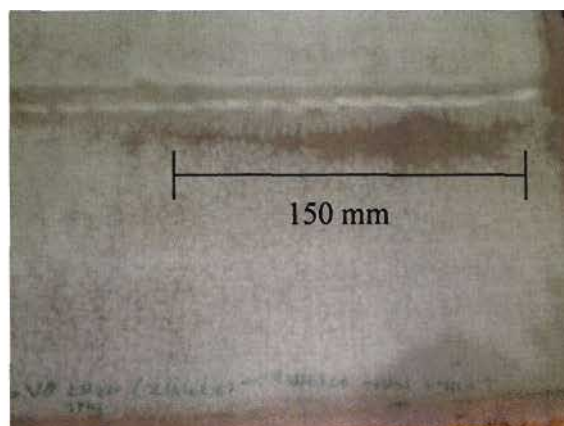


*Figure 9.4: The third laminate was similar in appearance to the previous two, aside from the region around the exit pipe. As seen, a small section appeared adequately embedded in resin, whilst the region that the exit pipe was directly placed upon appeared visibly resin-starved.*

This mould configuration also proved to be detrimental to the aluminium mould itself; a resin imprint resulting from the shade cloth, which was directly on the mould, was left on the mould surface and could not be removed without possibly damaging the mould even further. As a result, this mould could not be used for further work.

It appears that a poor laminate results from when using unidirectional E-glass and LR 20 resin in the vacuum-assisted resin infusion process. This result was unvarying in all of the three tests that were performed.

Tests were then undertaken to determine if hand lay-up manufacture of unidirectional E-glass laminates with LR20 resin yielded more promising results. In this work, the use of mohair and aluminium rollers as application tools was adopted. Resin was adequately applied to all surfaces of the materials on the mould; and a layer of porous bleeder cloth was placed upon the wet fabric. A layer of breather cloth was placed upon these materials, and the mould was covered with vacuum bag. A vacuum pressure of 80kPa, as in all the laminates fabricated in this work, was introduced into the system.



*Figure 9.5: The hand lay-up E-glass fabric upon introducing vacuum pressure into the enclosed mould*

The resin was allowed to gel for 4hrs and the vacuum inlet was sealed. The laminate was allowed to cure for an initial period of 30hrs, and the bag was removed. Upon removal of the vacuum bag, visible inspection of the laminate indicated that it was uniformly encapsulated in resin. As is the case with typical laminates fabricated using the hand lay-up process, the upper-most surface contained a smooth resin-rich layer, opposed to vacuum resin infusion samples which typically contain a rougher upper-most layer due to the peel-ply/shade cloth combination that is used.

To verify that this process was consistent in the production of laminates of a similar quality, a second sample of the same type was prepared in the exact manner. Upon removal, the laminate was visibly alike to the first laminate fabricated using the hand lay-up process, and was deemed satisfactory. Upon post-curing the laminates at  $65^{\circ}$  for 16hrs, the dimensions for the prospective test specimens were marked on the laminates. The weights of the laminates were 189g and 192g respectively, and the thicknesses were 1.58mm and 1.62mm respectively. This indicates that these laminates consisted of less matrix material than the irregular vacuum-assisted resin infusion ones, as they are lighter in weight suggesting a more uniform distribution of resin.





*Figure 9.6: Resin had embedded the fabric uniformly, and both laminates were similar in appearance. The laminates are marked with the specimen dimensions of the tests required.*

Once it had been determined that hand lay-up fabrication of unidirectional E-glass composites with LR20 resin was viable, the use of Prime 27 resin with unidirectional E-glass was investigated. The nine layers of  $280\text{mm}^2$  glass fabric, peel-ply cloth, and shade cloth were laid out on the mould with piping on extreme ends. The materials appeared to be completely infused after a period of 8mins after resin was initially introduced into the system, and the inlet pipe was sealed. The resin exit pipe was sealed after a period of 5hrs, and the system was allowed to cure for a period of 30hrs.

Upon removal of the laminate, inspection showed that the laminate was uniformly encapsulated in resin. A second laminate of the same type was manufactured in the exact manner, and the results were similar. These laminates were post-cured for 8hrs at  $65^\circ\text{C}$ . The weights of the laminates were 194g and 189g respectively and the thicknesses were 1.63mm and 1.60mm respectively. Use of this resin in the vacuum-assisted resin infusion of unidirectional E-glass thus appeared to be quite suitable.



*Figure 9.7: The resulting laminate from the vacuum-assisted resin infusion of E-glass with Prime 27 was uniform in appearance, and was free of visible inconsistencies*

## **9.2. Manufacture of 3K Woven Carbon Fibre Samples**

As there were known problems with the suitability of LR20 with vacuum-assisted resin infusion, it was decided that the initial testing on carbon fabric should be undertaken on material that was left-over from previous work. This was undertaken specifically to determine the viability of using LR20 resin with vacuum-assisted resin infusion with carbon fibre. Although the suitability would not necessarily be transferable to other carbon fabrics, it was thought that this will provide a greater assurance, as there was doubt following the glass tests. The fabric used was 3K woven carbon fibre cloth.

Although the fabric was 0.2mm in thickness, it was decided that the 250mm<sup>2</sup> test laminates would consist of only four layers, as this was only for test purposes. The material configuration within the mould consisted of the carbon material; a layer each of peel-ply and shade cloth. The resin inlet and exit pipes were located at extreme ends of the mould. Upon introduction into the system, resin embedded approximately one third of the material length in 18s. After this time, resin flow was substantially slower than in E-glass experiments. Resin flowed to approximately three quarter of the material length after a comparatively long time, 70mins, at which point flow abruptly stopped. Resin was observed to remain viscous in the sealed inlet pipe, although resin in the source had begun gelling. In this experiment, resin did not reach the exit pipe, despite the high vacuum pressure (80kPa). Figure 9.8 shows this laminate during infusion, and upon removal of the vacuum bag.

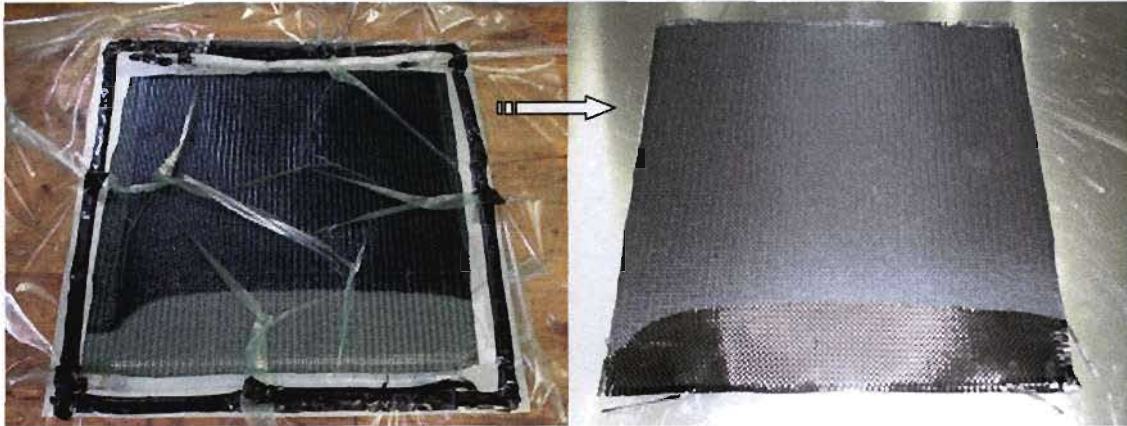


*Figure 9.8: Resin flow had abruptly stopped at 70mins, and the resulting laminate contained an area of fabric that was completely resin-starved*

Indeed, different material configurations within the mould could result in a complete infusion, but determination of these configurations was not the focus of this research. As with the E-glass test, the possibility of including layers of peel-ply and shade cloth on the under-side of the carbon fabric could be one of the solutions. However, it will not be viable, in any research, to utilise one mould per laminate as was the case when this configuration was adopted with the glass tests. As far as this particular laminate shows, it is best assumed that a size of  $200\text{mm}^2$  would be more appropriate for complete infusion of the fabric when using the material configuration that was used in the experiment. However, the laminates are required to be between 2-3mm, and the ply amount would be approximately 14 layers, and this could influence results further. Having samples of this size would not be conducive to the EMSE testing either, as it was determined that  $300\text{mm}^2$  was the smallest possible size for reliable results.

A hand lay-up using four layers of 3K woven carbon fabric with the same resin material was then manufactured. Resin was thoroughly applied to the mould surface and fabric layers using mohair and aluminium rollers, and a layer each of bleeder and breather cloth was placed upon the wet fabric. The materials were enclosed within a vacuum bag, and pressure of 80kPa was introduced into the system. Upon removal of the bag after a period of 30hrs, the laminate appeared visibly uniform, and was post-cured for 16hrs at  $65^\circ\text{C}$ .





*Figure 9.9: Hand lay-up fabrication using 3K carbon fibre fabric and LR20 epoxy resin.*

A vacuum-assisted resin infusion test with Prime 27 was not undertaken, as it was assumed that this fabric would be suitable with the resin. This assumption was made due to there only being documented problems with Prime 27 and unidirectional carbon fabric [83].

### **9.3 Manufacture of Stitched Carbon Fibre Samples**

Upon establishing the behaviour of 3K woven carbon fabric and LR20 with both manufacturing processes, tests were undertaken using the stitched carbon fabric purchased for this work. It was suggested that a final test to determine the suitability of LR20 resin with the vacuum-assisted resin infusion process be performed to determine if this was not a viable option with certainty [137].

It was known, from the previous test, that use of a single inlet and exit pipe for infusion of LR20 in carbon fabric was likely unsuitable. In addition, it was required to determine a repeatable manufacturing process for the fabrication of laminates at least  $300\text{mm}^2$  in size to suffice the EMSE testing requirement. Thus, a material size of  $310\text{mm}^2$  was used, and the weight of seven layers was 291g. The material configuration within the mould thus consisted of seven layers of  $310\text{mm}^2$  carbon fabric; one layer each of peel-ply and shade cloth above the fabric; two resin inlet pipes on extreme ends of the materials; and a single resin exit pipe along the midsection of the materials. This was the most appropriate configuration, despite it being known that surface imperfections would be present on the final laminate due to the inlet pipe.

The infusion process was performed in the exact manner as in the previous tests, and the material was left to cure for 30hrs initially. Resin flow during infusion was quite slow as expected; as resin took approximately 40mins to visibly embed the materials, despite there being two inlet pipes. Upon removal of the laminate 30 hrs later, visible inspection of the underside showed that resin did not flow consistently in this fabric as well. The mid-section of the laminate, where the exit pipe was located, remained completely resin-starved. It was initially assumed that this was due to lack of a flow medium on the under-surface; thus resin likely flowed on the path of least resistance (the shade cloth surface) and into the pipe as pressure was likely higher as resin flowed closer to the exit pipe. However, the laminate was machined through this region, and inspection showed the lower five layers were resin-starved. This indicates that use of a flow medium on the lower surface could also likely result in the middle layers being resin-starved within the laminate regardless of the surfaces being encapsulated.

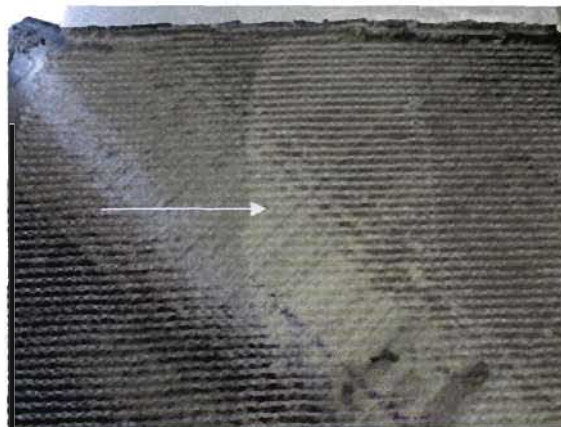


**Figure 9.10:** The area at the midsection of the laminate did not wet-out at all below the first ply. The wet-out regions appear a darker colour in the image while the un-wet fabric appears to be lighter in colour in this image.

Due to the high-cost of this fabric, one test was deemed sufficient for the purpose of this work. It was determined with certainty that use of LR20 in vacuum-assisted resin infusion was not suitable for the manufacture of the shielding material in this work, as promising repeatable results were not achieved in the five tests performed.

A sample fabricated with the same materials using the hand lay-up process was undertaken following this test. In the previous tests, the LR20 epoxy resin proved to be quite suitable for use with the hand lay-up process. The 310mm<sup>2</sup> seven-ply sample was manufactured in the manner

used in the previous tests, and was allowed to pre-cure under the influence of vacuum pressure for 5hrs. At that time, the inlet pipe was sealed and the sample was allowed to cure for 25hrs. Upon removal of the vacuum bag, visible inspection showed that the entire laminate was uniformly embedded in resin. The sample was then cured at 65 °C for a further 16hrs. A second sample of the same size was fabricated and cured in the exact manner. Upon curing, the samples were marked with the relevant test specimen dimensions and were subsequently cut to specification by the author. The weights of the laminates were 487g and 492g respectively; and the true thickness of these laminates was measured to be 4.2mm and 4.15mm respectively, which is substantially more than anticipated, indicating that the suspicion regarding the material thickness may not have been unfounded.



*Figure 9.11: Hand lay-up laminate using stitched carbon fibre and LR20 resin*

A stitched carbon fibre test specimen using Prime 27 resin was then undertaken via vacuum-assisted resin infusion. The material configuration within the mould consisted of the carbon fabric; a layer of both peel-ply layer and shade cloth; and resin inlet and exit pipes located at extreme ends of the mould. Upon starting infusion, approximately one third of the material was visibly embedded in 10s; and the materials appeared fully embedded within 10mins. This was less than a quarter of the time LR20 took to visibly embed the material with two inlet pipes, and is an apparent indication on the influence that resin viscosity has on the vacuum-assisted resin infusion process. The resin exit pipe was sealed after 5hrs, and the system was left to cure for 30hrs.

Upon removal of the laminate, the laminate appeared to be uniformly embedded in resin, and no visible irregularities were seen. The laminate was subsequently post-cured for 8hrs at 65 °C. A

second laminate consisting of the same materials was fabricated in the exact manner to ensure the result was repeatable. The weights of these laminates were 427g and 435g respectively; and the true thicknesses of these laminates were 4.25mm and 4.4mm respectively.

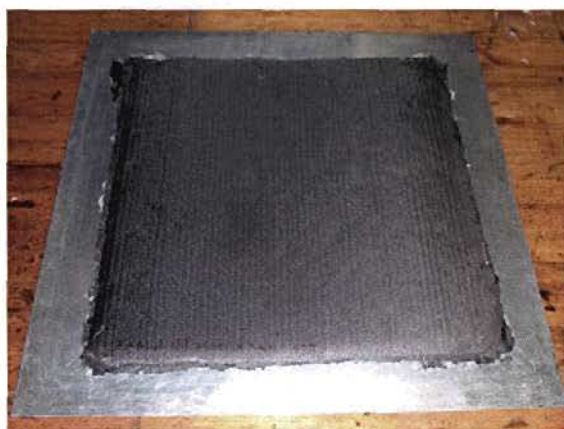


*Figure 9.12: Stitched carbon fibre laminate manufactured using Prime 27 resin by means of vacuum-assisted resin infusion*

#### **9.4 Manufacture of Unidirectional Carbon Fibre Samples**

As the unidirectional carbon fibre fabric was available in a maximum width of  $600\text{mm}^2$ , the sample size selected was  $300\text{mm}^2$ . Seven layers of the material, having a weight of 196g, were used, instead of the initial nine layers that were predicted in Table 9.1 This was due to the discrepancies between the predicted and true thicknesses that were found in the previous tests.

A hand lay-up using LR20 was first fabricated in the exact way as with the other samples. Vacuum pressure was then introduced into the system for 5hrs, and was then sealed off. The system was allowed to cure for a further 30hrs, and the laminate was removed. Inspection showed that it was sufficiently encapsulated in resin, and was deemed acceptable. The laminate was cured for a further 16hrs at  $65^\circ\text{C}$ . A second laminate of the same type was then manufactured to determine if the quality would be repeatable, which it was. The weights of the laminates were 264g and 260g respectively. The thicknesses of the laminates were 2.15mm and 2.10mm respectively.

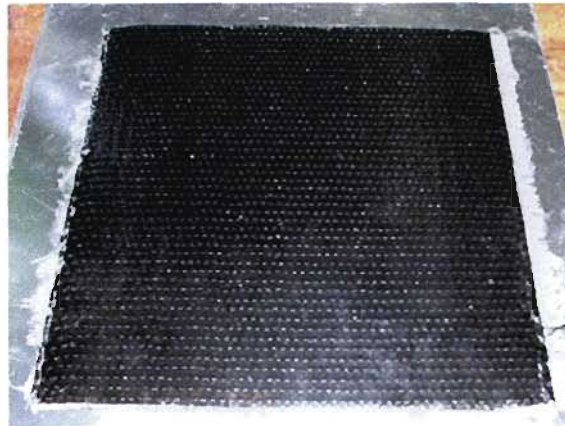


*Figure 9.13: Hand lay-up fabrication of unidirectional carbon fibre*

It was known that there is documented difficulty in infusing unidirectional carbon fibre with Prime 27 resin [83]. However, to determine the veracity of this, a test laminate was fabricated. As explained previously, for the results of this research to be significantly comparable, the manufacturing process and matrix material had to remain constant, as the structural materials were changing. This would only be the case if the vacuum-assisted resin infusion of unidirectional carbon yielded a promising result, which was reported to be unlikely.

The test laminate consisted of six layers of fabric and was 167g in weight. The material configuration in the mould consisted of the carbon fabric; a layer each of peel-ply and shade cloth; and piping on the extreme ends of the mould. Upon starting infusion, the materials appeared visibly embedded in resin after approximately 9mins. After 30hrs, the vacuum bag was removed and the laminate visibly appeared to be improperly infused. The laminate contained “patches” that were completely resin starved, most of which were towards the end of the laminate. The laminate that resulted from this test may be seen in Figure 9.14.

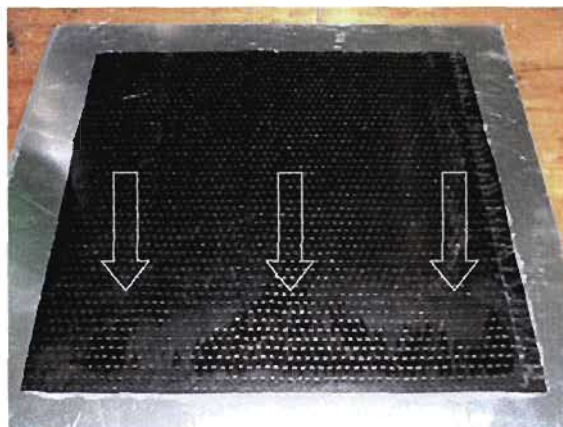


*Figure 9.14: Improperly infused unidirectional carbon fibre laminate fabricated using Prime 27 resin*

### **9.5 Manufacture of 12K Woven Carbon Fibre Samples**

Following testing on unidirectional carbon samples using the final material purchased, 12K woven carbon fibre, were manufactured. Again, as there were discrepancies between the approximated and true thicknesses of the glass and stitched carbon samples, only ten layers of 12K fabric were used in the manufacture of the laminates, as opposed to the estimated fourteen layers. The weight of ten layers of  $310\text{mm}^2$  fabric was found to be 198g.

A hand lay-up fabrication was prepared with LR20 epoxy resin in the exact manner as with the other fabrics. Vacuum pressure was introduced into the system for 5hrs, at which time it was sealed off. The materials were left to cure for a further 30hrs, and were removed from the vacuum bag. The laminate appeared to be uniformly embedded in resin, and was thus post-cured at  $65^\circ\text{C}$  for 16hrs. A second laminate was prepared in the exact manner, and the result was uniform. The laminates weighed 270g and 271g respectively; and the thicknesses were 2.2mm and 2.25mm respectively.





*Figure 9.15: Hand lay-up fabrication with 12K woven carbon fibre*

Although it was determined that use of Prime 27 would no longer be viable for the actual electromagnetic shielding materials, it was suggested that tests be performed to determine if 12K woven fabric is suitable for use with Prime 27 resin. The composite was manufactured using the vacuum-assisted resin infusion process. The material configuration within the mould consisted of ten layers of fabric; a layer each of peel-ply and shade cloth; and resin pipes at the extreme ends of the mould as before. The material took 8mins to visibly wet-out, and the exit pipe was sealed 5hrs upon starting the infusion. The vacuum bag was removed following an initial cure of 30hrs.

Visible inspection of the laminate showed that almost half of the surface area of the fabric that was on the aluminium mould did not receive any resin at all. This was not expected, and a second sample was manufactured to determine if this was an anomaly. The sample was prepared in the exact manner, and upon curing for 30hrs, was removed from the vacuum bag. The result displayed was similar to that of the first laminate.

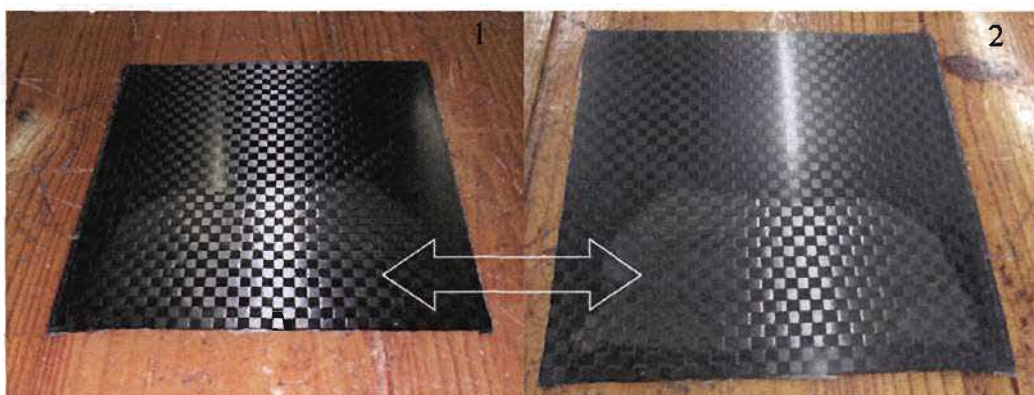


*Figure 9.16: An area of almost half of the 12K woven carbon fibre remained dry after infusion on both laminates*

There were no problems documented regarding the suitability of Prime 27 with woven carbon materials, and it was thought that this could be a problem with the mould configuration, rather than the material. To determine if this result would be uniform with a change in mould configuration, it was decided that a layer of shade cloth on the lower surface of the materials should be used.

Although this material configuration proved detrimental to the mould surface previously, it was the best approach to determine if the irregular infusion was a result of the 12K carbon fibre fabric. A layer each of shade cloth and peel-ply were placed on the base, followed by the rest of the materials as before. It was thought that this would aid resin flow on the under-side of the laminate, which was visibly resin-starved in the other two tests. However, a surprising outcome was seen upon infusion. Resin initially flowed around the carbon fabric; and flowed along the sides which contained only shade cloth and peel-ply layers, and straight into the resin exit pipe. Presumably, the resin flowed in this manner as this was the path of least resistance for the fluid to take. The material also took substantially longer to infuse, and only three quarter of the materials appeared wet after 30mins. This was not expected, as it was assumed that resin flow would be aided by the additional shade cloth layer. Interestingly, an area of the materials remained dry until almost 50mins passed. The area in question can be seen clearly in Figure 9.17. There was suspicion that this region received little resin below the upper shade cloth layer.



*Figure 9.17: The materials only appeared completely wet after 50mins*

The resin exit pipe was sealed 5hrs later, and the materials were left to cure for an additional 30hrs. Upon removal of the laminate, inspection showed that the laminate was visibly embedded in resin. The laminate was cured for 8hrs at 65°C. Upon curing, the laminate was marked and cut



into size for electrical testing. Inspection of the individual specimens showed that a number of fabric layers within the laminate remained dry during infusion. As expected, the abundance of dry fibres was found in the region that was suspected of receiving little resin during infusion. This was clearly visible due to the colour difference between the wet and dry fibres, as well as the by the difference in texture of the outer and middle regions.

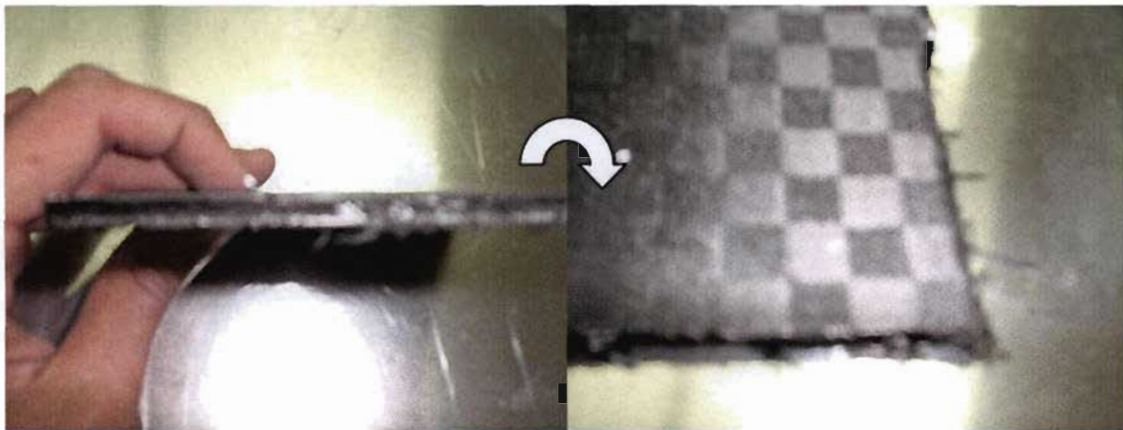


*Figure 9.18: The third 12K woven/Prime 27 composite. There were layers of dry fibre that were only apparent once the laminate was cut.*

## **9.6 Discussion on Manufacturing Processes**

It was found that the hand lay-up fabrication process, using LR20 epoxy resin, yielded repeatable production results. Use of LR20 epoxy resin with the vacuum-assisted resin infusion process resulted in laminates that were consistently poorly infused for both glass and carbon fabrics. Use of Prime 27 epoxy resin with the vacuum-assisted resin infusion process showed promising results when applied to glass and stitched carbon fabric. A poor laminate, as was expected, resulted when this resin was applied to unidirectional carbon fibre. However, this work also unexpectedly shows that poor laminates result when this resin is used with 12K woven carbon fibre as well.

As a goal of this research was to provide a series of data which was comparable, it was decided that only the hand lay-up manufacturing process using LR20 resin with LH281 hardener would be adopted following these initial tests. Despite the mechanical properties of this matrix material being inferior to that of Prime 27 resin with Prime 20 hardener in Tables 6.6 and 6.7, this was the

only manufacturing process and resin system which resulted in consistent laminates for all the fabrics used.

It was initially hoped that a single laminate could yield specimens for all of the required mechanical and electrical tests of the actual electromagnetic shielding materials. However, laminates would have to be at least 300mm by 700mm to allow for this. As mentioned, the oven at UKZN could comfortably accommodate laminates of a much smaller size than this, and post-curing was essential to obtain optimum mechanical properties.

The other alternative was to simultaneously prepare smaller laminates, such that they are fabricated from the same source materials, which could be housed in the oven simultaneously as well. The constituents of the structural materials were assumed to be constant for the most part, but there was some concern regarding the constituents of the matrix material, as fillers would be added in. It was therefore decided that it would be best if all of the samples were simultaneously manufactured in pairs of two, with one serving laminate serving as the EMSE test specimen, and the other serving as the laminate for mechanical and electrical resistivity testing specimens. This was decided to ensure that both laminates contained exactly the same materials.

In order to ensure that fibre volume fractions were similar in both laminates, it was apparent that same vacuum pressure had to be introduced into both systems when curing. In order to achieve this, two moulds were joined together by means of tacky tape along the sides and the fabric was laid up on either side of the joined section. A pipe was placed on the joined section to ensure the same pressure was experienced in both mould systems when required. When all the layers were adequately embedded in resin, the twin-mould system was sealed and enclosed in vacuum bagging. Vacuum pressure was introduced and as expected, the vacuum bag conformed to the rigid mould surface in both mould systems.



*Figure 9.19: Optimising the manufacturing process involved temporarily joining two moulds together for the purpose of introducing appropriate pressure into each system*

There were three vacuum pressure outlets available to the author for use in this work. This allowed for a total of six laminates to be fabricated on any given day. The metal oven supports that were described previously allowed for the post-curing of all six of the laminates simultaneously as well.

## **PART D: Final Designs, Results and Discussions**

## **CHAPTER 10: COMPOSITE MATERIAL DESIGN AND ANALYSIS**

Upon determining the manufacturing process that yielded promising results for all of the fabrics, work commenced on enhancing electrical conductivity in the basic laminates. The electrical resistances of the initial samples were measured, and were found to be in the range of  $5\text{--}20\ \Omega$  for carbon fibre specimens. The E-glass specimens could not be accurately measured on the available equipment, as it measured a maximum of  $999.99\ \text{M}\Omega$ , and these samples contained higher resistances than this. As explained in Chapters 5 and 6, the preferred methods to obtain electrical conductivity were selected as being addition of metal powders into the matrix material and inclusion of metal fabrics as layers when building the laminate itself.

In order to develop a reliable means of comparison, the exact same laminate should ideally be tested for both electrical and mechanical properties. Should the laminates be fabricated on different days or from different source materials, the margin of uncertainty widens. One cannot say with certainty that the results obtained from the testing of materials fabricated in this way are either accurate or comparable. However, manufacture of single laminates sufficiently large enough for both electrical and mechanical test specimens could not be manufactured at UKZN. Thus, to achieve a more reliable means of comparison with the resources available, the hand-lay up manufacturing process at UKZN was optimised to be conducive for the simultaneous manufacture of multiple laminates, as explained in Chapter 9, and this process was used for the manufacture of all the electromagnetic shielding materials on this work.

The materials that were selected for this work have been detailed in Chapter 6. In order to enhance electrical conductivity, metal powders were introduced in the matrix material; and electrically conductive fabrics were built in as actual layers in the composite laminate structure.

The relevant tests described in Chapter 8 were undertaken on all of the samples manufactured. Analytical data using the equations presented in Chapter 4 and Chapter 8, for electrical and EMSE results, and in Chapter 8, for elastic moduli, were analysed for all of the samples. The solutions for each of these analytical computations are not presented in this work, as these computations exceed 1000 pages, but sample calculations of each equation are presented in the Appendix D. Some of the test results are not presented in full tabulated form in this work as they

would be too extensive. Rather, scatter-point graphs containing these values are presented in the Appendices E and F as well. Images relating to material testing can be found in Appendix G.

## **10.1 Discontinuous Filler Material Designs**

As mentioned previously, the aim of this work was not to ascertain the exact percolation threshold of the composite materials, but rather to develop an understanding of the behaviour of the materials' properties when fillers are introduced in increasing quantities. The process of introducing foreign materials with the purpose of influencing material properties is referred to as "doping" [138], and in this work, the "dopants" were metals powders.

It was suggested that filler loading should not exceed 12-15% [137], and the maximum upper limit was therefore taken to be 15%. The lower limit was taken to be 0% filler loading, as this would provide the best indication in the change of material properties, and the intermediate limit was taken to be half way between these values, at 7.5% filler loading.

The filler loading in all laminates was introduced by percentage weight, rather than by percentage volume, of the total resin/hardener system. Effects of including aluminium powder; copper powder; and a mixture of aluminium and copper powder as discontinuous fillers were studied in this work.

### **10.1.1 Aluminium-doped Samples**

#### **10.1.1.1 Manufacture**

Aluminium was selected based on its light weight, low cost, and good electrical conductivity. It was known that galvanic corrosion could occur when aluminium is in the direct contact with carbon, but the effects of this are not focused in this research. The reason for this being that as aluminium was found to be the cheapest suitable metal powder, and should this powder result in providing an adequate shielding material that is replaceable at a lower cost, then this could negate the need to produce longer-lasting shielding materials at higher costs. In addition, it was found that shielding effectiveness is enhanced by connectivity, and aluminium was found to be the lightest of the suitable powders investigated. Therefore a greater volume of powder will be provided at comparative weights implying greater connectivity within the resin material.

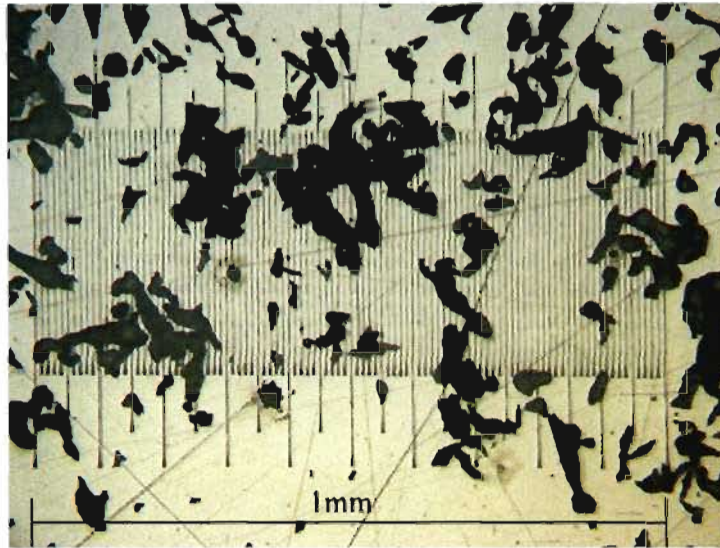


*Figure 10.1: Aluminium powder under a microscope*

As seen in Figure 10.1, the aluminium particles are quite random in size and shape. They were relatively small, in the order of  $10\text{-}50\ \mu\text{m}$  in size. It was decided that aluminium powder would be applied to all of the structural materials purchased, in order to determine what influence their introduction would have on the various carbon fabrics.

It was decided that only four layers of stitched fabric would be used in these samples, as it was thought that this would likely result in a laminate between 2-3mm. Ten layers of 12K woven carbon and seven layers of unidirectional carbon fibre were used, as this ply amount resulted in laminates of an acceptable thickness in the initial tests described in Chapter 9. Further laminates without fillers were fabricated, and the relevant tests and calculations were undertaken.

The samples containing 7.5% filler loading of aluminium powder were manufactured first. Upon preparing the undoped matrix material, 7.5% of finely sifted aluminium powder by weight was introduced and the system was thoroughly mixed by hand at 180rpm for 5mins. Upon mixing, the colour of the fluid was noticed to change from the normal light yellow colour to a grey colour almost immediately. The fluid also changed from being transparent to opaque proportionally with the colour change. The texture of the doped resin also appeared to be more viscous to that which contained no powder. This change is shown in Figure 10.2.



*Figure 10.2: The resin colour changed from being a transparent, light yellow colour to an opaque grey shade. The texture also changed, and became less viscous and rougher as filler loading increased.*

It was important to ensure that the same resin was used to prepare the laminate due for EMSE testing and its partner laminate for electrical and mechanical testing. The carbon fabrics on each twin-mould setup were embedded with resin from the same source, and allowed to cure under vacuum pressure for 30hrs.

The samples containing 15% filler loading were manufactured immediately following the previous samples. The powder was introduced in the exact manner as explained, and was stirred at 180 rpm for 5mins. The colour changed to a much darker shade of grey in this mixture, and appeared to be more viscous and rougher in texture than the system containing 7.5% filler loading. It was concluded that this is due to the higher filler loading. The laminates were fabricated in the exact manner as previously and were allowed to cure for 30hrs.

Upon removal of the laminates containing 7.5% filler loading, it was immediately noticed that the exposed surface areas of laminate were light grey in colour. The laminates containing 15% filler loading were then removed and found to be a darker shade of grey in colour. This was indicative of the matrix material used in each laminate and was anticipated. The laminates were post-cured for period of 16hrs at 65 °C. Images of these laminates, and all of the other laminates built in this work, can be seen in Appendix B; and thickness and weight data for the laminates can be found in Appendix C.

The thicknesses of all the laminates were quite comparable despite the increasing filler loading. Thickness was thus not influenced by the filler content. Weight, on the other hand was found to generally increase as filler loading increased.



It was mentioned that aluminium is a lightweight material, and hence it was assumed that a high degree of connectivity between the particles will exist in the matrix. To ascertain the accuracy of this assumption, the laminates were viewed under a microscope at 50x, 100x, 200x, and 400x magnification.

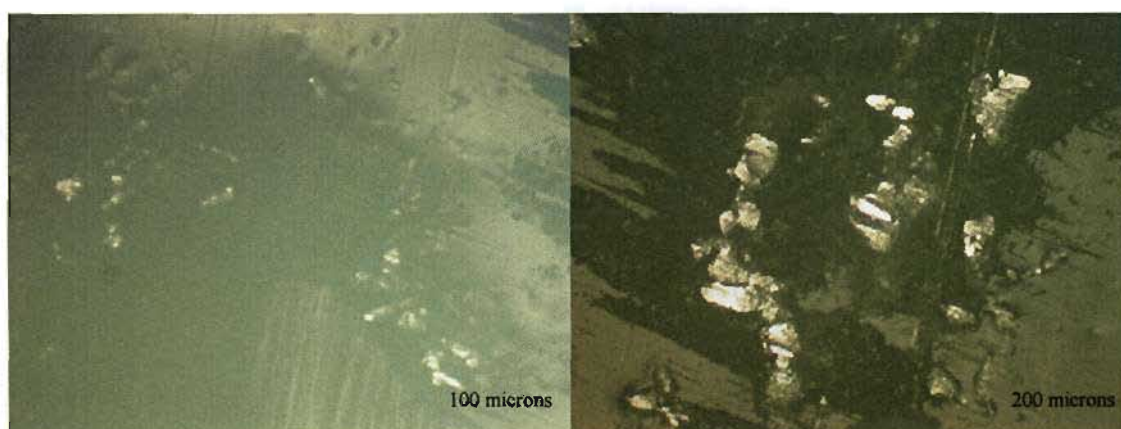


**Figure 10.3:** An image depicting 100x and 200x magnification of 7.5% aluminium filler side by side. As seen there are microscopic spaces between the metal particles within the composite.

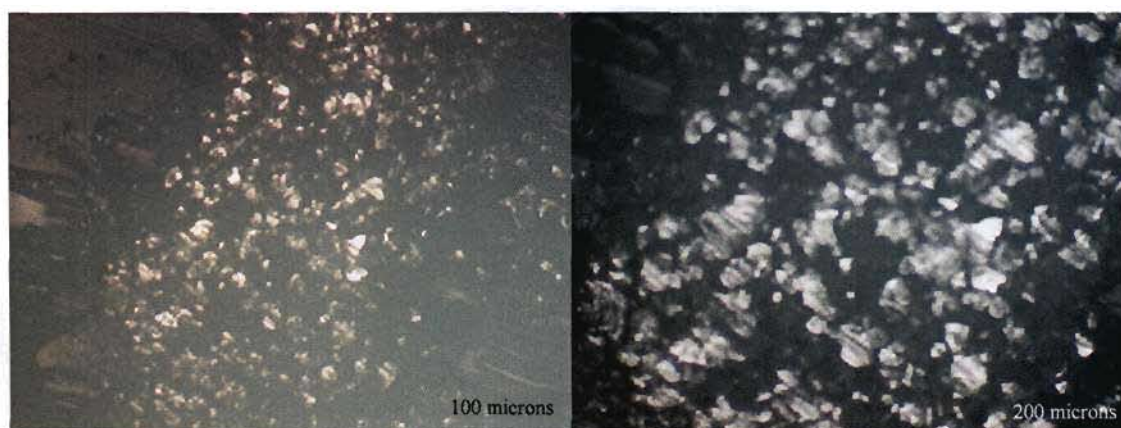


**Figure 10.4:** An image depicting 100x and 200x magnification of 15% aluminium loading samples. As seen, the extent of connectivity between the particles increased considerably, although there are still microscopic spaces between them.

Microscopic spaces, as expected did exist, although there appeared to be connectivity on a macroscopic scale before viewing the specimens under the microscope. However, the particles, as seen, were quite disordered within the matrix material. The specimens were then tested and their properties were analysed.

### 10.1.1.2 Results and Discussion of Stitched Carbon Fibre Samples

#### a. Mechanical Testing

The average mechanical properties are shown in Table 10.1 for this specimen. The values in the bracket in this table, and all other tables where applicable, represent the standard deviation value. At least six tests were conducted for these samples, as well as all of the others, and this provides a minimum of 90% confidence in the results, which is in accordance with the ASTM standards.

**Table 10.1: Average Mechanical Properties of Aluminium-Doped Stitched Carbon Fibre Laminates**

	0% Filler	7.5% Filler	15% Filler
<b>Tensile Strength (MPa)</b>	73 (3)	78 (9)	75 (3)
<b>Yield Strength (MPa)</b>	61 (3)	70 (8)	72 (3)
<b>Tensile Yield Elongation (%)</b>	1.0 (0.1)	0.8 (0.0)	0.8 (0.0)
<b>Break Elongation (%)</b>	3.1 (0.4)	3.9 (0.8)	3.7 (0.7)
<b>Flexural Strength (MPa) *</b>	N/A	N/A	N/A
<b>Elastic Modulus (GPa)</b>	14.1370 (1.4486)	8.5472 (0.3411)	8.1280 (0.9660)
<b>Compressive Strength (MPa)</b>	79 (4)	84 (2)	82 (7)

Note: \* Flexural strength was indeterminate as the specimens deflected excessively and touched the supports of the testing rig before failure – The low elastic moduli obtained is indicative of this

When compared with the undoped laminate, there was no significant difference in the tensile strength, and in fact a 7% increase was even observed between the undoped samples and the sample with 7.5% filler. A 3% decrease from this was observed as the filler loading was increased to 15%. The tensile strength of the stitched samples was very low for a carbon fibre composite as well; approximately 75 MPa for all of the samples. The yield elongation decreased proportionally with filler loading, but the break elongation appeared to increase. Failure in these specimens was observed to occur at the midsection of the specimen length, with splitting of the fibres in the  $\pm 45^\circ$  plane taking place.

The results for the flexural testing were also surprising; as the specimens did not fail and deflected significantly, such that they touched the supports during testing. This was quite unexpected for carbon fibre epoxy laminates, as they generally have a high modulus of elasticity. In order to determine if this was an anomaly with these laminates, the seven-layer stitched carbon laminate that was fabricated previously was tested. The results were identical, indicating that this was a property of this composite material. The elastic moduli of these laminates was calculated using equation (8.2), and the results were unsurprisingly low as well. It was, however, noticed that elastic modulus decreased with increasing filler loading.

The results for compressive testing showed an initial increase, and then a decrease in compressive strength. The change was not too significant, but was in accordance with the change displayed in tensile testing. Failure was observed to have occurred at the midsection, by splitting of fibres in the  $\pm 45^\circ$  plane. Compressive strength was observed to be approximately 10 MPa higher than tensile strength in the laminates. However, it has been found after consulting Prof. Adali at the School of Mechanical Engineering, UKZN, that compressive strength of carbon fibre laminates should likely be lower than their tensile strength due to micro-buckling of the fibres [139]. In his experience, Prof. Adali has only seen one example in which compressive strength equalled tensile strength [139].

#### b. Electrical Resistivity and Conductivity Testing

**Table 10.2: Electrical Properties of Aluminium-doped Stitched Carbon Fibre Laminates**

	0% Filler	7.5% Filler	15% Filler
<b>Resistance (<math>\Omega</math>)</b>	8.1000	7.2000	13.2000
<b>Resistivity (<math>\Omega \cdot \text{cm}</math>)</b>	1.8520	1.4456	2.7940
<b>Conductivity (<math>\Omega / \text{cm}</math>)</b>	0.5399	0.6917	0.3579
<b>Relative Conductivity * (<math>\times 10^{-3}</math>)</b>	3.8266	4.9021	2.5364

Note \* Relative to a copper plate of the same size measured on the same instrument

The electrical resistance results measured for the composites surprisingly indicated that resistance increased between 7.5% and 15% filler loading. This could be due to the instrument not measuring electrical resistance strictly in the current-carrying path of the laminate, as it provides

an indication of bulk resistance. The fibres were oriented in  $\pm 45^\circ$  in this stitched fabric, and this could have led to a discrepancy in the electrical resistance value obtained. In addition to this, the disordered arrangement of the electrically conductive particles within the matrix could also have influenced resistance measurements.

It was mentioned that the far-field region is of significance in this work, and thus the far-field EMSE equations presented in Chapter 4 were used to analytically calculate the required variables for these specimens. The frequency range used was between 750 MHz and 5 GHz, which was the same frequency range adopted for the actual EMSE testing. There were 801 data points in this frequency range, and thus results are presented by means scatter-point graphs. The calculations at all of these points are not presented as their computation exceeds several thousand pages, but sample calculations may be found Appendix D.

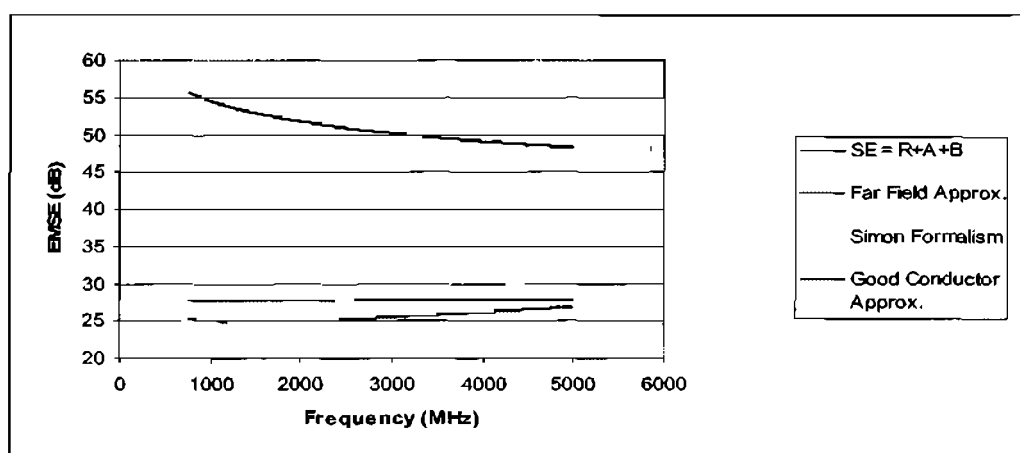


**Figure 10.5:** Comparative graph of EMSE (analytical) vs. Frequency for undoped stitched carbon fibre specimens

As seen in Figure 10.5, the EMSE value obtained from use of equations (4.14), (4.15) and (4.18) for the approximation of EMSE yield results that are in a great deal of agreement. However, these equations do not correlate with equation (4.6), and there was approximately 25 dB discrepancy between the results. For instance, it can be seen by use of equation (8.9) that EMSE provided by equation (4.6) indicates an average wave penetration of only 0.3%, whilst the rest of the equations indicate an average wave penetration of 4% through the shielding material. This discrepancy could be due to the use of the relative conductivity variable in equation (4.6) whereas the

conductivity variable was used in the other equations. Therefore, the results may not be exactly comparable.

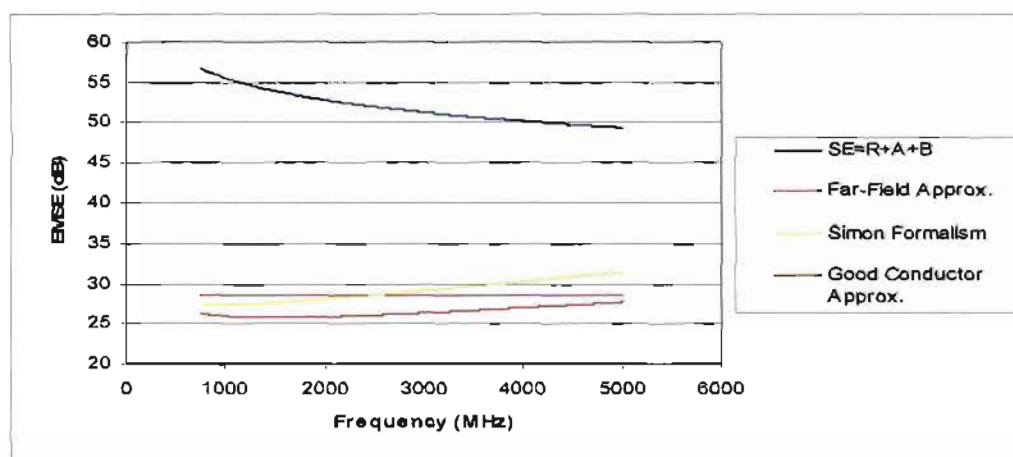


**Figure 10.6:** Comparative graph of EMSE (analytical) vs. Frequency for 7.5% aluminium-doped stitched carbon fibre specimens

As the equations yield values of EMSE which are proportional to electrical conductivity, it can be seen that higher EMSE results when materials with higher conductivity are used, as was the case in the 7.5% aluminium-doped sample in this case. As expected, the lower conductivity displayed by the 15% filler sample resulted in it possessing the lowest EMSE of the three stitched carbon samples.

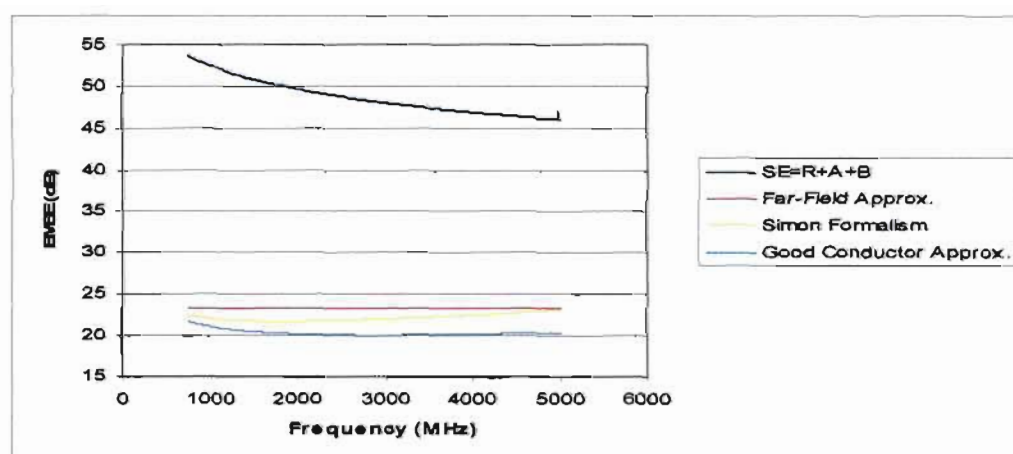


**Figure 10.7:** Comparative graph of EMSE (analytical) vs. Frequency for 15% aluminium-doped stitched carbon fibre specimens

Theoretical barrier impedance and skin depth values over the same frequency range have also been analytically computed using data obtained from electrical resistance testing for all samples. These results were computed by use of equations (4.16) and (4.20), and may be found in Appendix E.

It was mentioned in Chapter 4 that the analytical equations yield approximate results, and has previously been reported to not correlate with actual EMSE values in practice [40]. Thus, it was felt that a true indication of the shielding capabilities was best determined by actual EMSE testing, and comparing the obtained results relative to an aluminium plate, which is known to be an excellent shielding material in aircraft.

### c. Actual Electromagnetic Shielding Effectiveness Testing

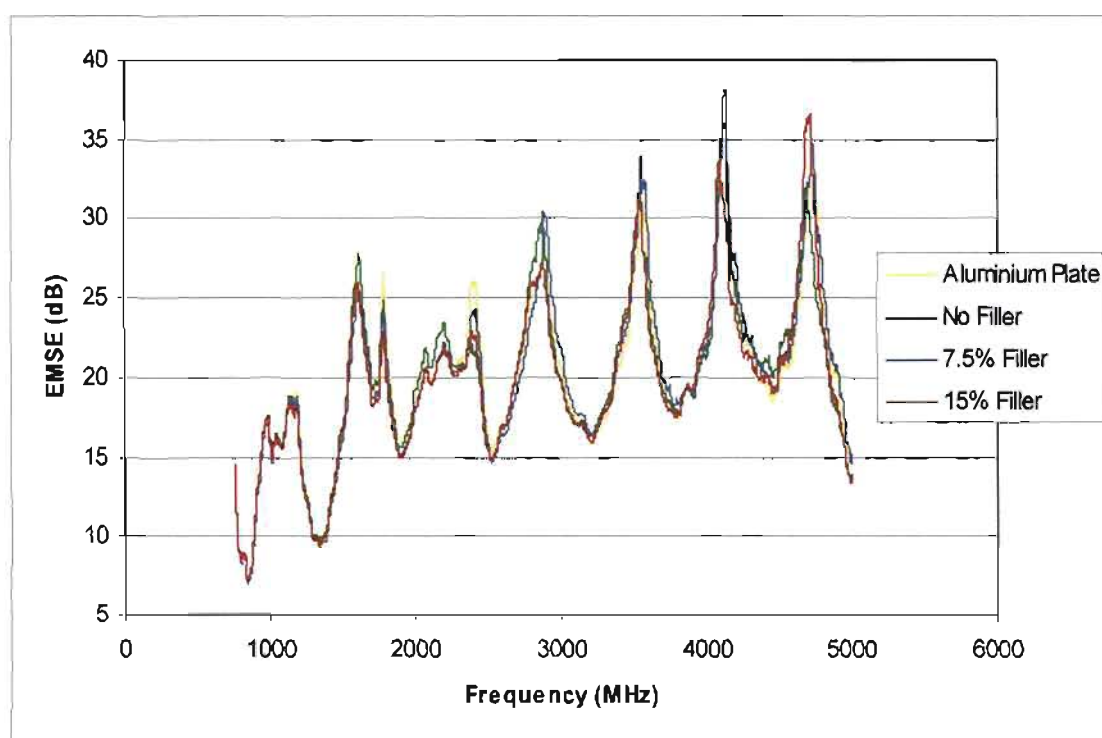


**Figure 10.8:** Actual EMSE vs. Frequency for undoped and aluminium-doped stitched carbon samples relative to an aluminium plate of the same size

The results indicate that the materials behave in a similar manner to aluminium in practice. From Figure 10.8 it may be seen that the sample with no filler can suffice the shielding requirement in the frequency range between 1.6 GHz to 3 GHz. Above this range, the 7.5% and 15% aluminium-

doped samples display superior shielding, with the former generally being better than the latter. However, diffraction on the aluminium plate could have resulted in EMSE appearing lower than the shielding materials at some of the data points [44].

Full scatter point graphs depicting Actual EMSE vs. Frequency; Transmission vs. Frequency; and Penetration vs. Frequency for all of the laminates in this work can be seen in Appendix F.

### 10.1.1.3 Results and Discussion of 12K Woven Carbon Fibre Samples

#### a. Mechanical Testing

**Table 10.3: Average Mechanical Properties of Aluminium-doped Woven Carbon Fibre Laminates**

	0% Filler	7.5% Filler	15% Filler
<b>Tensile Strength (MPa)</b>	821 (47)	659 (86)	613 (63)
<b>Yield Strength (MPa)</b>	780 (47)	659 (86)	613 (63)
<b>Tensile Yield Elongation (%)</b>	4.0 (0.2)	2.8 (0.2)	3.0 (0.2)
<b>Break Elongation (%)</b>	4.3 (0.4)	2.8 (0.2)	3.0 (0.2)
<b>Flexural Strength (MPa)</b>	531 (97)	597 (54)	645 (65)
<b>Elastic Modulus (GPa)</b>	72.9192 (19.6554)	51.0484 (6.9043)	44.0801 (1.9695)
<b>Compressive Strength (MPa)</b>	136 (16)	217 (48)	206 (32)

These samples displayed a much higher tensile strength and tensile yield point than the stitched samples. Failure in tensile testing was characterised by a loud “snapping” noise as the samples fractured at 0° on the midsection of the specimen length. The average results are shown in Table 10.3. The results show that tensile strength decreases with increasing filler loading, but elongation was found to initially decrease and then increase slightly thereafter.

Flexural testing showed that bending strength increased slightly with increasing filler loading. However, elastic moduli decreased quite significantly as filler increased. Failure in these samples

was characterised by a loud noise, but only minor fracture across the upper layers of the width of the midsection was observed.

The results obtained from compressive testing of these specimens were dubious, as localised crushing of the end surfaces was observed when the samples were returned from the test location. There was no visible failure on the specimen length, and the apparent compressive strength was much lower than tensile strength. While variance in results could be a result of the testing machine and tester, which was different from that used for the other mechanical tests, there was some doubt regarding these results.

#### **b. Electrical Resistivity and Conductivity Testing**

The electrical resistances were measured in accordance with the method described in Chapter 8. The result obtained indicated that electrical resistance increased between the undoped and 7.5% aluminium-doped samples. This could very likely have been due to the  $0^\circ/90^\circ$  fabric alignment. The thick 12K weaves could have resulted in erroneous results when bulk resistance was measured across the length, due to continuous overlapping of the fibres. Also, the disordered arrangement of the electrically conductive particles further influences resistance measurements. The resistance results obtained were higher than that of the stitched fabric.

**Table 10.4: Electrical Properties of Aluminium-doped Woven Carbon Fibre Laminates**

	<b>0% Filler</b>	<b>7.5% Filler</b>	<b>15% Filler</b>
<b>Resistance (<math>\Omega</math>)</b>	23.3000	50.0000	16.6000
<b>Resistivity (<math>\Omega \cdot \text{cm}</math>)</b>	4.8047	13.4163	4.4847
<b>Conductivity (<math>\Omega/\text{cm}</math>)</b>	0.2081	0.0745	0.2229
<b>Relative Conductivity * (<math>\times 10^{-3}</math>)</b>	1.4749	0.5282	1.5802

Note \* Relative to a copper plate of the same size measured on the same instrument

The same frequency range, 750 MHz to 5 GHz, was used for the analytical computation of EMSE in these samples. Again, the results of these computations are shown by means of graphs.



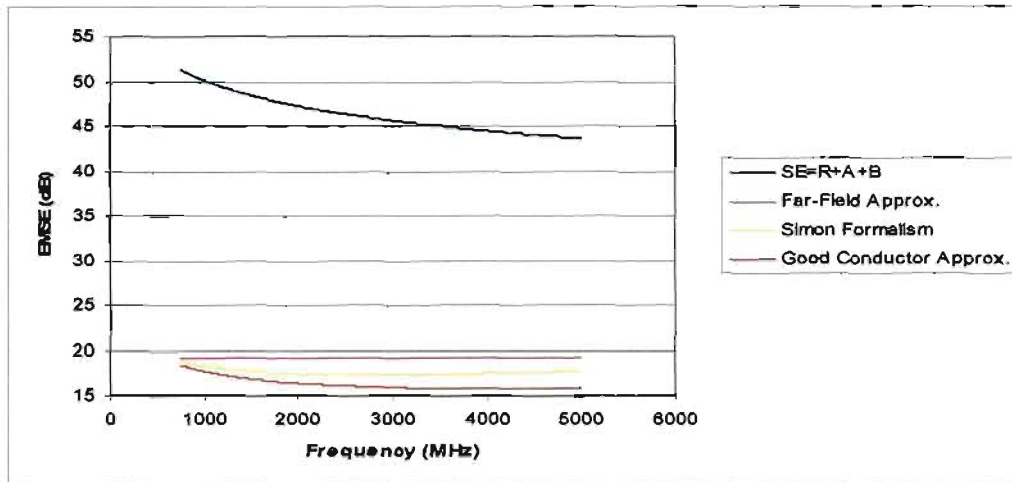


**Figure 10.9:** Comparative graph of EMSE (analytical) vs. Frequency for undoped woven carbon fibre specimens

As the electrical conductivity of these samples was not particularly high, the resulting EMSE was low when calculated using the equations as they are dependant on conductivity. However there were discrepancies with the analytical EMSE values, as the EMSE obtained from equation (4.6) implies an average wave penetration of 0.5%, whilst the EMSE obtained from equations (4.14), (4.15) and (4.18) indicate a much higher average wave penetration of 39%. This could be due to the use of the relative conductivity variable in the computation of equation (4.6), whilst the other equations were computed using the conductivity variable.

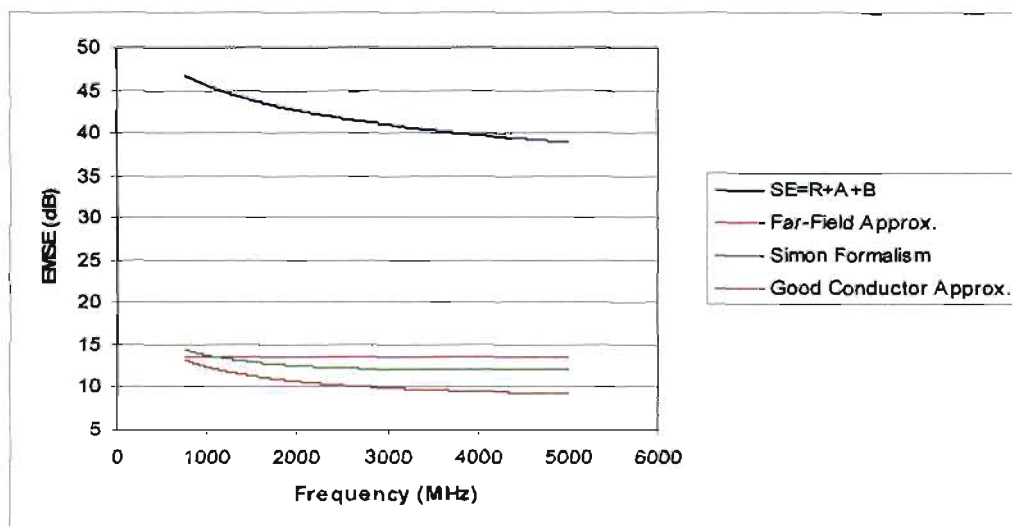


**Figure 10.10:** Comparative graph of EMSE (analytical) vs. Frequency for 7.5% aluminium-doped woven carbon fibre specimens

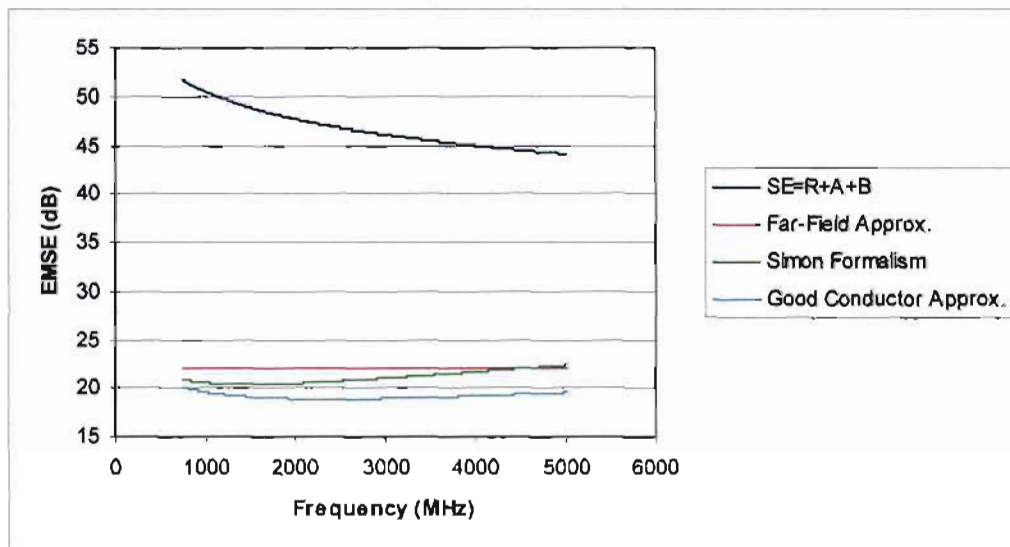


**Figure 10.11:** Comparative graph of EMSE (analytical) vs. Frequency for 15% aluminium-doped woven carbon fibre specimens

These results, as expected, show the lower conductivity displayed by the 7.5% aluminium-doped sample resulted in it theoretically possessing the lowest EMSE of the three woven carbon samples.

#### c. Actual Electromagnetic Shielding Effectiveness Testing

The EMSE of the aluminium-doped samples were measured, and the results showed that the 7.5% filler loading sample in fact contained the best EMSE of the woven carbon fibre samples. The undoped sample also proved to be adequate in emulating the quality of shielding found in aluminium, as is evidenced by the graph in Figure 10.12. The sample containing 15% aluminium filler did not display any significant improvement in shielding capabilities, but was the paramount shielding material prior to frequencies above 2 GHz.

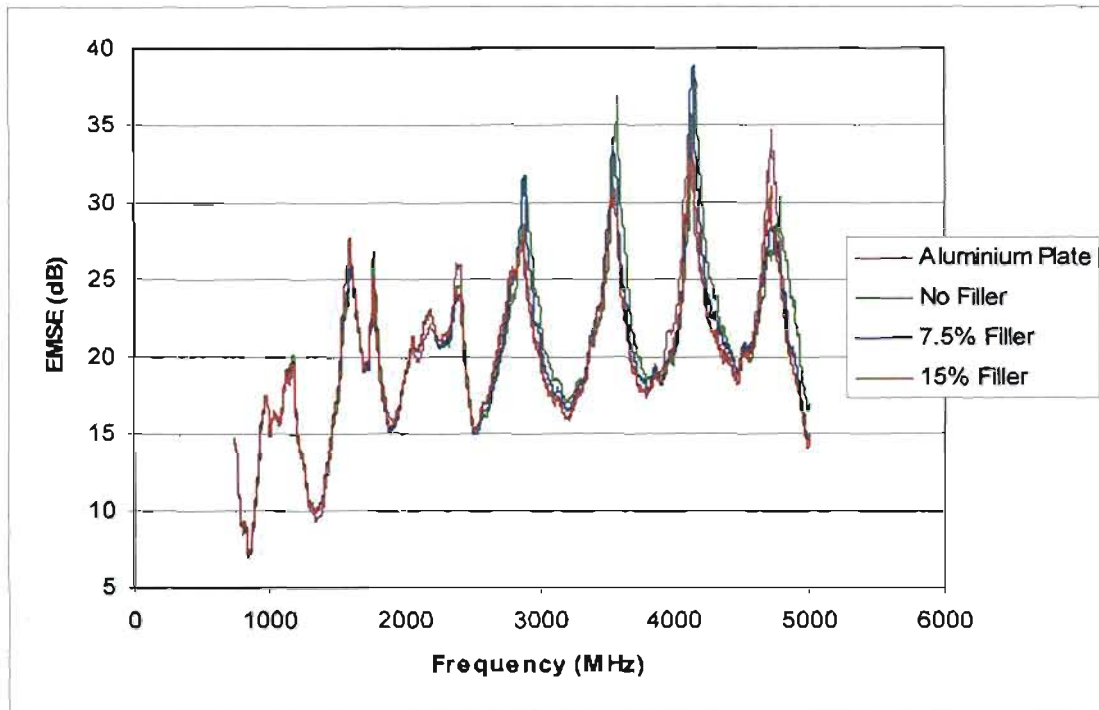


*Figure 10.12: Actual EMSE vs. Frequency of the undoped and aluminium-doped woven samples relative to an aluminium plate of the same size*

#### 10.1.1.4 Results and Discussion of Unidirectional Carbon Fibre Samples

##### a. Mechanical Testing

**Table 10.5: Average Mechanical Properties of Aluminium-doped Unidirectional Carbon Fibre Laminates**

	0% Filler	7.5% Filler	15% Filler
<b>Tensile Strength (MPa)</b>	841 (56)	796 (100)	704 (127)
<b>Yield Stress(MPa)</b>	839 (56)	777 (99)	628 (125)
<b>Tensile Yield Elongation (%)</b>	4.2 (0.0)	3.3 (0.3)	2.4 (0.5)
<b>Break Elongation (%)</b>	4.2 (0.3)	3.4 (03)	2.7 (0.4)
<b>Flexural Strength (MPa)</b>	1135 (39)	1068 (28)	1051 (33)
<b>Elastic Modulus (GPa)</b>	180.3777 (27.5470)	152.9789 (57.8662)	118.1243 (2.5305)
<b>Compressive Strength (MPa)</b>	155 (5)	237 (104)	236 (51)

The unidirectional specimens were tested in the direction parallel to fibre orientation for all of the mechanical tests. This orientation was selected as it was thought that this would be the most likely orientation in practice, and is also the direction of current flow in the material.

These samples displayed highest tensile strength when compared with the other carbon fabric results. This was expected, as this was a 100% unidirectional fabric. Failure in tensile testing was generally due to splitting at the 0° plane of the fibres on the outer regions of the midsection, and was characterised by “snapping” noises heard as the individual fibres snapped. The samples did not visibly snap at the midsection as with the woven and stitched samples. This was likely due to the higher strength of the unidirectional fibres. In some instances, delamination of the fibres in the fibre direction in the grip surfaces was observed. Such a problem was reported in [105], and the results of these samples were not included. As this phenomenon occurred at least once in every test, at least six unidirectional specimens were tested for every tensile test in this work. These results indicate that tensile strength is inversely proportional to filler loading, as are tensile yield and break elongations.

Flexural testing showed that bending strength decreased slightly with increasing filler loading. However, as in the woven samples, the elastic moduli decreased quite significantly. Failure in these samples was characterised by a loud noise, but only minor fracture across the outer layer along the width of the midsection was observed.

The compressive strength data obtained were dubious in these specimens, as there was visible evidence of localised crushing on the end surfaces of the specimens. There was no visible failure on the specimen length either. However, these results obtained show that compressive strength was substantially lower than tensile strength.

#### b. Electrical Resistivity and Conductivity Testing

The electrical resistances were measured in accordance with the method described in Chapter 8. The results obtained indicated that electrical resistance increased proportionally with filler loading, which was thought to be unlikely. However, it can be seen that the undoped unidirectional samples displayed a lower resistivity than the other carbon fabrics, which is likely due to the unidirectional fibre orientation in them. This likely provides a constant unidirectional current-carrying path in the laminates, and thus a lower bulk resistance was obtained from the test

instrument. Electrical resistance was measured in the direction perpendicular to fibres on the undoped specimen, and the resistance results were an order of magnitude higher than that obtained in the fibre direction. Thus, the inclusion of fillers could have influenced the unidirectional current-carrying path, as the particles were disordered in arrangement within the matrix material. In the doped samples, bulk resistance may not necessarily have been measured strictly across the fibre direction, as the particles included were of a lower resistance and were not necessarily aligned in the fibre direction within the composite.

**Table 10.6: Electrical Properties of Aluminium-doped Unidirectional Carbon Fibre Laminates**

	0% Filler	7.5% Filler	15% Filler
<b>Resistance (<math>\Omega</math>)</b>	5.9000	10.7000	11.0000
<b>Resistivity (<math>\Omega \cdot \text{cm}</math>)</b>	1.2421	2.7201	2.7563
<b>Conductivity (<math>\Omega / \text{cm}</math>)</b>	0.8050	0.3676	0.3627
<b>Relative Conductivity<sup>*</sup> (<math>\times 10^{-3}</math>)</b>	5.7053	2.6053	2.5710

Note <sup>\*</sup> Relative to a copper plate of the same size measured on the same instrument

The results of the analytical computations of EMSE in these samples using equations (4.6), (4.14), (4.15) and (4.18) are shown by means of graphs. The frequency range used was between, and including, 750 MHz to 5 GHz. Theoretical results of skin depth and barrier impedance vs. frequency have been computed using equations (4.16) and (4.20), and may be seen in Appendix E.

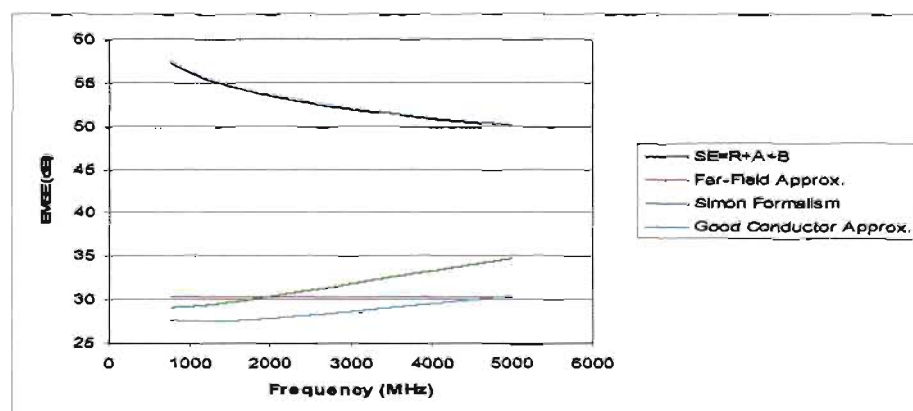


**Figure 10.13: Comparative graph of EMSE (analytical) vs. Frequency for undoped unidirectional carbon fibre specimens**

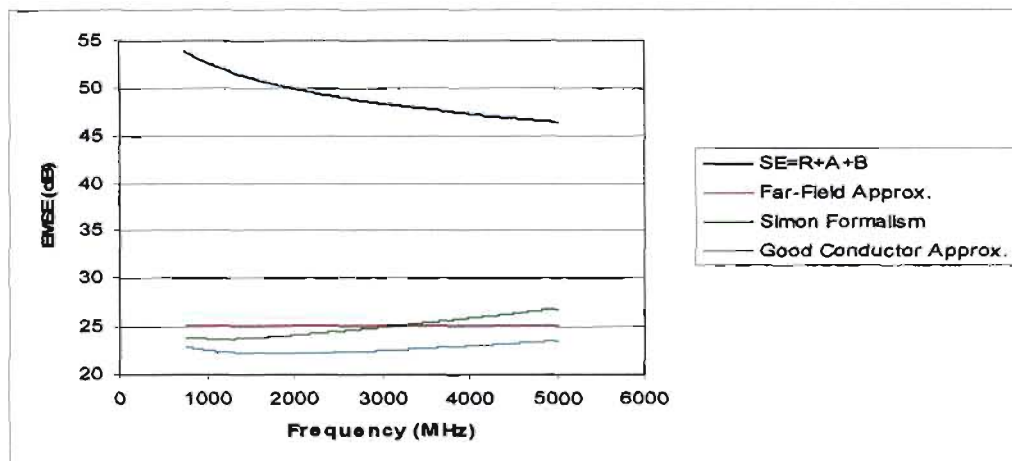


**Figure 10.14:** Comparative graph of EMSE (analytical) vs. Frequency for 7.5% aluminium-doped unidirectional carbon fibre specimens

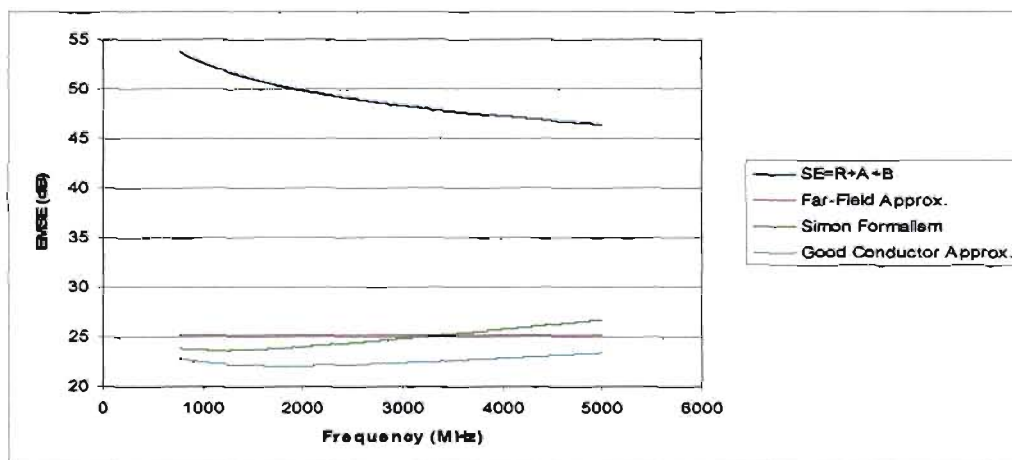


**Figure 10.15:** Comparative graph of EMSE (analytical) vs. Frequency for 15% aluminium-doped unidirectional carbon fibre specimens

The analytical results are dependant on electrical conductivity. The high electrical conductivity displayed by unidirectional materials resulted in these samples theoretically displaying a higher EMSE than the other carbon fabric laminates.

### c. Electromagnetic Shielding Effectiveness

The EMSEs of the unidirectional samples were measured, and the results showed that the unidirectional laminates generally contained excellent inherent shielding capabilities. The

undoped sample was found to be slightly inferior in shielding performance opposed to those with fillers, which was more plausible. The 7.5% aluminium-doped sample showed an improvement, and even displayed the highest EMSE of all the samples at approximately 4.5-4.7 GHz, but the 15% aluminium-doped sample matched the shielding displayed by aluminium over the entire frequency range in question to a greater degree.

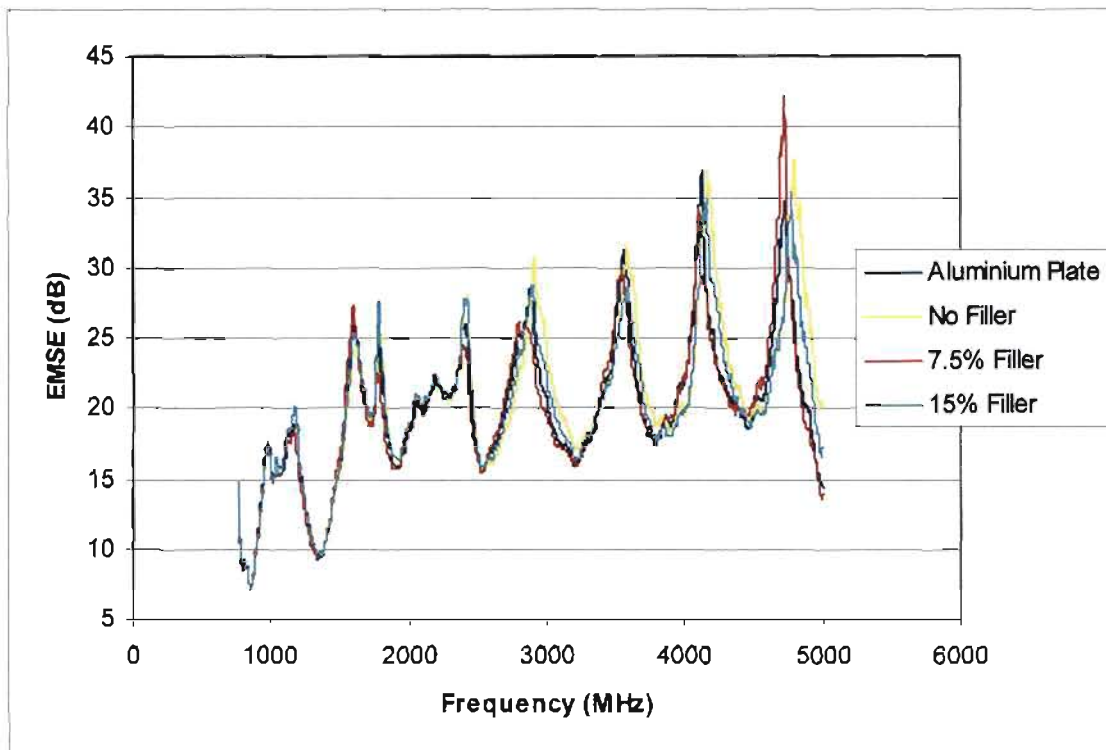


*Figure 10.16: Actual EMSE vs. Frequency of the undoped and aluminium-doped unidirectional samples relative to an aluminium plate of the same size*

## **10.1.2 Copper-doped Samples**

### **10.1.2.1 Manufacture**

Copper was selected based on its high electrical conductivity. Copper is inherently heavier than aluminium in weight, and as mass is proportional to volume, it was known that there would be less copper particles introduced by percentage weight into the same resin quantity. The copper particles were also found to be significantly smaller in size ( $0.5\text{--}10\ \mu\text{m}$ ) when compared with aluminium particles. There was some suspicion that weight and size may negatively influence



EMSE properties, as it was assumed there would be significantly less connectivity achieved between these particles as opposed to aluminium particles.

However, it was known that EMSE is not strictly dependant on connectivity, but is enhanced by connectivity of the particles [5]. Copper is known to display significantly superior electrical conductivity when compared with aluminium, and it was thought that copper powder could result in laminates that display improved shielding despite the lack of connectivity. In addition, Chung [5], explicitly states that smaller particles as filler materials often result in superior shielding due to the skin effect.

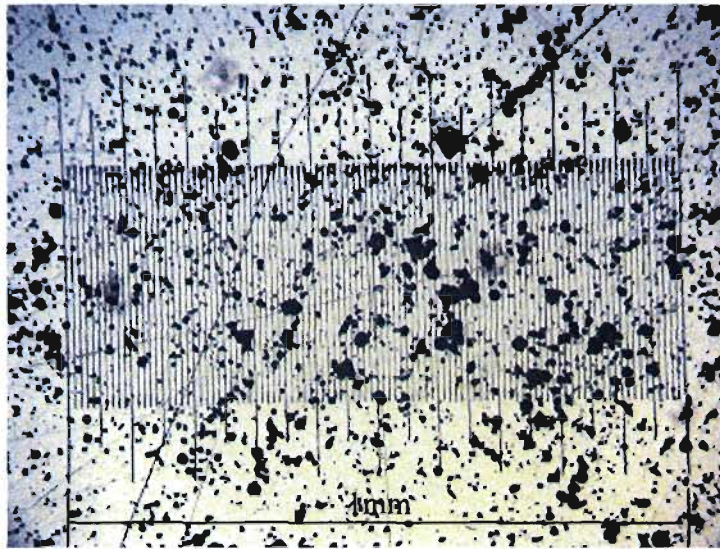


*Figure 10.17: Copper powder particles under a microscope*

All of the copper-filled samples were fabricated using the twin-mould system to ensure the matrix material of all test specimens was consistent in composition. The samples were manufactured using the hand lay-up process, which was performed in the exact manner used for previously described samples.

Prior to introduction into the undoped resin, the copper powder was thoroughly sifted, to ensure that the particles did not cluster together in the matrix. Due to the mass of the particles, they had begun to sink to the bottom of the container upon introduction into the resin source. The material was thoroughly mixed for 5mins at 180rpm, with careful attention being paid to the bottom and sides of the container. The resin also changed in colour, texture and viscosity, with increasing copper loading. The 7.5% copper-doped mixture was reddish-brown in colour, and the 15%



copper-doped mixture was a darker brown shade. It was also noted that the copper-doped resins were more viscous and smoother in texture opposed to the aluminium-doped resins. Figure 10.18 indicates the resin colour change as increasing filler loading was applied.



*Figure 10.18: The resin colour changed from being a transparent, light yellow colour to an opaque reddish-brown shade. The texture also changed, but was not as rough as the aluminium-enriched fluid, as filler loading increased.*

When the laminates were cured, they were observed to be dark brown in colour, due to the resin used. The specimens were viewed under a microscope to determine the level of connectivity between the particles within the matrix. The results show that there was indeed significantly less connectivity between the copper particles opposed to aluminium.

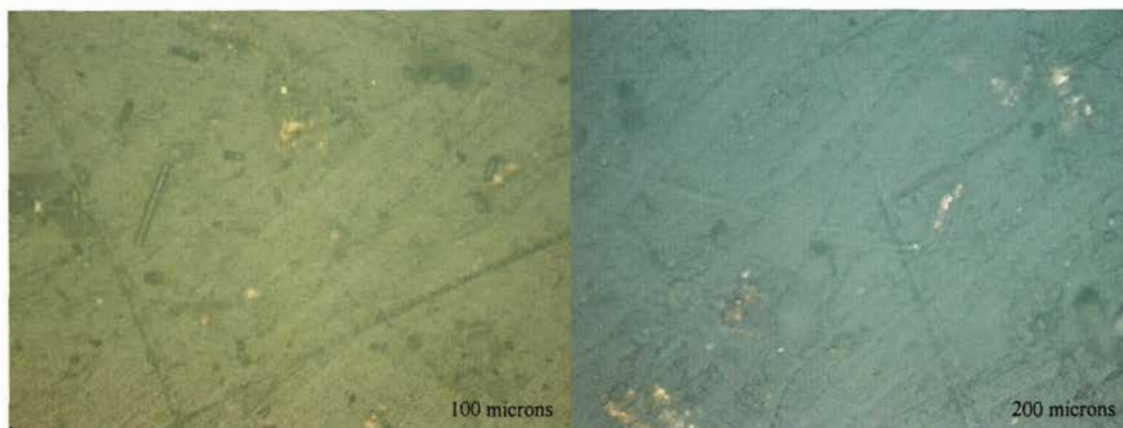


**Figure 10.19:** An image depicting 100x and 200x magnification of 7.5% copper filler side by side. Larger microscopic spaces between the copper particles, opposed to the aluminium powder samples, were clearly evident.

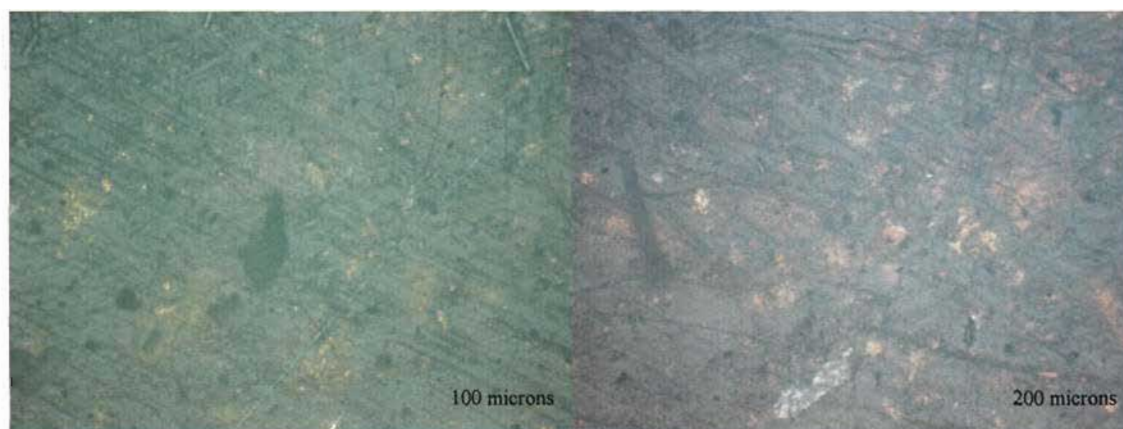


**Figure 10.20:** An image depicting 100x and 200x magnification of 15% copper loading samples. The difference in connectivity between the 15% copper-doped samples and 7.5% copper doped samples is clearly evident.

### 10.1.2.2 Results and Discussion of Stitched Carbon Fibre Samples

#### a. Mechanical Testing

**Table 10.7: Average Mechanical Properties of Copper-doped Stitched Carbon Fibre Laminates**

	0% Filler	7.5% Filler	15% Filler
<b>Tensile Strength (MPa)</b>	73 (3)	75 (5)	78 (3)
<b>Yield Strength (MPa)</b>	61 (3)	61 (5)	58 (3)
<b>Tensile Yield Elongation (%)</b>	1.0 (0.1)	0.8 (0.0)	0.8 (0.0)
<b>Break Elongation (%)</b>	3.1 (0.4)	3.0 (0.7)	3.8 (0.7)
<b>Flexural Strength (MPa) *</b>	N/A	N/A	N/A
<b>Elastic Modulus (GPa)</b>	14.1370 (1.4486)	11.2049 (1.1467)	10.0191 (1.0395)
<b>Compressive Strength (MPa)</b>	79 (4)	96 (5)	90 (2)

Note: \* Flexural strength was indeterminate as the specimens deflected excessively and touched the supports of the testing rig before failure – The low elastic moduli obtained is indicative of this

The results obtained from tensile testing were similar to that of the aluminium-filled samples. The copper-doped samples had low tensile strengths, which did increase slightly as filler loading increased. Tensile failure was characterised by separation of the fibres at midsection of the specimen at  $\pm 45^\circ$ .

The samples deflected excessively during flexural testing and bending strength was thus indeterminate. The samples displayed a low elastic modulus, which decreased proportionally with increasing filler loading.

Compressive failure was characterised by failure in the midsection of the specimen length at  $\pm 45^\circ$ . As with tensile strength, compressive strength was seen to increase in the doped samples. However, a decrease in compressive strength was seen between the 7.5% copper-doped samples and the 15% copper-doped sample. The compressive strength obtained was significantly higher than tensile strength as well, which appears to be incorrect.

### b. Electrical Resistivity and Conductivity Testing

**Table 10.8: Electrical Properties of Copper-doped Stitched Carbon Fibre Laminates**

	0% Filler	7.5% Filler	15% Filler
Resistance ( $\Omega$ )	8.1000	21.0000	23.2000
Resistivity ( $\Omega \cdot \text{cm}$ )	1.8520	4.2941	4.8768
Conductivity ( $\Omega / \text{cm}$ )	0.5399	0.2328	0.2050
Relative Conductivity <sup>*</sup> ( $\times 10^{-3}$ )	3.8266	1.6503	1.4513

Note<sup>\*</sup> Relative to a copper plate of the same size measured on the same instrument

The results of the analytical computations of EMSE in these samples are again shown by means of comparative graphs. The graph depicting the analytical results of the undoped stitched carbon specimen was presented in Figure 10.5.

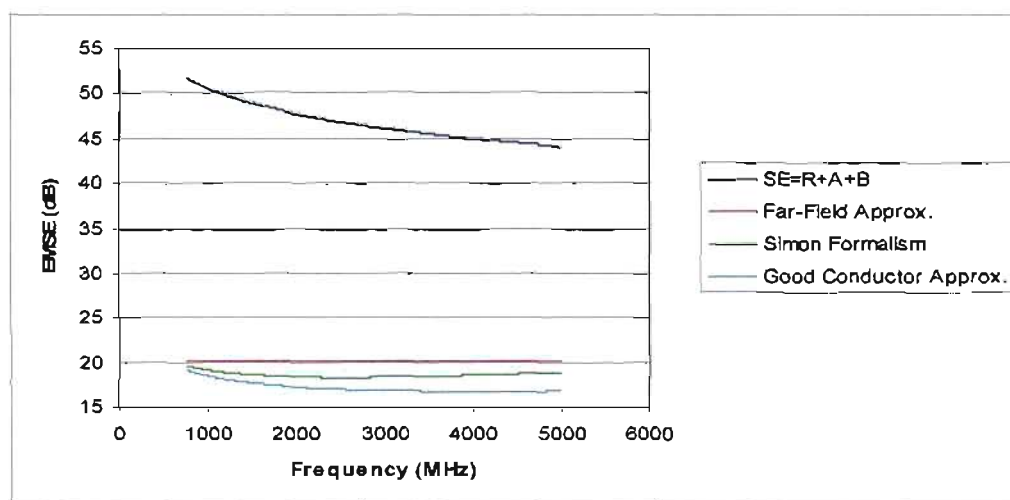


**Figure 10.21: Comparative graph of EMSE (analytical) vs. Frequency for 7.5% copper-doped stitched carbon fibre specimens**

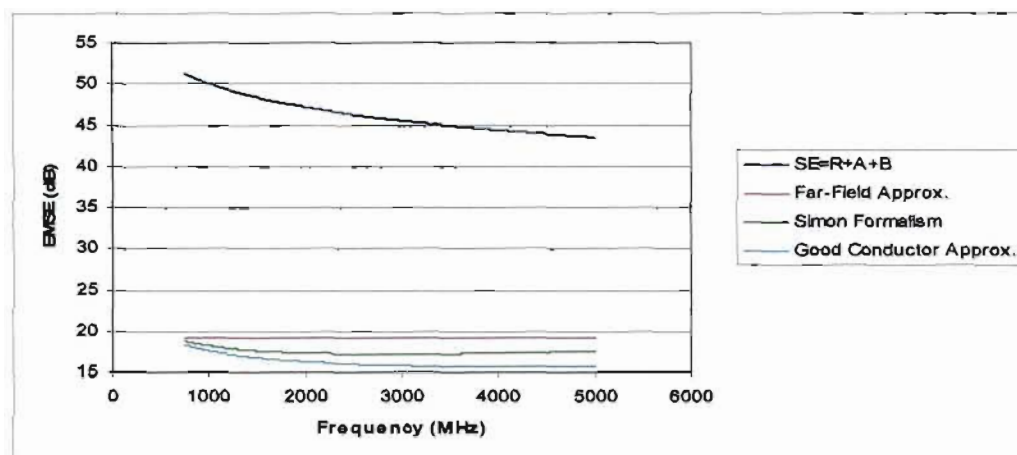


*Figure 10.22: Comparative graph of EMSE (analytical) vs. Frequency for 15% copper-doped stitched carbon fibre specimens*

The results from Figures 10.21 and 10.22 again show that the results obtained from equations (4.14), (4.15) and (4.18) were in agreement, whilst equation (4.6) did not correlate with these results. In Figure 10.22 for example, from use of equation (8.9), equations (4.14), (4.15) and (4.18) yields an average EMSE that implies an average wave penetration of 14%, whilst equation (4.6) yields an average EMSE that indicates an average wave penetration of 0.6%. However, as mentioned earlier, these results are not exactly comparable, as equation (4.6) uses the relative conductivity variable, as opposed to the conductivity variable which is used in the other equations.

### c. Electromagnetic Shielding Effectiveness Testing

The actual EMSEs of the samples were measured, and the results showed that the shielding capabilities did indeed improve with increasing filler loading. Apart from the 4.5-4.7 GHz range, the sample which contained 15% copper powder displayed superior shielding quality compared with the EMSE displayed by the undoped and 7.5% copper-doped samples. The 15% copper-doped sample displayed similar EMSE as the aluminium plate over the entire range of frequency in question.

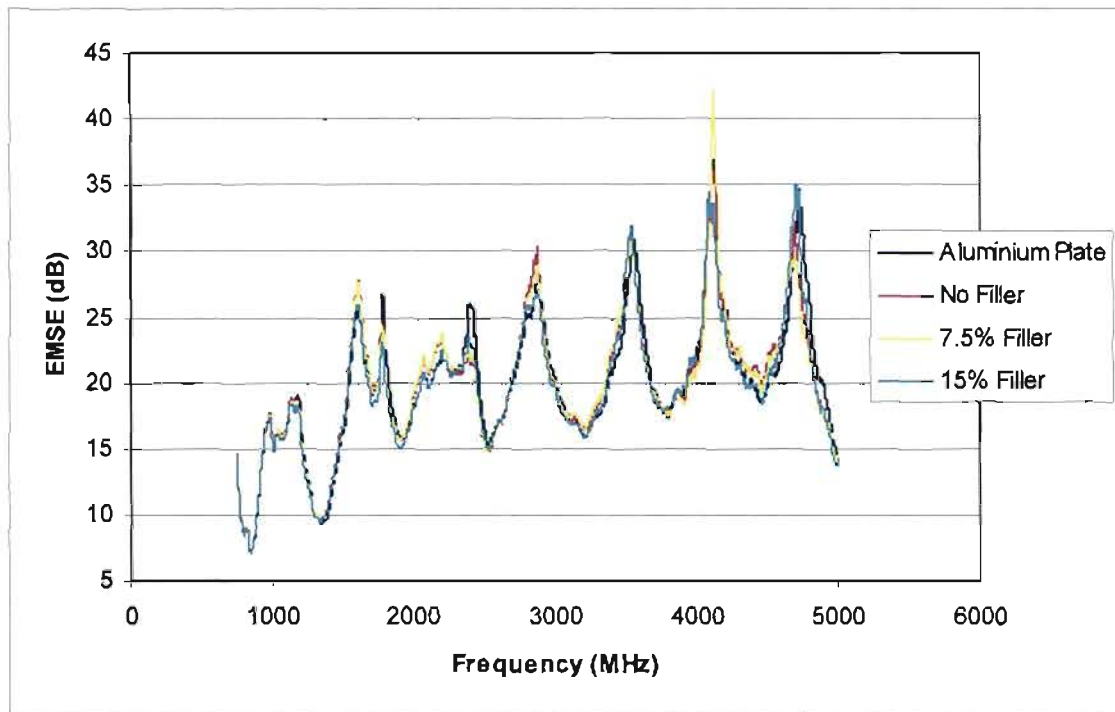


**Figure 10.23:** Actual EMSE vs. Frequency of the undoped and copper-doped stitched carbon fibre specimens relative to an aluminium plate of the same size

### 10.1.2.3 Results and Discussion of 12K Woven Carbon Fibre Samples

#### a. Mechanical Testing

**Table 10.9: Average Mechanical Properties of Copper-doped Woven Carbon Fibre Laminates**

	0% Filler	7.5% Filler	15% Filler
<b>Tensile Strength (MPa)</b>	821 (47)	636 (76)	661 (61)
<b>Yield Strength (MPa)</b>	780 (47)	636 (76)	660 (61)
<b>Tensile Yield Elongation (%)</b>	4.0 (0.2)	2.9 (0.2)	3.0 (0.2)
<b>Break Elongation (%)</b>	4.3 (0.4)	2.9 (0.2)	3.0 (0.2)
<b>Flexural Strength (MPa)</b>	531 (97)	828 (75)	752 (108)
<b>Elastic Modulus (GPa)</b>	72.9192 (19.6554)	44.9735 (3.0181)	51.4442 (3.3115)
<b>Compressive Strength (MPa)</b>	136 (16)	263 (38)	269 (8)

The tensile test results showed that tensile strength decreased with introduction of copper particles into the matrix. However, the tensile strength was slightly lower for the 7.5% copper-doped specimen than in the 15% copper-doped specimen. However, this was thought to be insignificant, as it was by 3%. Tensile strength decreased by 22% between 0% filler and 7.5% filler loadings. It is quite unlikely that tensile strength will significantly increase should filler loading higher than 15% be introduced. During testing, failure was characterised by a loud noise, and the specimens were generally observed to fail along the midsection at the 0° plane in a fibre snap.

Flexural testing showed that bending strength increased by 42% as filler loading increased to between the undoped and 7.5% copper-doped sample, but then decreased by 11% between the 7.5% and 15% copper-doped samples. The variance in elastic moduli behaved in an inversely proportional manner to the variance in bending strength. That is, elastic modulus was higher for specimens with lower bending strength. Failure in these samples was characterised by a loud noise, but only a minor fracture across the width of the midsection was observed.

The compressive test results were considered to be an inaccurate indication of the actual compressive strength possessed by the materials, as localised crushing of the end surfaces of the specimens were observed to have taken place.

#### **b. Electrical Resistivity and Conductivity Testing**

The results obtained from the electrical resistance measurements indicated that electrical resistance increased significantly with increasing filler loading, which seemed unlikely. As with the aluminium-doped samples, this increase could very likely have been due to the  $0^\circ/90^\circ$  fabric alignment and the disordered arrangement of particles within the composite.

**Table 10.10: Electrical Properties of Copper-doped Woven Carbon Fibre Laminates**

	<b>0% Filler</b>	<b>7.5% Filler</b>	<b>15% Filler</b>
<b>Resistance (<math>\Omega</math>)</b>	23.3000	28.0000	64.0000
<b>Resistivity (<math>\Omega \cdot \text{cm}</math>)</b>	4.8047	7.1758	16.4937
<b>Conductivity (<math>\Omega / \text{cm}</math>)</b>	0.2081	0.1393	0.0606
<b>Relative Conductivity * (<math>\times 10^{-3}</math>)</b>	1.4749	0.9876	0.4297

Note \* Relative to a copper plate of the same size measured on the same instrument

The analytical EMSE results for the undoped woven carbon sample are presented in Figure 10.9. The results for the copper-doped samples are presented in Figures 10.24 and 10.25 respectively.



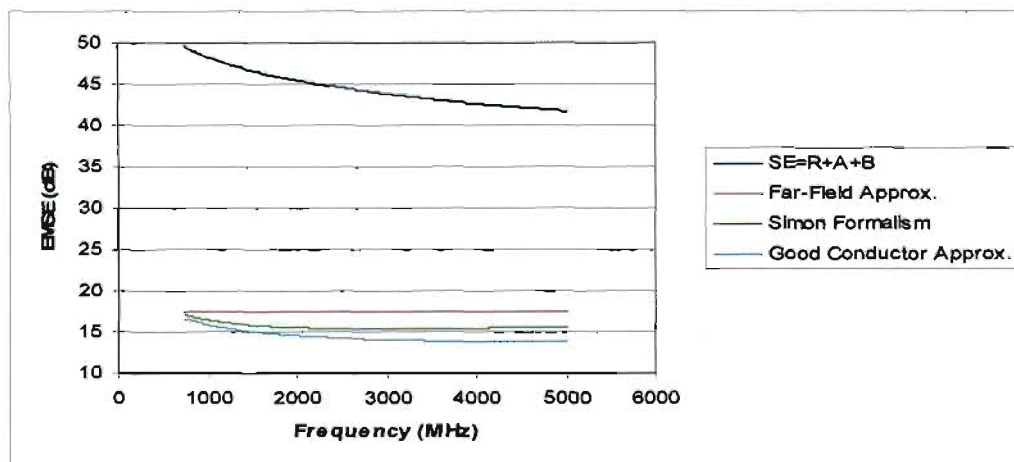


**Figure 10.24:** Comparative graph of EMSE (analytical) vs. Frequency for 7.5% copper-doped woven carbon fibre specimens

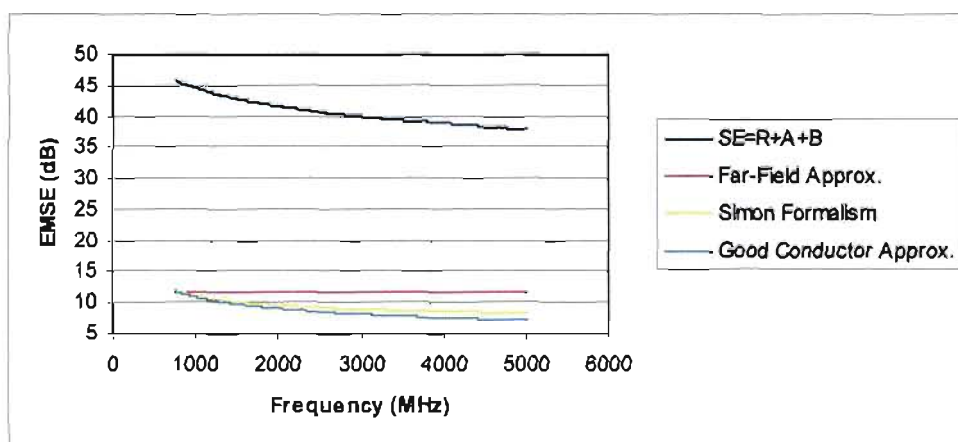


**Figure 10.25:** Comparative graph of EMSE (analytical) vs. Frequency for 15% copper-doped woven carbon fibre specimens

Due to the high electrical resistance measured for the sample with 15% filler loading, the resulting theoretical EMSE values were substantially lower than in the undoped and 7.5% copper-doped samples, which contained lower electrical resistances.

### c. Electromagnetic Shielding Effectiveness

The EMSE of the copper-doped samples was measured, and the results showed that the 15% filler loading sample did indeed possess the best shielding quality of the woven samples. The sample with no filler also proved to be adequate in simulating EMSE found in aluminium, and the sample with 7.5% filler displayed higher EMSE at 4.7 GHz. However, the sample containing 15% filler displayed very similar EMSE to that of the aluminium plate for the entire frequency range. Thus, it was unlikely that the value obtained from the electrical resistance testing was accurate, as this would have been indicative in the actual EMSE testing as well.

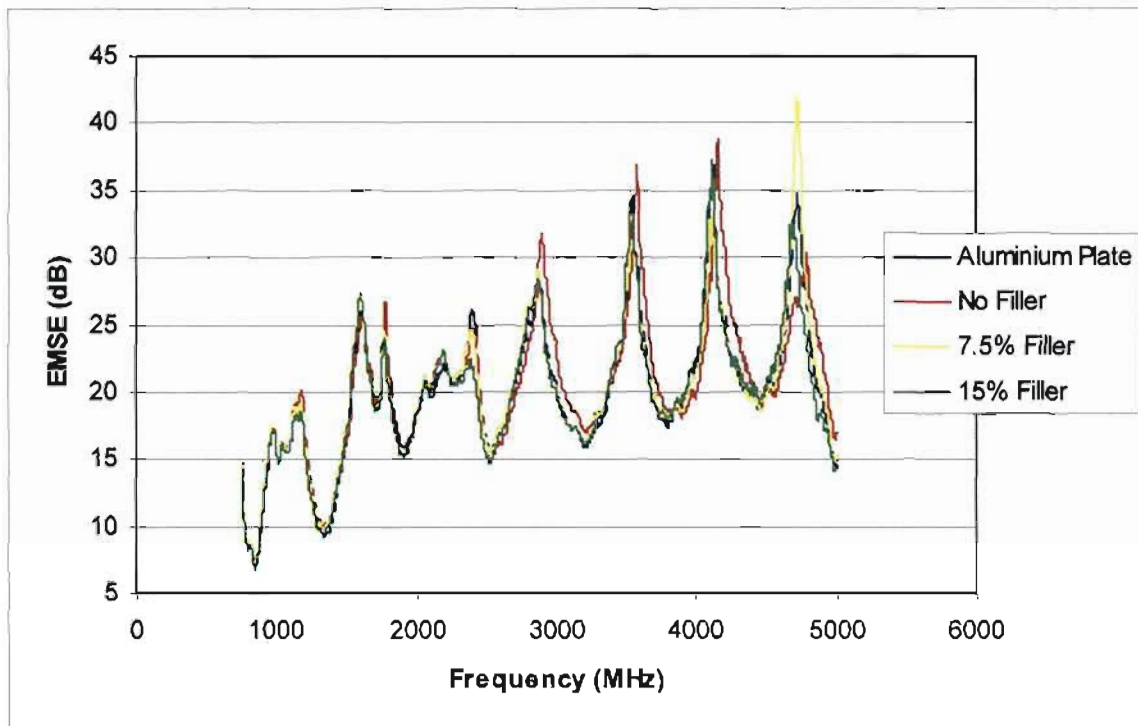


**Figure 10.26:** Actual EMSE vs. Frequency of the undoped and copper-doped woven samples relative to an aluminium plate of the same size

#### 10.1.2.4 Results and Discussion of Unidirectional Carbon Fibre Samples

##### a. Mechanical Testing

**Table 10.11: Average Mechanical Properties of Copper-doped Unidirectional Carbon Fibre Laminates**

	0% Filler	7.5% Filler	15% Filler
<b>Tensile Strength (MPa)</b>	841 (56)	769 (39)	739 (106)
<b>Yield Strength (MPa)</b>	839 (56)	740 (38)	695 (106)
<b>Tensile Yield Elongation (%)</b>	4.2 (0.0)	3.4 (0.1)	3.2 (0.3)
<b>Break Elongation (%)</b>	4.2 (0.3)	3.5 (0.2)	3.4 (0.3)
<b>Flexural Strength (MPa)</b>	1135 (39)	1036 (121)	1161 (67)
<b>Elastic Modulus (GPa)</b>	180.3777 (27.5470)	118.3419 (17.3473)	141.1579 (14.8274)
<b>Compressive Strength (MPa)</b>	155 (5)	231 (47)	275 (30)

Failure in tensile testing was alike to the other unidirectional carbon fibres tested, with splitting of the fibres at 0° on the outer regions of the midsection, and characterised by “snapping” noises. These results indicate that tensile strength is inversely proportional to filler loading, as are yield and break elongations. However, the reductions in tensile strength and elongations were lower than those observed in the aluminium-doped unidirectional samples. This could have been due to the lower concentration of particles within the matrix material.

Flexural testing showed an initial decrease in bending strength and elastic moduli between 0% filler and 7.5% filler loading, and then a slight increase between 7.5% and 15% filler loading. Failure in these samples was again characterised by a loud noise, but only a minor fracture perpendicular to the fibre direction across the outer layer midsection was observed.

Failure in compressive strength tests were due to crushing of the end surfaces, and were thus not considered as being a correct indication of the true compressive strength of the laminates. Failure of this type was consistent in all of these specimens.

### b. Electrical Resistivity and Conductivity Testing

**Table 10.12: Electrical Properties of Copper-doped Unidirectional Carbon Fibre Laminates**

	0% Filler	7.5% Filler	15% Filler
Resistance ( $\Omega$ )	5.9000	11.3000	14.3000
Resistivity ( $\Omega \cdot \text{cm}$ )	1.2421	2.6402	3.2496
Conductivity ( $\Omega / \text{cm}$ )	0.8050	0.3787	0.3077
Relative Conductivity <sup>*</sup> ( $\times 10^{-3}$ )	5.7053	2.6842	2.1808

Note <sup>\*</sup> Relative to a copper plate of the same size measured on the same instrument

The results of the analytical computations of EMSE displayed by the copper-doped samples are presented in Figures 10.27 and 10.28. The results for the undoped sample are shown in Figure 10.13. The relationship between EMSE and electrical current has been explained previously. The concerns, and possible reasons, regarding the unexpected increase in electrical resistance as filler loadings increased have been addressed previously, and the concerns are relevant to these samples as well.

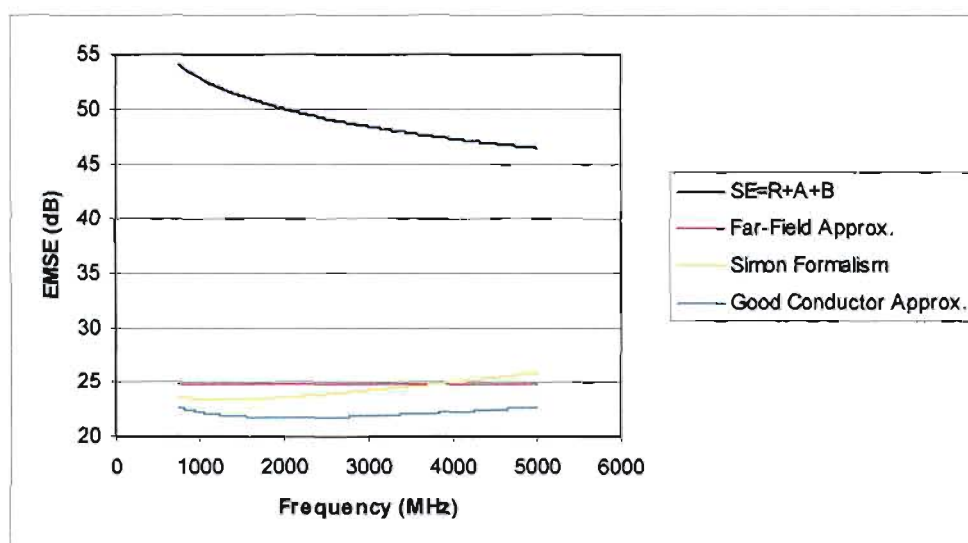


**Figure 10.27: Comparative graph of EMSE (analytical) vs. Frequency for 7.5% copper-doped unidirectional carbon fibre specimens**

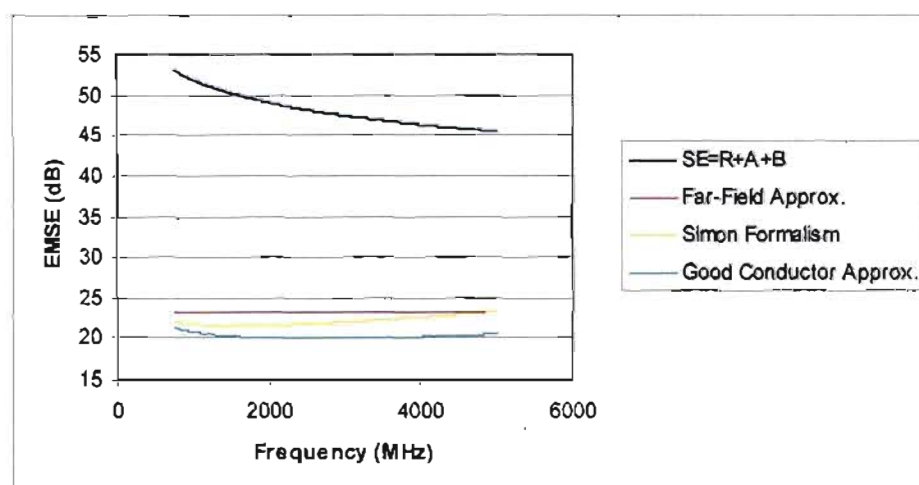


**Figure 10.28:** Comparative Graph of EMSE (analytical) vs. Frequency for 15% copper-doped unidirectional carbon fibre specimens

### c. Electromagnetic Shielding Effectiveness

As reported, unidirectional carbon fibre specimens were found to inherently display excellent EMSE without inclusion of filler materials. However, samples with fillers provide enhanced shielding performance. The sample which contained 7.5% copper powder displayed shielding capabilities superior to that of aluminium up until a frequency of approximately 3 GHz. However, the 15% copper-doped sample displayed a general improvement in the shielding performance found in undoped unidirectional carbon fibre laminates over the entire frequency range when compared with the aluminium sheet material.

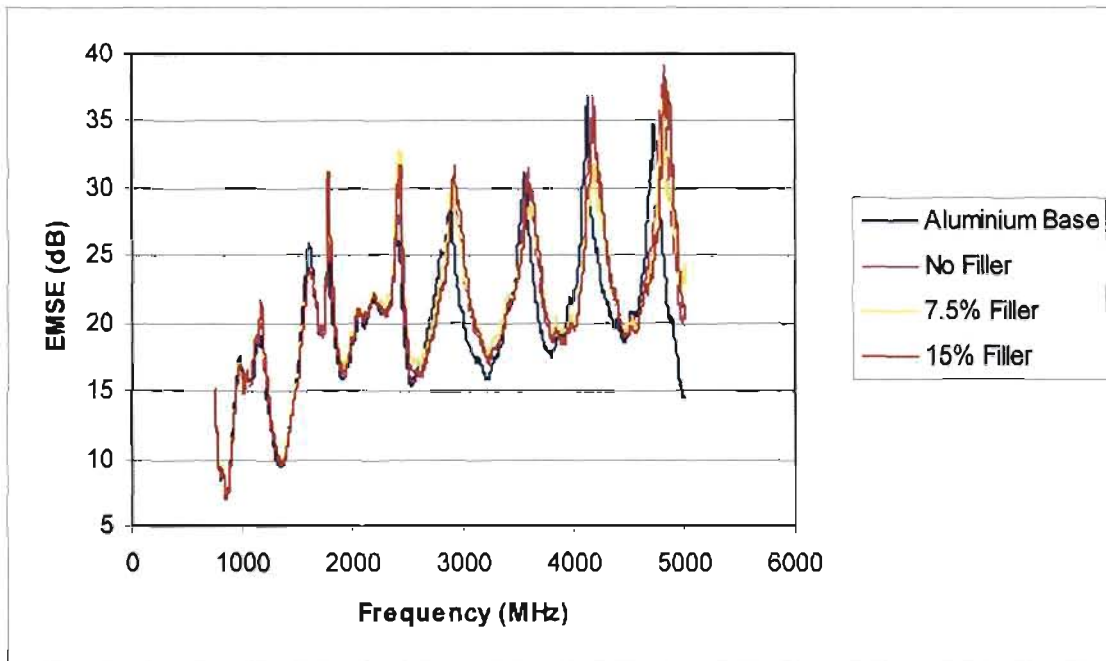


*Figure 10.29: Actual EMSE vs. Frequency of the copper-filled unidirectional fibre samples relative to an aluminium plate of the same size*

### 10.1.3 Hybrid Powder-doped Samples

#### 10.1.3.1 Manufacture

It was known that aluminium powders provided superior connectivity between the particles, whilst copper particles possess superior electrical conductivity. Designs consisting of a “hybrid powder” of aluminium and copper particles were implemented, as it was thought that a material with both superior connectivity and superior electrical conductivity would result as opposed to the materials with just aluminium and copper alone.

It was seen that the mechanical properties of the samples consisting of copper powder were slightly better than the aluminium-doped samples. This was likely due to there being a lower concentration of particles present in the matrix material, thus providing a stronger fibre/matrix bond.

The ratio selected for inclusion of copper and aluminium particles was 1:1 by percentage weight. The size difference between the larger aluminium particles and smaller copper particles was quite evident when viewed together, as in Figure 10.30.

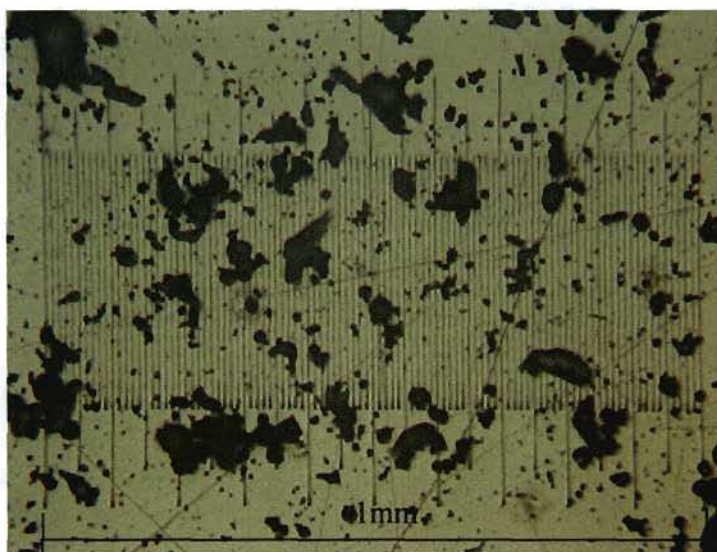


*Figure 10.30: Hybrid powder consisting of aluminium and copper particles. The larger particles are generally aluminium, whilst the smaller particles are generally copper.*

In preparation of the hybrid powder, the aluminium and copper particles were placed together in a separate container and were thoroughly mixed and sifted, to prevent clumping of the individual particles when the doped resin was prepared. The undoped resin was prepared and the hybrid powder was introduced. The mixture was thoroughly stirred at 180rpm for 5mins. The solution was observed to be a dull grey colour, due to the higher concentration of aluminium particles in the system, as shown in Figure 10.31. The texture and viscosity were also observed to change, as in the other doped resins.



*Figure 10.31: The resin colour changed from being a transparent, light yellow colour to an opaque dull grey shade.*



The laminates were fabricated in the usual way adopted in this work, and were post cured at 65 °C for 16hrs. The laminates were observed to contain dull grey surface layers when removed, denoting the properties of the doped resin used. The laminates were viewed under a microscope, and as expected connectivity improved significantly as filler loading increased, as shown in Figures 10.32 and 10.33.

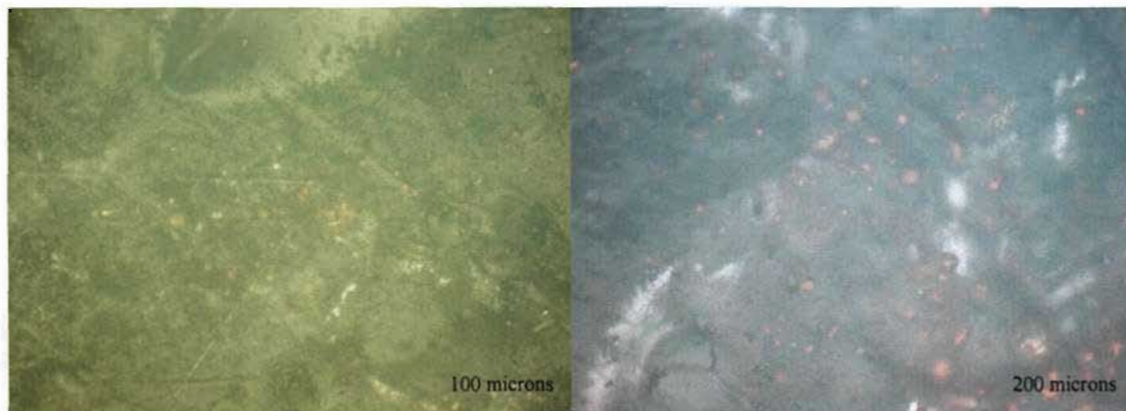


**Figure 10.32:** An image depicting 100x and 200x magnification of a 7.5% hybrid powder-doped laminate side by side. The dispersion of copper and aluminium particles in the system is clearly evident.

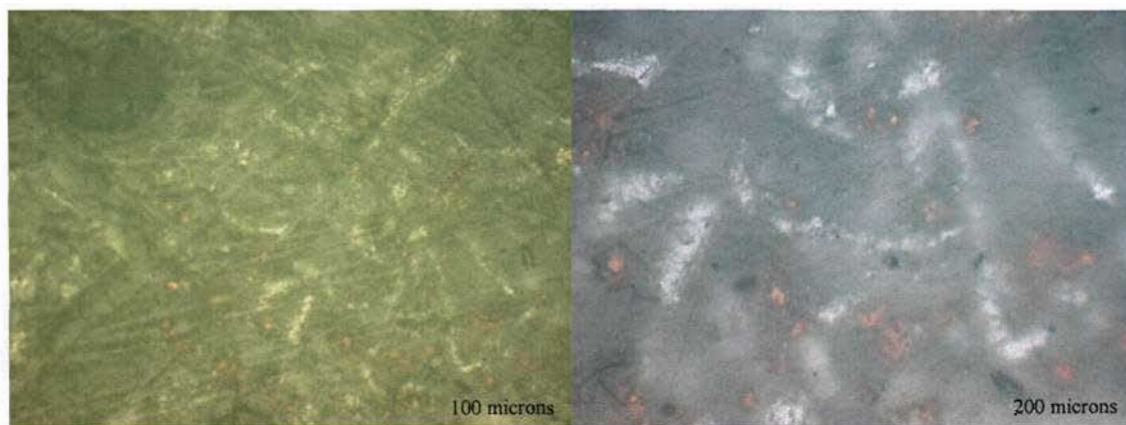


**Figure 10.33:** An image depicting 100x and 200x magnification of 15% hybrid powder-doped samples. The dominance of aluminium in providing connectivity was still evident, due to the size of the particles.



### 10.1.3.2 Results and Discussion of Stitched Carbon Fibre Samples

#### a. Mechanical Testing

**Table 10.13: Average Mechanical Properties of Hybrid Powder-doped Stitched Carbon Fibre Laminates**

	0% Filler	7.5% Filler	15% Filler
<b>Tensile Strength (MPa)</b>	73 (3)	54 (5)	70 (5)
<b>Yield Strength (MPa)</b>	61 (3)	51 (5)	61 (5)
<b>Tensile Yield Elongation (%)</b>	1.0 (0.1)	1.0 (0.1)	1.0 (0.0)
<b>Break Elongation (%)</b>	3.1 (0.4)	2.6 (0.4)	3.9 (0.8)
<b>Flexural Strength (MPa) *</b>	N/A	N/A	N/A
<b>Elastic Modulus (GPa)</b>	14.1370 (1.4486)	7.0351 (0.3499)	7.0941 (0.3739)
<b>Compressive Strength (MPa)</b>	79 (4)	63 (4)	72 (3)

Note: \* Flexural strength was indeterminate as the specimens deflected excessively and touched the supports of the testing rig before failure – The low elastic moduli obtained is indicative of this

The results obtained from tensile testing were in correlation with the poor results obtained for previous stitched samples containing discontinuous fillers. However, there was a significant decrease in tensile strength and elongation between the undoped samples and the 7.5% hybrid powder-doped samples. The failure, as in previous stitched carbon samples, was characterised by separation of the fibres at  $\pm 45^\circ$  at the midsection of the specimens.

The flexural strength was indeterminate due to excessive deflection of the specimen during testing. The samples displayed lower elastic moduli than the aluminium-doped and copper-doped stitched samples as well.

The results for compressive strength in these stitched specimens again indicated that compressive strength was higher than tensile strength, which appears doubtful. Compressive failure occurred by fibre separation at  $\pm 45^\circ$  at the midsection of the specimens.

### b. Electrical Resistivity and Conductivity Testing

**Table 10.14: Electrical Properties of Hybrid Powder-doped Stitched Carbon Fibre Laminates**

	0% Filler	7.5% Filler	15% Filler
Resistance ( $\Omega$ )	8.1000	26.3000	42.2000
Resistivity ( $\Omega \cdot \text{cm}$ )	1.8520	6.1734	9.6962
Conductivity ( $\Omega / \text{cm}$ )	0.5399	0.1619	0.1031
Relative Conductivity <sup>*</sup> ( $\times 10^{-3}$ )	3.8266	1.1479	0.7308

Note <sup>\*</sup> Relative to a copper plate of the same size measured on the same instrument

The result obtained show that electrical resistance significantly increased between 0% filler and 15% filler loadings. Again, this could have been due to the disordered powder arrangement influencing readings.

The electrical resistance results showed an increase in resistance as filler loading increased. The results of the analytical computations of EMSE in these samples are again shown by means of comparative graphs in Figures 10.34 and 10.35. The graph depicting the theoretical shielding performance of the undoped specimens are presented in Figure 10.5

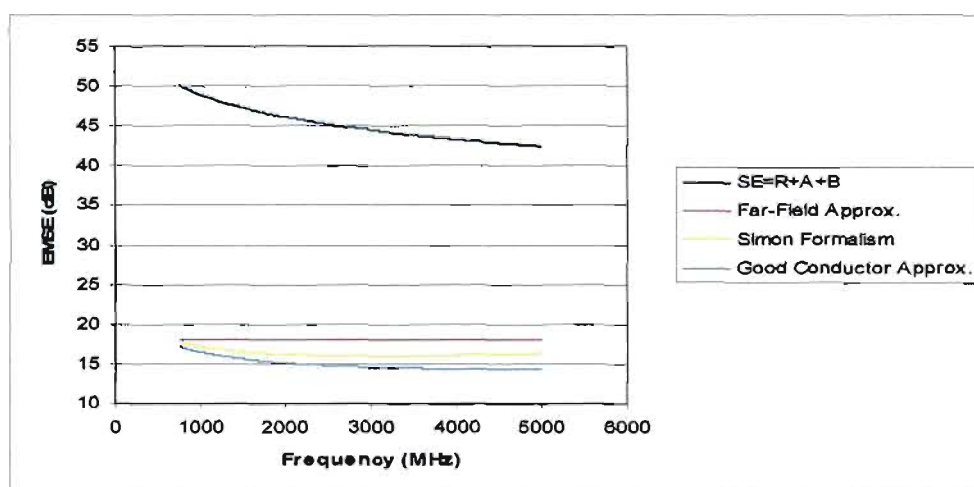


**Figure 10.34: Comparative graph of EMSE (analytical) vs. Frequency for 7.5% hybrid powder-doped stitched carbon fibre specimens**

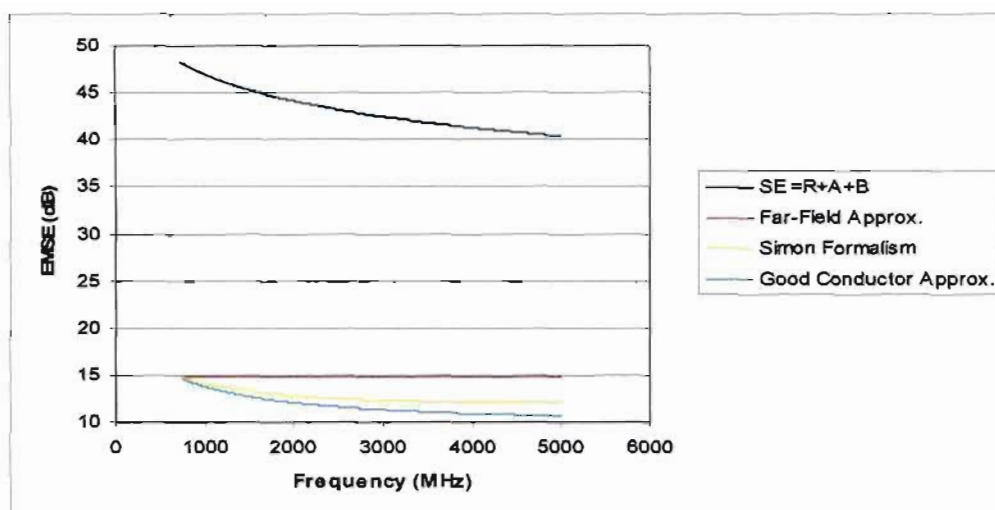


*Figure 10.35: Comparative graph of EMSE (analytical) vs. Frequency for 15% hybrid powder-doped stitched carbon fibre specimens*

As electrical resistance increased with filler loading, a decrease in EMSE was found by analytical calculation. The assumptions on why resistance increased with filler loading were previously discussed, and the opinion was the same in this case. The true indication of the shielding quality was found by actual EMSE testing.

### c. Electromagnetic Shielding Effectiveness

The EMSE of the samples was measured, and the results showed that the shielding capabilities did indeed improve with filler loading. The specimen with 15% filler was found to display the best shielding performance, and generally appeared to be superior to that of the aluminium plate over frequency range in question. The sample with 7.5% filler was observed to be slightly inferior to the aluminium plate over some frequencies, but did provide improved shielding when compared with the undoped stitched carbon fibre sample. Figure 10.36 shows the EMSE results obtained from testing.

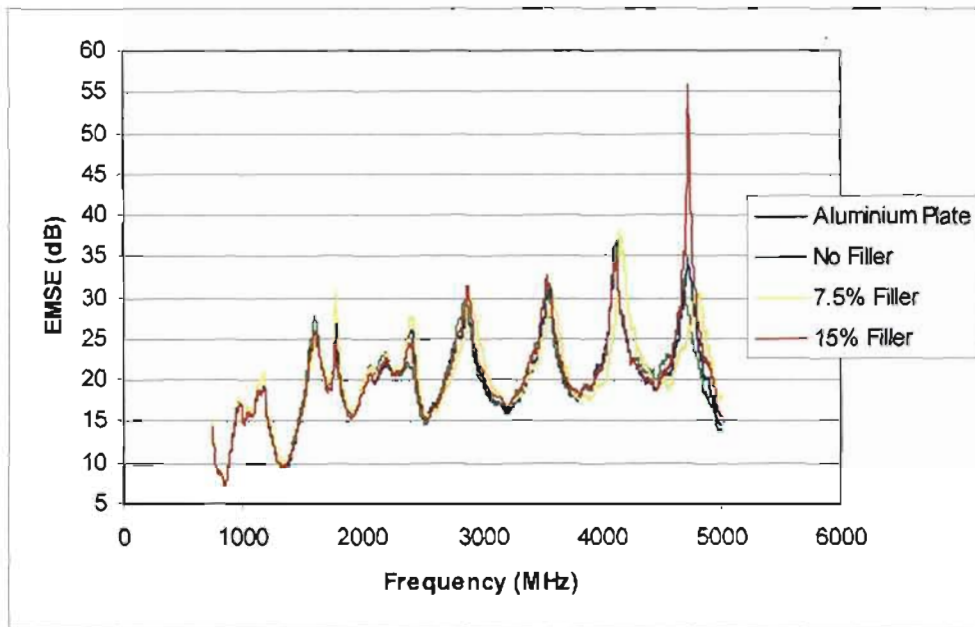


*Figure 10.36: Actual EMSE vs. Frequency of the Hybrid Powder-doped Stitched Carbon Samples relative to an aluminium plate*

#### 10.1.3.3 Results and Discussion of 12K Woven Carbon Fibre Samples

##### a. Mechanical Testing

**Table 10.15: Average Mechanical Properties of Hybrid Powder-doped Woven Carbon Fibre Laminates**

	0% Filler	7.5% Filler	15% Filler
Tensile Strength (MPa)	821 (47)	636 (44)	595 (38)
Yield Strength (MPa)	780 (47)	636 (44)	595 (38)
Tensile Yield Elongation (%)	4.0 (0.2)	3.1 (0.1)	3.0 (0.1)
Break Elongation (%)	4.3 (0.4)	3.1 (0.2)	3.0 (0.1)
Flexural Strength (MPa)	531 (97)	832 (136)	890 (53)
Elastic Modulus (GPa)	72.9192 (19.6554)	47.9290 (2.8186)	47.3399 (2.3406)
Compressive Strength (MPa)	136 (16)	269 (8)	165 (10)

The tensile test results show that tensile strength decreased by 22% upon introduction of 7.5% filler into the matrix. Tensile strength, yield elongation and break elongation continued to decrease with increasing filler loading. Failure, as in the previous woven specimens, was characterised by a loud noise and the specimens were generally observed to fail at the midsection along the 0° plane in a fibre breakage.

Flexural testing showed that bending strength increased with increasing filler loading. The elastic moduli, however, decreased proportionally with increasing filler loading. However, the decrease in elastic modulus between 7.5% and 15% filler loadings was not significant, with only a 1% reduction observed. Failure in these samples was characterised by a loud noise but, as in the other 12K woven carbon specimens, only minor fracture across the width of the midsection was observed.

The compressive strength data obtained was not considered as being reliable indication of the materials true compressive strength, as localised crushing was observed to have occurred during testing.

#### b. Electrical Resistivity and Conductivity Testing

**Table 10.16: Electrical Properties of Hybrid Powder-doped Woven Carbon Fibre Laminates**

	<b>0% Filler</b>	<b>7.5% Filler</b>	<b>15% Filler</b>
<b>Resistance (<math>\Omega</math>)</b>	23.3000	64.0000	46.0000
<b>Resistivity (<math>\Omega \cdot \text{cm}</math>)</b>	4.8047	16.2088	10.8975
<b>Conductivity (<math>\Omega / \text{cm}</math>)</b>	0.2081	0.0616	0.0917
<b>Relative Conductivity * (<math>\times 10^{-3}</math>)</b>	1.4749	0.4372	0.6503

Note \* Relative to a copper plate of the same size measured on the same instrument

The results obtained indicated that electrical resistance initially increased significantly when comparing the undoped specimen to the specimen with 7.5% filler loading. Resistance decreased by 28% between the 7.5% and 15% filler loading specimens. Possible explanations on why the materials displayed behaviour of this nature when electrical measurements were undertaken have been mentioned previously, and were thought to be the same in this case. Theoretical EMSE data

was obtained by use of equations (4.6), (4.14), (4.15) and (4.18), and the results are presented by means of comparative graphs. The comparative graph of the undoped sample may be seen in Figure 10.9.

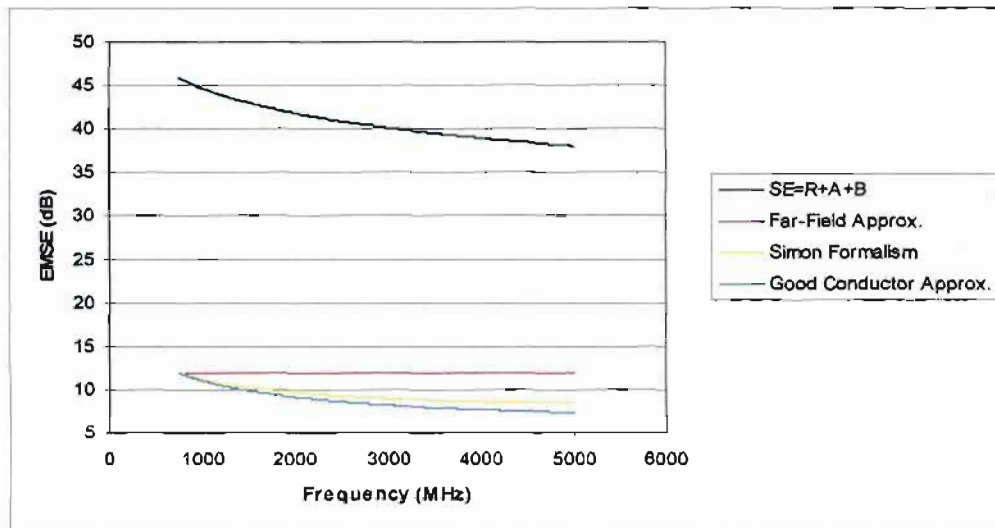


*Figure 10.37: Comparative graph of EMSE (analytical) vs. Frequency for 7.5% hybrid powder-doped woven carbon fibre specimens*

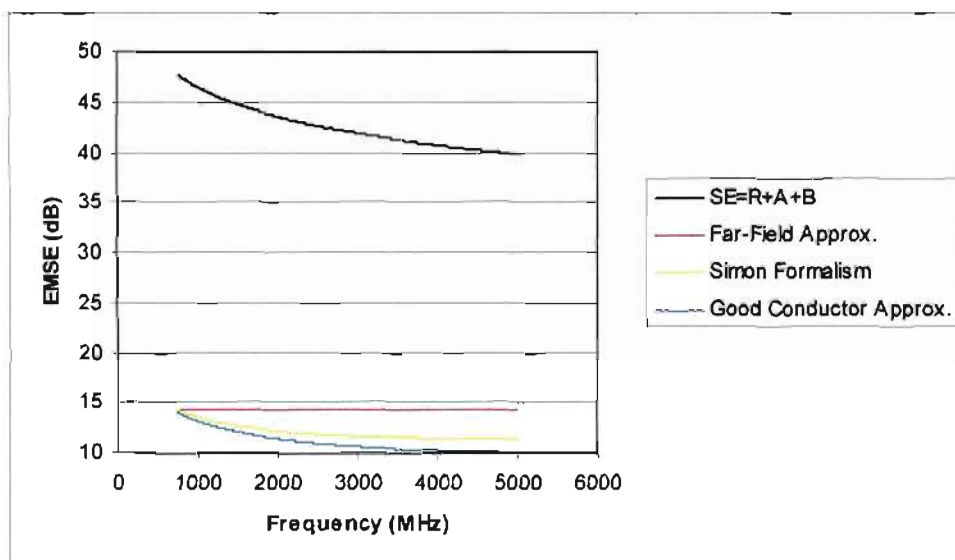


*Figure 10.38: Comparative graph of EMSE (analytical) vs. Frequency for 15% hybrid powder-doped woven carbon fibre specimens*

### c. Electromagnetic Shielding Effectiveness Testing

The actual EMSE test results show that EMSE does indeed increase with increasing filler loading. The specimen with 7.5% filler displayed good shielding characteristics, and closely matched the EMSE of the aluminium plate. The sample with 15% filler was slightly superior in shielding performance, although not significantly. Again the sample with no filler did display excellent shielding as well, but was slightly inferior to those with filler materials.

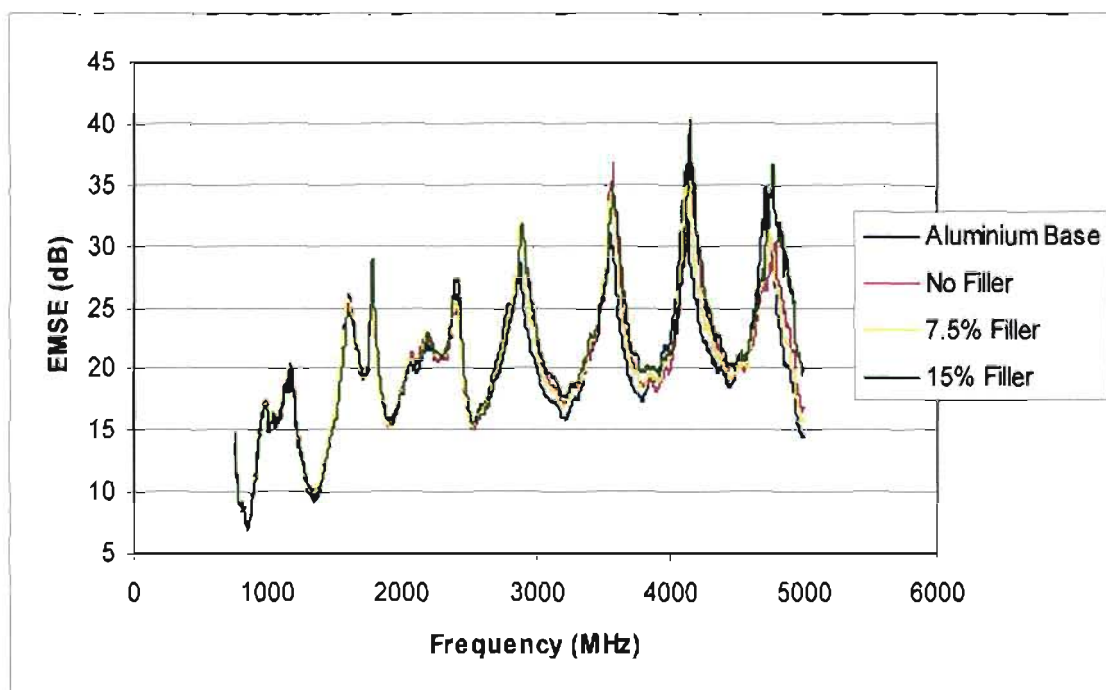


**Figure 10.39:** Actual EMSE vs. Frequency of the hybrid powder-doped woven carbon fibre specimens relative to an aluminium plate of the same size

#### 10.1.3.4 Results and Discussion of Unidirectional Carbon Fibre Samples

##### a. Mechanical Testing

**Table 10.17: Average Mechanical Properties of Hybrid Powder-doped Unidirectional Carbon Fibre Laminates**

	<b>0% Filler</b>	<b>7.5% Filler</b>	<b>15% Filler</b>
<b>Tensile Strength (MPa)</b>	841 (56)	767 (43)	904 (51)
<b>Yield Strength (MPa)</b>	839 (56)	750 (43)	875 (52)
<b>Tensile Yield Elongation (%)</b>	4.2 (0.0)	3.9 (0.1)	4.2 (0.1)
<b>Break Elongation (%)</b>	4.2 (0.3)	4.0 (0.1)	4.4 (0.2)
<b>Flexural Strength (MPa)</b>	1135 (39)	1023 (43)	1148 (106)
<b>Elastic Modulus (GPa)</b>	180.3777 (27.5470)	120.9705 (3.9832)	122.6269 (19.9027)
<b>Compressive Strength (MPa)</b>	155 (5)	133 (49)	177 (6)

Failure in tensile testing was alike to the other unidirectional carbon fibres tested, with splitting of the fibres at the 0° plane along the outer regions of the midsection, and was characterised by “snapping” noises heard as the individual fibre failed. However, the results indicate an initial decrease in both strength and elongation from 0% filler to 7.5% filler loadings, and then an increase in strength and elongation between 7.5% and 15% filler loading.

Flexural testing results were similar to tensile results in that an initial decrease in bending strength and elastic moduli between no filler and 7.5% filler loading was observed, and an increase between 7.5% and 15% filler loading was observed. Failure in these samples was again characterised by a loud noise at failure, but only minor fracture across the outer layer along the width of the midsection was observed.

Compressive failure was due to localised crushing at the end surfaces of the specimen once again.



### b. Electrical Resistivity and Conductivity Testing

**Table 10.18: Electrical Properties of Hybrid Powder-doped Unidirectional Carbon Fibre Laminates**

	0% Filler	7.5% Filler	15% Filler
Resistance ( $\Omega$ )	5.9000	25.8000	31.0000
Resistivity ( $\Omega \cdot \text{cm}$ )	1.2421	6.6743	7.1300
Conductivity ( $\Omega / \text{cm}$ )	0.8050	0.1498	0.1402
Relative Conductivity * ( $\times 10^{-3}$ )	5.7053	1.0618	0.9939

Note \* Relative to a copper plate of the same size measured on the same instrument

The electrical resistance measurements showed an increase as filler loading increased in the specimens. As stated previously, this could likely be due to the disordered arrangement of particles within the composite materials. The results of the analytical computations of EMSE in the hybrid powder-doped specimens are presented in Figures 10.40 and 10.41. The results for the undoped sample are presented in Figure 10.13. As expected, these results indicate a theoretical decrease in EMSE due to measured conductivity decreasing.

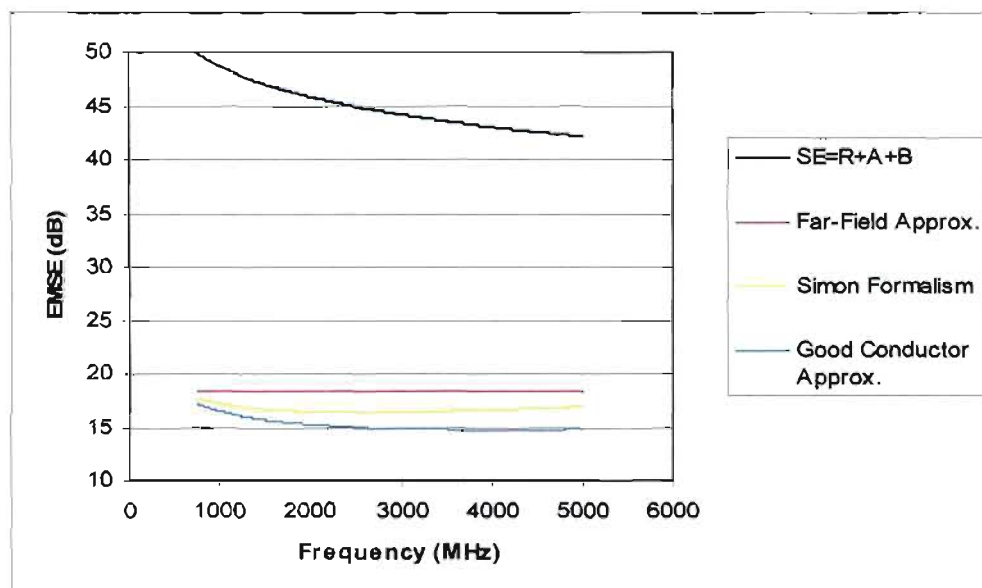


**Figure 10.40: Comparative graph of EMSE (analytical) vs. Frequency for 7.5% hybrid powder-doped unidirectional carbon fibre specimens**

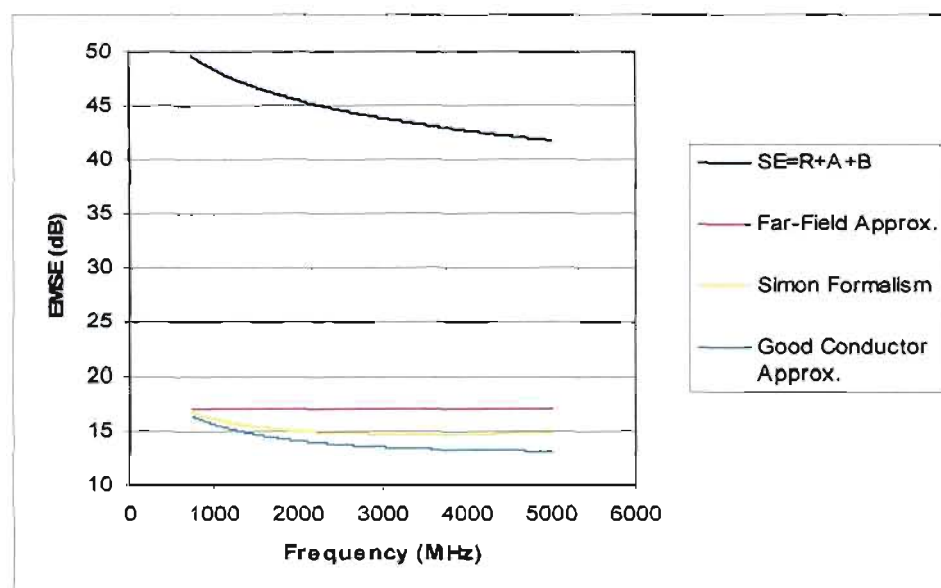


**Figure 10.41:** Comparative graph of EMSE (analytical) vs. Frequency for 15% hybrid powder-doped unidirectional carbon fibre specimens

The EMSE results obtained for the specimen with 7.5% filler loading when equation (4.6) was used indicated an average wave penetration of 1%; whilst the other equations indicated an average wave penetration of 31% in the specimens. The EMSE results for the specimen with 15% filler loading when equation (4.6) was used indicated an average wave penetration of 0.6%; whilst the other equations imply an average wave penetration of 25% throughout the shielding material. The possible reason for these discrepancies was explained previously.

### c. Electromagnetic Shielding Effectiveness

The results indicated that the sample with 7.5% filler loading adequately emulated the EMSE displayed by aluminium. The sample with 15% filler loading was superior to the aluminium plate up to a frequency of 3.8 GHz, but shielding performance slightly diminished after this frequency. The reduction was not particularly significant, as its EMSE was only slightly less than that of the aluminium plate. The samples containing filler materials were superior in shielding to the undoped sample.

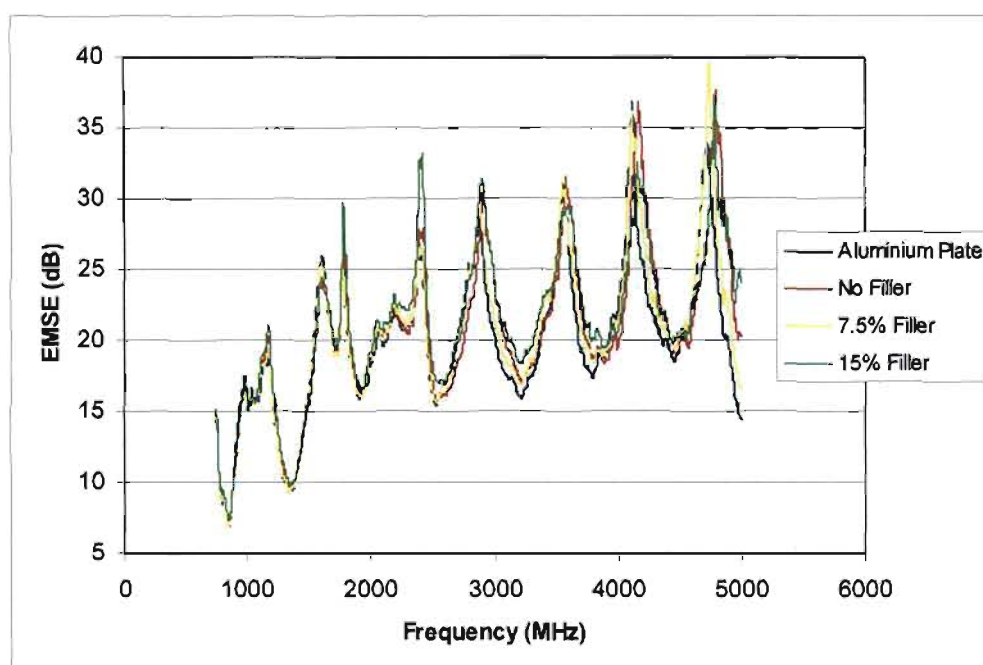


**Figure 10.42:** Actual EMSE vs. Frequency of the hybrid-doped unidirectional samples relative to an aluminium plate of the same size

#### 10.1.4 Discussion on Metal Powder Samples

The samples enriched with metal powder have displayed enhanced shielding quality compared to their respective undoped samples. Despite the undoped carbon fibre epoxy laminates already possessing inherent electromagnetic shielding capabilities, a noticeable improvement in EMSE with the inclusion of discontinuous filler materials was noted.

However, a general decrease in mechanical properties was also found in some laminates, as was expected. In some cases, bending strength did increase, although there was a substantial decrease in tensile modulus in all samples which contained fillers compared to their respective undoped samples. However, the case of the 15% hybrid powder-doped unidirectional specimens, tensile strength unexpectedly increased with increasing filler loading as well. However, the specimen also displayed inferior EMSE compared with the 7.5% hybrid powder-doped sample. The stitched carbon samples also displayed an increase in tensile strength as filler loading increased in some of the experiments, but the mechanical properties of this material was extremely poor. It is felt that those laminates would not be suitable for structural applications in practice. However, the woven,

and most notably the unidirectional samples, displayed excellent strength even after the fillers were introduced, and should suffice a variety of structural aircraft applications in practice.

There was initially some suspicion that connectivity between the particles may influence shielding quality. It was generally seen that the samples with higher filler loadings (15%) yielded higher EMSE values in the actual EMSE testing. The lack of connectivity between the copper particles in particular did not result in poor shielding quality due to lack of connectivity between the particles. This reaffirms the conclusions on connectivity and shielding made by Chung [5] and Yang *et al.* [11]. However, it was quite apparent that the samples with 15% powder displayed better shielding quality, and this was likely due both to the extent of connectivity between the particles and to the general increase in electrically conductive particles within the matrix itself. The disordered arrangement of metal particles could also have influenced the bulk resistance measurements, and thus higher values than anticipated were obtained.

The analytical results obtained by use of equations did not provide a true indication of shielding quality in practice. Even if a different means of determining electrical resistance was adopted (which was particularly sought after, but found to be unavailable in SA as explained in Chapter 8), the trend of the analytical graphs would not change, as is evident from the various graphs presented. The theoretical results obtained from using equations (4.14), (4.15) and (4.18) were in some correlation with each other, but did not correspond with the results obtained by using equation (4.6). The possible reason was the use of relative conductivity in equation (4.6) whilst the conductivity variable was used in the other equations.

The shielding performance of the materials developed was found to be excellent in practice, and most of the materials were successful in emulating, and improving, the EMSE found in aluminium. Further discussions regarding cost, strength and shielding of these materials are presented in Chapter 11.

## **10.2 Continuous Filler Material Designs**

It was known that composites materials with metal powder filler materials would likely not suffice for the purpose of lightning strike protection. Lightning protection was not the primary goal of this work and the specific application of the electromagnetic shielding material in practice

was unknown. With this in mind, it was thought that it could very well be used on external aircraft surfaces, thus becoming exposed to lightning strike.

Upon reviewing literature and consulting industry professionals, indications were that a metal mesh would be the most cost-effective method to provide electromagnetic shielding for external aircraft surfaces, as this material is known to suffice the purpose of lightning strike protection as well. For this purpose, Alumesch 401, the metal mesh material detailed in Chapter 6, was selected. The material, known to consist of finely woven aluminium material, was viewed under a microscope to determine its fibre orientation. As can be seen in Figure 10.43, the fibres were aligned in a highly ordered structure. It was anticipated that this would result in more effective shielding, as there would be a continuous current-carrying path in composites containing this material.

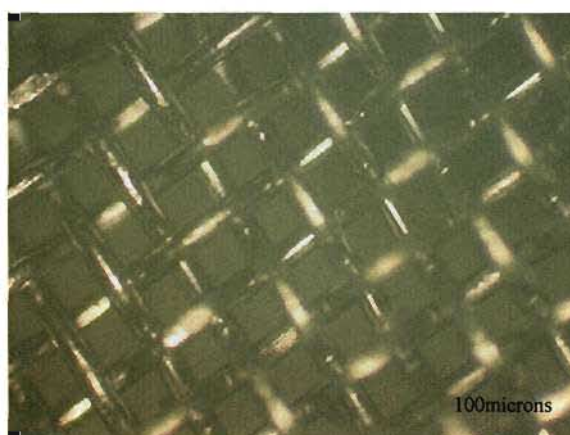


*Figure 10.43: Alumesch 401 when viewed at 100x magnification*

It was known that galvanic corrosion may result when aluminium is placed in direct contact with carbon. Although it was not the focus of this research to investigate possible degradation effects, or prevention thereof, it was decided that a layer of glass fibre fabric should be placed between the carbon and aluminium materials to limit the possibility of corrosion damage. This approach is currently used in industry [64].

#### 10.2.1 Manufacture

The same carbon fabrics used in the discontinuous filler material laminates were used for these designs as well. The designs selected for this work consisted of single and double layers of

Alumesh 401 in the composite respectively. The laminates were built with the metal fabric as the first layer (or first two layers for the designs containing two metal layers), followed by a single layer of unidirectional E-glass fabric, and the carbon materials above. The samples were manufactured with the 80/20 E-glass layer oriented with the 80% fibre side parallel to the direction that the specimens would be tested at.

These samples were fabricated using the twin mould process as well, to ensure each of the samples contained the same matrix material. The laminates were cured at 65 °C for 16hrs. Images of these laminates can be seen in Appendix B. Thickness and weight data for these laminates may be seen in Appendix C. From that data, weight in these laminates was proportional to the amount of fabrics used within the composite. Thickness increased as well and, unlike the powder-filled laminates, was proportional to the amount of materials included. This was due to the substantial dry thicknesses that the glass and Alumesh 401 possess (unidirectional E-glass was 0.2mm in thickness, and Alumesh 401 was 0.12mm in thickness).

#### 10.2.2 Results and Discussion of Stitched Carbon Fibre Samples

##### a. Mechanical Testing

**Table 10.19: Average Mechanical Properties of Mesh/Stitched Carbon Fibre Laminates**

	No Mesh	1 Ply Mesh	2 Ply Mesh
<b>Tensile Strength (MPa)</b>	73 (3)	76 (4)	83 (7)
<b>Yield Strength (MPa)</b>	61 (3)	58 (5)	61 (6)
<b>Tensile Yield Elongation (%)</b>	1.0 (0.1)	0.9 (0.0)	0.8 (0.0)
<b>Break Elongation (%)</b>	3.1 (0.4)	1.4 (0.1)	1.6 (0.2)
<b>Flexural Strength (MPa)</b>	N/A	N/A	N/A
<b>Elastic Modulus (GPa)</b>	14.1370 (1.4486)	10.5774 (2.0314)	8.8211 (2.5678)
<b>Compressive Strength (MPa)</b>	79 (4)	73 (4)	75 (1)

Note: \* Flexural strength was indeterminate as the specimens deflected excessively and touched the supports of the testing rig before failure – The low elastic moduli obtained is indicative of this

The results from tensile testing showed that strength increased as the mesh material content increased. However, there was a decrease in yield and break elongations as the metal fabric content increased as well. The increase in strength could very well have been due to the glass and metal fabrics, as the stitched carbon specimens displayed poor strength previously.

The flexural strength in these samples could not be obtained, as with the other stitched samples, due to excessive deflection of the specimen during testing. The specimens did, however, display reductions in elastic moduli as content of metal fabric increased.

Compressive test results showed a reduction in compressive strength in the specimens with metal mesh. However, inspection of the samples showed damage just below both grip surfaces of the specimens. This could have been a result of buckling of the specimens during testing, but was not confirmed by the tester.

#### b. Electrical Resistivity and Conductivity Testing

**Table 10.20: Electrical Properties of Mesh/Stitched Carbon Fibre Laminates**

	0% Filler	7.5% Filler	15% Filler
<b>Resistance (<math>\Omega</math>)</b>	8.1000	0.5890	0.7500
<b>Resistivity (<math>\Omega \cdot \text{cm}</math>)</b>	1.8520	0.1358	0.1975
<b>Conductivity (<math>\Omega / \text{cm}</math>)</b>	0.5399	7.3597	5.0622
<b>Relative Conductivity * (<math>\times 10^{-3}</math>)</b>	3.8266	52.1580	35.8759

Note \* Relative to a copper plate of the same size measured on the same instrument

The result obtained indicated that electrical resistance decreased significantly between no mesh and one mesh layer, but surprisingly increased between one and two layers. This seems very unlikely, as there was now more metal, which should result in a lower resistance.

The results of the analytical computations of EMSE in these samples are again shown by means of graphs in Figures 10.44 and 10.45. The graph depicting the shielding performance of specimen without filler materials was presented in Figure 10.5. As expected, these results show that the laminate with one mesh layer theoretically displays the best EMSE. However, results obtained from equations (4.14), (4.15) and (4.18) were no longer in the same degree of correlation with

these samples as they were in the discontinuous samples. The possible reason could be that equation (4.18) is only valid for samples which were electrically thin, and these were not. Equations (4.14) and (4.15) were in some degree of accordance as well, but there was between 5dB and 15dB between their results.

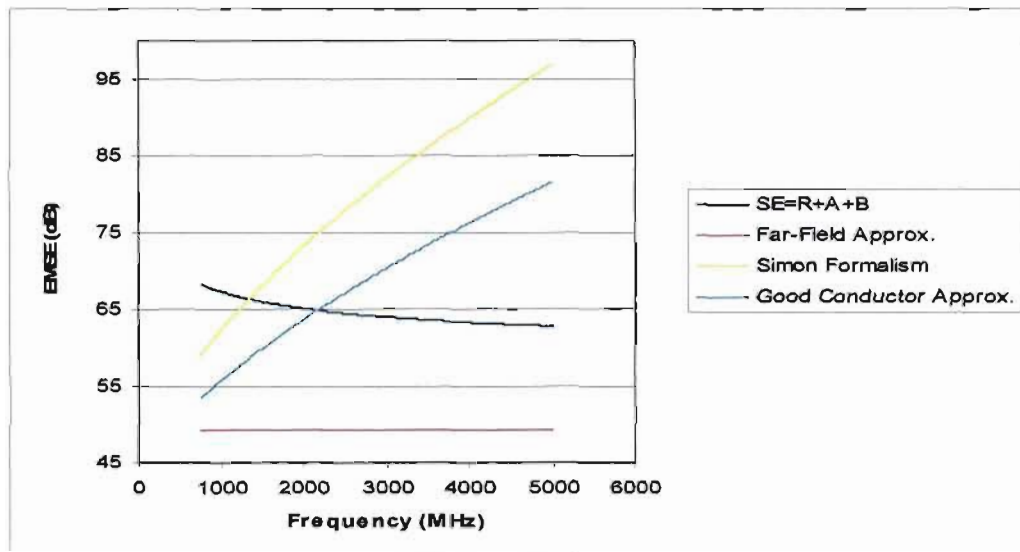


*Figure 10.44: Comparative graph of EMSE (analytical) vs. Frequency for stitched carbon with one metal mesh layer*

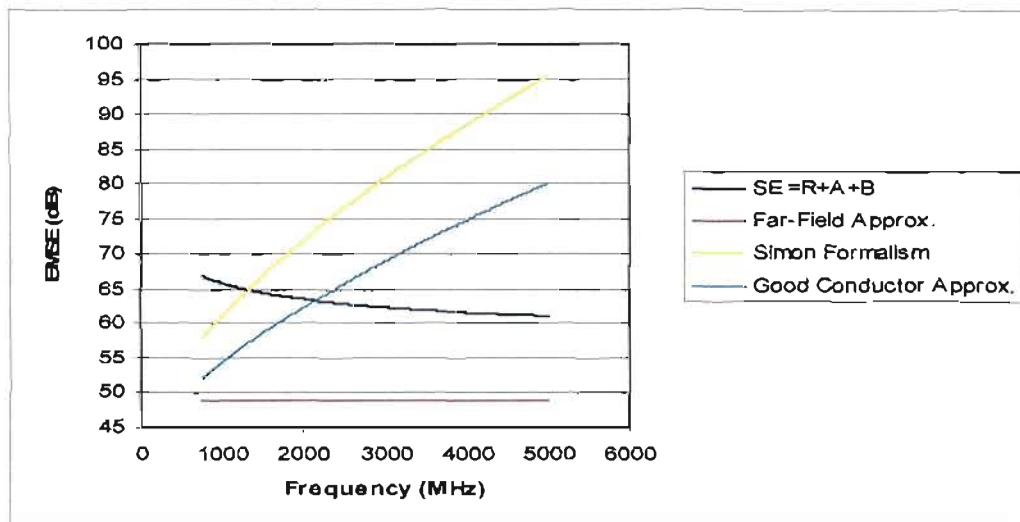


*Figure 10.45: Comparative graph of EMSE (analytical) vs. Frequency for stitched carbon with two metal mesh layers*



### c. Electromagnetic Shielding Effectiveness

The EMSE of the samples was measured, and the results showed that the shielding capabilities did indeed improve with the addition of metal fabric. However, there was no significant difference in shielding quality between the sample containing one and two metals layers. The samples both generally matched the EMSE of aluminium throughout the frequency range.

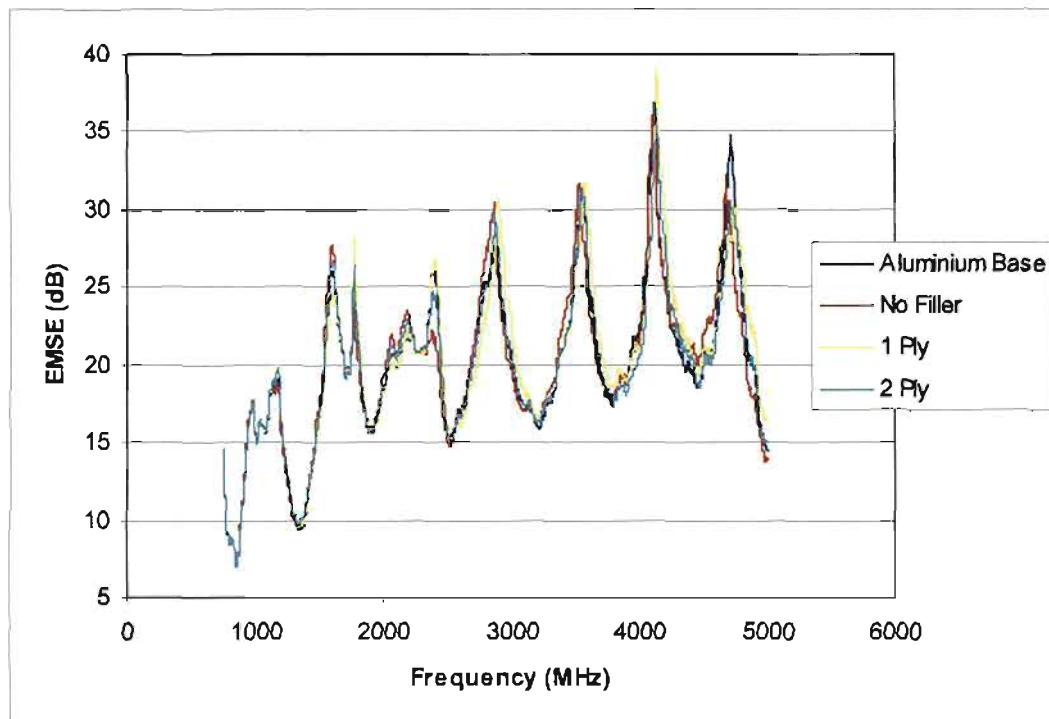


**Figure 10.46:** Actual EMSE vs. Frequency of the metal mesh/stitched samples relative to an aluminium plate

### 10.2.3 Results and Discussion of 12K Woven Carbon Fibre Samples

#### a. Mechanical Testing

**Table 10.21: Average Mechanical Properties of Mesh/Woven Carbon Fibre Laminates**

	No Mesh	1 Ply	2 Ply
<b>Tensile Strength (MPa)</b>	821 (47)	704 (36)	648 (57)
<b>Yield Strength (MPa)</b>	780 (47)	702 (36)	642 (57)
<b>Tensile Yield Elongation (%)</b>	4.0 (0.2)	3.2 (0.2)	3.1 (0.1)
<b>Break Elongation (%)</b>	4.3 (0.4)	3.2 (0.2)	3.1 (0.1)
<b>Flexural Strength (MPa)</b>	531 (97)	753 (167)	877 (90)
<b>Elastic Modulus (GPa)</b>	72.9192 (19.6554)	49.7243 (4.0911)	51.0282 (3.7724)
<b>Compressive Strength (MPa)</b>	136 (16)	145 (20)	138 (30)

Tensile test results showed that strength, yield elongation and break elongation decreased as metal fabric content increased in the laminates. Failure in these samples was characterised by fracture of the glass and metal fabrics first. This was expected, as the glass fabric was the weaker component in the composite. Failure in the mesh likely followed from fracture of the glass.

Flexural testing showed that bending strength increased with increasing metal fabric content in the laminates. There was a significant decrease in elastic modulus between the sample without mesh and the sample with one mesh layer, but a slight increase was observed between the samples with one mesh and two mesh layers.

Inspection of the compressive test specimens showed failure was due to crushing of the end surfaces on the laminate. Thus, the results obtained were likely not a true indication of the compressive strength of the specimen.

b. Electrical Resistivity and Conductivity Testing

**Table 10.22: Electrical Properties of Mesh/Woven Carbon Fibre Laminates**

	No Mesh	1 Ply	2 Ply
Resistance ( $\Omega$ )	23.3000	0.4800	0.6800
Resistivity ( $\Omega \cdot \text{cm}$ )	4.8047	0.1004	0.1555
Conductivity ( $\Omega / \text{cm}$ )	0.2081	9.9554	6.4298
Relative Conductivity <sup>*</sup> ( $\times 10^{-3}$ )	1.4749	0.7055	0.4556

Note <sup>\*</sup> Relative to a copper plate of the same size measured on the same instrument

The electrical resistance measurements showed a significant drop in resistance upon the inclusion of the single metal mesh layer. However, electrical resistance was observed to increase slightly in the specimens with two metal mesh layers. As expected, the analytical EMSE results show that the sample with one mesh layer theoretically displays the best shielding performance. The analytical EMSE results for the woven carbon sample without a metal mesh layer are presented in Figure 10.9. The results for the samples with metal mesh are presented in Figures 10.47 and 10.48.

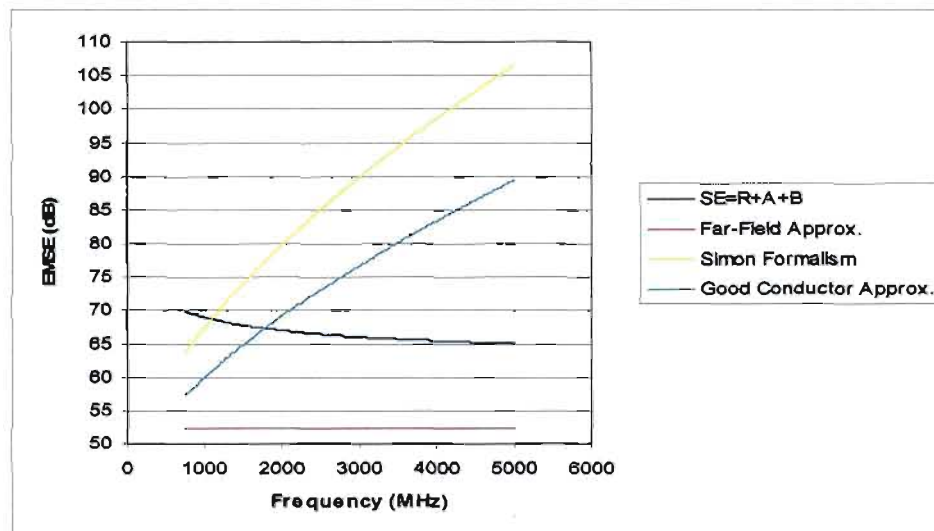


**Figure 10.47: Comparative graph of EMSE (analytical) vs. Frequency for woven carbon fibre specimens with one metal mesh layer**

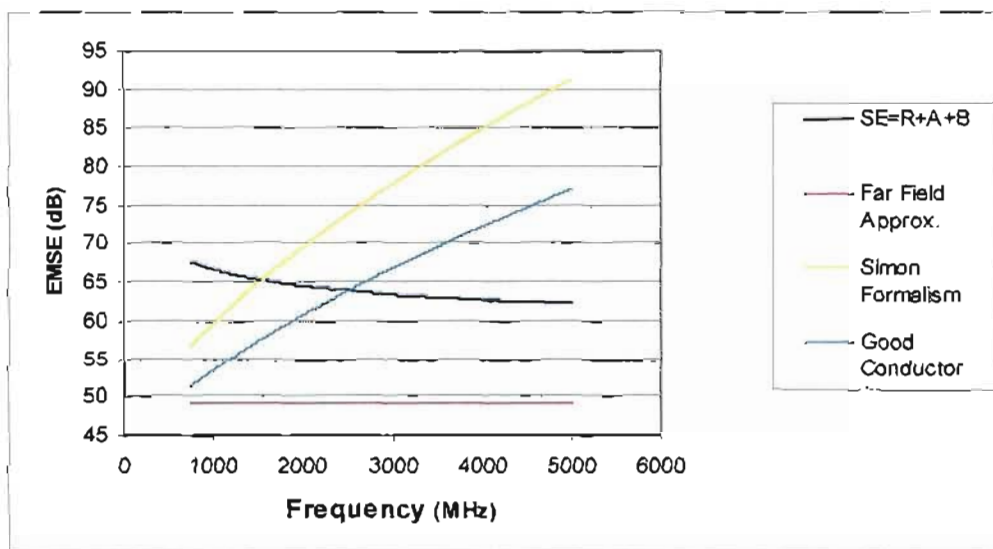


**Figure 10.48:** Comparative graph of EMSE (analytical) vs. Frequency for woven carbon fibre specimens with two metal mesh layers

As seen in the figures, results obtained from equations (4.14) and (4.15) were in some correlation, as in the stitched carbon specimens with metal mesh fabric.

#### c. Electromagnetic Shielding Effectiveness

There was some concern regarding the lower electrical conductivity displayed in the laminate containing two mesh layers. However, the actual EMSE testing showed that the sample with two mesh layers did provide the best shielding quality, and was significantly superior in shielding performance when compared to the aluminium plate. The sample with one mesh layer closely emulated the shielding quality found in aluminium, and was certainly not a poor shielding material by any means. As mentioned previously, woven carbon without filler materials did display good EMSE, and thus use of filler materials further enhanced its shielding quality.

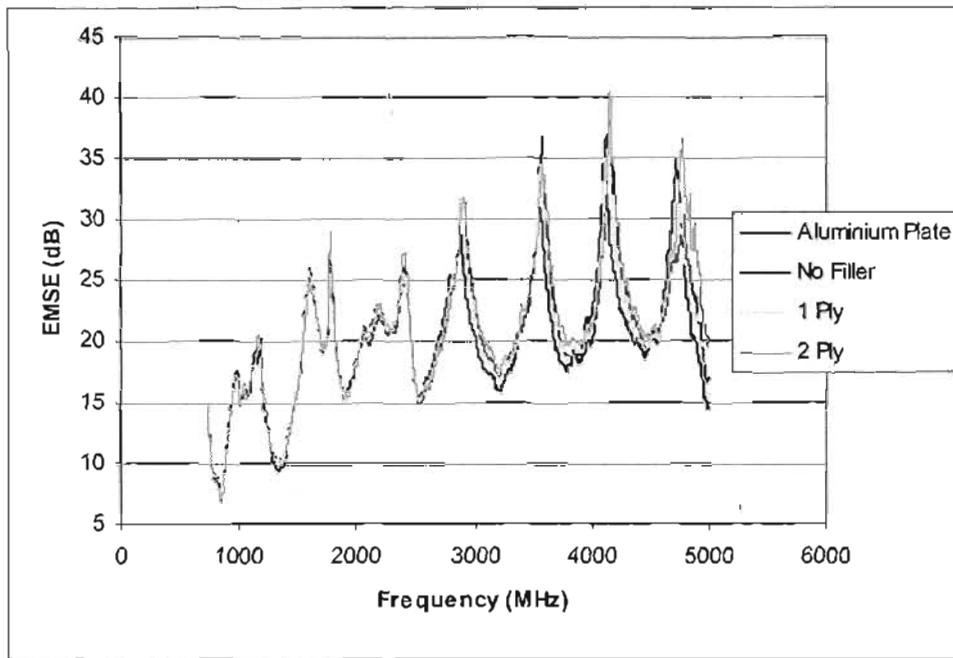


*Figure 10.49: Actual EMSE vs. Frequency of the metal mesh/woven carbon fibre specimens relative to an aluminium plate of the same size*

#### 10.2.4 Results and Discussion of Unidirectional Carbon Fibre Samples

##### a. Mechanical Testing

**Table 10.23: Average Mechanical Properties of Mesh/Unidirectional Carbon Fibre Laminates**

	No Mesh	1 Ply	2 Ply
Tensile Strength (MPa)	841 (56)	521 (65)	549 (32)
Yield Strength (MPa)	839 (56)	339 (65)	523 (32)
Tensile Yield Elongation (%)	4.2 (0.0)	2.4 (1.4)	4.9 (0.3)
Break Elongation (%)	4.2 (0.3)	3.7 (0.7)	5.2 (0.3)
Flexural Strength (MPa)	1135 (39)	550 (68)	326 (60)
Elastic Modulus (GPa)	180.3777 (27.5470)	109.2479 (19.1618)	121.9785 (12.0782)
Compressive Strength (MPa)	155 (5)	158 (46)	158 (16)

Failure in tensile testing was characterised by fracture in the glass and metal fabrics. Tensile strength decreased significantly between the laminate without metal and the laminate with one metal mesh layer. There was a 5% increase in tensile strength between the sample with one and two metal mesh layers. The results also indicated an initial decrease in both yield and break elongations between the sample without a metal mesh layer and the sample with a single metal mesh layer. However, elongations increased considerably between the single-mesh layer sample and double-mesh layer sample.

There was a significant decrease in bending strength, with over 50% reduction between the samples without metal and the samples with one mesh layer. Bending strength decreased by a further 40% in the sample with two mesh layers. The elastic modulus decreased significantly between the samples without metal to the samples with one layer of metal. However, there was a slight increase in elastic modulus as the metal content increased thereafter.

The results for compressive testing were poor once again. Failure did not occur in the specimen, but once again, the grip surfaces were observed to have crushed.

#### b. Electrical Resistivity and Conductivity Testing

**Table 10.24: Electrical Properties of Mesh/Unidirectional Carbon Fibre Laminates**

	0% Filler	7.5% Filler	15% Filler
<b>Resistance (<math>\Omega</math>)</b>	5.9000	0.7300	0.2900
<b>Resistivity (<math>\Omega \cdot \text{cm}</math>)</b>	1.2421	0.1858	0.0732
<b>Conductivity (<math>\Omega / \text{cm}</math>)</b>	0.8050	5.3816	13.6511
<b>Relative Conductivity (<math>\times 10^{-3}</math>)</b>	5.7053	38.1396	96.7444

Note \* Relative to a copper plate of the same size measured on the same instrument

The results show a decrease in electrical resistivity as metal content increased, which was expected. As expected, the analytical computations of EMSE show an increase with increasing conductivity, and thus the sample with two mesh layers displays the best theoretical EMSE. There was a greater correspondence between the results obtained from equations (4.14) and (4.15) for the unidirectional carbon samples with one metal mesh layer, but the results obtained from

equations (4.14) and (4.15) were in significantly less correlation in the unidirectional carbon samples with two metal mesh layers. The graphs are shown in Figures 10.50 and 10.51 below.

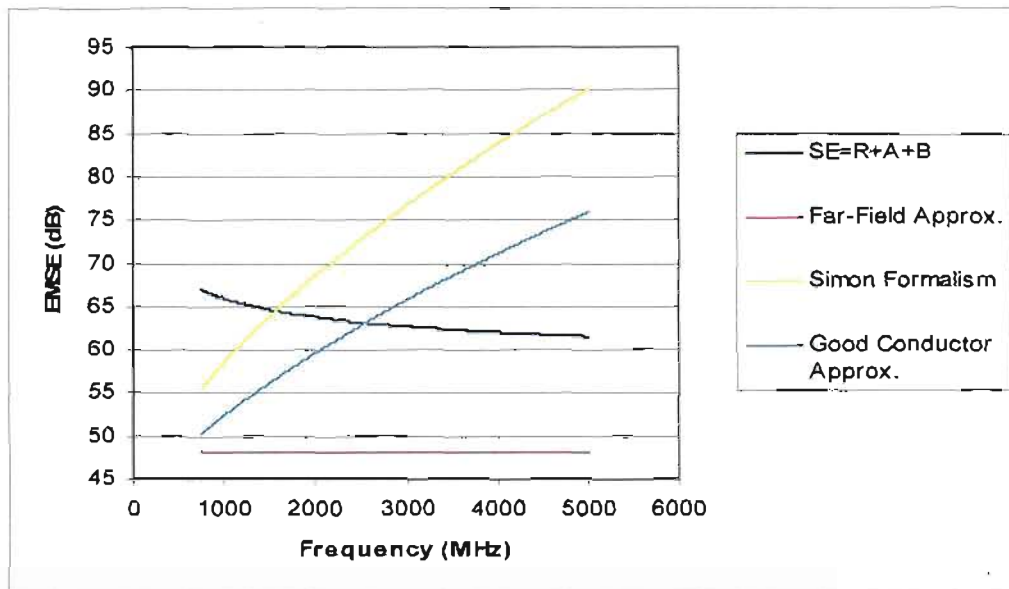


**Figure 10.50:** Comparative graph of EMSE (analytical) vs. Frequency for unidirectional carbon fibre specimens with one metal mesh layer

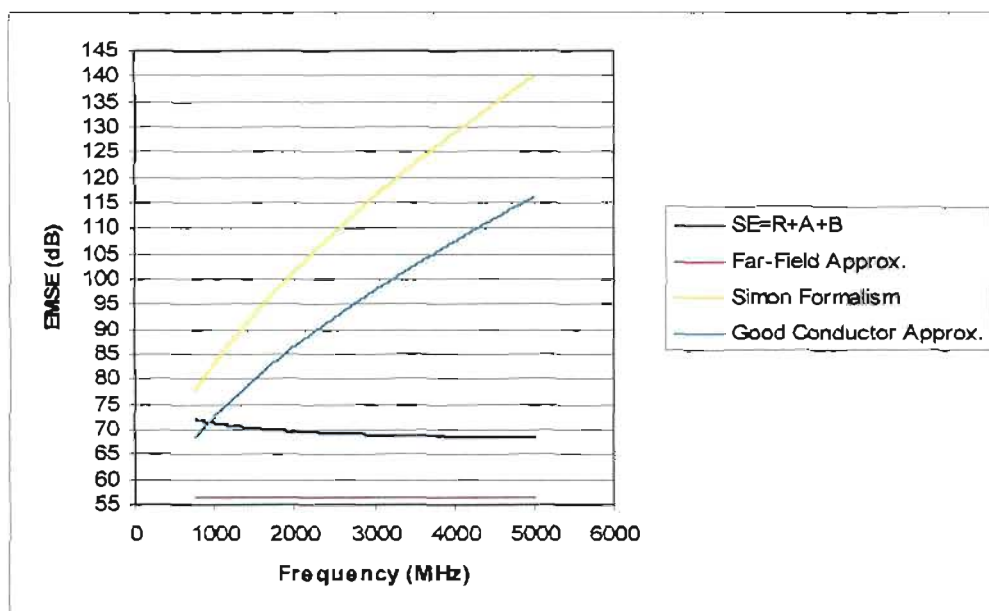


**Figure 10.51:** Comparative graph of EMSE (analytical) vs. Frequency for unidirectional carbon fibre specimens with two metal mesh layers

### c. Electromagnetic Shielding Effectiveness

The actual results from the EMSE testing showed that both the single and double mesh layers are adequate in displaying the shielding performance of an aluminium sheet. The sample with two mesh layers did not appear to provide any significant improvement of the single layer composite. Both materials were found to be superior to the sample without filler.

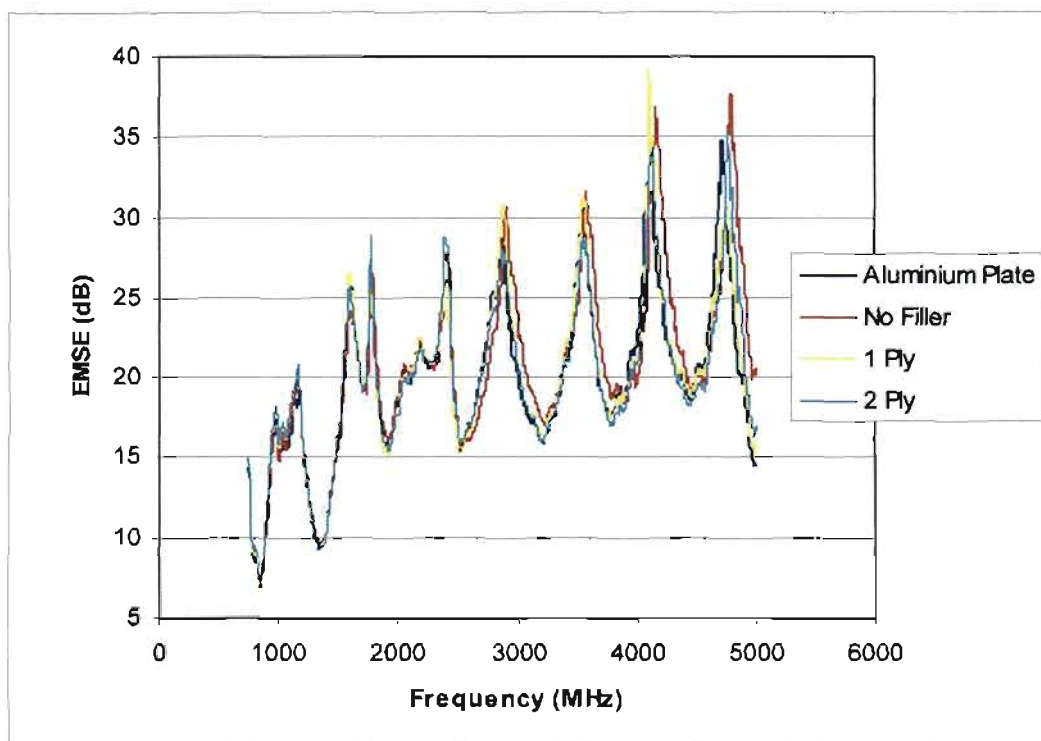


**Figure 10.52:** Actual EMSE vs. Frequency of the metal mesh/unidirectional carbon fibre samples relative to an aluminium plate of the same size

#### 10.2.5 Discussion on Metal Mesh Samples

Theoretically, EMSE should increase with an increase in electrical conductivity in materials. This is due to shielding theoretically being a function of electrical conductivity in the analytical equations. However, Chung [5] and Yang *et al.* [11] have stated that high conductivity is not a strict criterion for shielding, although it should enhance shielding performance due to connectivity. As seen from the actual EMSE test results, composite shielding specimens containing continuous materials seemingly offer no significant improvements in electromagnetic shielding performance when compared with the specimens containing discontinuous filler



materials. By no means was the shielding displayed by these materials of a poor quality; it was just not significantly superior to the shielding displayed by the specimens containing discontinuous filler materials.

However, the low bulk resistance values displayed by these materials indicate their suitability for lightning strike protection. This would likely not be the case for samples with discontinuous fillers, as there were microscopic spaces between the particles, and thus less connectivity between them. The continuous weaves of the material maintains a constant current-carrying path. However, damage due to tensile and bending test show that this continuous current-carry path ceases, due to fracture of the fibres. The damage is visible on a macroscopic level, and images of this, along with images of some other mechanical failures described to have taken place in this work, can be seen in Appendix F.

As seen in the results presented, the theoretical EMSE results from equations (4.14), (4.15) and (4.18) were not in the same degree of correlation as they were in the discontinuous specimens. It was thought that this was likely due to the fact that the electrical resistivities of the samples with continuous fillers were lower than the samples with discontinuous fillers. To verify this, the analytical EMSE results of copper (using its true conductivity value of  $5.8 \times 10^5 \Omega/\text{cm}$  [17]) were computed over the same frequency range. The graphs in figure 10.53 and 10.54 do indeed show a significant lack of correlation, seemingly due to the higher conductivity of this material. Although it may seem that equations (4.14) and (4.15) are in some degree of correlation, the results obtained from equation (4.14) indicate absorption is the dominant mechanism, whilst the results from equation (4.15) indicate reflection is the dominant mechanism.

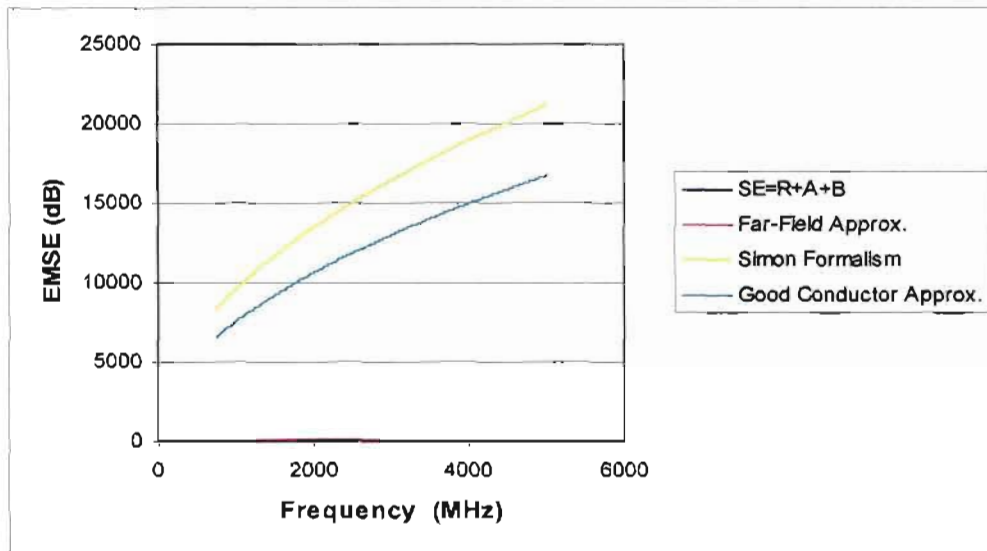


Figure 10.53: Theoretical EMSE results of a copper plate

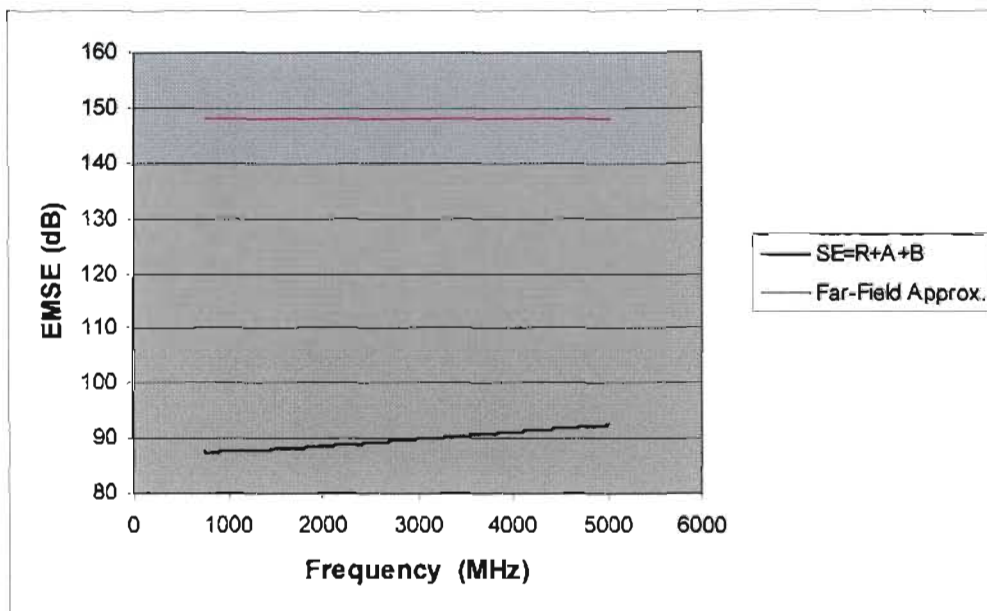


Figure 10.54: Theoretical EMSE results of a copper plate (equations (4.6) and (4.18))

### 10.3 General Discussion on Test Results

The tensile and flexural results show that tensile strength generally decreased with increasing filler loading in all specimens; flexural strength generally increased in the unidirectional and woven carbon specimen, whilst it was not obtained in the stitched carbon specimens due to

excessive deflection; and elastic modulus was generally observed to decrease with increasing filler loading in the specimens.

There was some concern regarding the compressive strength results. It was known that compressive strength of composites is quite poor [84,139]. There are numerous documented reports on erroneous compressive strength in composites [105,140,141]. However, Piggot [141] reports that compressive strength is determined by the failure mode which gives the lowest value, which apparently, in the case of the higher modulus specimens, was due to crushing on the end surfaces. It was known that compressive strength should likely be lower in carbon fibre reinforced composites due to micro-buckling of the fibres, but the results obtained for the stitched carbon specimens indicate a slightly higher compressive strength, compared with tensile strength (which could likely be due to the different test location and test equipment [105]).

The electrical resistance test results showed an increase in resistance as filler loading increased in some specimens. The possible reasons for this were addressed earlier. There was some suspicion that the electrical resistivity value obtained using the available equipment was slightly higher than the true resistivity value of the materials, as was evidenced when measuring copper and aluminium sheet metal on the same instrument. However, despite this, the resistivity values obtained were still much lower than  $100\ \Omega\cdot\text{cm}$ , and in most cases were lower than  $10\ \Omega\cdot\text{cm}$ . This indicates that the materials will theoretically serve as good shielding materials in practice. The actual EMSE test results, which are the best indication of true shielding performance in the materials, showed an increase in EMSE with increasing filler loading, which was expected. Barrier impedance and skin depth results, presented in Appendix E, show that these variables are proportional to electrical conductivity. Therefore, the specimens with the metal mesh displayed the lowest values and appear to be very suitable for lightning strike dissipation.

The possible cause for lack of correlation between the results obtained from analytical EMSE equations and actual testing has been explained. However, as seen from the trends of the various analytical EMSE graphs, it appears that the theoretical results will never correspond with actual results over the entire frequency range in question. It also appears that the lack of correlation between the analytical results obtained from use of the various equations increases as electrical conductivity of the specimens increase.

## **CHAPTER 11: COST AND STRENGTH VS. SHIELDING**

### **ANALYSES**

The materials designed in this work were developed, and displayed excellent shielding characteristics. However, it was required that the net value which these materials provide to aircraft be determined, in order to ascertain whether it would be of benefit to implement them into future designs.

Two studies were initiated for this purpose viz. strength vs. shielding and cost vs. shielding. As mentioned previously, electromagnetic shielding materials do not follow generic designs. Thus, the intention of the study was not to determine a single material for electromagnetic shielding, but to determine the suitability of several materials for possible use.

However, shielding performance does not increase by a single tangible value, as seen by the experimental results in Chapter 10. Also, shielding is a function of frequency and thus the shielding performance displayed at a particular frequency is not comparable with shielding performance displayed at a different frequency.

For this study it was decided that the materials would be benchmarked against aluminium, which is commonly used in aircraft for its lightweight, shielding performance, and strength properties. The formula developed to determine relative shielding quality was:

$$\% \text{ Difference} = \frac{SE_{\text{Aluminium}} - SE_{\text{Composite}}}{SE_{\text{Aluminium}}} \times 100 \quad (11.1)$$

Where:  $SE_{\text{Aluminium}}$  = shielding effectiveness of aluminium at a frequency

$SE_{\text{Composite}}$  = shielding effectiveness of composite at the same frequency

For this study, it was desired to have a percentage difference predominantly greater than 0, or as close to 0 as possible. This implies that the SE found in the shielding material is superior, or similar to that found in aluminium over the entire frequency range in question (750 MHz to 5 GHz). The results are shown in Appendix H. The results show that although the samples with no filler materials display higher SE when compared with aluminium and the other materials at some

frequencies, they have difficulty in maintaining a high quality over the entire frequency range. That is, they also display the lowest SE values in certain frequency ranges. As mentioned in Chapter 10, there was no substantial benefit in including a second metal mesh layer, as there was little difference between these specimens when compared with specimens containing a single metal mesh layer. The samples with 7.5% discontinuous filler loading generally maintained adequate SE over the entire frequency range and the samples with 15% discontinuous filler loading generally showed improvement over this as well.

As aircraft are exposed to a wide frequency range in practice, the samples with higher filler loadings were found to be more suitable, as they maintain shielding quality over the entire frequency range.

### **11.1 Strength vs. Shielding Analysis**

Reliable results for all of the composite materials' properties could not be established with assurance in this work. For instance, bending strength of stitched carbon specimens was indeterminate, as the specimens deflected excessively during testing; and compressive strengths were obtained using different testing equipment at a different test location, and those conditions may not have been comparable to that at UKZN. Thus in order to develop a reliable means of comparison, tensile strength; yield elongation; break elongation; and elastic modulus were selected as the comparison data in this work. It was found that this data is typically used in industry for the comparison of material data as well, and very seldom is reference made to flexural or compressive strengths.

**Table 11.1 Mechanical Properties of Aluminium and its Alloys [Amended from 142]**

<b><u>Material</u></b>	<b><u>Tensile Strength</u></b> <b><u>(MPa)</u></b>	<b><u>Yield Strength</u></b> <b><u>(MPa)</u></b>	<b><u>Break</u></b> <b><u>Elongation (%)</u></b>	<b><u>Elastic Modulus</u></b> <b><u>(GPa)</u></b>
Aluminium Alloys	35-500	100-550	1-45	70-79
2014-T6	480	410	13	73
6061-T6	310	270	17	70
7075-T6	550	480	11	72

The 2mm aluminium sheet material purchased was measured to have a mass density of  $2695\text{kg/m}^3$ , which correlates to the mechanical data of 6061-T6 aluminium, as this material is

reported to have a mass density of  $2700\text{kg/m}^3$ . However, the values in Table 11.2 were obtained by using the data from the mechanical testing of the various shielding materials presented in Chapter 10, compared against the mechanical properties of 7075-T6 aluminium. This aluminium material was selected, as it contains the best mechanical properties of the aluminium materials presented in Table 11.1, and thus provides a conservative estimate in the differences between strength and stiffness properties found in these materials.

**Table 11.2: Differences in Tensile Strength, Yield Strength and Elastic Moduli between Composite Shielding Materials and Aluminium**

Material	% Difference in Tensile Strength	% Difference in Yield Strength	% Difference in Elastic Modulus
Undoped Stitched CF	-86.7	-87.3	-80.4
Undoped Woven CF	49.3	62.5	1.3
Undoped UD CF	52.9	74.8	150.5
7.5% Al Stitched	-85.8	-85.4	-88.1
7.5% Al Woven	19.8	37.3	-29.1
7.5% Al UD	44.7	61.9	112.5
7.5% Cu Stitched	-86.4	-87.3	-84.4
7.5% Cu Woven	15.6	32.5	-37.6
7.5% Cu UD	39.8	54.2	64.3
7.5% Hybrid Stitched	-90.2	-89.4	-90.2
7.5% Hybrid Woven	15.6	32.5	-33.5
7.5% Hybrid UD	39.5	56.3	67.9
15% Al Stitched	-86.4	-85	-88.7
15% Al Woven	11.5	27.7	-38.8
15% Al UD	28	30.8	64.1
15% Cu Stitched	-85.8	-87.9	-86.1
15% Cu Woven	20.2	37.5	-28.6
15% Cu UD	34.4	44.8	96
15% Hybrid Stitched	-87.3	-87.3	-90.2
15% Hybrid Woven	8.2	24	-34.3
15% Hybrid UD	64.4	82.3	70.3
1 Ply Stitched	-86.2	-87.9	-85.3
1 Ply Woven	28	46.3	-31
1 Ply UD	-5.3	-29.4	51.7
2 Ply Stitched	-84.9	-87.3	-87.8
2 Ply Woven	17.8	33.8	-29.2
2 Ply UD	-0.2	9	69.3

Note: A negative percentage difference in Table 11.2 implies that aluminium is the superior material in that property

It can be seen that the stitched carbon fibre samples are significantly inferior to aluminium in all properties. This material will thus not suffice as a structurally supportive agent in practice. It can

be seen that the unidirectional carbon fibre composite specimens with discontinuous fillers are superior in tensile and yield strengths when compared with aluminium, and possess higher elastic moduli opposed to aluminium. The 12K woven carbon fibre specimens possessed lower elastic moduli opposed to aluminium, in the range of 45-70 GPa, but possessed higher tensile and yield strengths opposed to aluminium. The unidirectional specimens containing metal mesh were inferior to aluminium in tensile strength, but possessed a higher elastic modulus.

As discontinuous filler loading in composites increased, shielding was observed to generally increase. However, as explained in Chapter 10, increasing filler loading generally resulted in a reduction in strength and elastic moduli. However, as seen in Table 11.2, the strengths of doped woven and unidirectional carbon-fibre specimens were still significantly superior to that found in aluminium. The elastic moduli of the doped unidirectional specimens was also substantially higher than that of aluminium as well.

## **11.2 Cost vs. Shielding Analysis**

The strength properties of the shielding materials developed in this work in comparison to aluminium, which is typically used for electromagnetic shielding in aircraft, have been explained. The actual cost analysis of the raw materials that constitute the composite material can be seen in Appendix I.

As expected, the cost of the laminate increases as raw material content increases. Samples with metal mesh were found to be the most costly composites, due solely to the comparatively high cost of the metal mesh fabric. The increase in cost of the samples containing discontinuous filler materials was negligible, due to the low cost of these materials.

The comparative cost analysis of the composites with aluminium can be seen in Table 11.3 below. The negative percentage value denotes that the composites are more expensive compared to aluminium. As expected, the composites are significantly more expensive than aluminium.

The table also shows the percentage increase in the cost of the electrically-enhanced composites over the base laminate. Inclusion of metal powders result in an increase of approximately 2-3% in the composites, whilst use of metal mesh results in an increase of approximately 80% in the composites.

**Table 11.3: Comparative Cost Analysis of Composite Shielding**

Material	Cost of 300mm <sup>2</sup> Material	Cost of 1m <sup>2</sup> Material	% Cost Increase in Laminate with Filler	% Difference in Cost With Aluminium
Undoped Stitched CF	101.35	1126.06	N/A	-305.4
Undoped Woven CF	224.14	2490.40	N/A	-796.5
Undoped UD CF	181.75	2019.48	N/A	-627.0
7.5% Al Stitched	103.29	1147.64	1.92	-313.1
7.5% Al Woven	227.52	2528.00	1.51	-810.1
7.5% Al UD	184.34	2048.24	1.42	-637.4
7.5% Cu Stitched	104.50	1161.12	3.11	-318.0
7.5% Cu Woven	227.32	2525.78	1.42	-809.3
7.5% Cu UD	182.83	2031.49	0.59	-631.3
7.5% Hybrid Stitched	103.69	1152.09	2.31	-314.8
7.5% Hybrid Woven	227.45	2527.20	1.48	-809.8
7.5% Hybrid UD	183.85	2042.77	1.15	-635.4
15% Al Stitched	104.99	1166.51	3.59	-319.9
15% Al Woven	229.03	2544.83	2.19	-816.1
15% Al UD	184.88	2054.27	1.72	-639.5
15% Cu Stitched	106.29	1181.02	4.88	-325.2
15% Cu Woven	228.82	2542.43	2.09	-815.3
15% Cu UD	183.90	2043.35	1.18	-635.6
15% Hybrid Stitched	105.76	1175.10	4.36	-323.0
15% Hybrid Woven	228.19	2535.50	1.81	-812.8
15% Hybrid UD	184.28	2047.54	1.39	-637.1
1 Ply Stitched	190.47	2116.35	87.94	-661.9
1 Ply Woven	312.97	3477.49	39.64	-1151.9
1 Ply UD	269.01	2989.00	48.01	-976.0
2 Ply Stitched	273.96	3043.96	170.32	-995.8
2 Ply Woven	396.42	4404.63	76.86	-1485.7
2 Ply UD	352.14	3912.70	93.75	-1308.6

Note: A negative percentage difference in Table 11.3 implies that aluminium is cheaper

However, in weight-critical applications, such as aircraft, it is also necessary to refer a figure-of-merit referred to as shielding density (SD) [17]. The SD value was devised to relate EMSE per unit weight per unit area of a shielding material, to present an indication which shielding materials would be most suitable for weight-critical applications. [17]. It is important to note that SD does not provide an indication of actual EMSE, but rather provides an indication of which materials possess the greatest amount of shielding in relation to weight [17]. Thus, materials with the same SD value do not possess the same EMSE. SD is presented by equation (11.2) on page 170.



$$SD = SE (W/A) \quad (11.2) \quad [17]$$

Where: SE = shielding effectiveness (dB)

$$W/A = \text{weight per unit area of material thickness (g/m}^2 / \mu\text{m)} \quad (11.3) \quad [17]$$

From qualitative inspection of equation (11.3), it can be seen that the SD of aluminium with density of  $2695\text{kg/m}^3$  will be  $2.695\text{g/m}^2 / \mu\text{m}$ . The average mass densities and W/A values of the carbon fibre laminates are presented in Table 11.4. As seen, the results show that the carbon fibre laminates are between 45-58% lighter in weight opposed to aluminium.

**Table 11.4: Mass Densities, % Difference in Weight between Aluminium, and W/A Values**

Material	Average Mass Density ( $\text{kg/m}^3$ )	% Difference in Mass Density between Aluminium	W/A ( $\text{g/m}^2 / \mu\text{m}$ )
Undoped Stitched CF	1119.78	58.4	1.120
Undoped Woven CF	1273.31	52.8	1.273
Undoped UD CF	1317.29	51.1	1.317
7.5% Al Stitched	1277.64	52.6	1.278
7.5% Al Woven	1374.97	49.0	1.375
7.5% Al UD	1432.10	46.9	1.432
7.5% Cu Stitched	1384.82	48.6	1.385
7.5% Cu Woven	1435.28	46.7	1.435
7.5% Cu UD	1412.15	47.6	1.412
7.5% Hybrid Stitched	1259.95	53.2	1.260
7.5% Hybrid Woven	1392.30	48.3	1.392
7.5% Hybrid UD	1392.14	48.3	1.392
15% Al Stitched	1360.52	49.5	1.361
15% Al Woven	1417.14	47.4	1.417
15% Al UD	1404.58	47.9	1.405
15% Cu Stitched	1427.91	47.0	1.428
15% Cu Woven	1494.10	44.6	1.494
15% Cu UD	1460.63	45.8	1.461
15% Hybrid Stitched	1349.06	49.9	1.349
15% Hybrid Woven	1444.89	46.4	1.445
15% Hybrid UD	1468.32	45.5	1.468
1 Ply Stitched	1250.94	53.6	1.251
1 Ply Woven	1409.81	47.7	1.410
1 Ply UD	1307.30	51.5	1.307
2 Ply Stitched	1222.46	54.6	1.222
2 Ply Woven	1406.96	47.8	1.407
2 Ply UD	1279.18	52.5	1.279

In many cases, the composite shielding materials displayed greater shielding performance opposed to the aluminium base when the EMSE experimental results were analysed in Chapter 10. Even the undoped specimens were found to be only slightly inferior to aluminium in shielding quality. Thus, qualitative inspection of equation (11.3) shows that the composite shielding materials possess a lower SD at any given frequency in the range used in this work, simply due to their W/A values being between 45-58% less than that of aluminium.

Lighter materials that provide similar EMSE are more desired in many aircraft applications, and the composite materials adequately suffice this requirement, and are superior to aluminium in this regard.

Therefore, the composite shielding materials, which although are more expensive to install in aircraft, do provide valuable weight savings, and are clearly superior in terms of SD. However, with the increasing fuel costs, the net return is likely far greater with composite materials, which are lighter in weight.

### **11.3 Discussion on Strength vs. Shielding and Cost vs. Shielding**

The woven carbon and unidirectional carbon composite materials are suitable for high strength applications. The unidirectional carbon specimens possess greater tensile strengths and elastic moduli opposed to aluminium; whilst the woven carbon specimens possess greater tensile strength but lower elastic moduli opposed to aluminium. In addition, the materials are much lighter in weight when compared with aluminium. Thus, the SD of the materials is much lower than that of aluminium which is desired in weight-critical applications such as aircraft [5,17]. In addition, cost savings also come from the generally non-corrosive nature of composite, and their excellent fatigue resistance, which implies a longer in-service life.

The cost of the raw materials to develop the composite material is far greater than the cost of aluminium sheet material of similar size. However, the long-term cost savings in using composite materials directly comes from weight savings and manufacturing cost savings when developing more complex shapes. Research in development of secondary bonding mechanisms of these composite electromagnetic shielding materials is currently underway at UKZN. Successful development of a five-sided box-shaped laminate has been performed in this work, and will be explained in Chapter 12.

Implementing the composite electromagnetic shielding materials developed in this work is solely the choice of the aircraft developer. It will depend on factors such as projected aircraft life-span and the purpose of the aircraft in practice. For instance, undoped shielding materials could suffice shielding in regions that are not prone to high frequencies, whilst composites containing metal meshes will be required in regions prone to lightning strike.

The many benefits, such as higher strength compared to aluminium; high SE comparable and exceeding that displayed in aluminium; the much lighter weight of the composite components; and potential long-term return make them more desired in today's aircraft in the opinion of this author. However, it is imperative that the different regions are identified by the aircraft developer to avoid over-compensating, and subsequently incurring additional expense by implementing the more costly composite shielding materials in regions which the cheaper ones could suffice.

## **CHAPTER 12: FABRICATION OF COMPLEX-SHAPED LAMINATES**

The electromagnetic shielding materials developed have proven to display many potential cost-saving features, despite their relatively high start-up costs. However, composite materials containing holes, slits or other apertures present problems in maintaining a high quality of electromagnetic shielding [17].

For this reason, a separate secondary bonding study is currently underway at UKZN. In this work, investigation was made to determine if a multiple-sided laminate could be successfully fabricated. There were some concerns by interested persons regarding the drapability of carbon fabrics, if potential “one-shot” processes were to adequately work. A box-shaped laminate was designed to determine if the process was feasible.

### **12.1 Design of the Mould**

As mentioned, apertures or other discrepancies between shielding materials could result in degradation of shielding performance in practice. For this reason, bonded surfaces should maintain the shielding quality provided by the shielding material itself [143]. Thus, to limit the amount of surfaces that would require secondary bonding, a five-sided box mould, for the manufacture of a five-sided box laminate, was designed. The mould had to contain surfaces that could be easily separated, in order to allow the laminate to be removed without damage.

The mould consisted of a base, and four side surfaces. The surfaces all contained draft angles of  $45^\circ$  to allow for easy removal of the mould upon curing. The material used for the mould was 4.5mm thick aluminium sheet metal, obtained from Aluminium City, Durban, SA. The draft angles were bent into the sheet metal, and the triangular aluminium pieces were cut and welded to the corners of the base. The computer aided design (CAD) drawings in Appendix J describe the base and sides of the mould.

It was decided that the surfaces would be held together by means of hinges on three sides, and with steel clips of the fourth side. Countersunk holes were drilled on the inner surfaces of each

side, to allow for the hinges to fit without visibly indenting the laminate surfaces. The final box mould is shown in Figures 12.1 and 12.2.

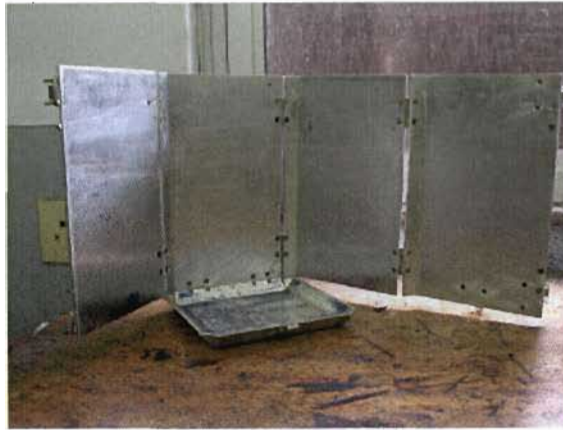


*Figure 12.1: The open box-mould with the sides unclipped*



*Figure 12.2: The box-mould with the sides clipped in place*

## **12.2 Manufacture of the Box-Shaped Laminate**

The laminate was fabricated using LR20 epoxy resin, with LH281 hardener, which was applied to the surfaces by means of an aluminium roller. The material was laid on the inner surfaces of the mould, with the fabric draped from one end of each side to the extreme end. Strips of the same length were applied in the same way to the angled surfaces. Upon completely encapsulating the

system in resin, layers of bleeder and breather cloth were placed over the materials, and the system was enclosed in a vacuum bag. Vacuum pressure of 80kPa was introduced into the system. The laminate was allowed to remain under the influence of vacuum pressure for 5hrs, and was subsequently allowed to cure for 30hrs. The vacuum bag was then removed, and the laminate was post cured at 65 ° C for 16hrs. The laminate was then removed as anticipated.



*Figure 12.3: The laminate being removed from the mould*

### **12.3 Concluding Remarks on Box-Shaped Laminates**

A suitable means of fabricating multi-sided parts has been established. The mould designed in this work adequately served to provide a five-sided carbon fibre box. There were no problems experienced with the drapability of carbon fabric, and this was likely due to inclusion of sufficient draft angles in the mould design. A box-shaped structure of this type can be used for housing on-board electronic equipment or avionics, and only requires one surface to be bonded, thus limiting shielding performance degradation.



*Figure 12.4: The final box-shaped laminate*

EMSE measurements of the box, or specimens with apertures, do not provide a true indication of the EMSE, due to leakage through the aperture. Thus, a true indication of the EMSE of enclosures can only be undertaken upon bonding a panel on the open-sided end of these objects. As mentioned, the secondary bonding study at UKZN will address these concerns upon completion.

## **CHAPTER 13: DISCUSSION ON RADAR CROSS SECTION**

To conclude this work, a study on radar cross section (RCS) was undertaken on the shielding materials. Although radar cross-section (RCS) measurements are usually undertaken on entire systems, such as an entire aircraft, investigation on the RCS displayed by the individual 300mm<sup>2</sup> shielding materials was undertaken.

### **13.1 Concepts of Radar Cross-Section**

RCS measurements are of particular importance to stealth of the aircraft [144], which is not the area of study in this work. Stealth involves reflecting as little power back to the radar source as possible to avoid early detection [144]. RCS measurements are thus dependant on the amount of power returned from a particular target to the transmitting radar [144]. The power that is reflected back to the radar is referred to as the “backscatter”, or “backscattered power” [144,145].

The quantity of RCS is determined by three factors [144]:

1. Geometric cross section, which refers to the projected area that the target presents to the radar. This is dependant on where the object is flying in relation to the radar [144].
2. Reflectivity, which refers to the fraction of power that is reflected back by the target [144].
3. Directivity, which refers to the power that is scattered back in the direction of the source radar [144].

These three factors determine the RCS of a target object. They are related by:

$$\sigma = A \times \frac{P_{scatter}}{(A)(P_{intercepted})} \times \frac{P_{backscatter}}{\left(\frac{1}{4\pi}\right)P_{scatter}} = 4\pi \left( \frac{P_{backscatter}}{P_{intercepted}} \right) \quad (13.1) \quad [144]$$

Where:  $\sigma$  = RCS (m<sup>2</sup>)

$A$  = geometric cross-section (m<sup>2</sup>)

$P_{intercepted}$  = power intercepted by the target

$P_{scatter}$  = power scattered by the target



$P_{backscatter}$  = power backscattered by the target

The RCS measurements were undertaken at UP in this work, and were performed on the same equipment used for EMSE testing. The results, provided in terms of  $S_{11}$  scatter parameters, were undertaken over the frequency range of 2 GHz to 5 GHz. The results obtained were for RCS in terms of dBsm (decibels relative to a square meter).

$$RCS_{dBsm} = 10 \log \left( \frac{\sigma}{1m^2} \right) \quad (13.2) \quad [145]$$

Where:  $RCS_{dBsm}$  = radar cross-section (dBsm)

Equation (13.2) can be rewritten as:

$$\sigma = 10^{\left( \frac{RCS_{dBsm}}{10} \right)} \quad (13.3)$$

The linear results of RCS were computed using equation (13.3), and  $\sigma$  vs. Frequency graphs can be found in Appendix K for all of the shielding materials (The tabulated data is not presented as there are 401 data points within the frequency range, and the results are too extensive). Inspection of the data shows that the shielding materials return a strong backscatter in the direction of the radar, which was generally constant. The strong backscatter was due to the surface finish on the materials, which like many fibre composites, was not perfectly smooth along the entire surface area. This was mainly the case for the stitched carbon specimens as their surface finishes were particularly uneven. The woven and unidirectional carbon specimens displayed a generally consistent RCS over the entire frequency range in question.

### **13.2 Discussion on RCS**

The RCS measurements undertaken in this work were for the basic 300mm<sup>2</sup> shielding specimens. However, a true indication for complete RCS is best undertaken on the aircraft system, as RCS measurements are geometry-dependant [144]. The RCS measurements are usually provided in the form of polar plots for these complex shapes.

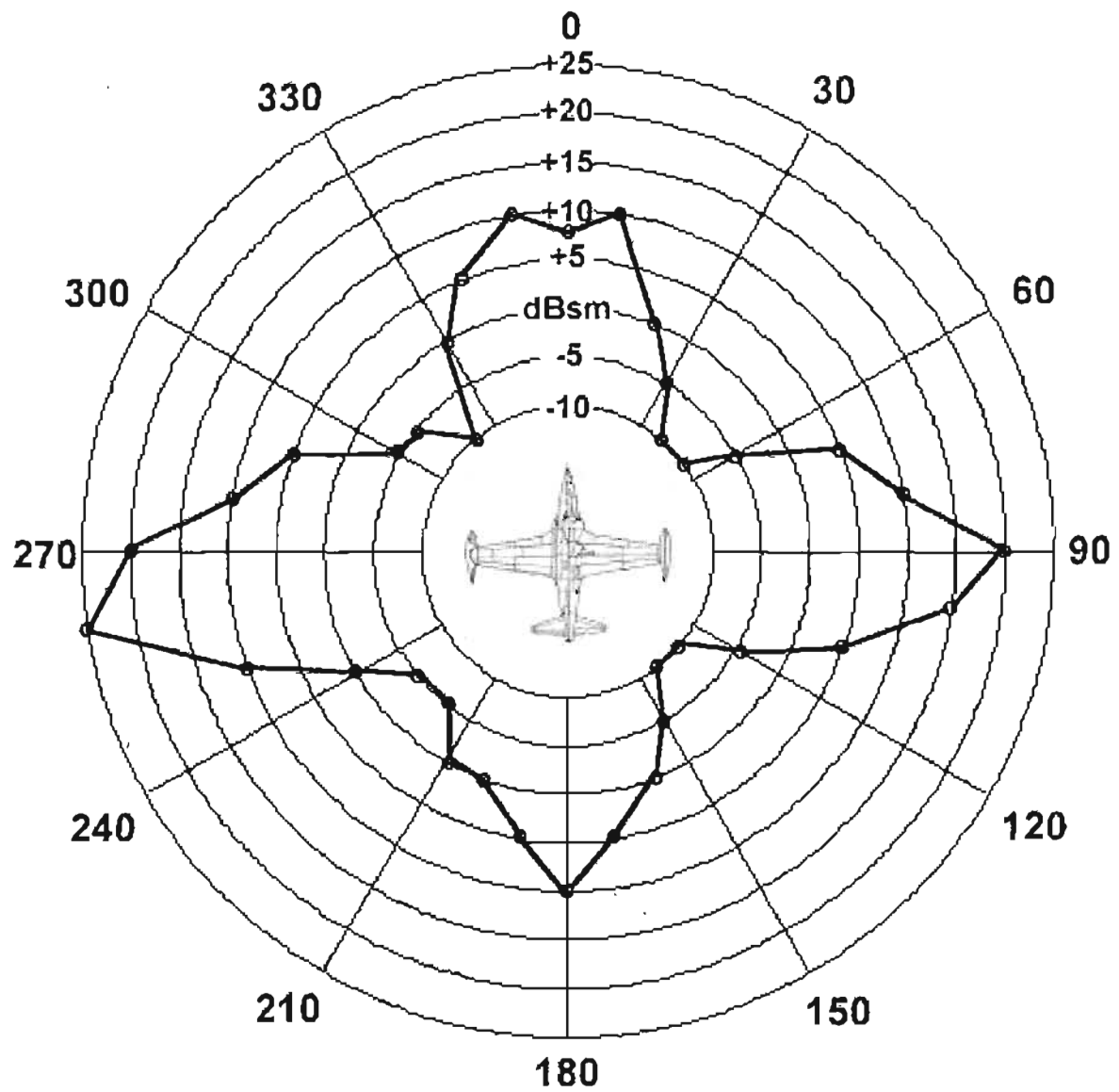


*Figure 13.1: RCS polar plot of the T-33 aircraft [144]*

RCS measurements are quite dependant on the location of the aircraft in relation to the radar [144]. It has been found that RCS varies significantly with location, frequency, wavelength and fidelity of the receiver [144].

## **CHAPTER 14: CONCLUSIONS**

The successful development of fibre composite electromagnetic shielding materials has been achieved in this work. The shielding performance displayed, particularly from specimens with discontinuous filler materials, were found to be superior to aluminium at many frequencies. The samples with continuous metal filler materials were found to display similar shielding performance to those with discontinuous fillers, but have valuable properties such as higher electrical conductivity when lightning strike is considered. For locations exposed to lightning strike, materials with continuous fillers are recommended, as it was successfully determined that their electrical resistance is less than  $1\ \Omega$ , which is required in those regions.

The samples containing stitched carbon fibre as a possible structural-reinforcement were found to display poor shielding. The undoped-epoxy based laminates containing this material displayed poor strength as well, which was unexpected.

The woven carbon specimens displayed excellent strength, but lower elastic moduli, when compared with aluminium. This composite material was also found to be the most costly to install in aircraft as well.

The unidirectional carbon specimens have displayed excellent electromagnetic shielding and structural properties. Shielding specimens with this material have displayed comparable, and in some cases higher, shielding performance when compared with aluminium. These specimens were also found to display significantly higher strength and elastic moduli opposed to aluminium.

The initial cost of installing composite materials in aircraft has been found to be higher than metal components. However, there are many disadvantages associated with metals such as higher weight, fatigue, and corrosion damage. In addition, there are many attractive long-term benefits that composite materials provide, and their use will certainly result in higher efficiency and higher performance vehicles.

It is thus the author's opinion that the composite materials should be implemented in prospective airborne vehicles. A wide range of materials that provide excellent shielding performance, and high strength capabilities, have been developed and the choice of which materials to implement is at the discretion of the aircraft developer.



## **APPENDICES**

## APPENDIX A: METAL PROPERTIES [17]

**Table A1: Metal Properties**

(1) Metal	(2) Relative Conduct. $\sigma_r$	(3) Relative Permbly. $\mu_r @ \leq 10\text{kHz}$	(4) Product $\sqrt{\sigma_r \mu_r}$ $A = k_1 \sqrt{\sigma_r \mu_r}$	(5) Quotient $\sqrt{\sigma_r / \mu_r}$ $R = k_2 \sqrt{\sigma_r / \mu_r}$	(6) Relative Reflection $R_{dB}$
1. Silver	1.064	1	1.03 dB	1.3	+0.3 dB
2. Copper (Solid)	1.00	1	1	1	0
3. Copper (Flame Spray)	0.10	1	0.32	0.32	-10.0
4. Gold	0.70	1	0.88	0.88	-1.1
5. Chromium	0.664	1	0.81	0.81	-1.8
6. Aluminum (Soft)	0.63	1	0.78	0.78	-2.1
7. Aluminum (Tempered)	0.40	1	0.63	0.63	-4.0
8. Aluminum (Household Foil, 1 mil)	0.53	1	0.73	0.73	-2.8
9. Aluminum (Household Foil, 1 mil)	0.61	1	0.78	0.78	-2.1
10. Aluminum (Flame Spray)	0.036	1	0.19	0.19	-14.4
11. Brass (91% Cu, 9% Zn)	0.47	1	0.69	0.69	-3.3
12. Brass (66% Cu, 34% Zn)	0.35	1	0.52	0.52	-5.7
13. Magnesium	0.38	1	0.61	0.61	-4.3
14. Zinc	0.305	1	0.57	0.57	-4.9
15. Tungsten	0.314	1	0.56	0.56	-5.0
16. Beryllium	0.33	1	0.53	0.53	-5.5
17. Cadmium	0.232	1	0.48	0.48	-6.3
18. Platinum	0.17	1	0.42	0.42	-7.6
19. Tin	0.151	1	0.39	0.39	-8.2
20. Tantalum	0.12	1	0.33	0.33	-9.6
21. Lead	0.079	1	0.28	0.28	-11.0
22. Monel (67 Ni, 30 Cu, 2 Fe, 1 Mn)	0.041	1	0.20	0.20	-13.9
23. Manganese	0.039	1	0.20	0.20	-14.1
24. Titanium	0.036	1	0.19	0.19	-14.4
25. Mercury (Liquid)	0.018	1	0.13	0.134	-17.4
26. Nichrome (65 Ni, 12 Cr, 23 Fe)	0.0012	1	0.035	0.035	-29.2
27. Superalloy	0.023	100,000	53.7	0.0005	-65.4
28. 78 Permalloy	0.108	8,000	29.4	0.0037	-48.7
29. Purified Iron	0.17	5,000	29.2	0.0058	-44.7
30. Conetic AA	0.031	20,000	28.7	0.0011	-58.8
31. 4-79 Permalloy	0.0314	20,000	25.1	0.0013	-58.0
32. Mumetal	0.0289	20,000	24.0	0.0012	-58.4
33. Permendur (50 Cu, 1-2V, & Fe)	0.247	800	14.1	0.018	-35.1
34. Hypernick	0.0345	4,500	12.5	0.0028	-51.1
35. 45 Permalloy (1200 Anneal)	0.0384	4,000	12.4	0.0031	-50.2
36. 45 Permalloy (1050 Anneal)	0.0384	2,500	9.80	0.0039	-48.1
37. Hot-Rolled Silicon Steel	0.0384	1,500	7.59	0.0051	-45.9
38. Sinimax	0.0192	3,000	7.59	0.0025	-51.9
39. 42 Silicon Iron (Grain Oriented)	0.037	1,500	7.45	0.0050	-46.1
40. 42 Silicon Iron	0.029	500	3.81	0.0076	-42.4
41. 16 Alfenol	0.0113	4,500	7.13	0.0016	-56.0
42. Hiperco	0.069	650	6.70	0.010	-39.7
43. Monimax	0.0216	2,000	6.57	0.0033	-49.7
44. 50% Nickel Iron	0.0384	1,000	6.20	0.0062	-44.2
45. 45-25 Perminvar	0.091	400	6.03	0.015	-36.4
46. Commercial Iron (0.2% impure)	0.17	200	5.83	0.29	-30.7
47. Cold-Rolled Steel	0.17	180	5.53	0.031	-30.2
48. Nickel	0.23	100	4.70	0.047	-26.6
49. Stainless Steel (1Cu, 18Cr, 8Ni, & Fe)	0.02	200	2.00	0.010	-40.0
50. Rhometal (36 Ni)	0.019	1,000	4.36	0.0044	-47.2
51. Netic 53-6	0.172	300	7.18	0.024	-32.4

**APPENDIX B: IMAGES OF ELECTROMAGNETIC SHIELDING  
MATERIALS**

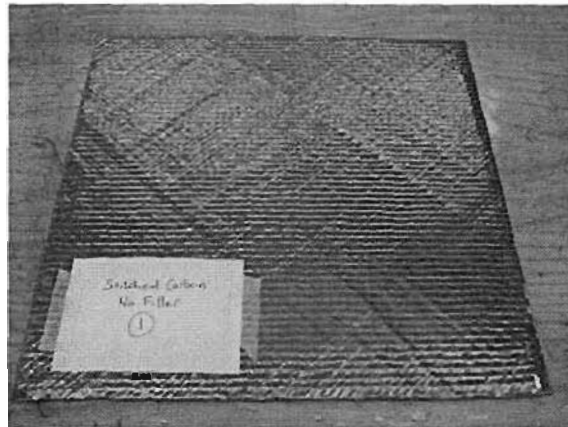


Figure B1: Undoped Stitched sample

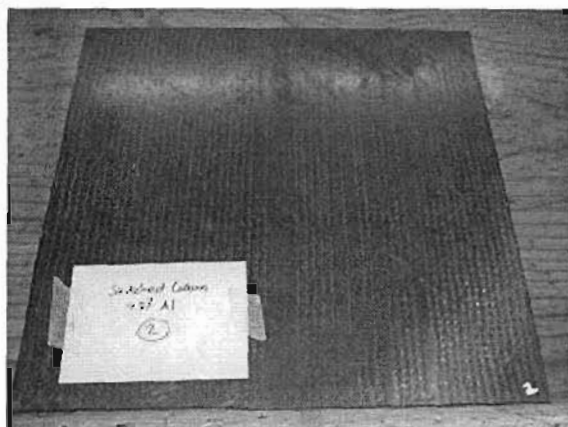


Figure B2: 7.5% Aluminium-doped Stitched sample

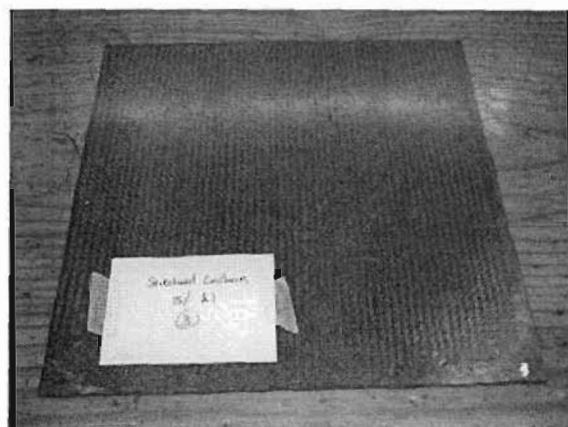


Figure B3: 15% Aluminium-doped Stitched sample

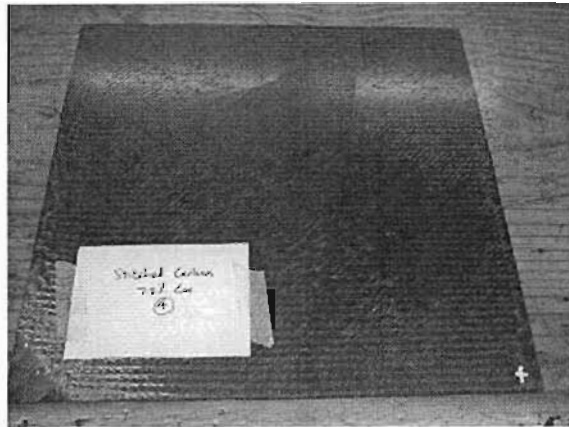


Figure B4: 7.5% Copper-doped Stitched sample

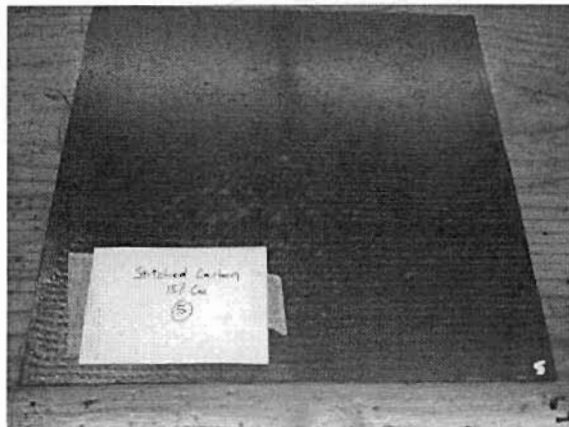


Figure B5: 15% Copper-doped Stitched sample

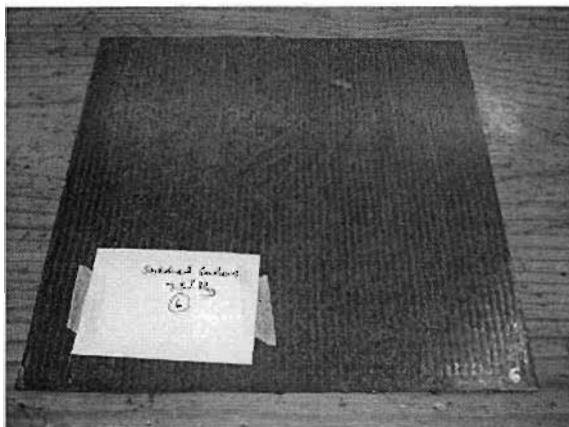


Figure B6: 7.5% Hybrid-doped Stitched sample



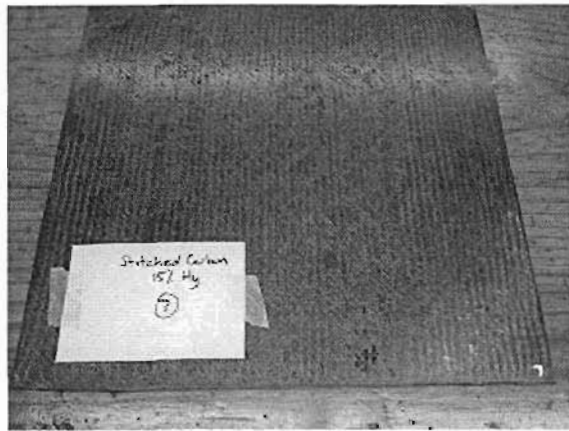


Figure B7: 15% Hybrid-doped Stitched sample



Figure B8: 1 Ply Mesh/Stitched sample

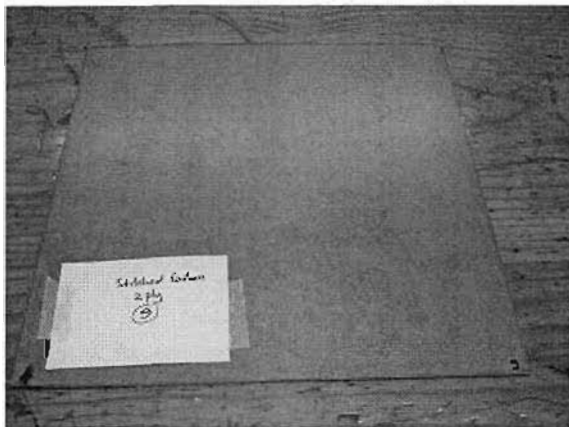


Figure B9: 2 Ply Mesh/Stitched sample

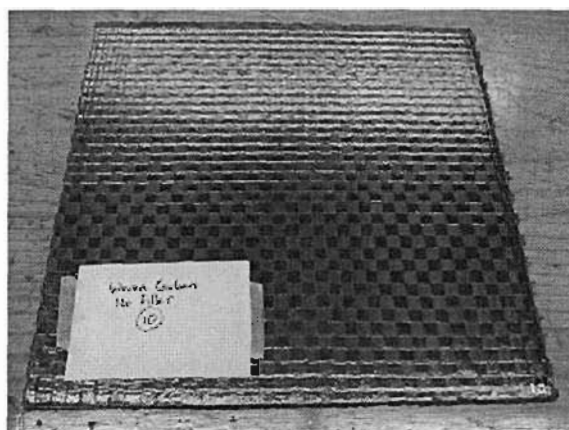


Figure B10: Undoped Woven sample

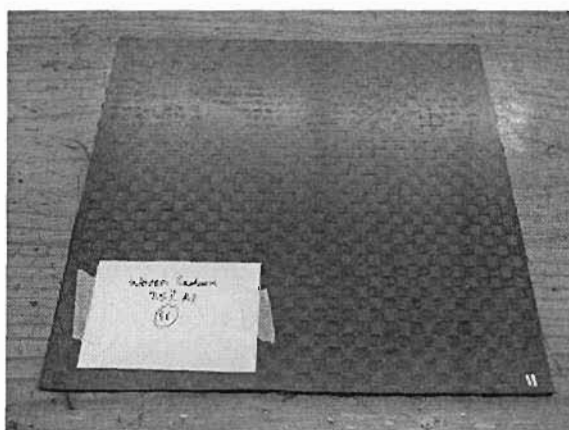


Figure B11: 7.5% Aluminium-doped Woven sample

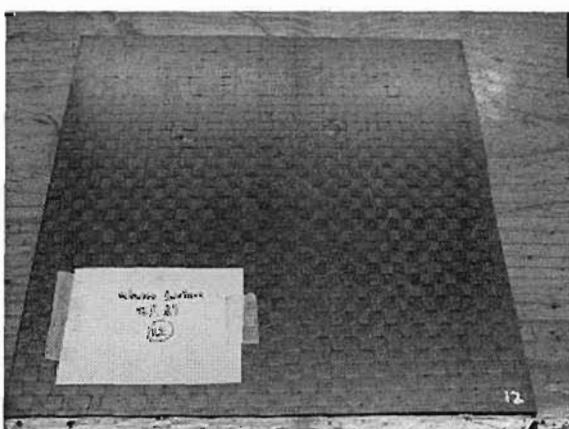


Figure B12: 15% Aluminium-doped Woven sample

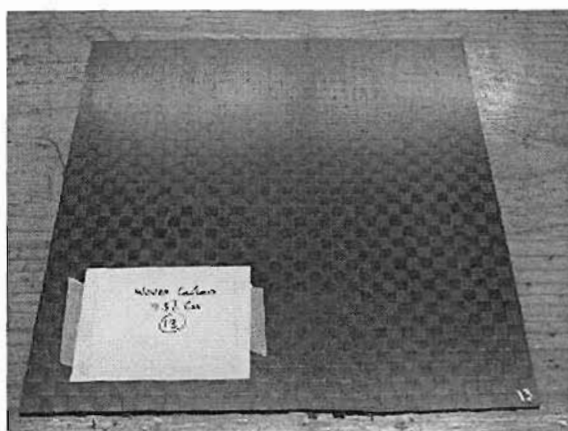


Figure B13: 7.5% Copper-doped sample

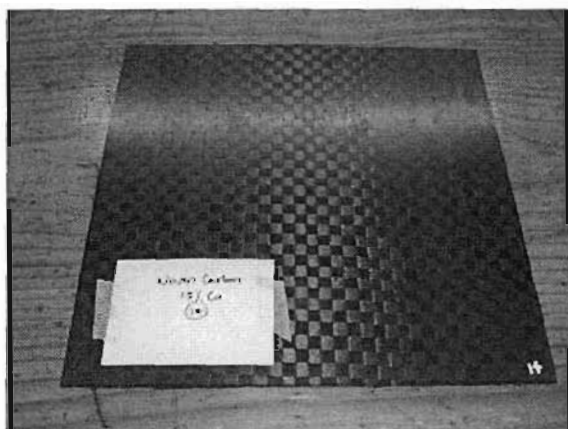


Figure B14: 15% Copper-doped sample

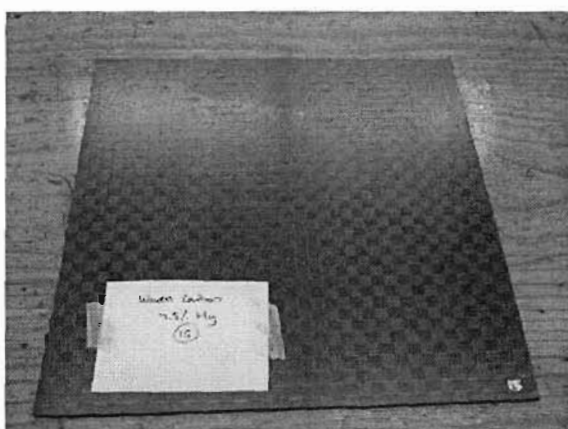


Figure B15: 7.5% Hybrid-doped sample

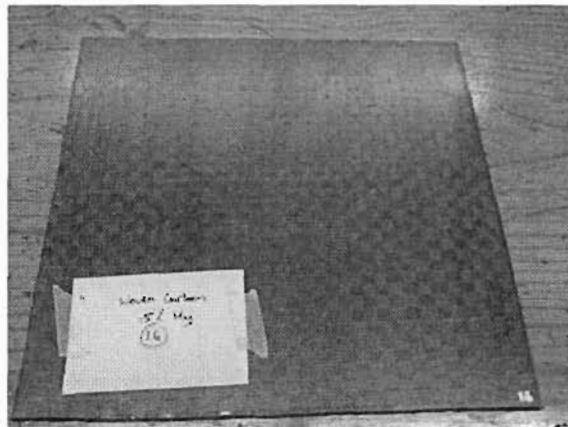


Figure B16: 15% Hybrid-doped sample

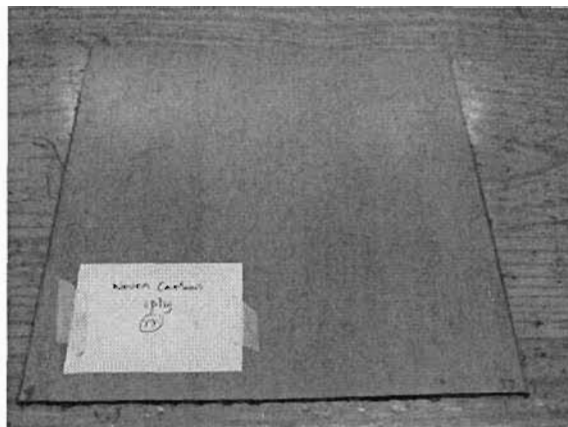


Figure B17: 1 Ply Mesh/Woven sample

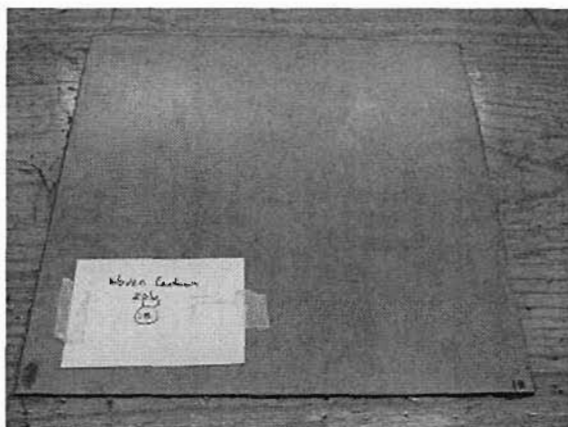


Figure B18: 2 Ply Mesh/Woven sample

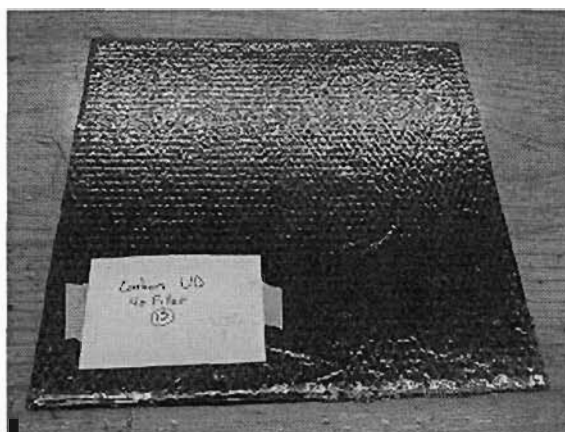


Figure B19: Undoped Unidirectional sample

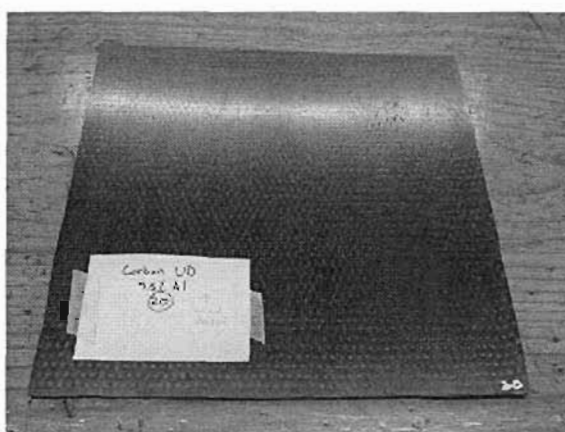


Figure B20: 7.5% Aluminium-doped Unidirectional sample

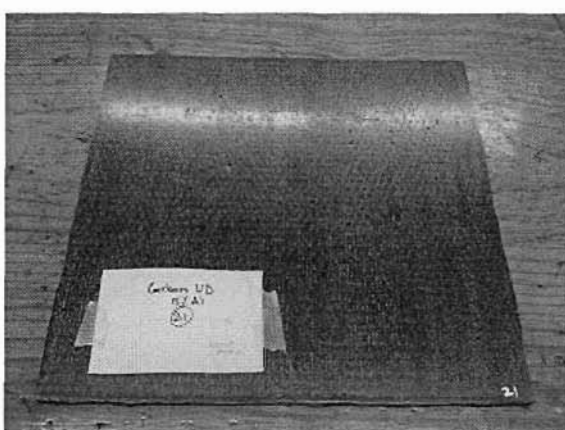


Figure B21: 15% Aluminium-doped Unidirectional sample

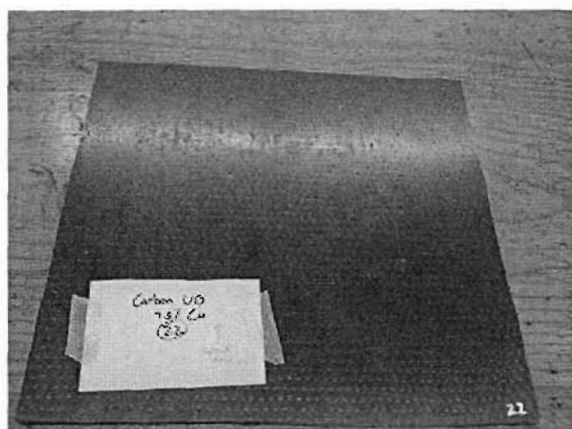


Figure B22: 7.5% Copper-doped Unidirectional sample

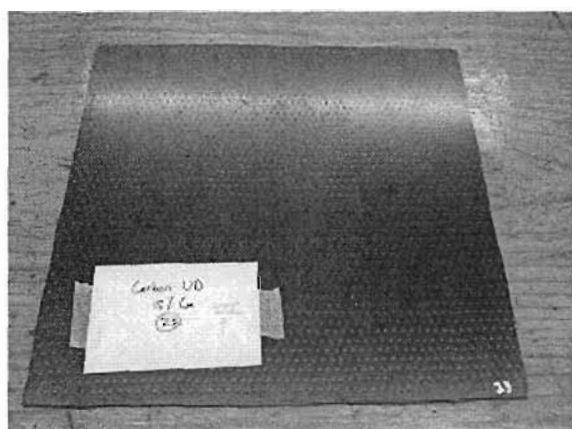


Figure B23: 15% Copper-doped Unidirectional sample

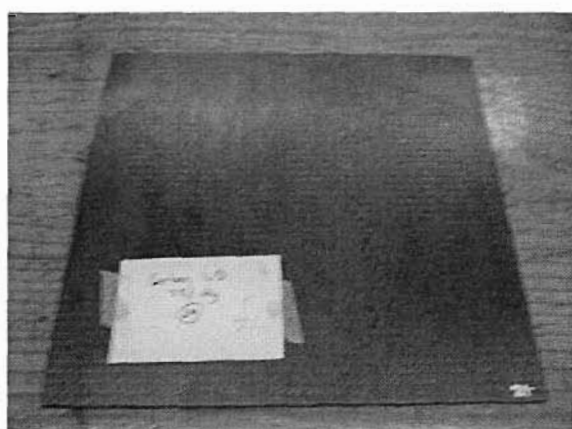


Figure B24: 7.5% Hybrid-doped Unidirectional sample

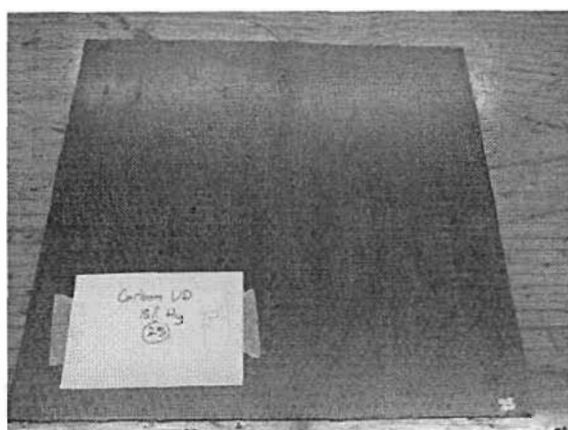


Figure B25: 15% Hybrid-doped Unidirectional sample

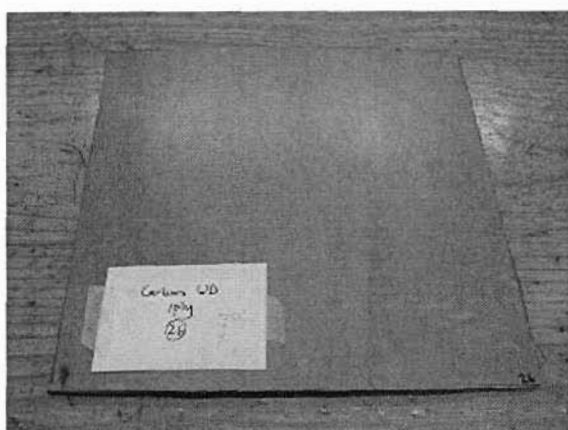


Figure B26: 1 Ply Mesh/Unidirectional sample

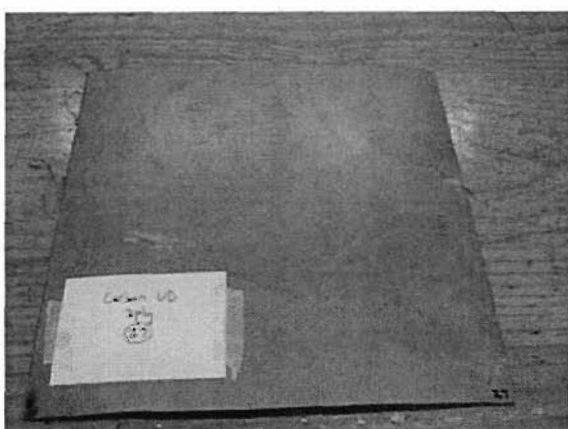


Figure B27: 2 Ply Mesh/Unidirectional sample

## **APPENDIX C: LAMINATE THICKNESS AND WEIGHT DATA**

**Table C1: Weights and Thicknesses of the Aluminium-doped Stitched Carbon Fibre Laminates compared to the Base Laminate**

	0% Aluminium Filler		7.5% Aluminium Filler		15% Aluminium Filler	
	Sample 1	Sample 2	Sample 1	Sample 2	Sample 1	Sample 2
<b>Weight of 4-ply Virgin Fabric (g)</b>	164.0	164.3	165.2	164.2	165.0	164.7
<b>Weight of Laminate (g)</b>	211	215	235.2	242.0	251.2	269.2
<b>Thickness of Laminate (mm)</b>	2.13	2.10	2.15	2.00	2.13	2.12

**Table C2: Weights and Thicknesses of the Aluminium-doped 12K Woven Carbon Fibre Laminates compared to the Base Laminate**

	0% Aluminium Filler		7.5% Aluminium Filler		15% Aluminium Filler	
	Sample 1	Sample 2	Sample 1	Sample 2	Sample 1	Sample 2
<b>Weight of 10-ply Virgin Fabric (g)</b>	190.1	189.3	189.5	190.3	189.6	189.5
<b>Weight of Laminate (g)</b>	263.8	277.1	314.2	323.1	340.2	334.5
<b>Thickness of Laminate (mm)</b>	2.37	2.35	2.60	2.55	2.65	2.64



**Table C3: Weights and Thicknesses of the Aluminium-doped Unidirectional Carbon Fibre Laminates compared to Base Laminate**

	0% Aluminium Filler		7.5% Aluminium Filler		15% Aluminium Filler	
	Sample 1	Sample 2	Sample 1	Sample 2	Sample 1	Sample 2
<b>Weight of 7-ply Virgin Fabric (g)</b>	188.2	189.4	189.4	190.0	189.2	188.8
<b>Weight of Laminate (g)</b>	291.6	277.9	321.2	316.8	326.2	318.5
<b>Thickness of Laminate (mm)</b>	2.40	2.40	2.60	2.35	2.65	2.45

**Table C4: Weights and Thicknesses of the Copper-doped Stitched Carbon Fibre Laminates compared to Base Laminate**

	0% Copper Filler		7.5% Copper Filler		15% Copper Filler	
	Sample 1	Sample 2	Sample 1	Sample 2	Sample 1	Sample 2
<b>Weight of 4-ply Virgin Fabric (g)</b>	164.0	164.3	164.7	165.3	164.9	164.4
<b>Weight of Laminate (g)</b>	211.2	215.1	248.9	262.1	274.1	278.5
<b>Thickness of Laminate (mm)</b>	2.13	2.10	2.00	2.10	2.10	2.20

**Table C5: Weights and Thicknesses of the Copper-doped 12K Woven Carbon Fibre Laminates compared to Base Laminate**

	0% Copper Filler		7.5% Copper Filler		15% Copper Filler	
	Sample 1	Sample 2	Sample 1	Sample 2	Sample 1	Sample 2
Weight of 10-ply Virgin Fabric (g)	190.1	189.3	189.2	190.5	189.7	189.4
Weight of Laminate (g)	263.8	277.1	311.1	315.4	324.7	334.2
Thickness of Laminate (mm)	2.37	2.35	2.35	2.50	2.40	2.50

**Table C6: Weights and Thicknesses of the Copper-doped Unidirectional Carbon Fibre Laminates compared to Base Laminate**

	0% Copper Filler		7.5% Copper Filler		15% Copper Filler	
	Sample 1	Sample 2	Sample 1	Sample 2	Sample 1	Sample 2
Weight of 7-ply Virgin Fabric (g)	188.2	189.4	190.2	190.1	188.9	189.5
Weight of Laminate (g)	285.6	281.1	292.1	293.8	304.6	300.1
Thickness of Laminate (mm)	2.40	2.38	2.31	2.30	2.30	2.30

**Table C7: Weights and Thicknesses of the Hybrid Powder-doped Stitched Carbon Fibre Laminates compared to Base Laminate**

	0% Hybrid Filler		7.5% Hybrid Filler		15% Hybrid Filler	
	Sample 1	Sample 2	Sample 1	Sample 2	Sample 1	Sample 2
<b>Weight of 4-ply Virgin Fabric (g)</b>	164.0	164.3	164.3	165.1	165.0	164.7
<b>Weight of Laminate (g)</b>	211.2	215.1	239.5	248.1	267.1	273.2
<b>Thickness of Laminate (mm)</b>	2.13	2.10	2.10	2.20	2.20	2.25

**Table C8: Weights and Thicknesses of the Hybrid Powder-doped 12K Woven Carbon Fibre Laminates compared to Base Laminate**

	0% Hybrid Filler		7.5% Hybrid Filler		15% Hybrid Filler	
	Sample 1	Sample 2	Sample 1	Sample 2	Sample 1	Sample 2
<b>Weight of 10-ply Virgin Fabric (g)</b>	190.1	189.3	190.1	189.8	190.2	190.2
<b>Weight of Laminate (g)</b>	263.8	277.1	318.0	314.8	326.8	316.9
<b>Thickness of Laminate (mm)</b>	2.37	2.35	2.65	2.40	2.55	2.40

**Table C9: Weights and Thicknesses Hybrid Powder-doped Unidirectional Carbon Fibre Laminates compared to Base Laminate**

	0% Hybrid Filler		7.5% Hybrid Filler		15% Hybrid Filler	
	Sample 1	Sample 2	Sample 1	Sample 2	Sample 1	Sample 2
<b>Weight of 7-ply Virgin Fabric (g)</b>	188.2	189.4	188.9	189.2	189.1	189.2
<b>Weight of Laminate (g)</b>	285.6	281.1	311.0	307.7	312.5	308.6
<b>Thickness of Laminate (mm)</b>	2.40	2.38	2.50	2.45	2.40	2.30

**Table C10: Weights and Thicknesses of the Metal Mesh, Glass and Stitched Carbon Fibre Laminates compared to Base Laminate**

	Mesh Absent		1 Mesh Layer		2 Mesh Layers	
	Sample 1	Sample 2	Sample 1	Sample 2	Sample 1	Sample 2
<b>Weight of 4-ply Virgin Fabric (g)</b>	164.0	164.3	165.2	164.8	164.5	165.3
<b>Weight of Laminate (g)</b>	211.2	215.1	251.5	249.5	263.3	259.3
<b>Thickness of Laminate (mm)</b>	2.13	2.10	2.20	2.25	2.35	2.40

**Table C11: Weights and Thicknesses of the Mesh/12K Woven Carbon Fibre Laminates compared to Base Laminate**

	Mesh Absent		1 Mesh Layer		2 Mesh Layers	
	Sample 1	Sample 2	Sample 1	Sample 2	Sample 1	Sample 2
<b>Weight of 10-ply Virgin Fabric (g)</b>	190.1	189.3	189.0	190.2	189.5	189.3
<b>Weight of Laminate (g)</b>	263.8	277.1	304.2	302.3	315.5	311.3
<b>Thickness of Laminate (mm)</b>	2.37	2.35	2.40	2.38	2.50	2.45

**Table C12: Weights and Thicknesses of the Mesh/Unidirectional Carbon Fibre Laminates compared to Base Laminate**

	Mesh Absent		1 Mesh Layer		2 Mesh Layers	
	Sample 1	Sample 2	Sample 1	Sample 2	Sample 1	Sample 2
<b>Weight of 7-ply Virgin Fabric (g)</b>	188.2	189.4	189.2	190.3	190.1	189.5
<b>Weight of Laminate (g)</b>	285.6	281.1	293.2	289.2	293.8	299.1
<b>Thickness of Laminate (mm)</b>	2.40	2.38	2.45	2.50	2.55	2.60

## **APPENDIX D: SAMPLE CALCULATIONS**

Sample calculations using the theoretical equations presented are shown. These calculations were performed for each specimen at the data intervals referred to in the report. To maintain uniformity, the data for the calculations are performed in this Appendix using data from undoped carbon fibre specimens.

### **Mechanical Testing**

Elastic Modulus using equation (8.2) with the first deflection measurement of undoped stitched carbon fibre specimen 1:

Data: Specimen width = 11.45mm  
 Specimen depth = 3.9 mm  
 Load span = 80mm  
 Support span = 39.2 mm  
 Load measurement 1 = 25.58 N  
 Deflection measurement 1 = 0.06 mm

$$\triangleright E_x = \frac{Pcl^2}{8Iw_{\max}} = \frac{3 \times 25.58 \times 80 \times 39.2^2}{2 \times 8 \times 11.45 \times 3.9^3 \times 0.06} = 14.468 \text{ GPa}$$

The elastic moduli for all of the specimens were calculated in the same way. At least 5 load and deflection measurements being recorded and the average elastic moduli were obtained from those measurements.

### **Electrical Resistance Testing**

Electrical resistance measurements were undertaken on the 4-ply stitched carbon fibre samples, and electrical resistivity and conductivity were obtained using equation (4.1):

Data: Measured resistance: 8.1  $\Omega$   
 Specimen width: 10.11cm  
 Specimen length: 10.17 cm  
 Specimen depth: 0.23 cm

$$R = \frac{\rho l}{A} = \frac{l}{\sigma A}$$

$$\triangleright \rho = \frac{8.1 \times 10.11 \times 0.23}{10.17} = 1.9 \Omega \cdot \text{cm}$$

$$\triangleright \sigma = \frac{1}{1.9} = 0.539 \Omega / \text{cm}$$

### Analytical EMSE; Skin Depth; and Barrier Impedance calculations:

The theoretical EMSE was obtained by use of equations (4.6), (4.14), (4.15) and (4.18). Equations (4.9), (4.12) and (4.13) were used to obtain the individual losses, and equation (4.16) was used for skin depth:

$$\begin{aligned}
 &\triangleright R_{dB} = 108.1 - 10 \log_{10}(\mu_r f / \sigma_r) = 108.1 - 10 \log_{10} \left( \frac{1 \times 750}{3.83 \times 10^{-3}} \right) = 55.1 dB \\
 &\triangleright A_{dB} = 1.32 t \sqrt{f \sigma_r \mu_r} = 1.32 \times 0.23 \times \sqrt{750 \times 3.83 \times 10^{-3} \times 1} = 0.51 dB \\
 &\triangleright B_{dB} = 20 \log_{10}(1 - e^{-2t \sqrt{\pi f \mu \sigma}} e^{-j 2t \sqrt{\pi f \mu \sigma}}) = 20 \log_{10}(1 - e^{-2 \times 0.0023 \times \sqrt{\pi \times 750 \times 10^6 \times 4 \pi \times 10^{-7} \times 539}}) = -1.5 dB \\
 &\triangleright \delta = \sqrt{\frac{1}{\mu_0 \pi f \sigma}} = \sqrt{\frac{1}{4 \pi \times 10^{-9} \times \pi \times 750 \times 0.539}} = 0.25 cm
 \end{aligned}$$

Equation (4.6):

$$\triangleright = R_{dB} + A_{dB} + B_{dB} = 55.1 + 0.51 + 0 = 55.61 dB$$

Simon Formalism (4.14):

$$\triangleright = 50 + 10 \log_{10}(\rho f)^{-1} + 1.7 t (f / \rho)^{\frac{1}{2}} = 50 + 10 \log_{10}(1.9 \times 750)^{-1} + 1.7 \times 0.23 \times (750 / 1.9)^{\frac{1}{2}} = 26.4 dB$$

Good Conductor Approx (4.15):

$$\triangleright 10 \log_{10} \left( \frac{\sigma}{32 \pi f \epsilon_0} \right) + 20 \frac{d}{\delta} \log(e) = 10 \log_{10} \left( \frac{0.539}{32 \times \pi \times 750 \times 8.815 \times 10^{-14}} \right) + 20 \left( \frac{0.23}{0.25} \right) \log(2.178) = 25.2 dB$$

Far-field Approx (4.19):

$$\triangleright = 20 \log_{10} \left( 1 + \frac{Z_0 \sigma d}{2} \right) = 20 \log_{10} \left( 1 + \frac{377 \times 0.539 \times 100 \times 2.3 \times 10^{-3}}{2} \right) = 27.7 dB$$

Barrier impedance was obtained by use of equation (4.20):

$$Z_B = 369 \sqrt{\mu_r f / \sigma_r} \left( 1 - e^{-\frac{t}{\delta}} \right)^{-1} = 369 \sqrt{1 \times 750 / 3.83 \times 10^{-3}} \left( 1 - 2.718^{\frac{-0.23}{0.25}} \right)^{-1} = 0.27 \Omega / sq$$

This approach was performed for all 27 specimens over 801 data points between 750-5000 MHz.

## **APPENDIX E: THEORETICAL BARRIER IMPEDANCE AND SKIN DEPTH RESULTS**

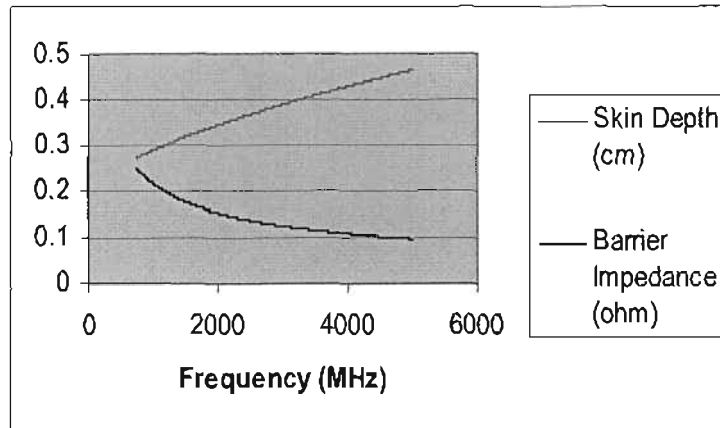


Figure E1: Undoped stitched carbon fibre specimen

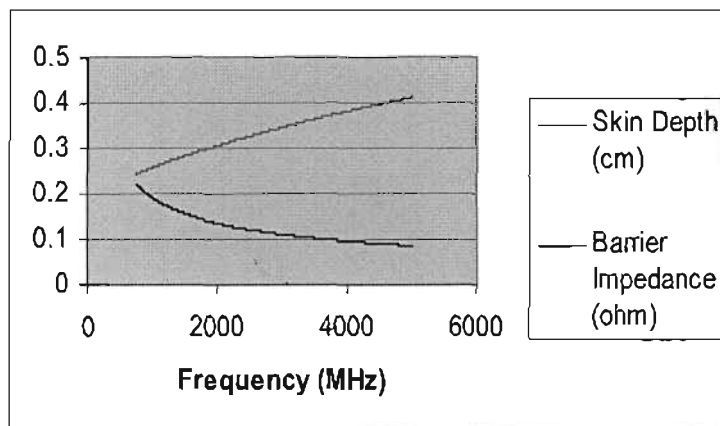


Figure E2: 7.5% Aluminium-doped stitched carbon fibre specimen

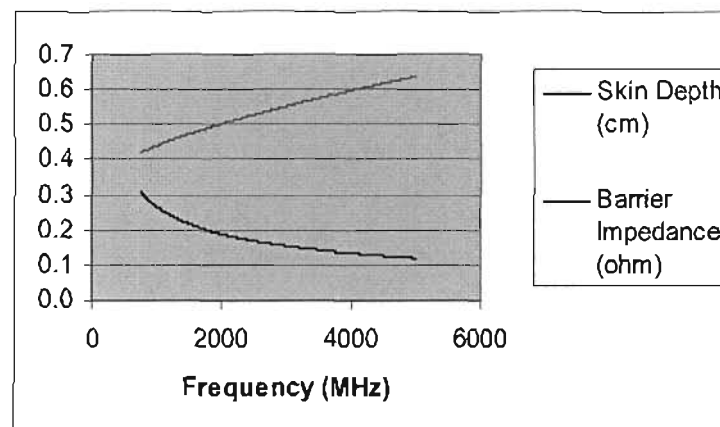


Figure E3: 15% Aluminium-doped stitched carbon fibre specimen



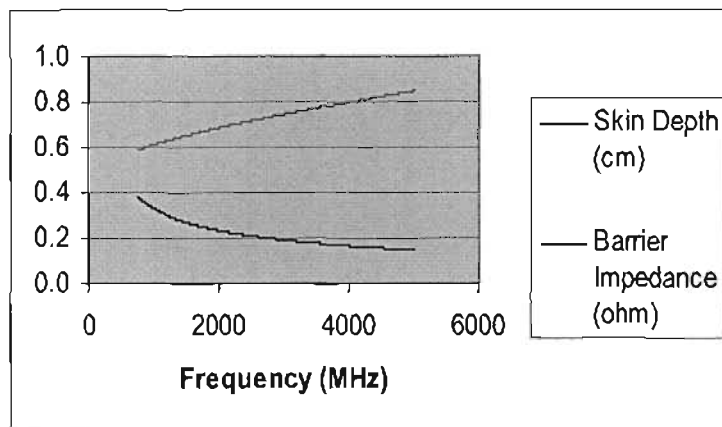


Figure E4: 7.5% Copper-doped stitched carbon fibre specimen

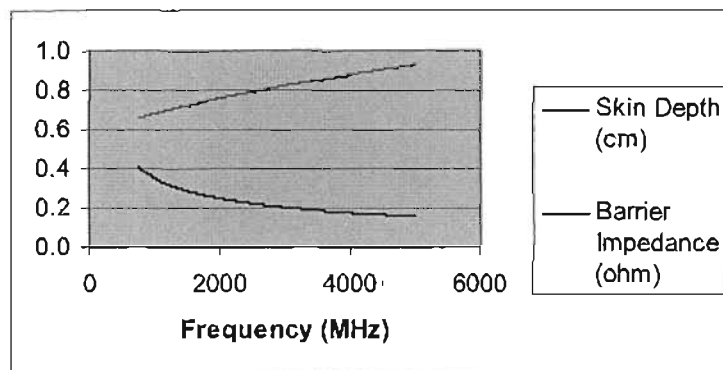


Figure E5: 15% Copper-doped stitched carbon fibre specimen

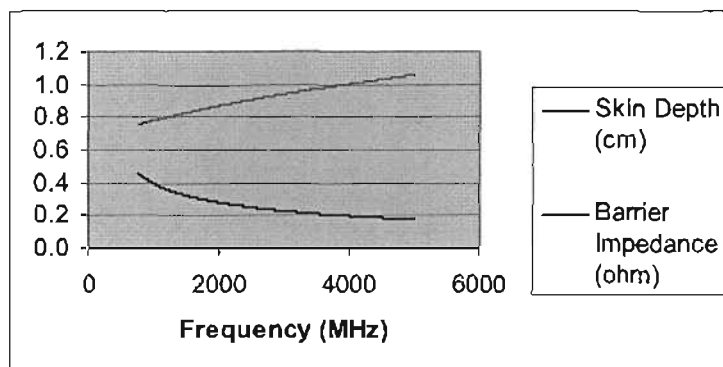


Figure E6: 7.5% Hybrid powder-doped stitched carbon fibre specimen

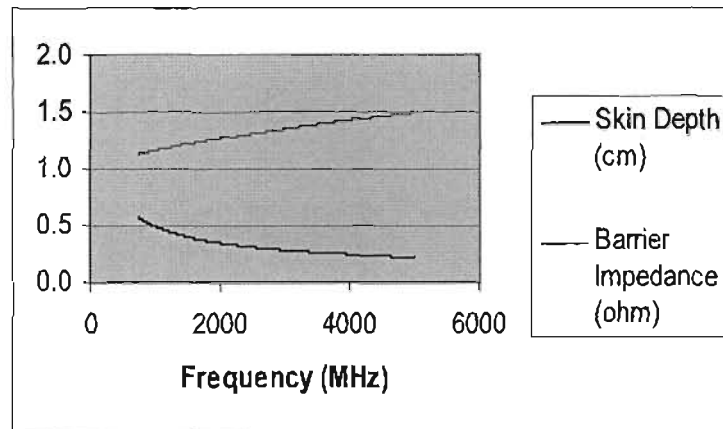


Figure E7: 15% Hybrid powder-doped stitched carbon fibre specimen

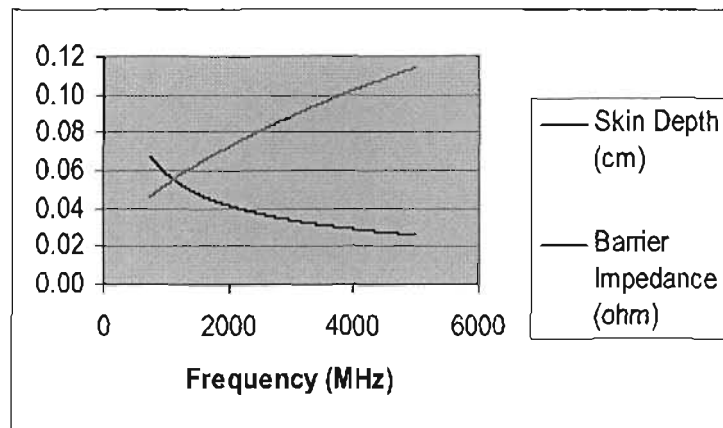


Figure E8: 1 ply Alumesht/stitched carbon fibre specimen

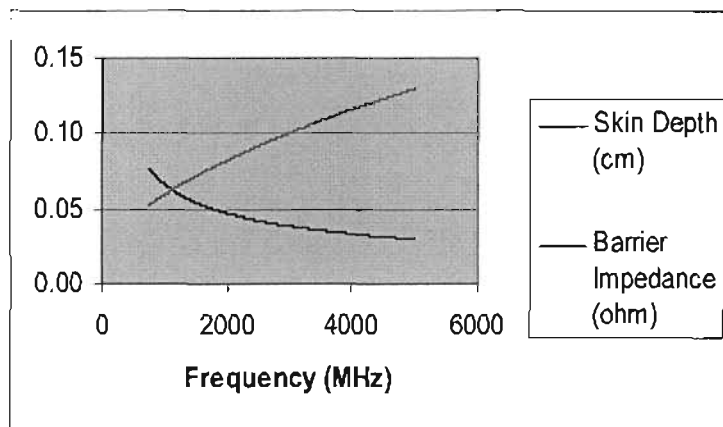


Figure E9: 2 ply Alumesht/stitched carbon fibre specimen

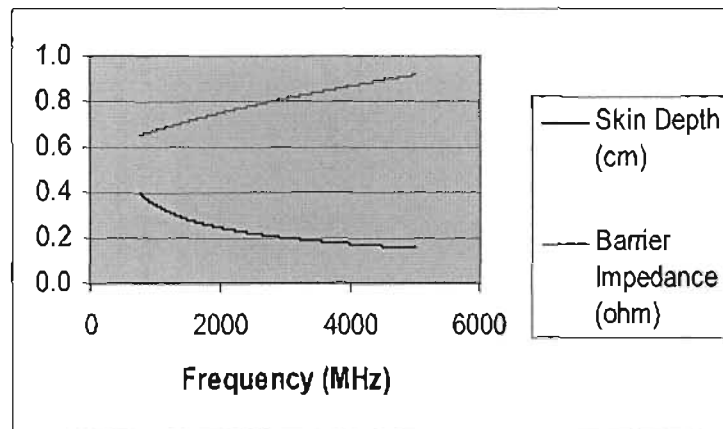


Figure E10: Undoped woven carbon fibre specimen

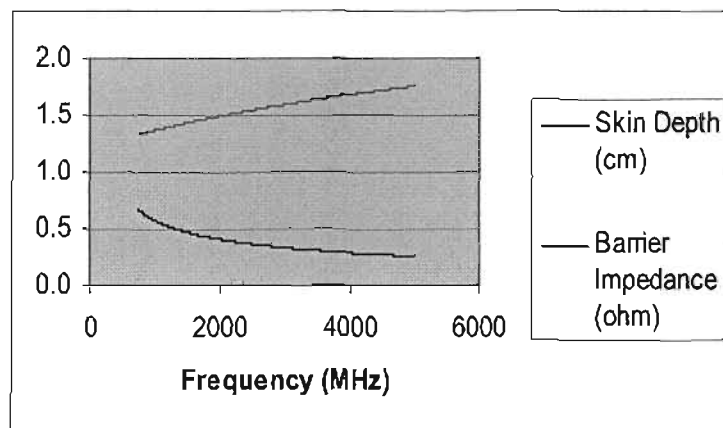


Figure E11: 7.5% Aluminium-doped woven carbon fibre specimen

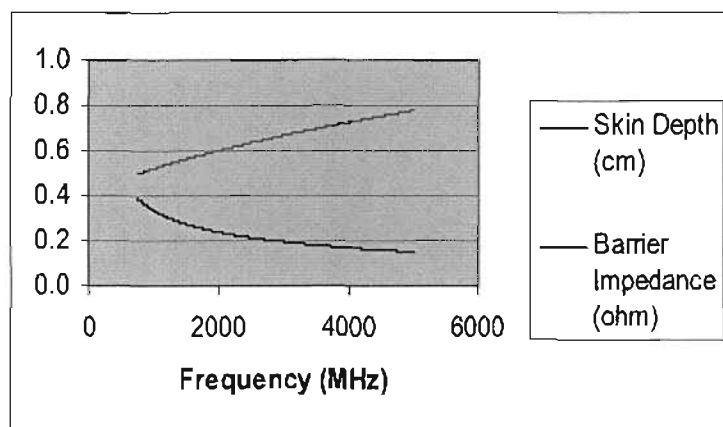


Figure E12: 15% Aluminium-doped woven carbon fibre specimen

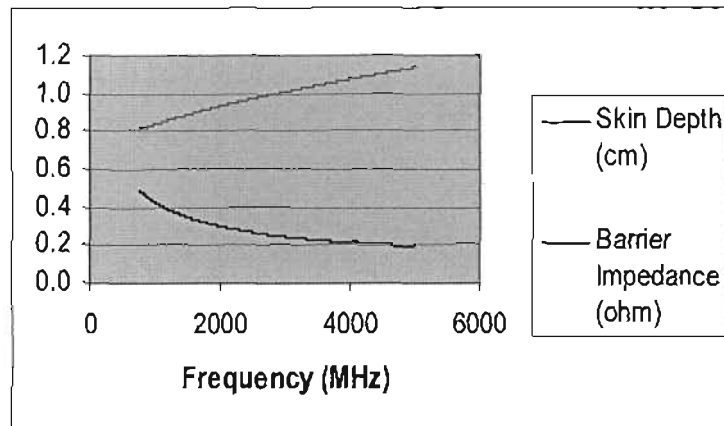


Figure E13: 7.5% Copper-doped woven carbon fibre specimen

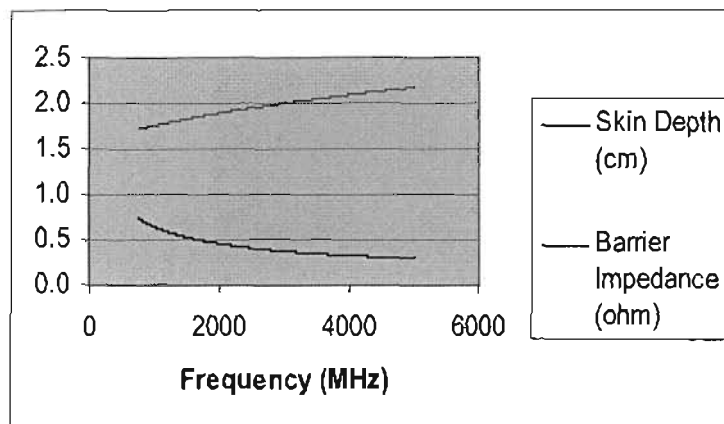


Figure E14: 15% Copper-doped woven carbon fibre specimen

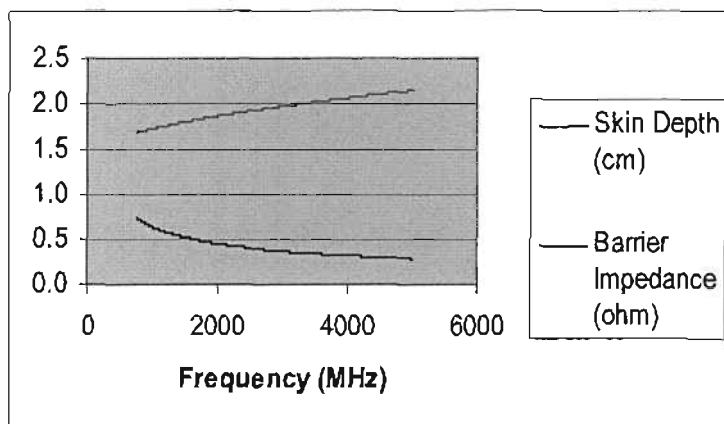


Figure E15: 7.5% Hybrid powder-doped woven carbon fibre specimen

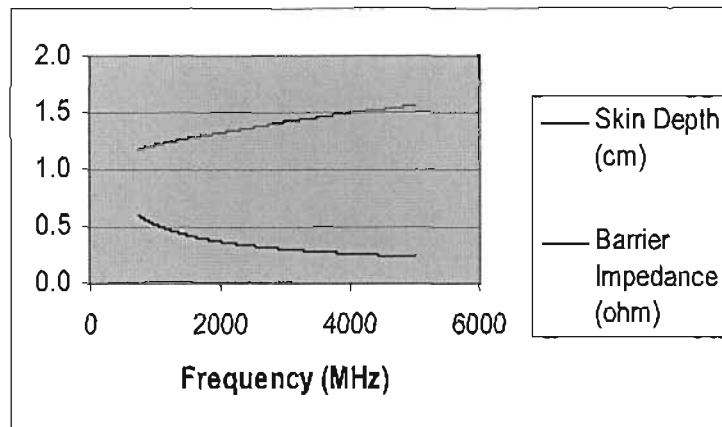


Figure E16: 15% Hybrid powder-doped woven carbon fibre specimen

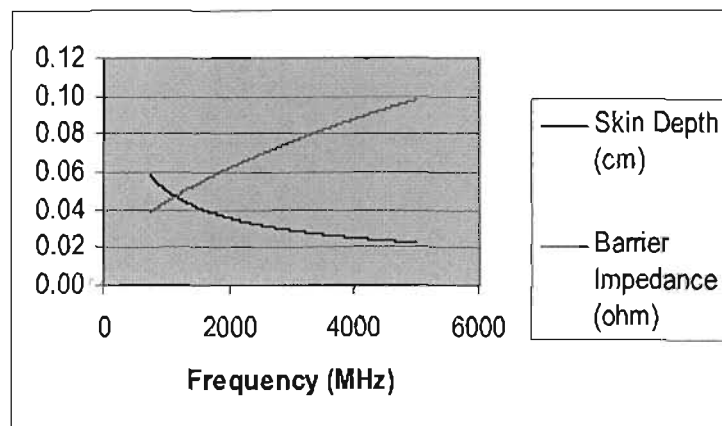


Figure E17: 1 ply Alumesb/woven carbon fibre specimen

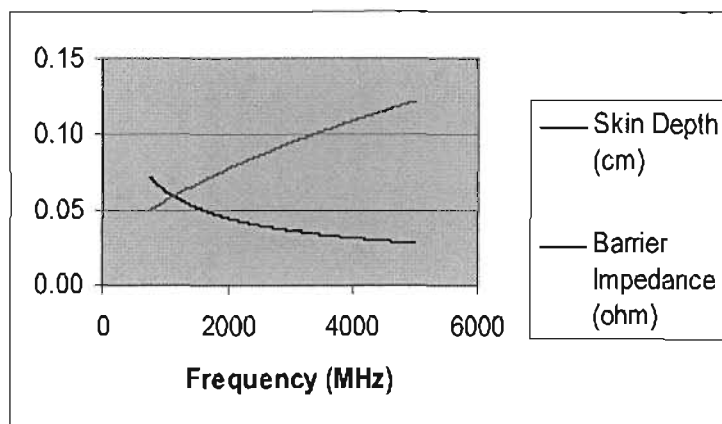


Figure E18: 2 ply Alumesb/woven carbon fibre specimen

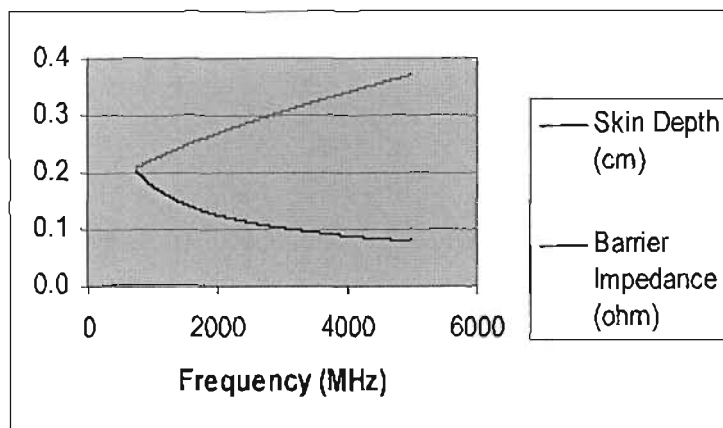


Figure E19: Undoped unidirectional carbon fibre specimen

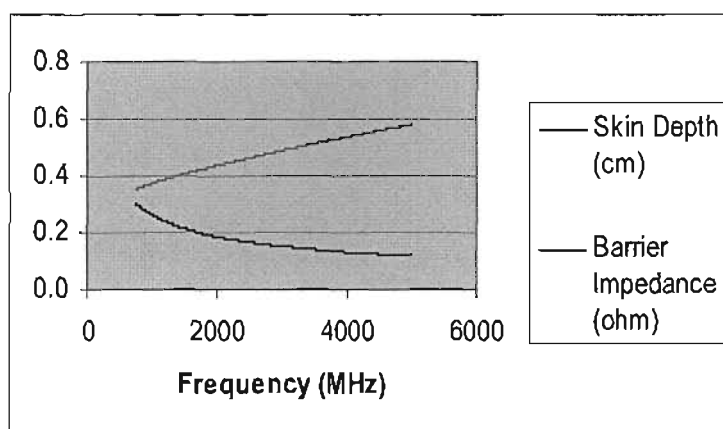


Figure E20: 7.5% Aluminium-doped unidirectional carbon fibre specimen

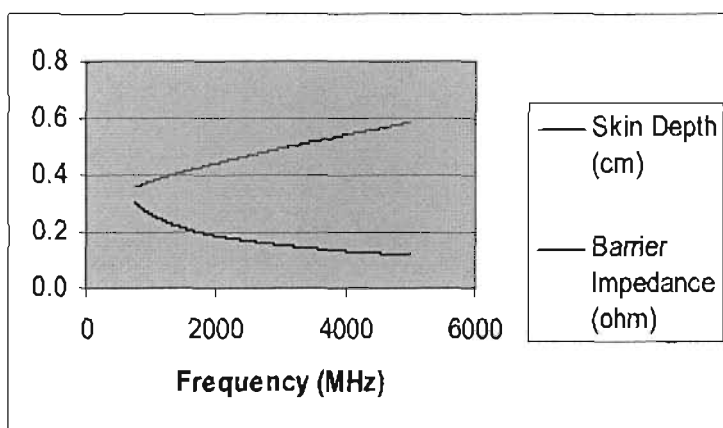


Figure E21: 15% Aluminium-doped unidirectional carbon fibre specimen

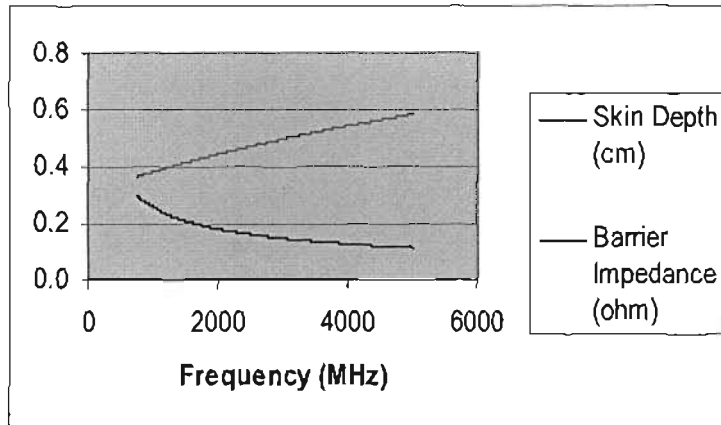


Figure E22: 7.5% Copper-doped unidirectional carbon fibre specimen

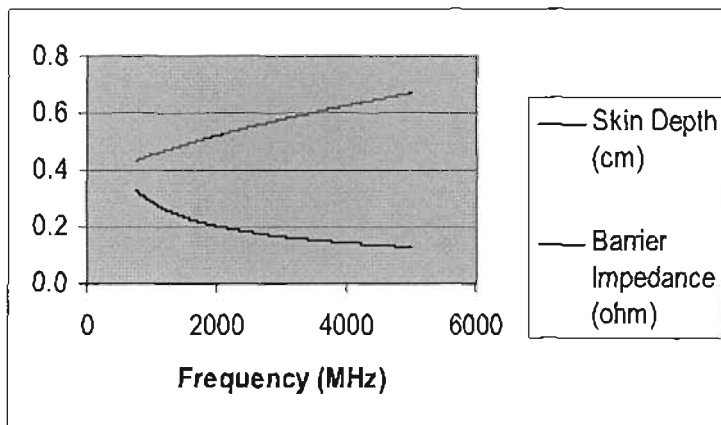


Figure E23: 15% Copper-doped unidirectional carbon fibre specimen

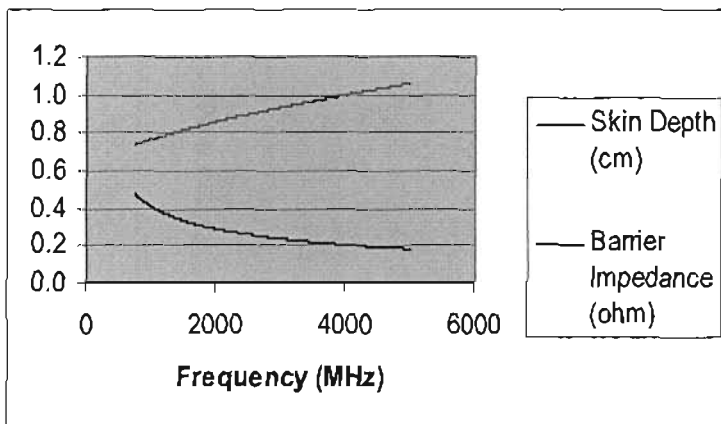


Figure E24: 7.5% Hybrid powder-doped unidirectional carbon fibre specimen

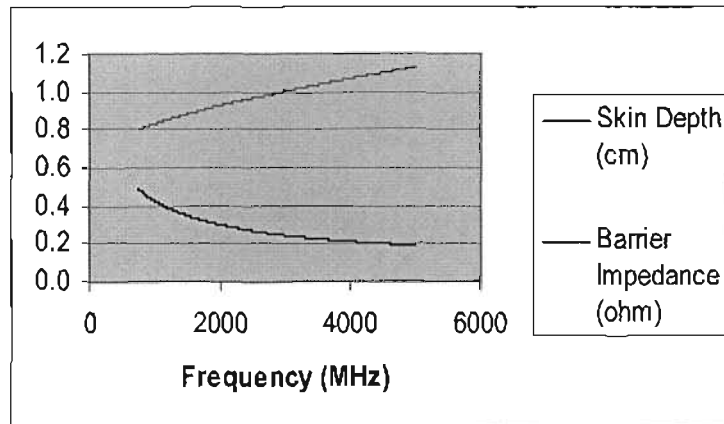


Figure E25: 15% hybrid powder-doped unidirectional carbon fibre specimen

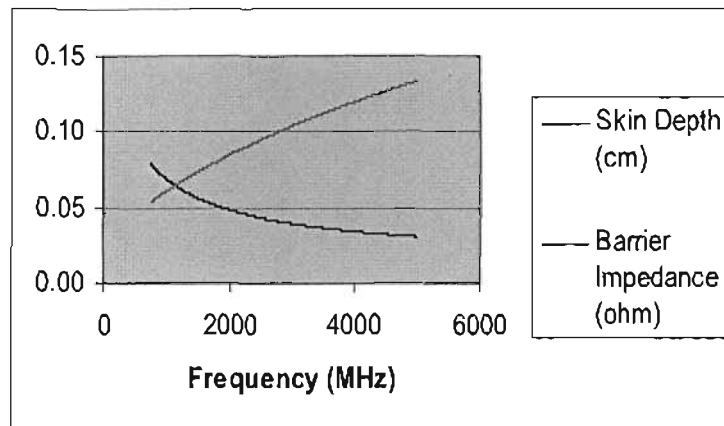


Figure E26: 1 ply Alumesb/unidirectional carbon fibre specimen

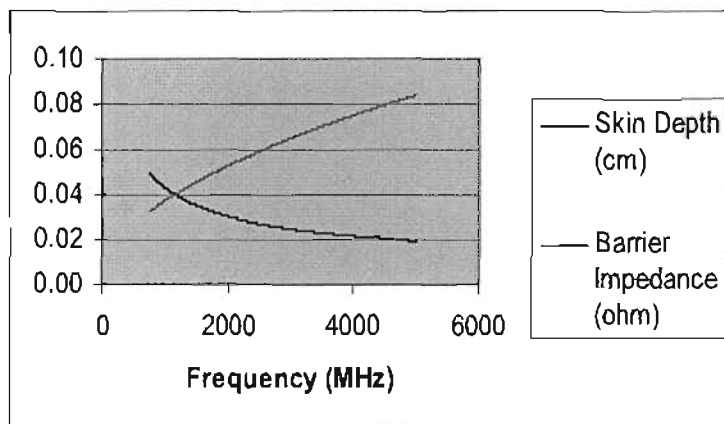


Figure E27: 2 ply Alumesb/unidirectional carbon fibre specimen



## **APPENDIX F: ACTUAL TESTING EMSE RESULTS**

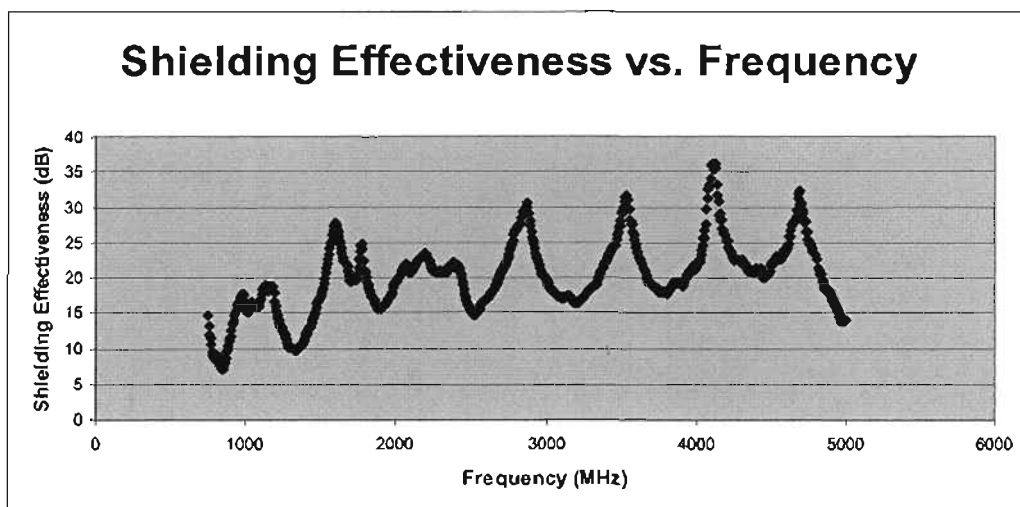
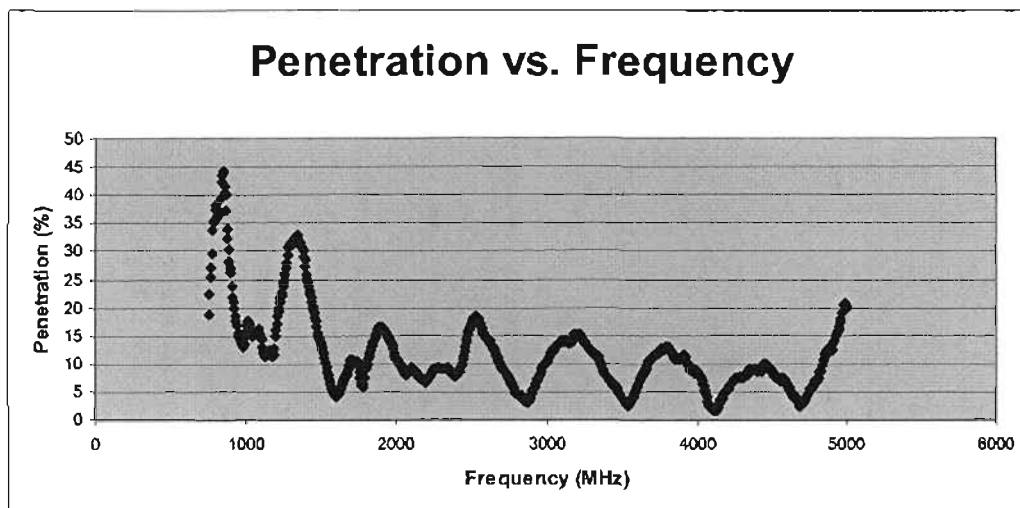
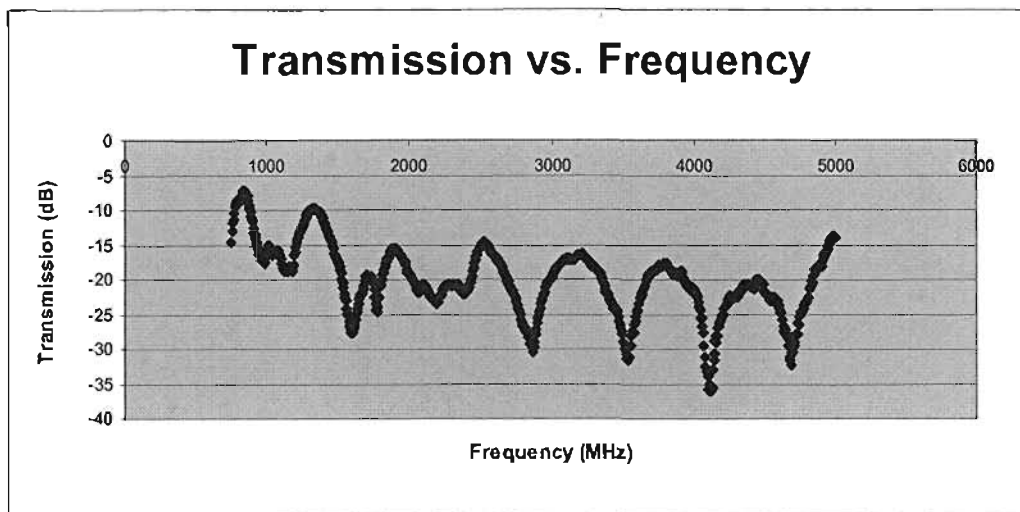
Actual EMSE measurements over the 801 data points were presented by means of Transmission in dB for all specimens. Equations (8.7) and (8.8) were used to obtain the results in terms of EMSE. This approach was used to obtain EMSE for all 27 specimens over 801 data points each time. The sample calculation presented is for undoped stitched carbon fibre at 750 MHz. Percentage penetrations through the shielding materials was obtained by use of equation (8.9).

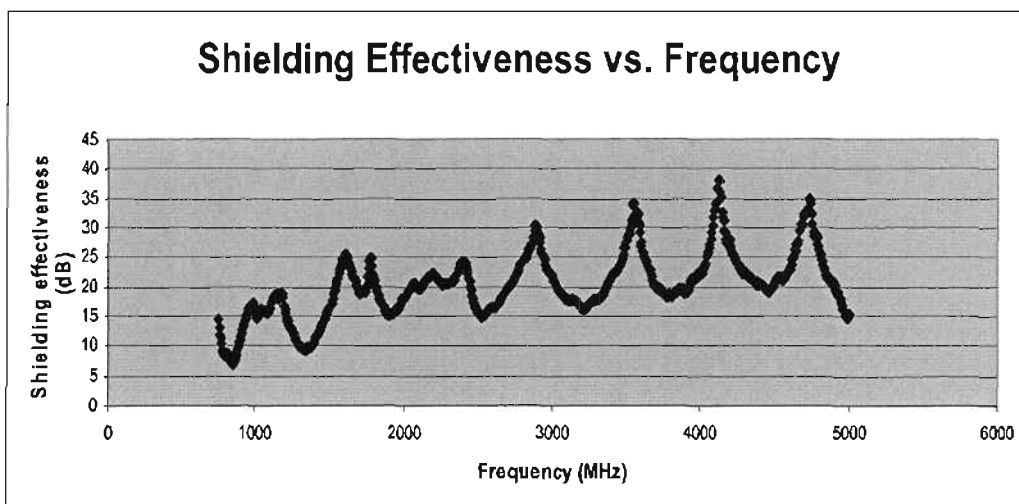
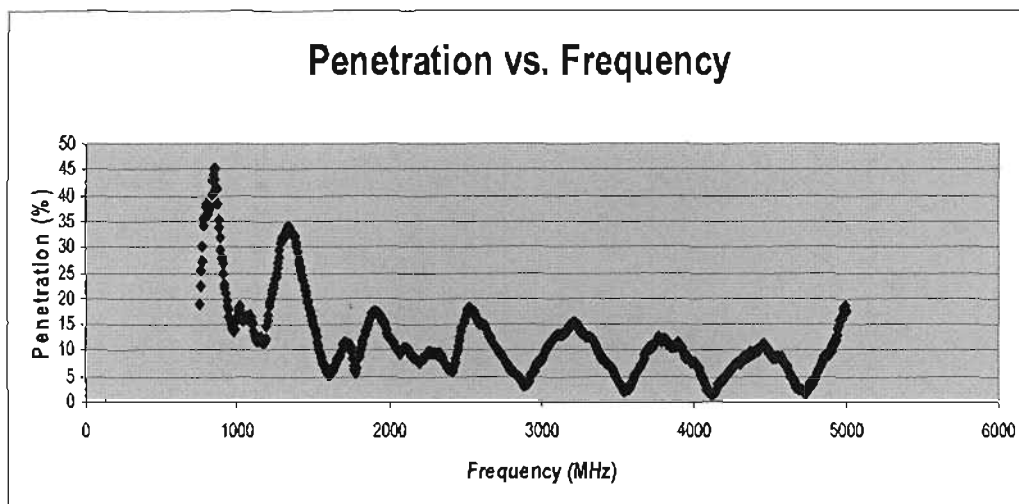
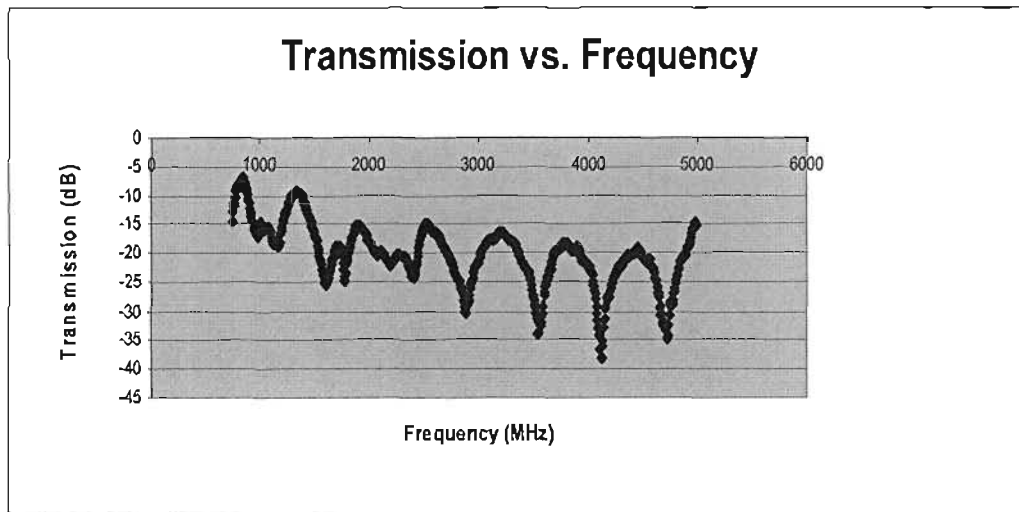
$$\triangleright T_R = 10^{\frac{T_{dB}}{20}} = 10^{\frac{-14.58}{20}} = 0.1860$$

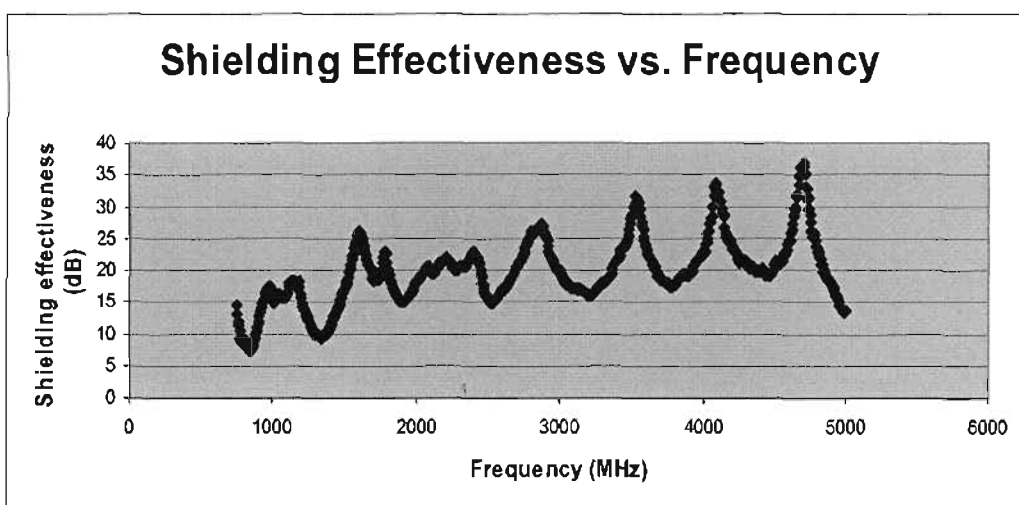
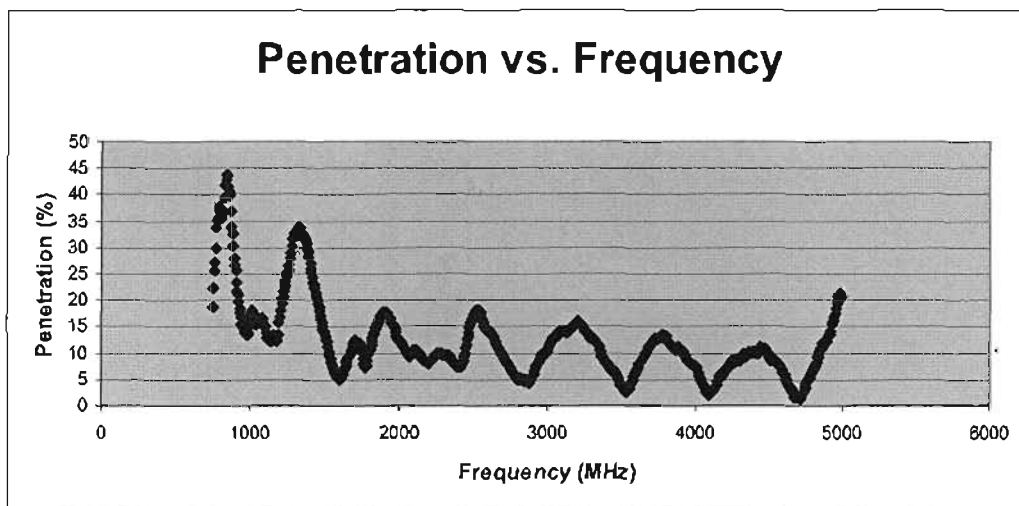
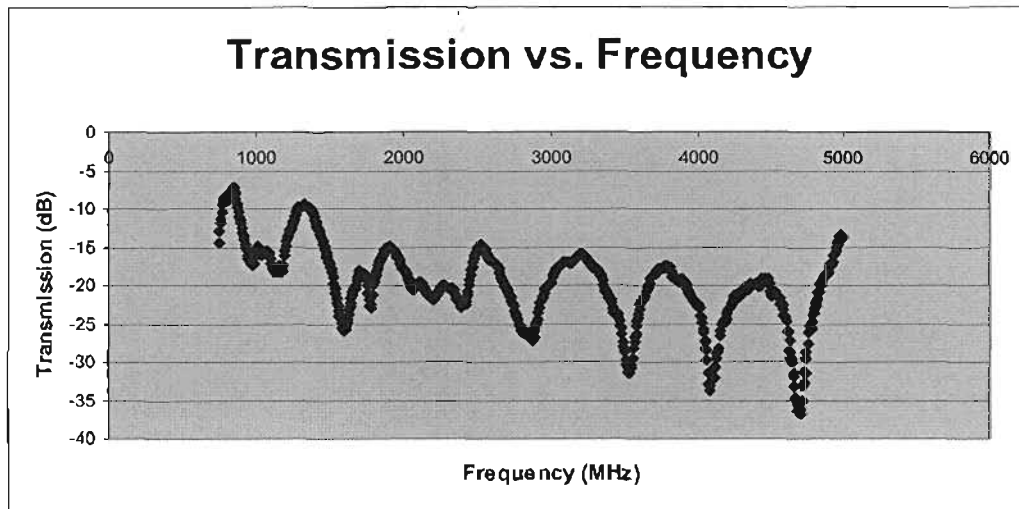
$$\triangleright SE = \log \frac{1}{T_R} = \log \frac{1}{0.1860} = 14.58 dB$$

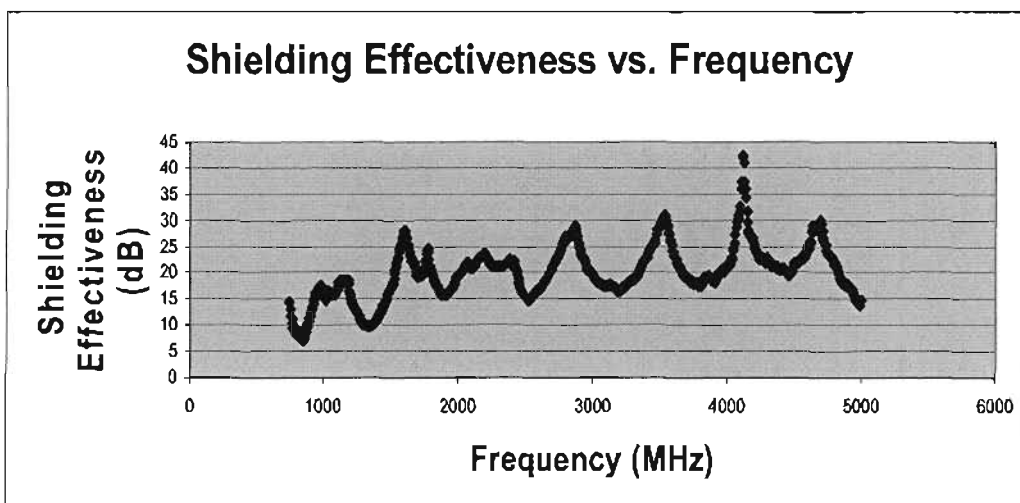
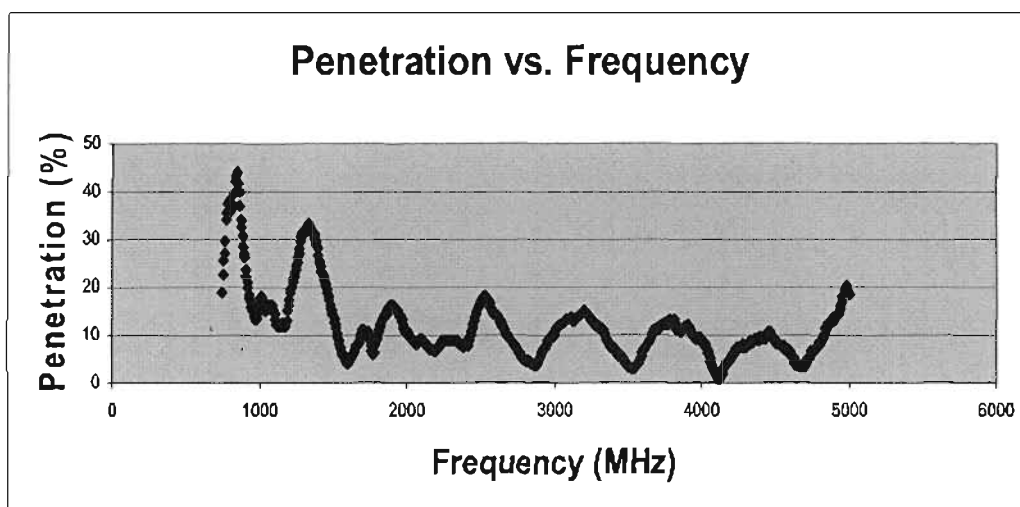
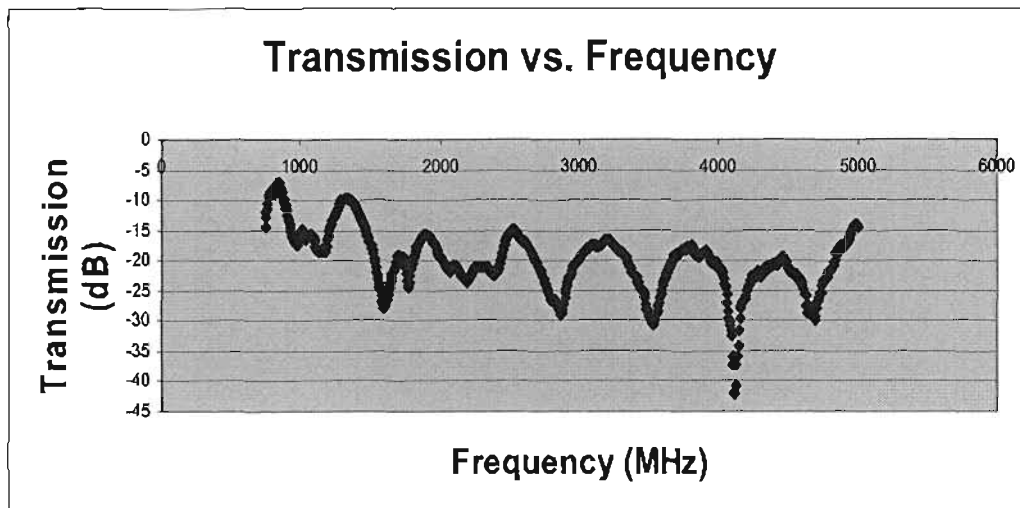
$$\triangleright \% \text{ penetration} = 10^{\frac{T_{dB}}{20}} \times 100 = 10^{\frac{-14.58}{20}} \times 100 = 18.60\%$$

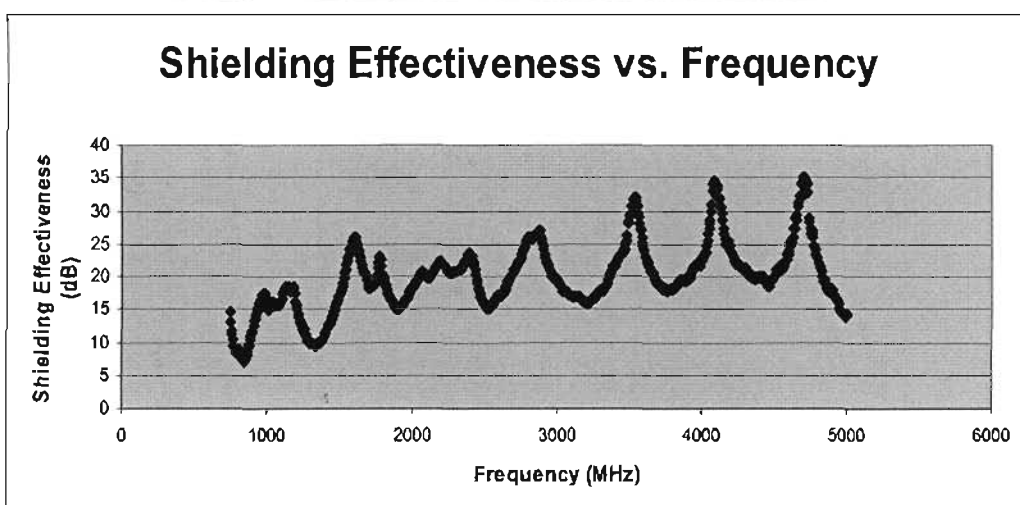
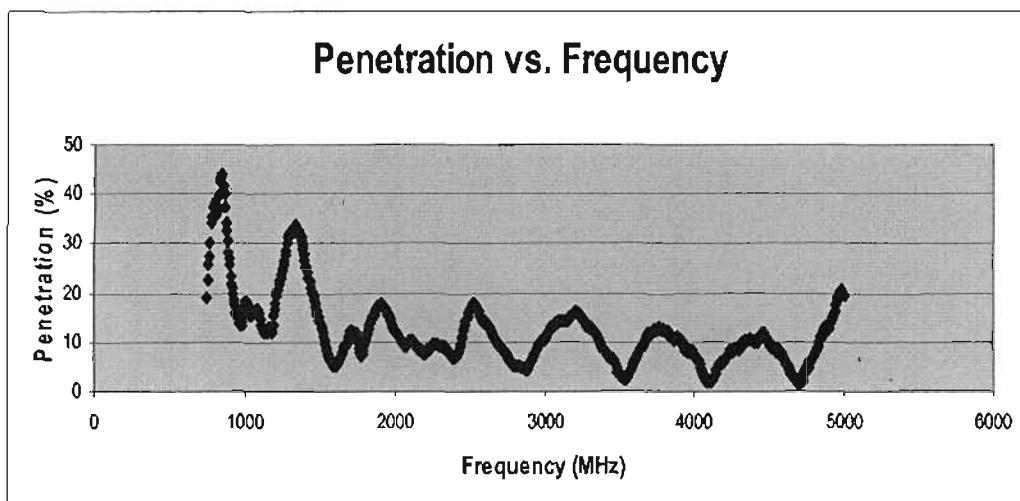
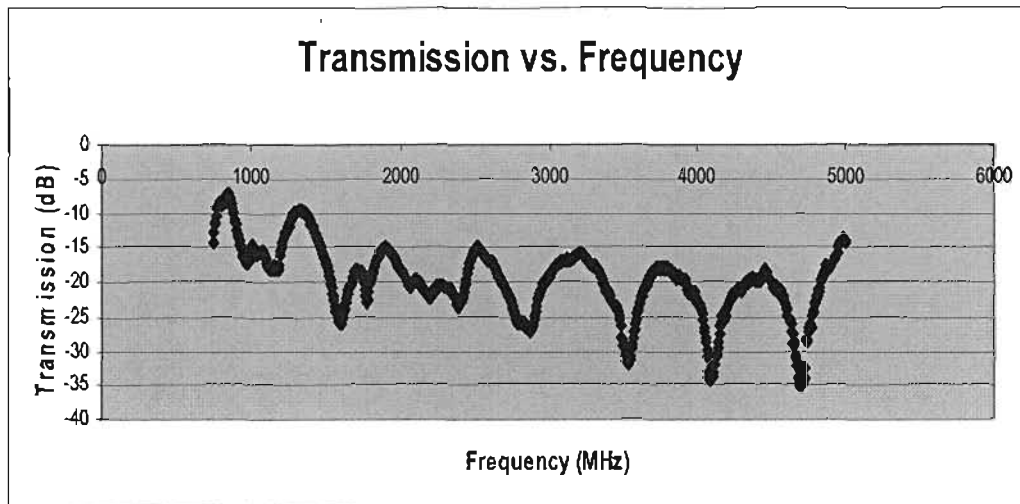
The results for 801 data points for all specimens are provided by means of graphs, which are shown from page 211 to 237:

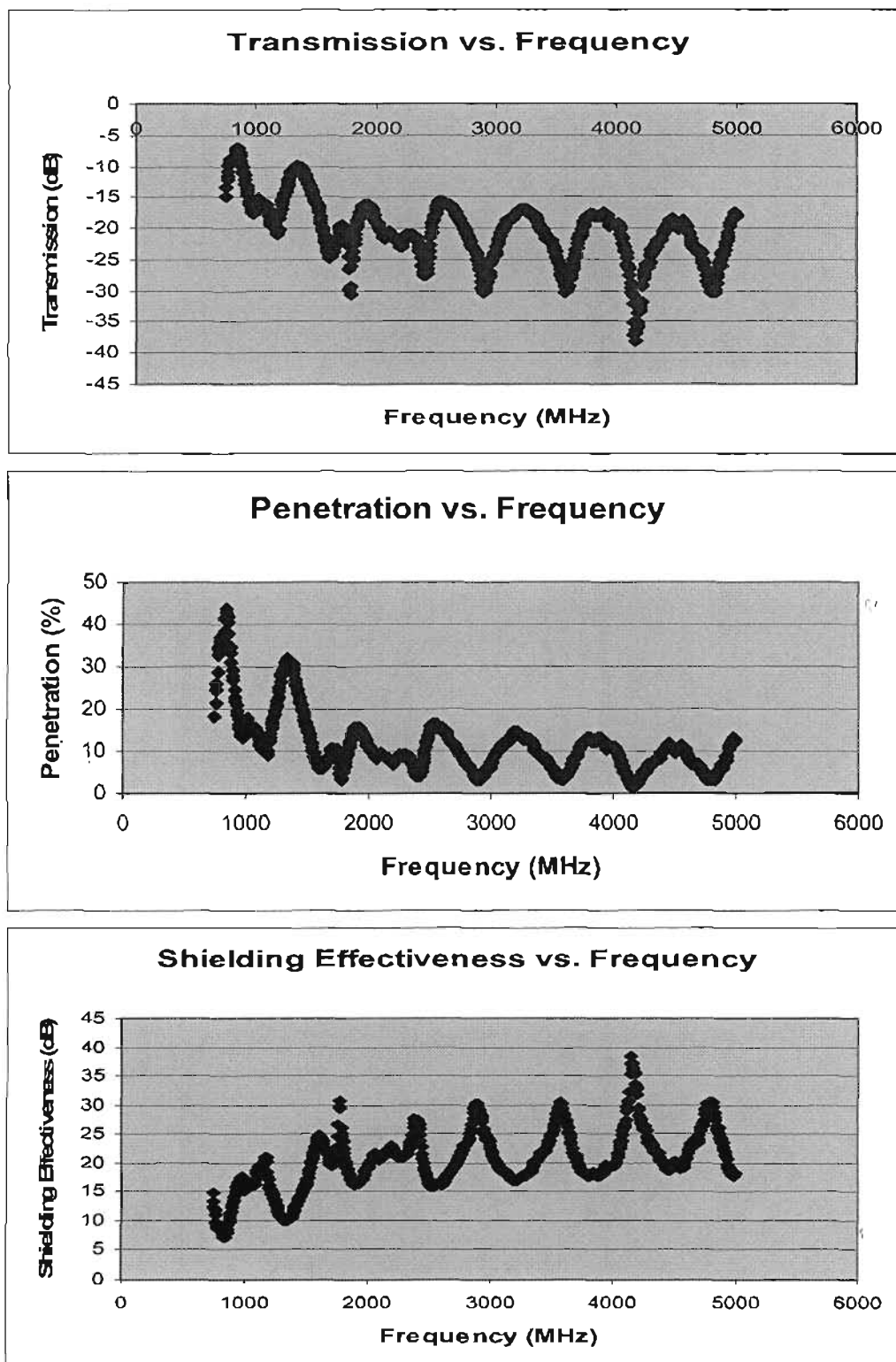
**F1: Undoped Stitched Carbon Fibre Specimens**

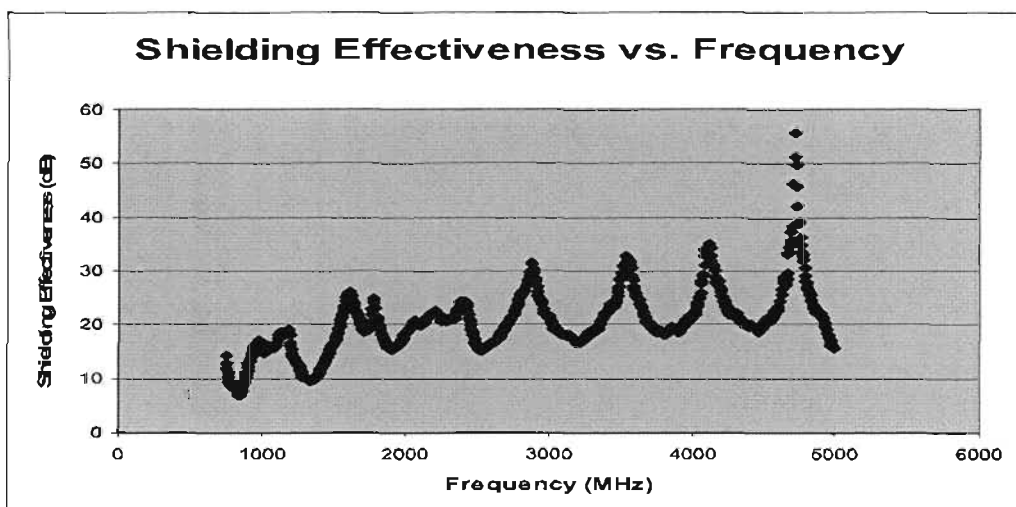
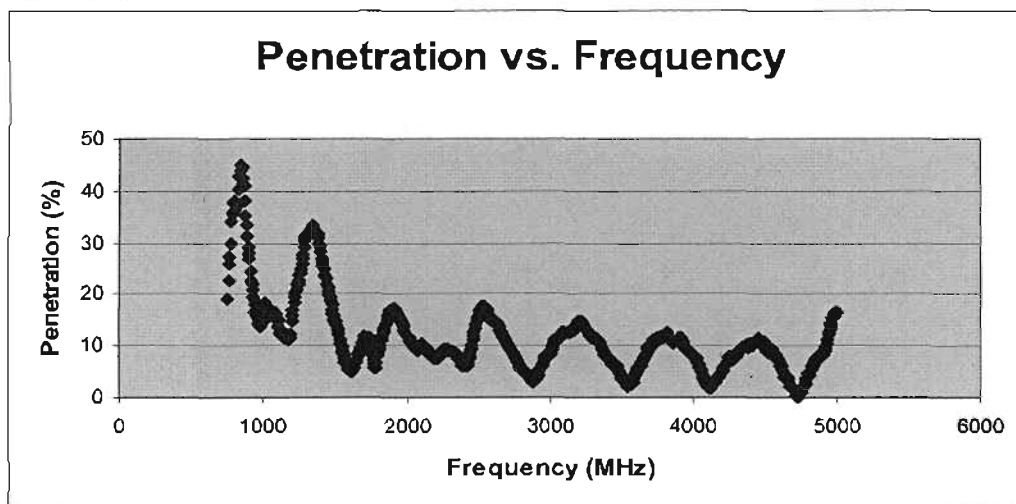
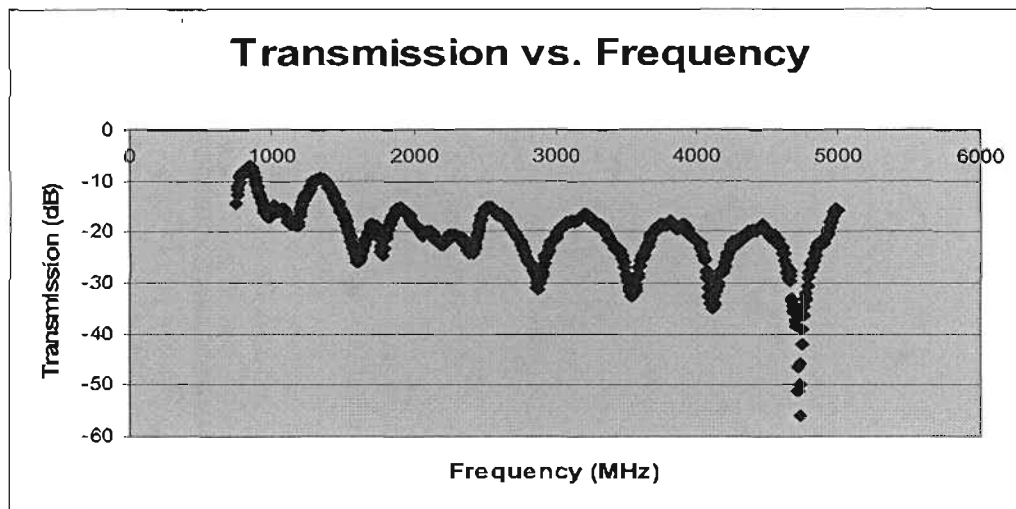
**F2: 7.5% Aluminium-doped Stitched Carbon Fibre Specimens**

**F3: 15% Aluminium-doped Stitched Carbon Fibre Specimens**

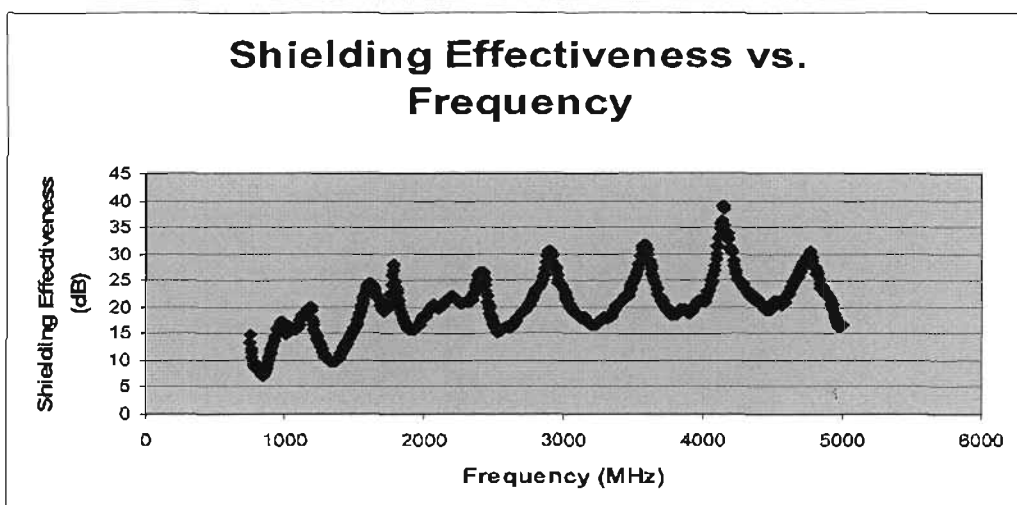
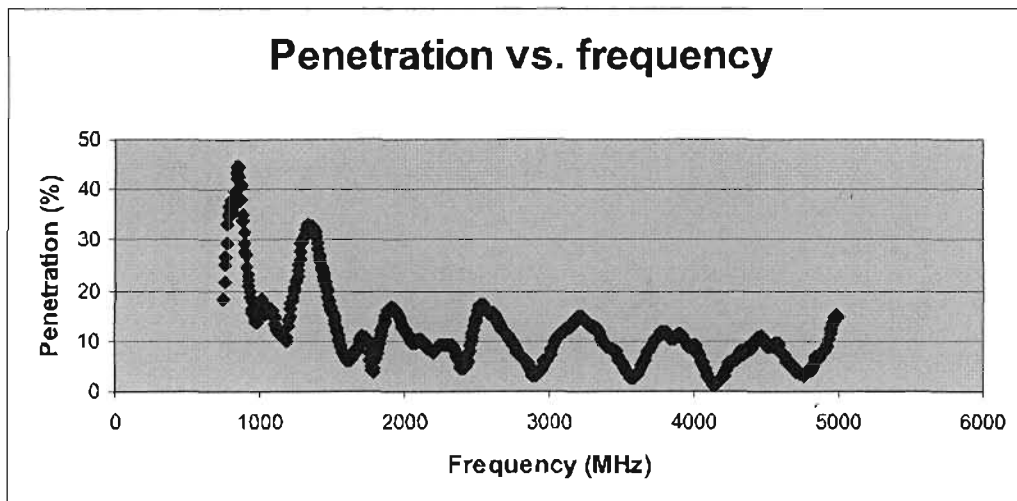
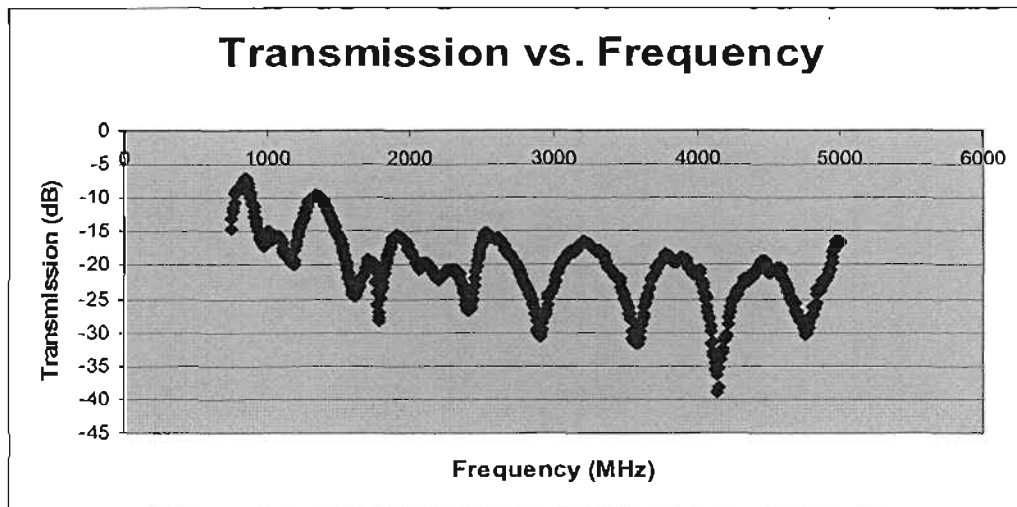
**F4: 7.5% Copper-doped Aluminium Stitched Carbon Fibre Specimens**

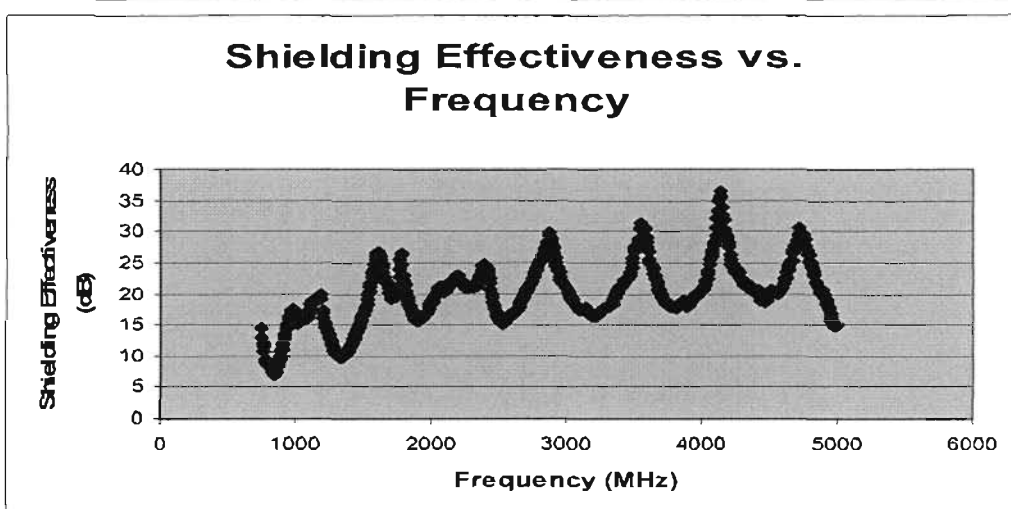
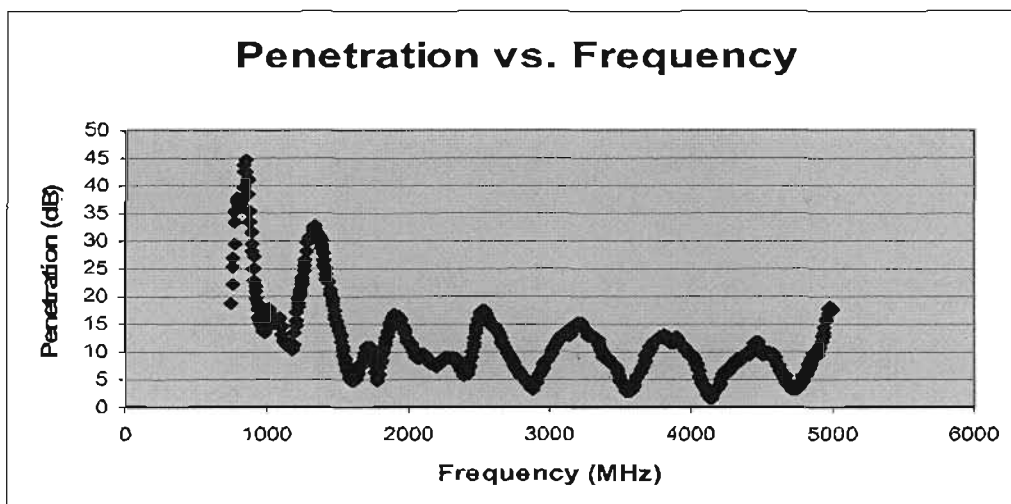
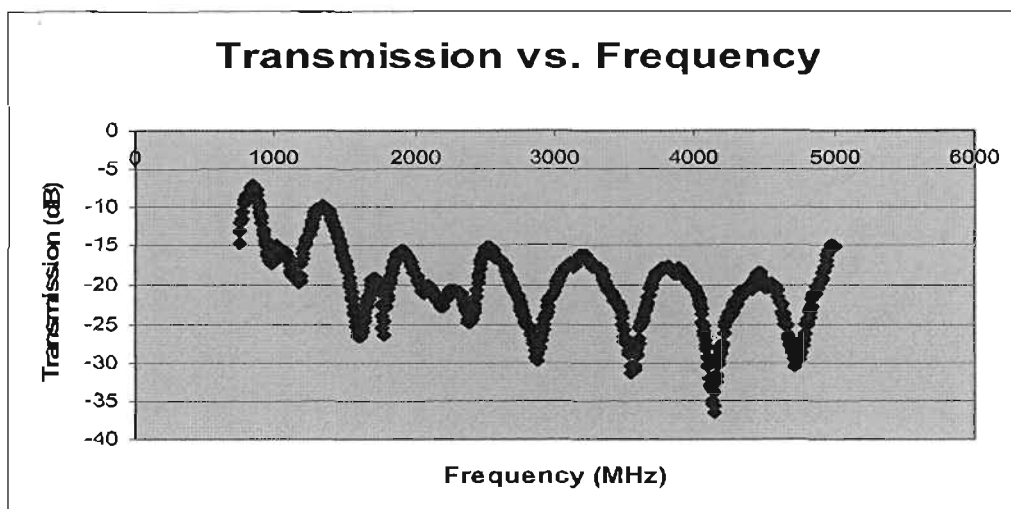
**F5: 15% Copper-doped Stitched Carbon Fibre Specimens**

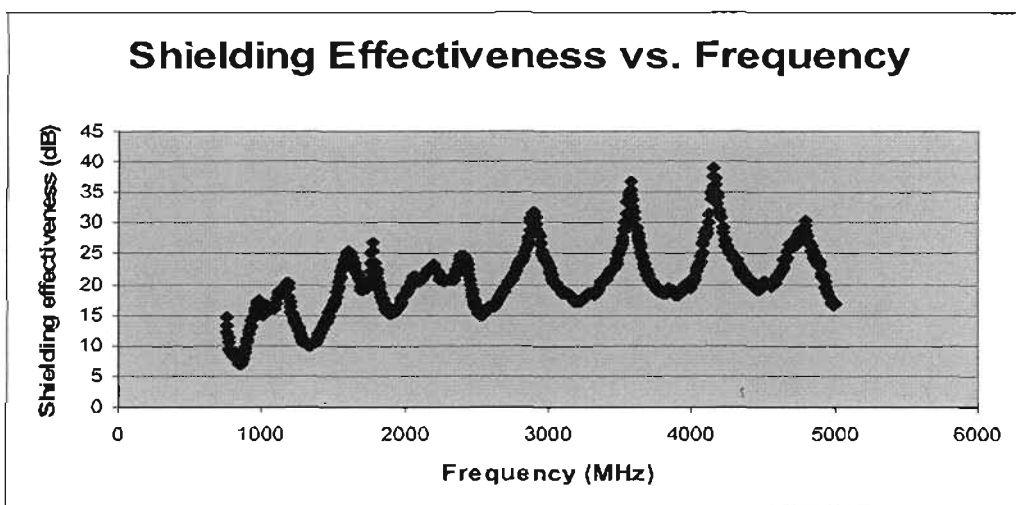
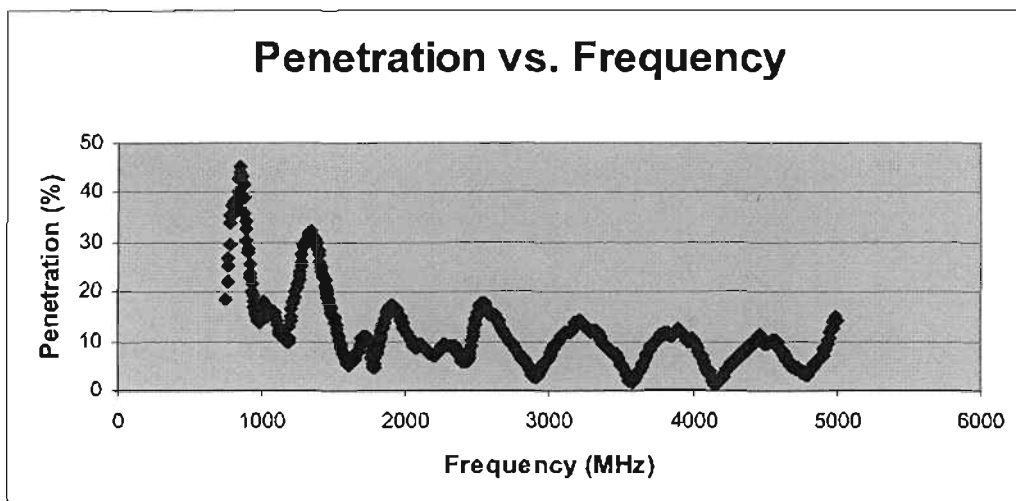
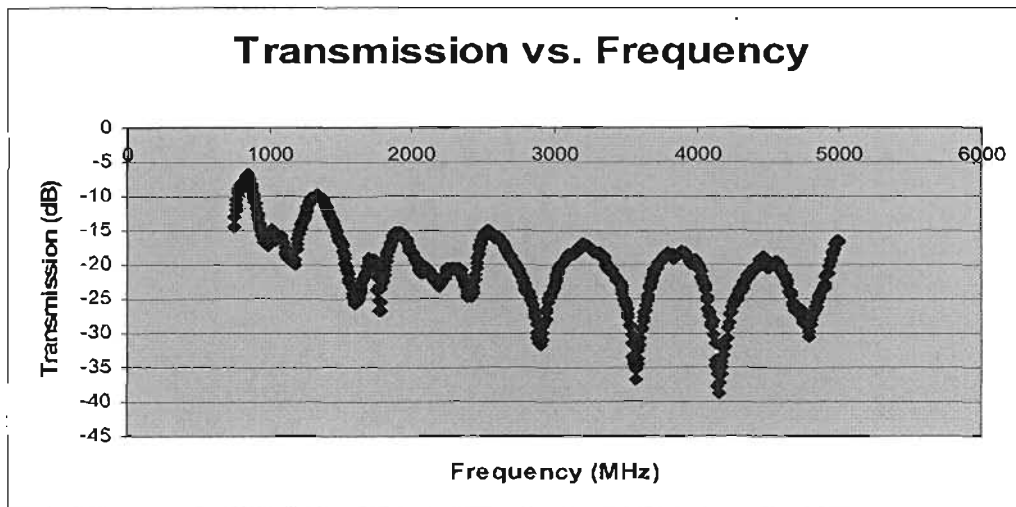
**F6 7.5% Hybrid Powder-doped Stitched Carbon Fibre Specimens**

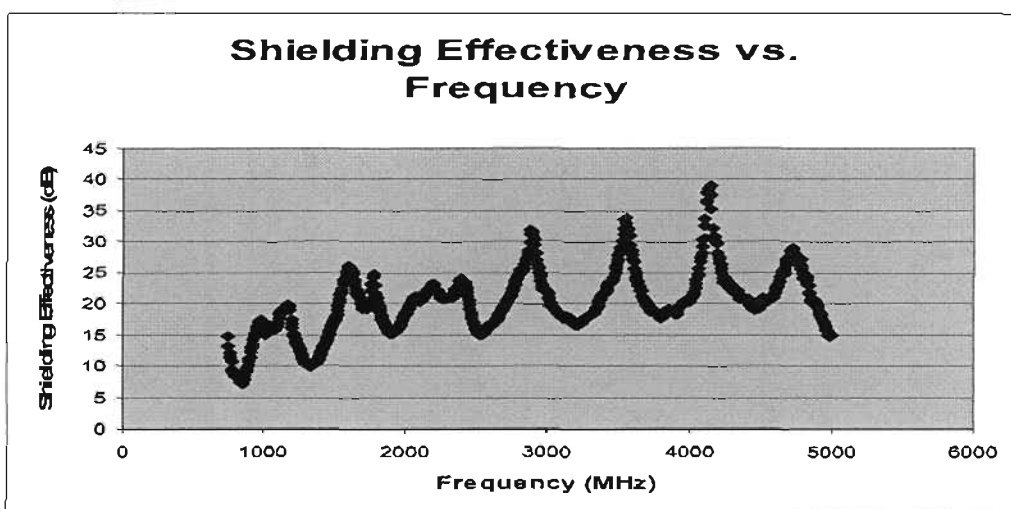
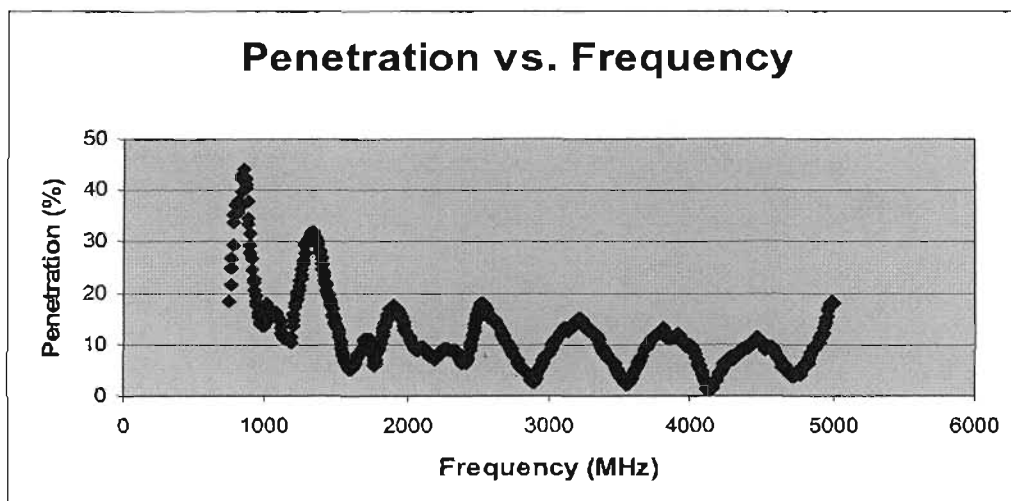
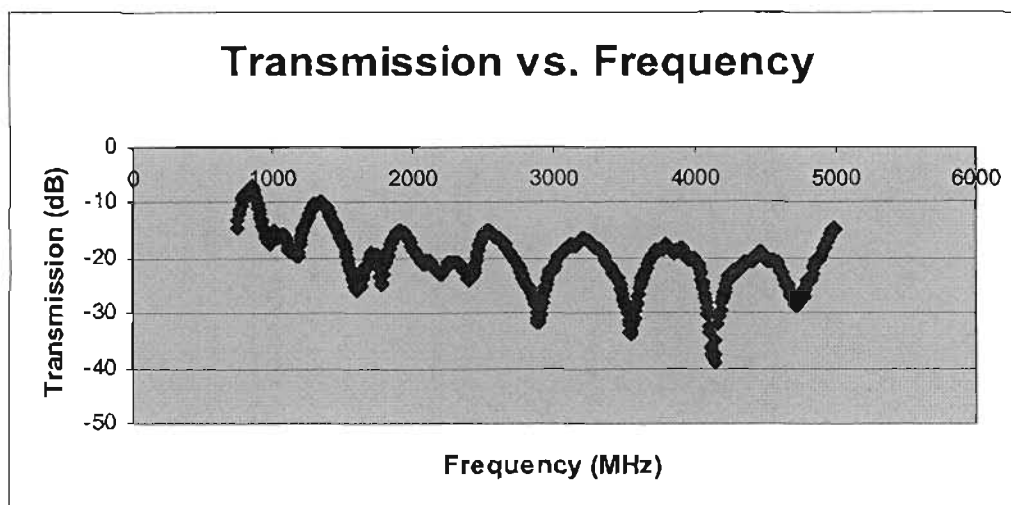
**F7: 15% Hybrid powder-doped Stitched Carbon Fibre Specimens**

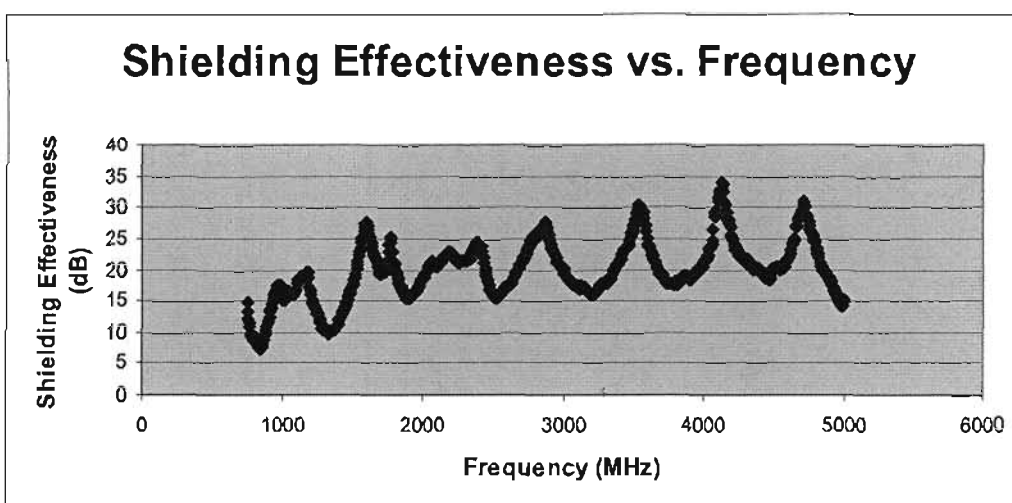
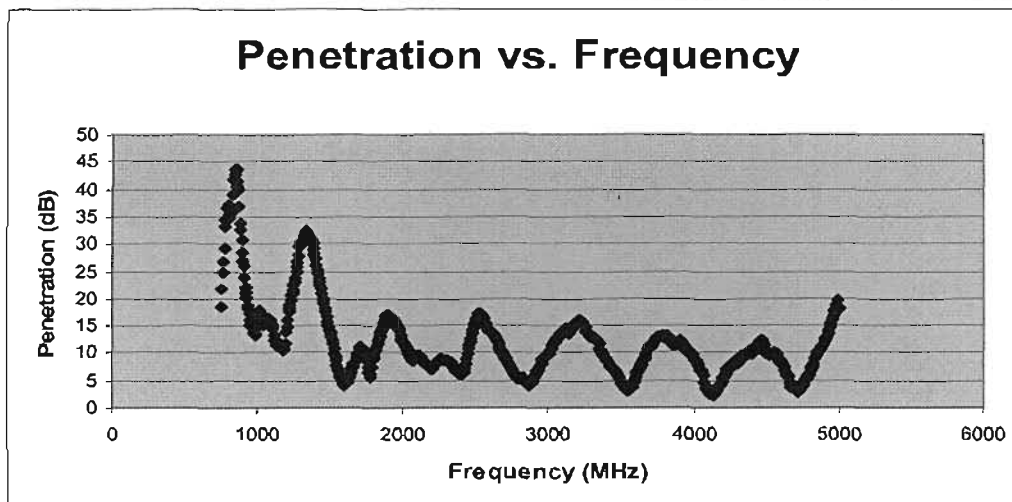
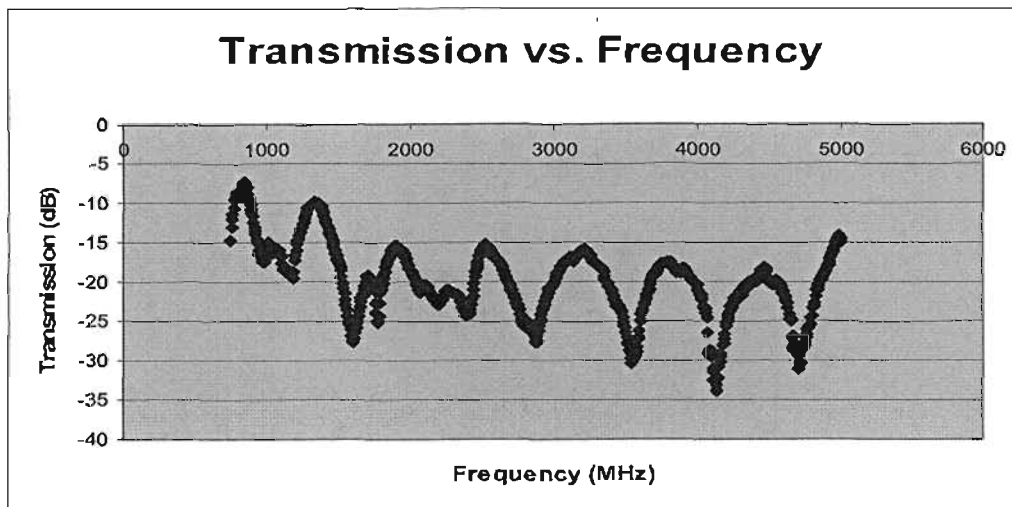


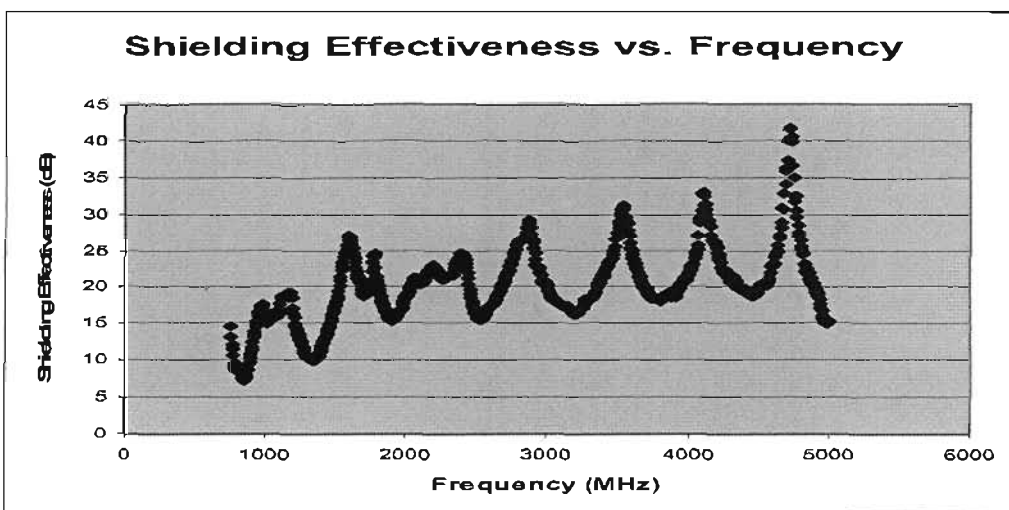
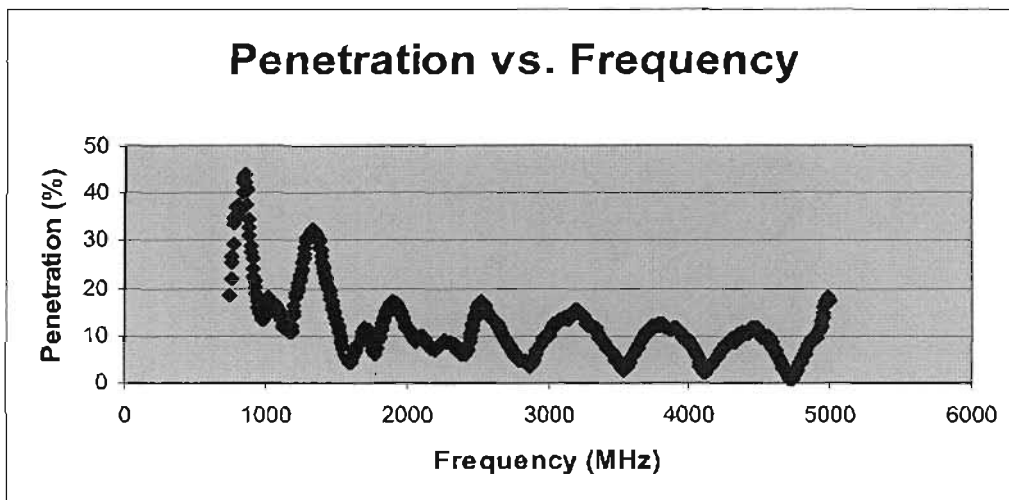
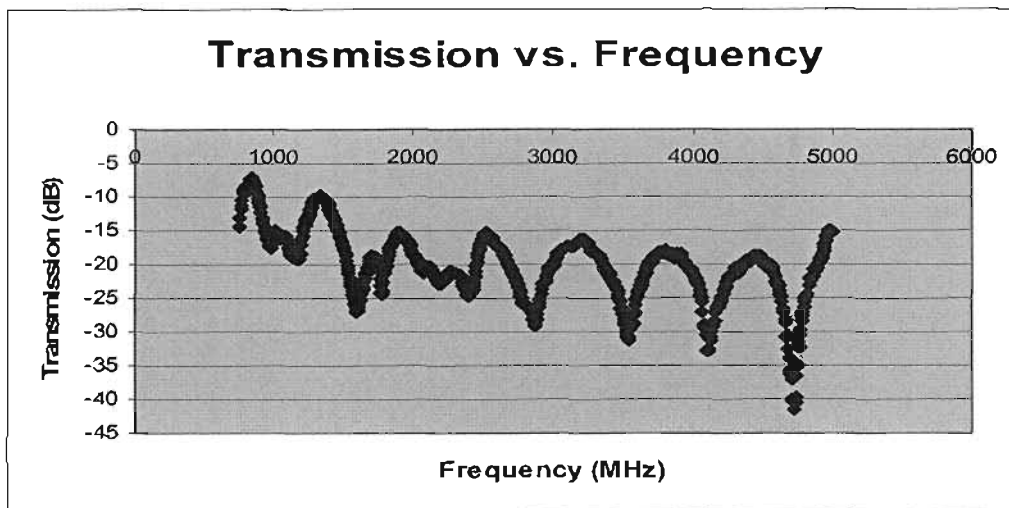
**F8: 1 Ply Mesh/Stitched Carbon Fibre Specimens**

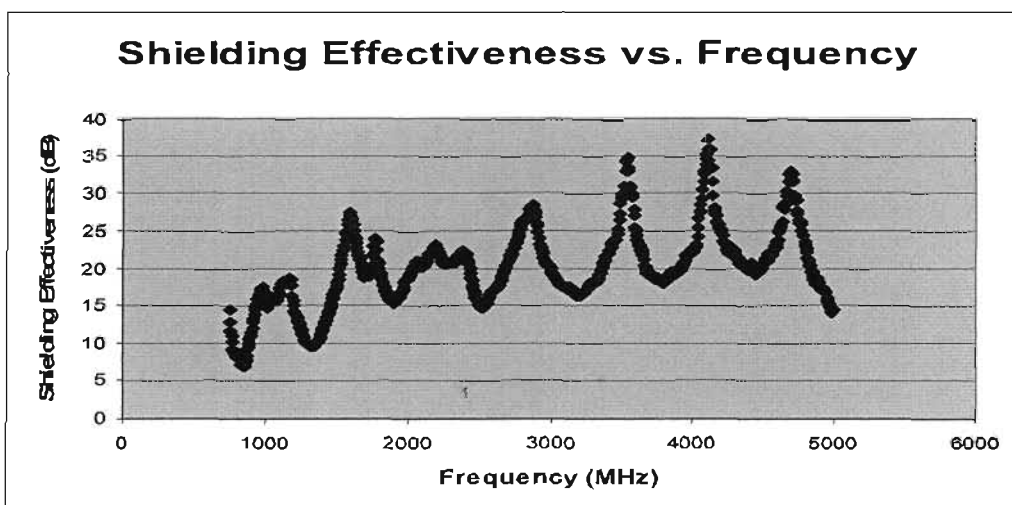
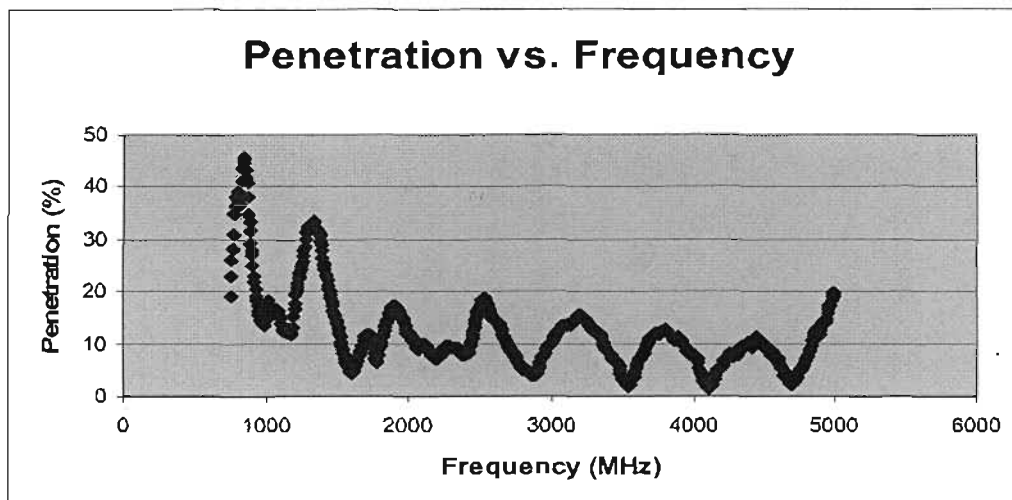
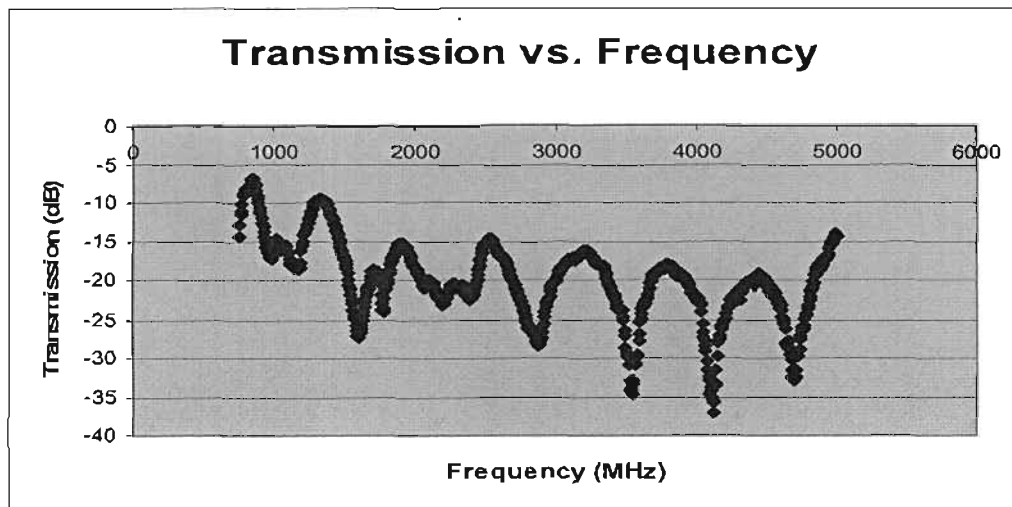
**F9: 2 Ply/Mesh Stitched Carbon Fibre Specimens**

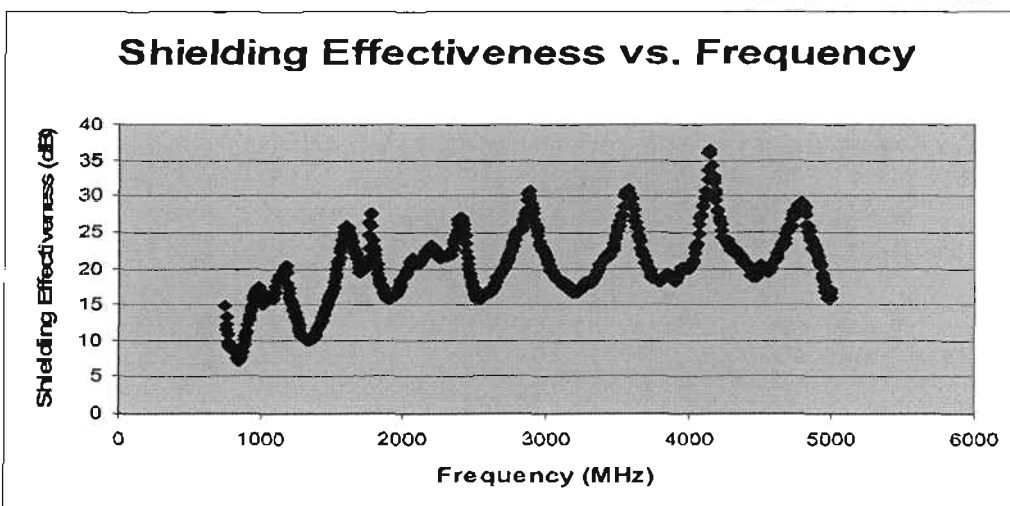
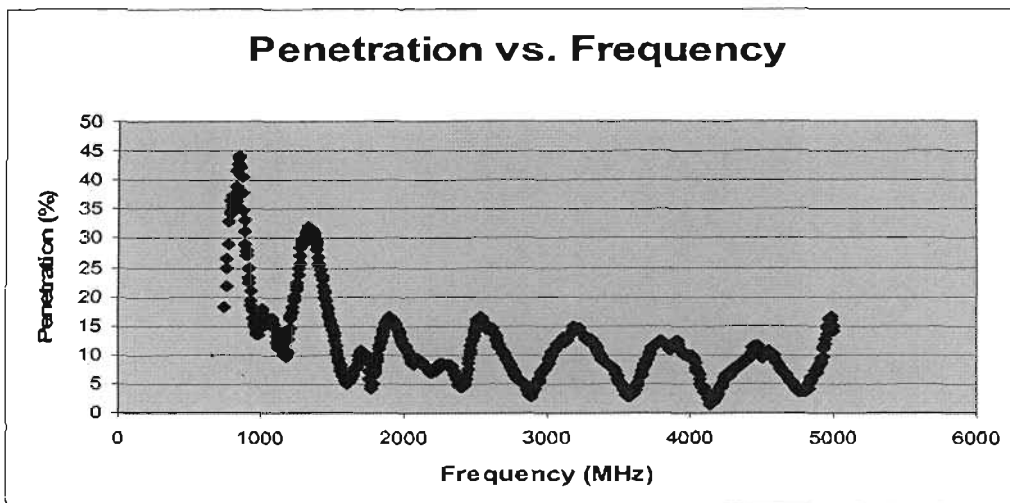
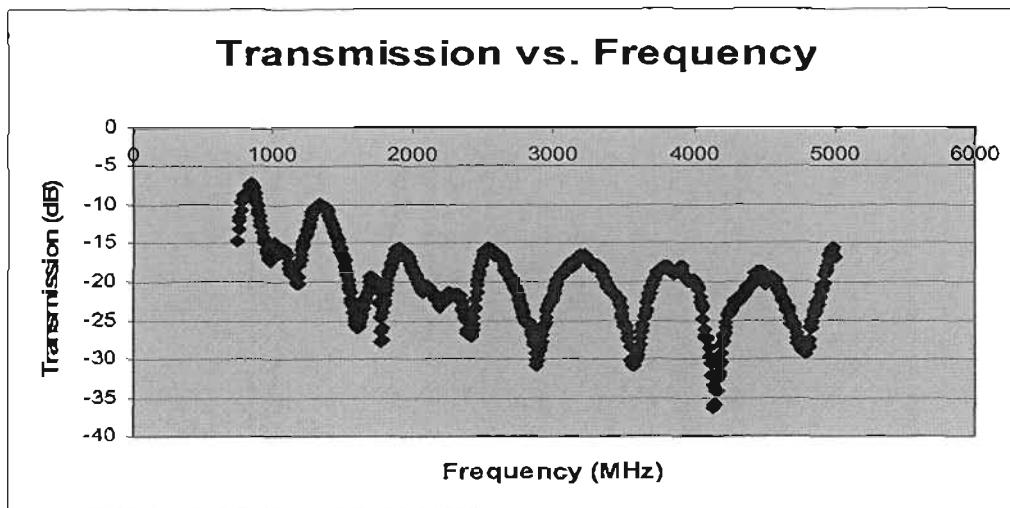
**F10: Undoped Woven Carbon Fibre Specimens**

**F11: 7.5% Aluminium-doped Woven Carbon Specimens**

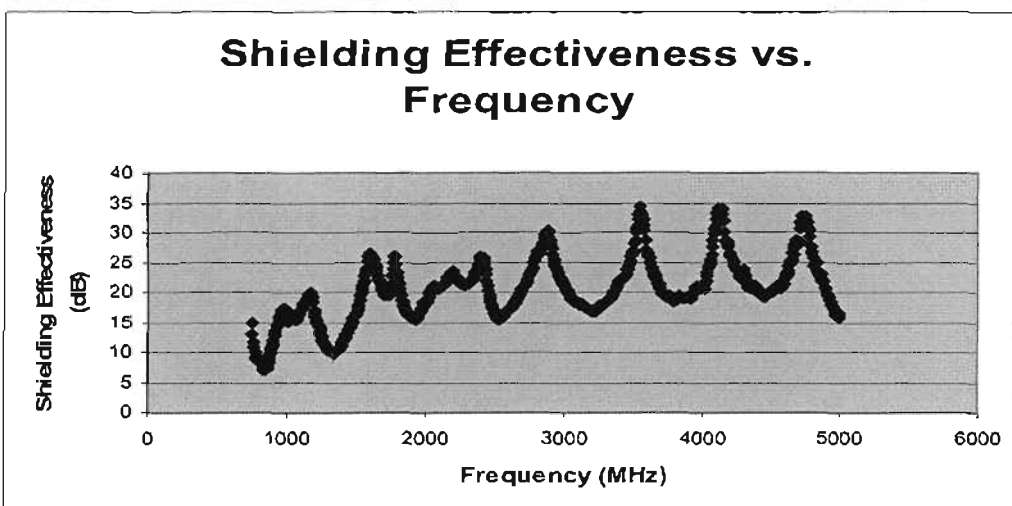
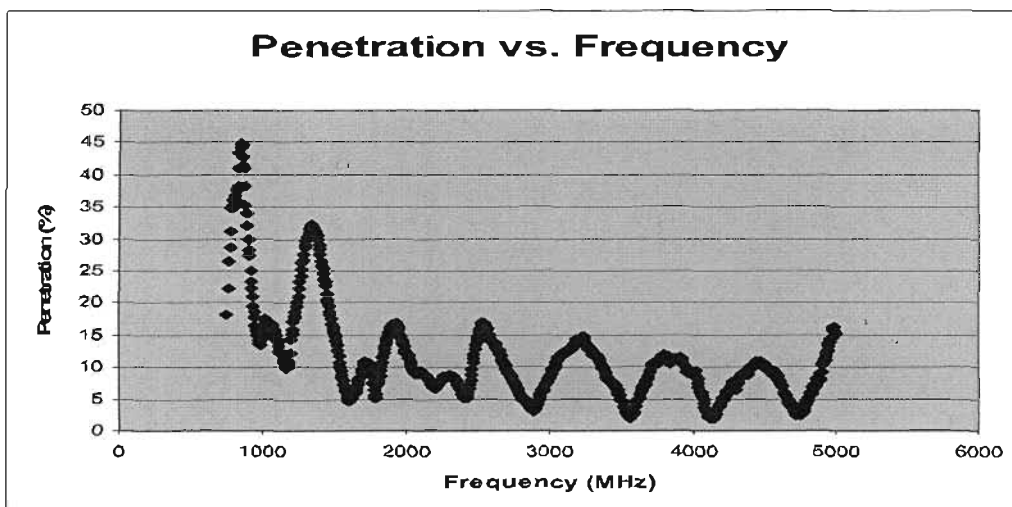
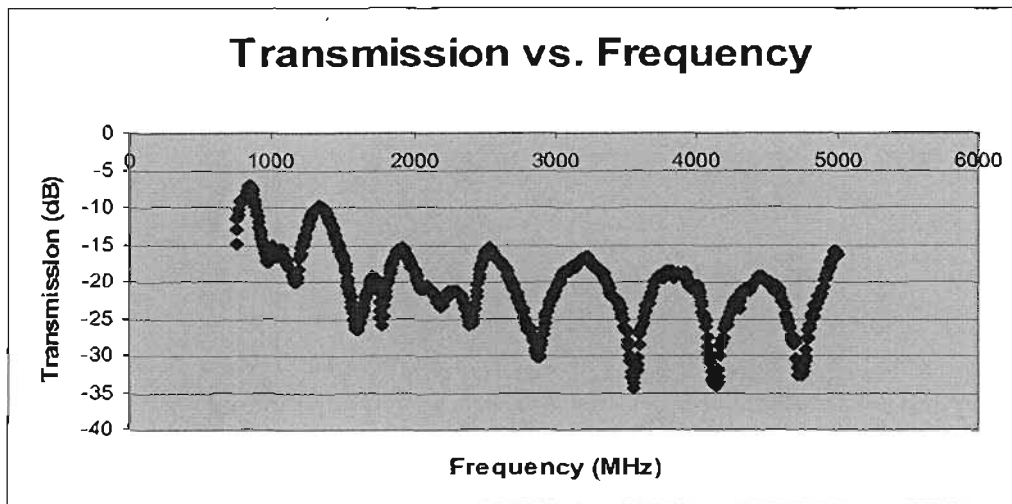
**F12: 15% Aluminium-doped Woven Carbon Specimens**

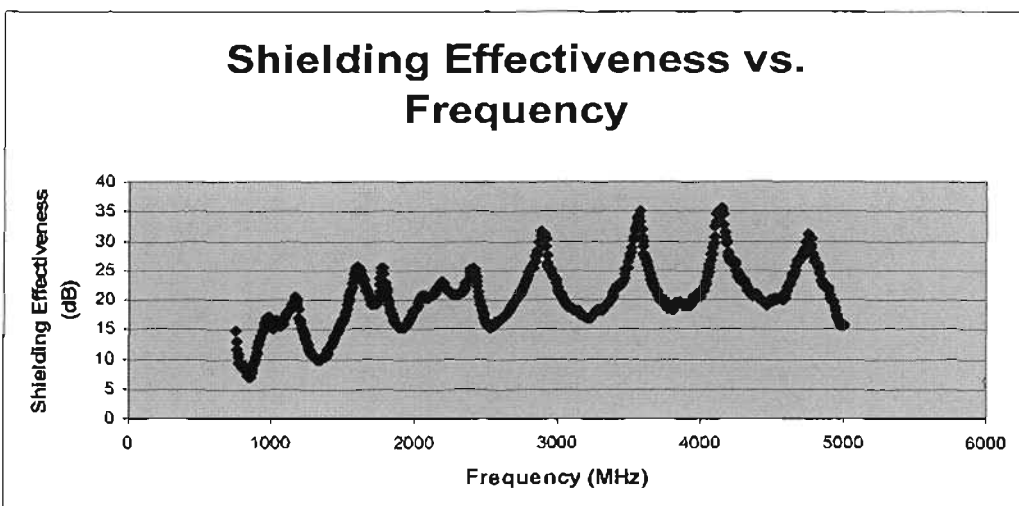
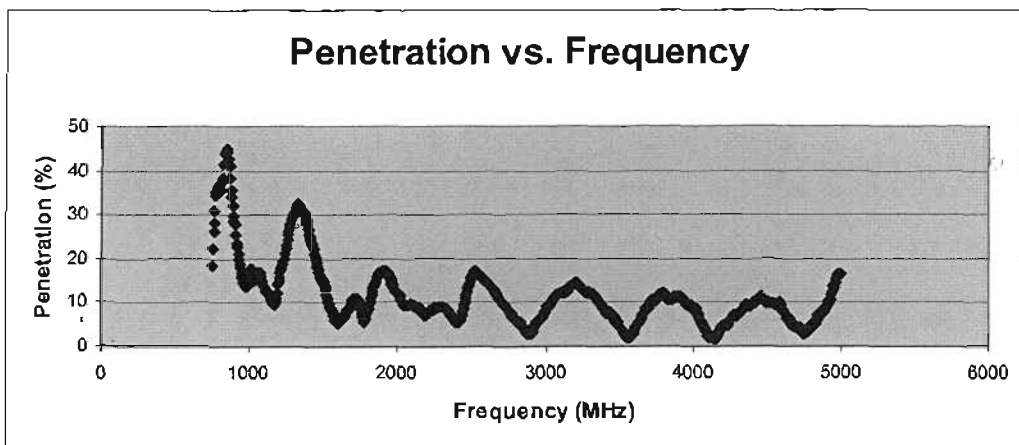
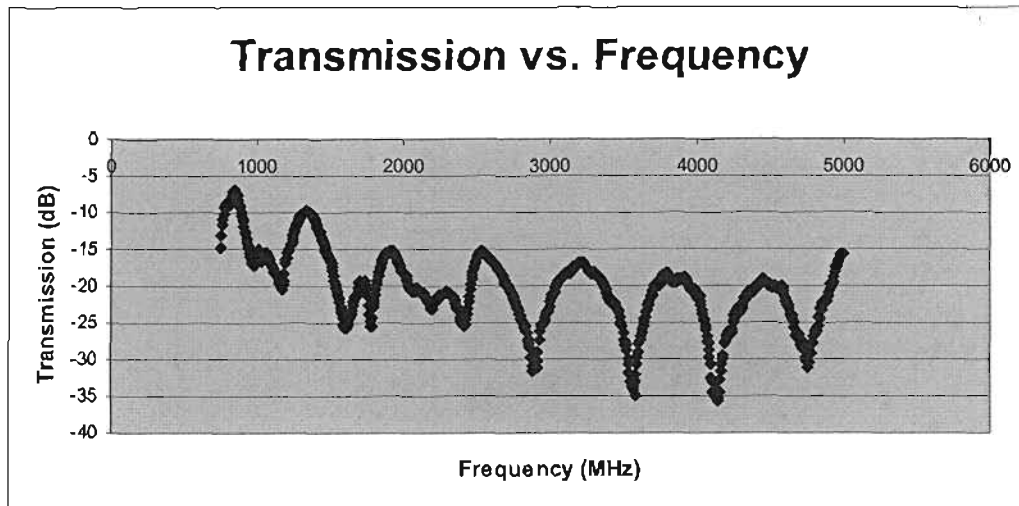
**F13: 7.5% Copper-doped Woven Carbon Specimens**

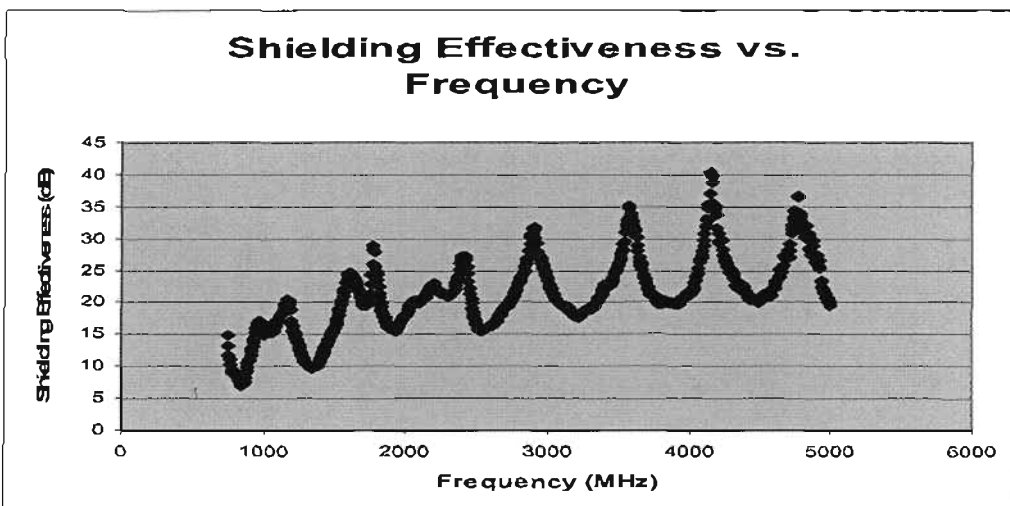
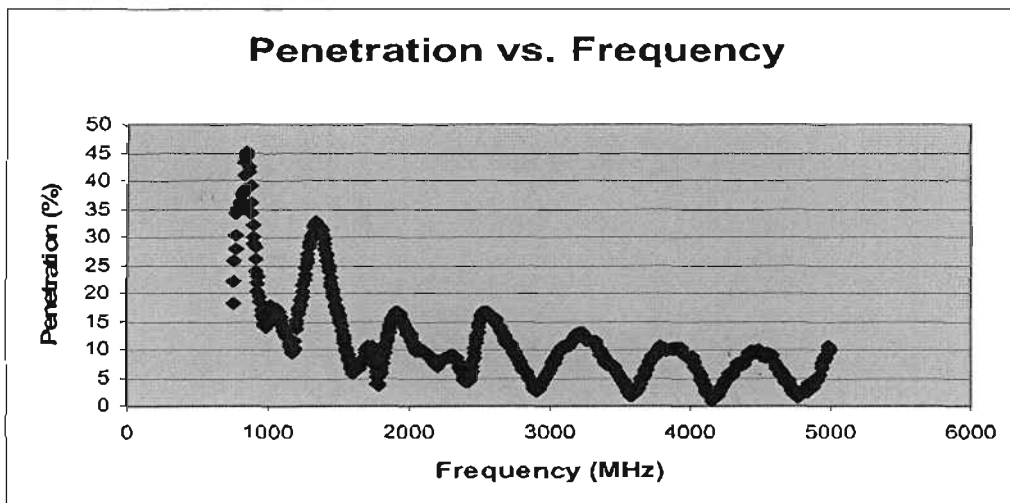
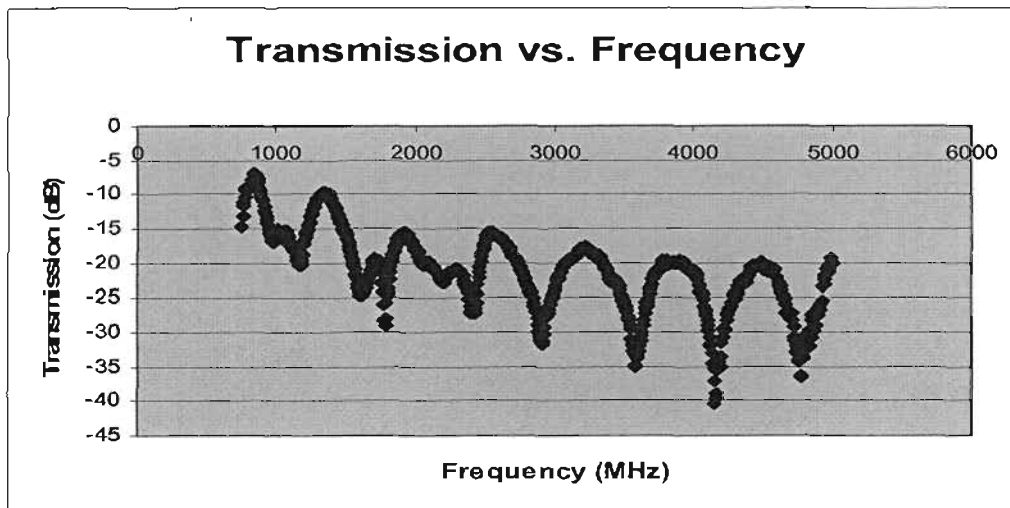
**F14: 15% Copper-doped Woven Carbon Specimens**

**F15: 7.5% Hybrid powder-doped Woven Carbon Specimens**

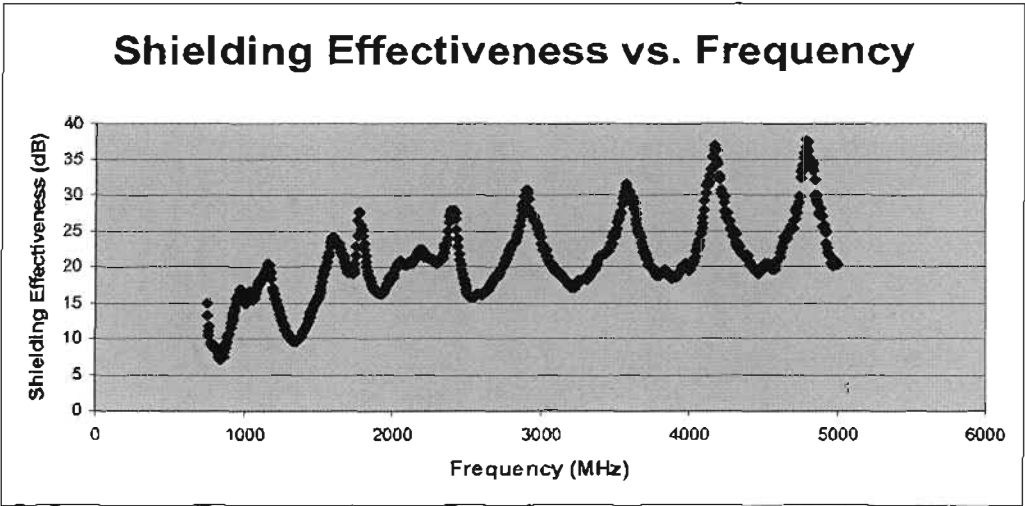
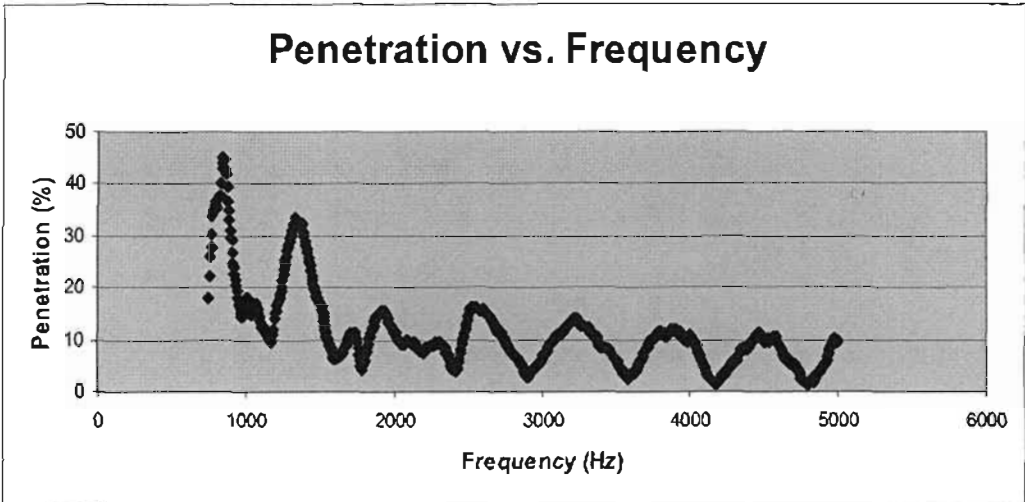
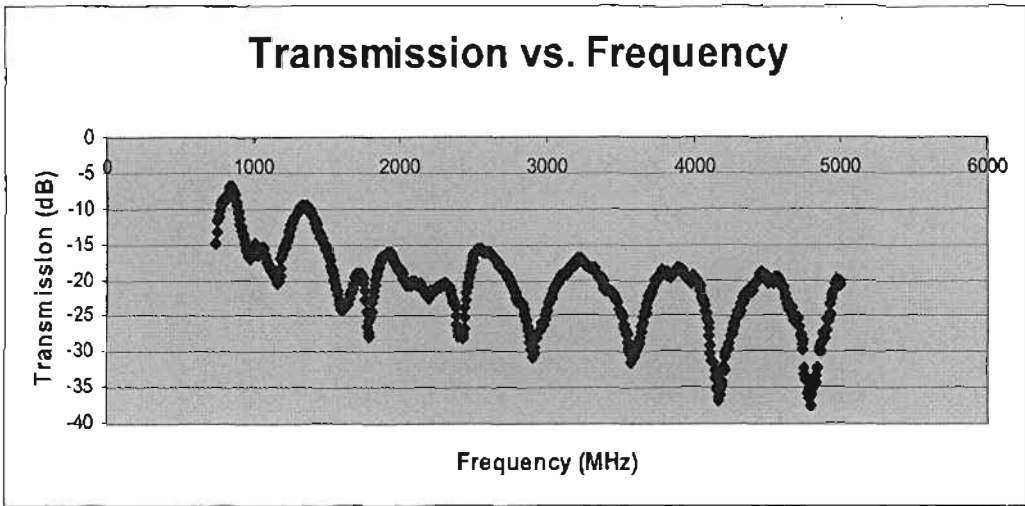


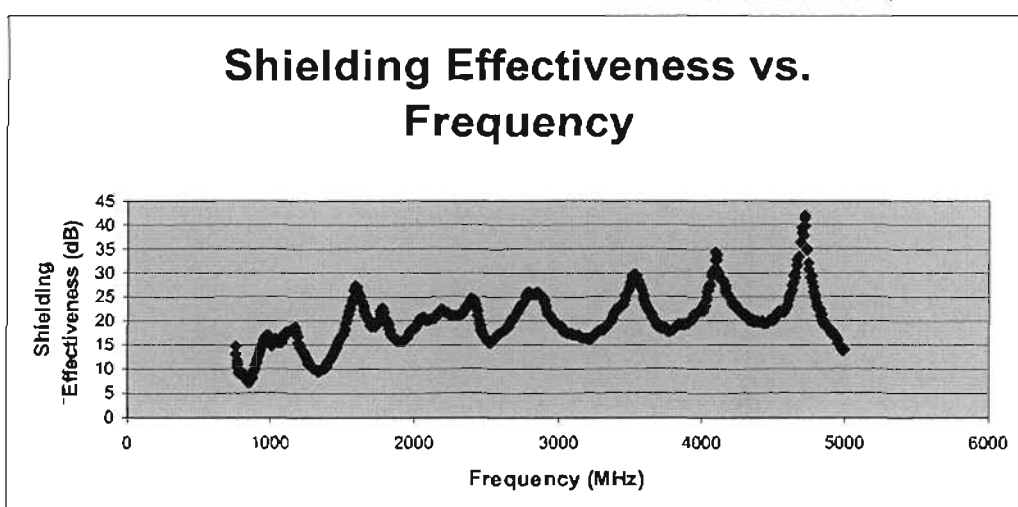
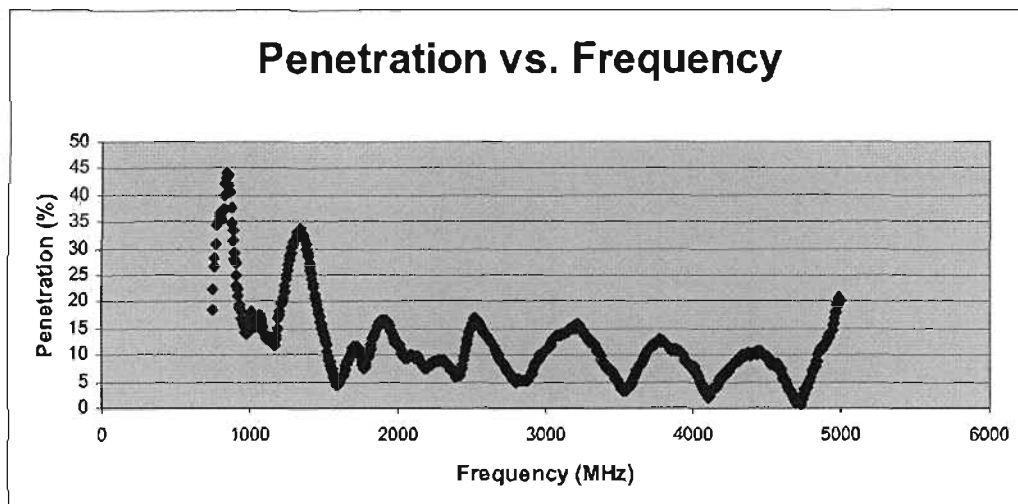
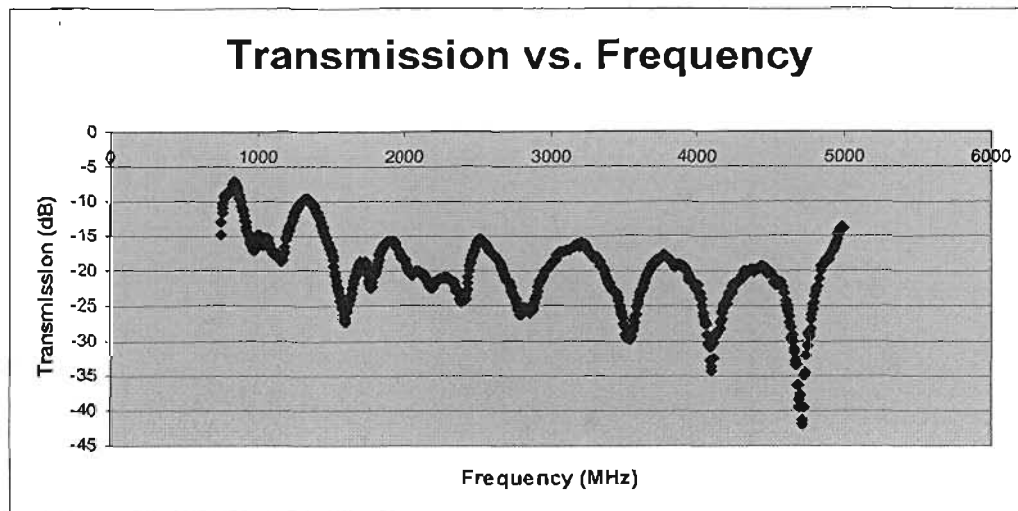
**F16: 15% Hybrid Powder-doped Woven Carbon Specimens**

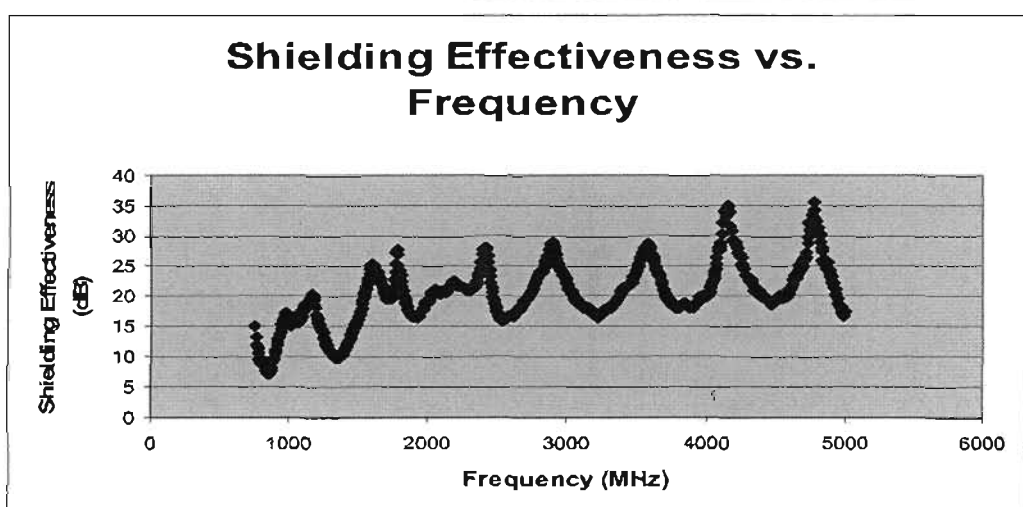
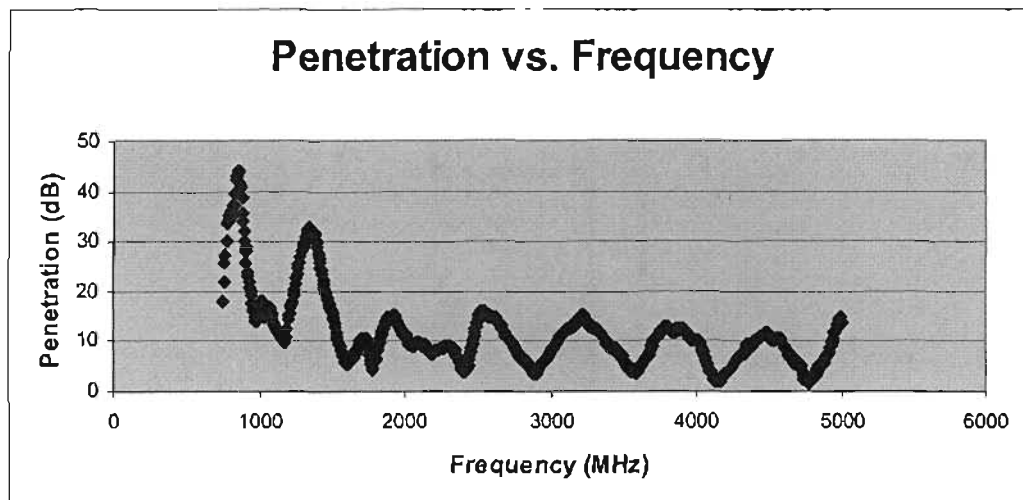
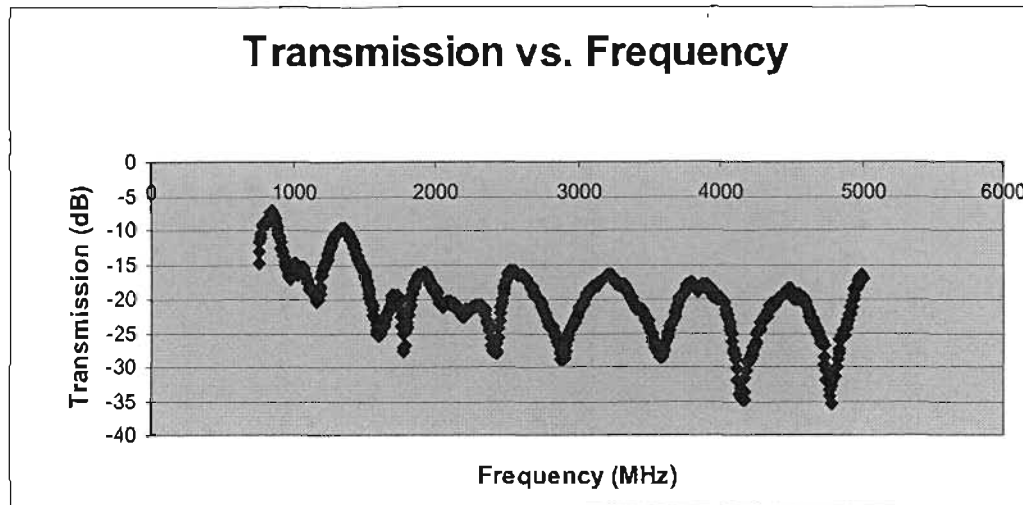
**F17: 1 Ply Mesh/Woven Carbon Specimens**

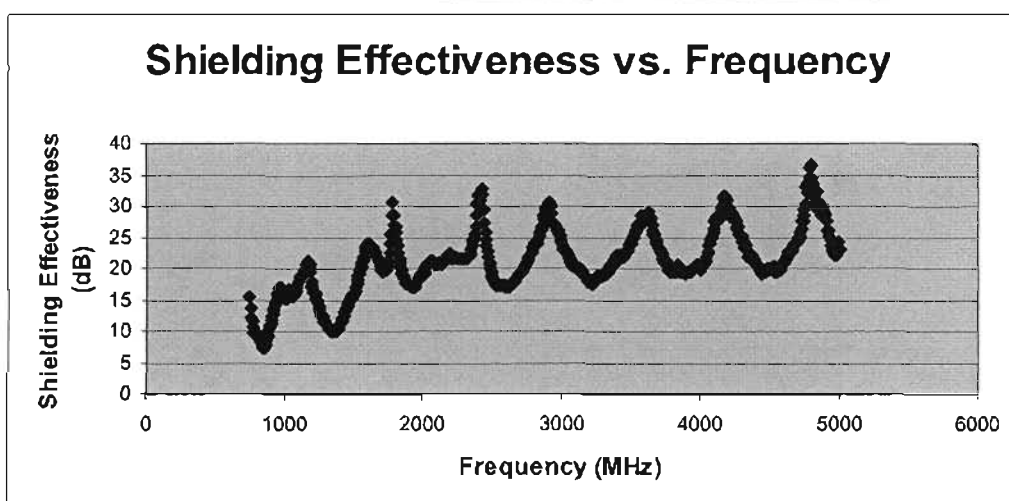
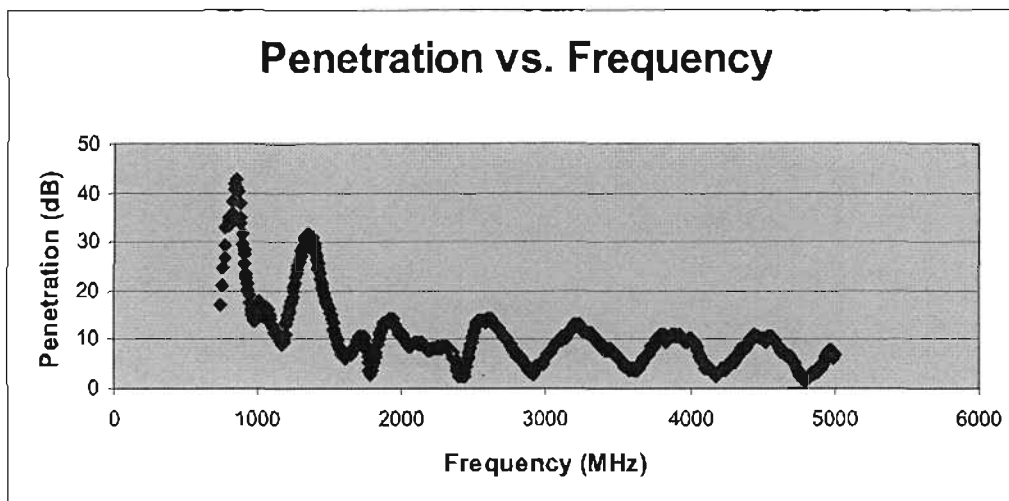
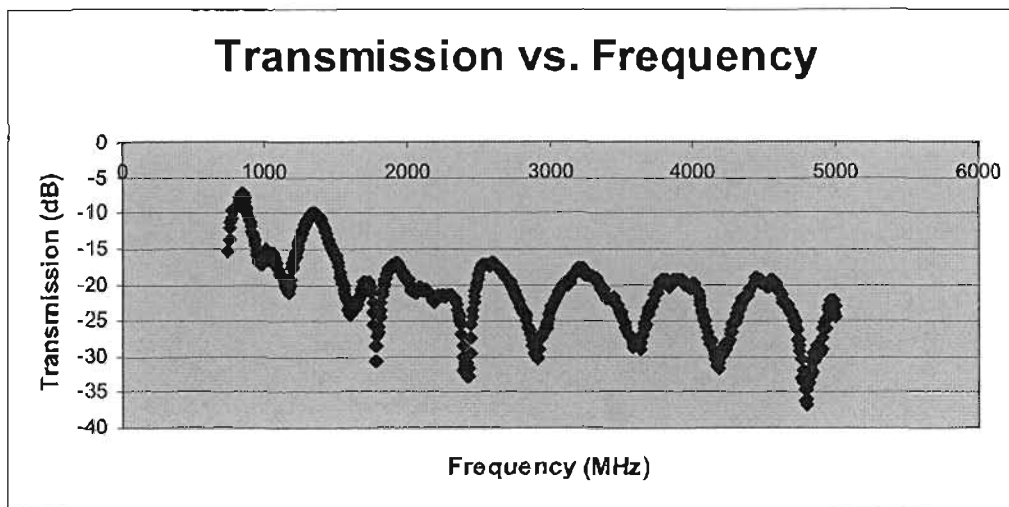
**F18: 2 Ply Mesh/Woven Carbon Specimens**

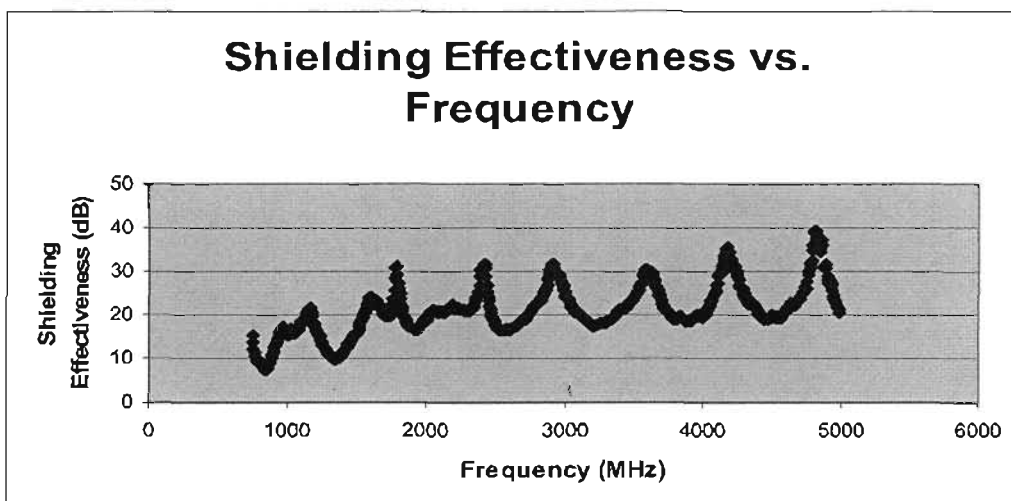
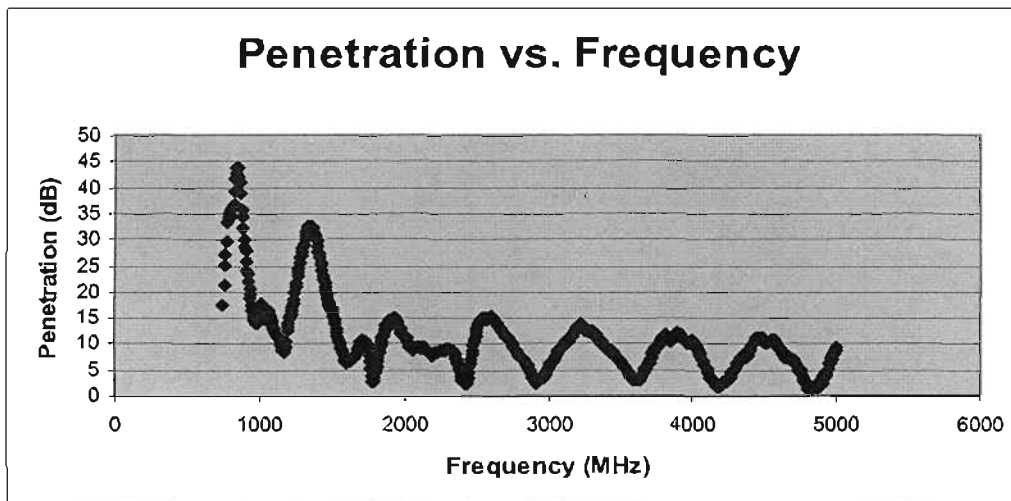
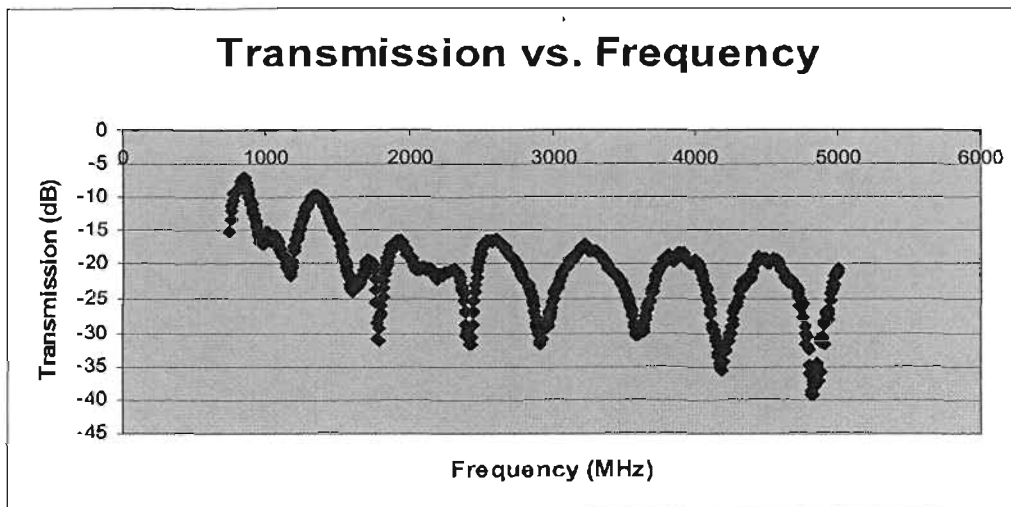
F19: Undoped Unidirectional Carbon Specimens



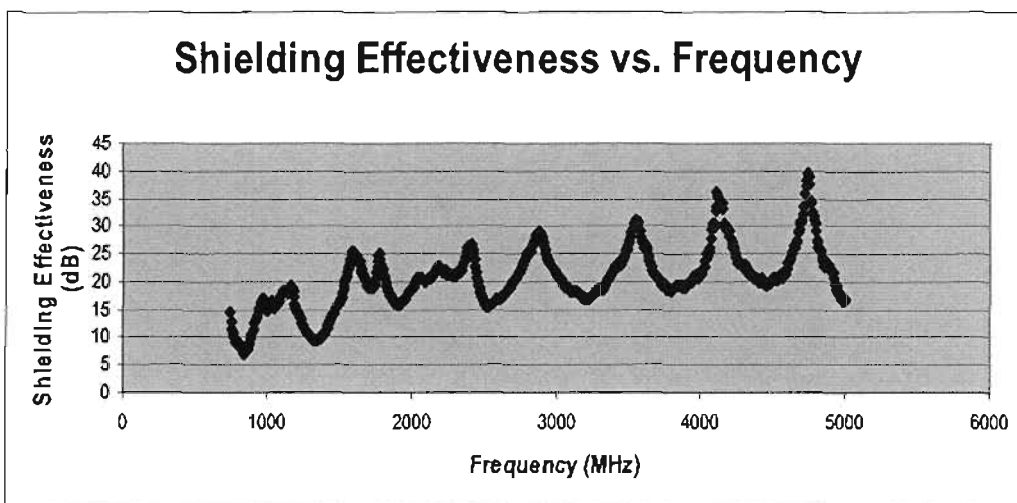
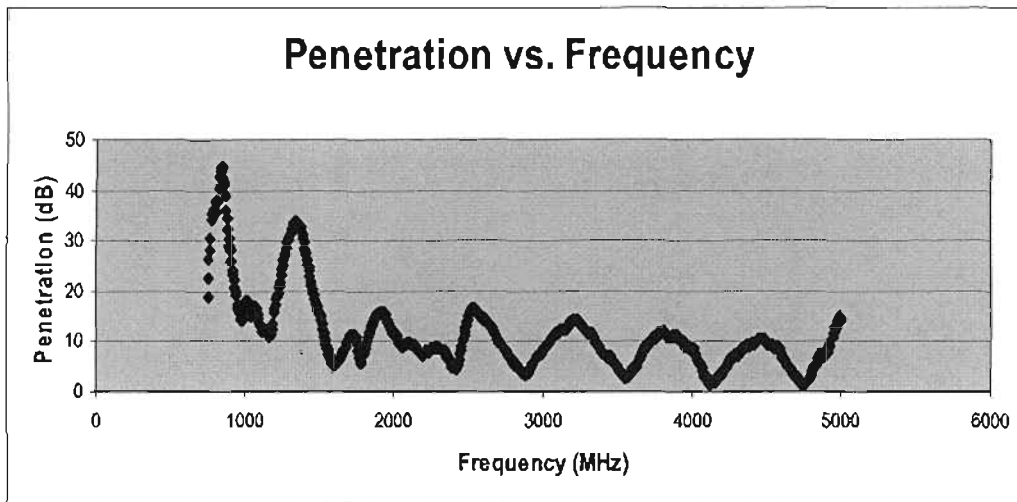
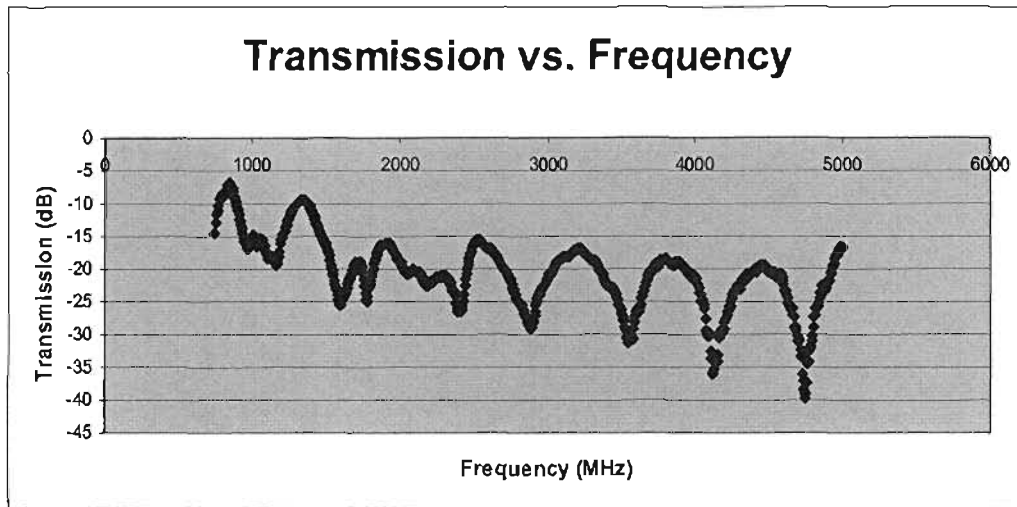
**F20: 7.5% Aluminium-doped Unidirectional Carbon Specimens**

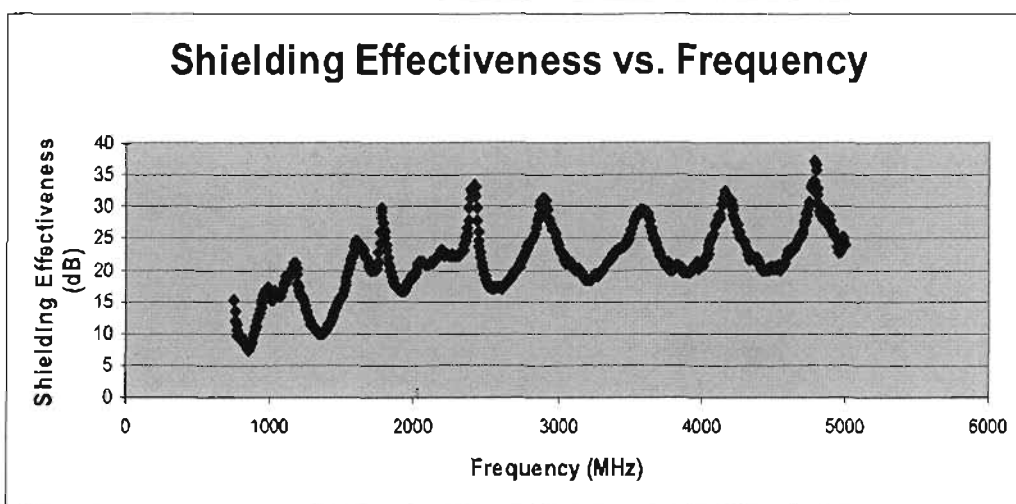
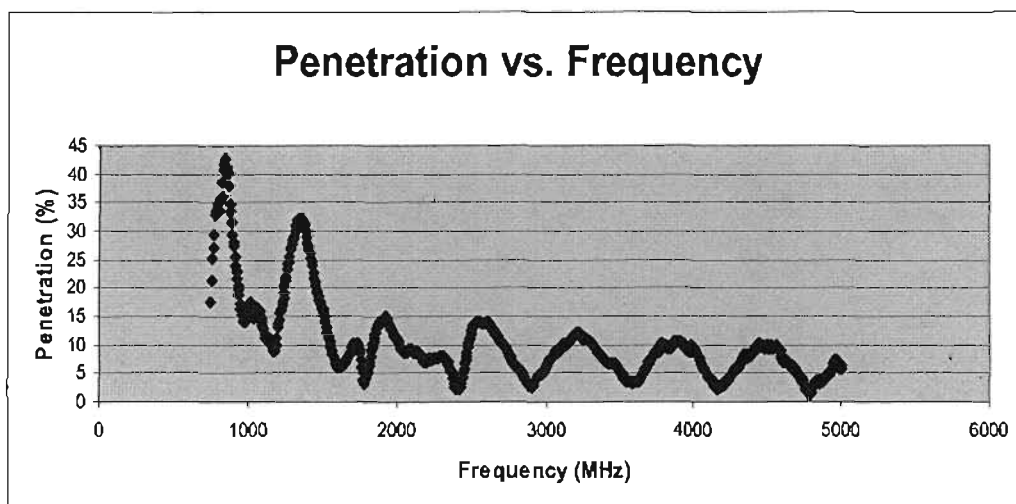
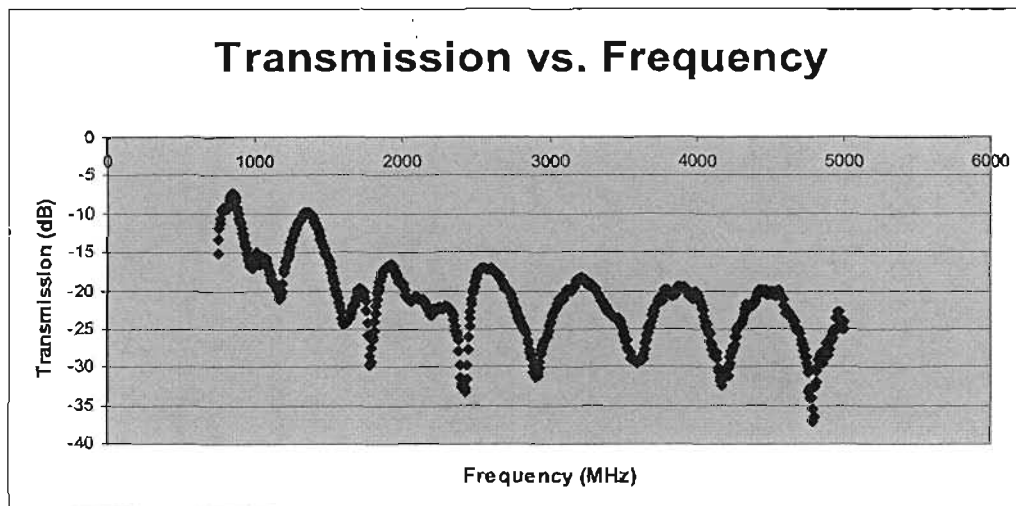
**F21: 15% Aluminium-doped Unidirectional Carbon Specimens**

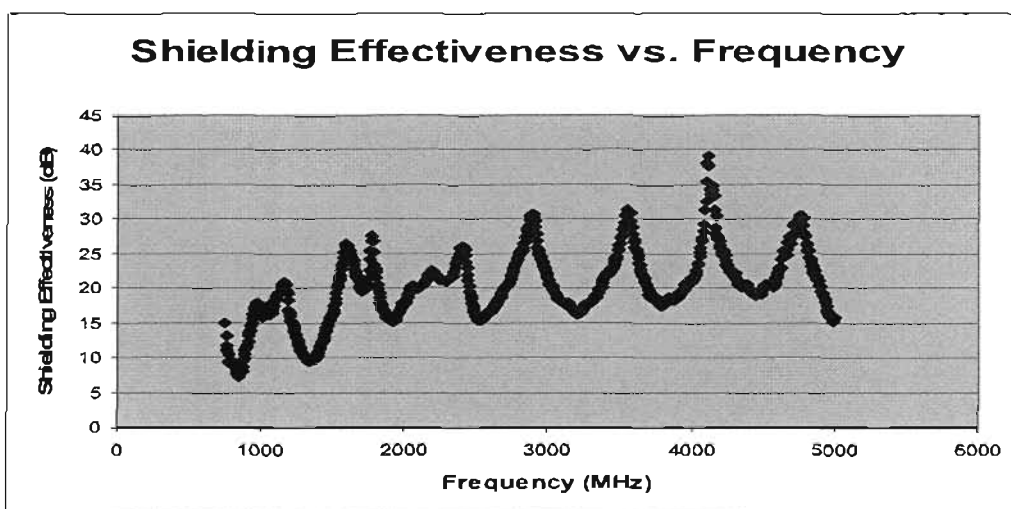
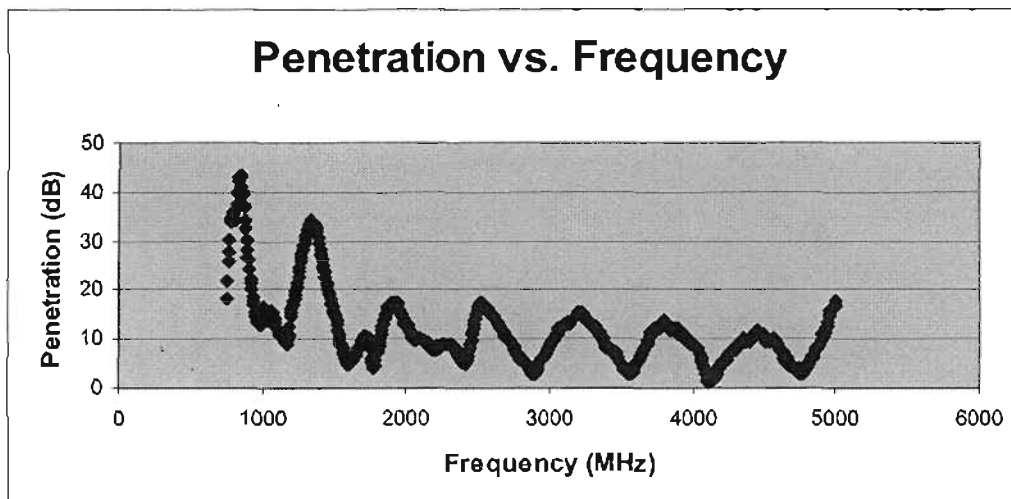
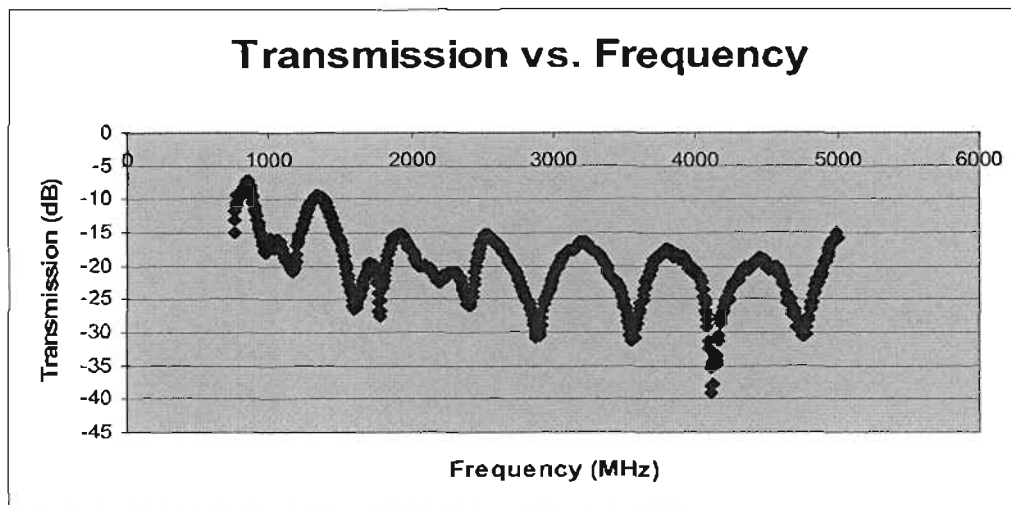
**F22: 7.5% Copper-doped Unidirectional Specimens**

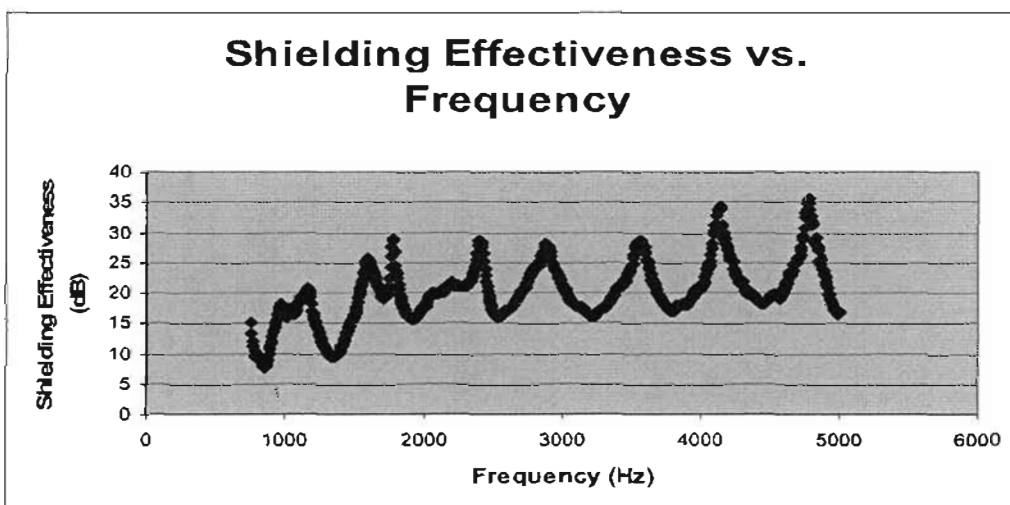
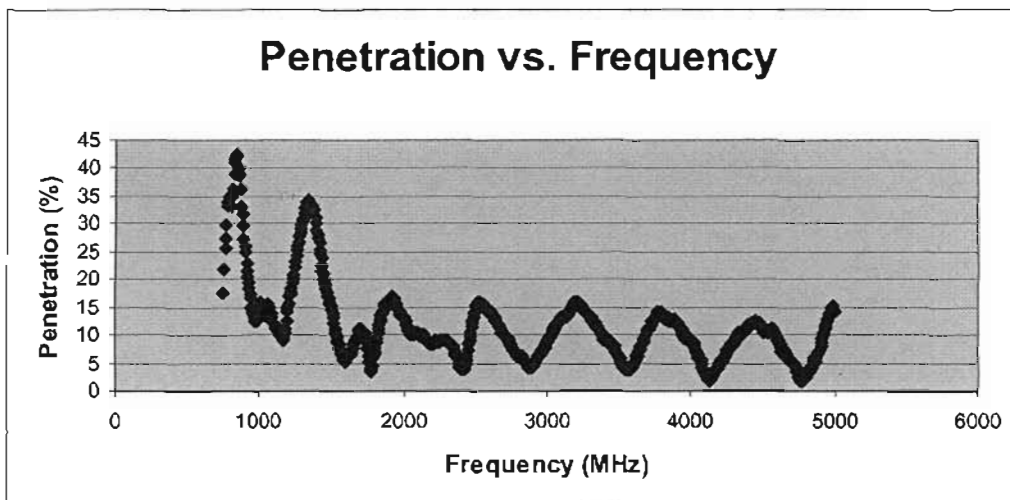
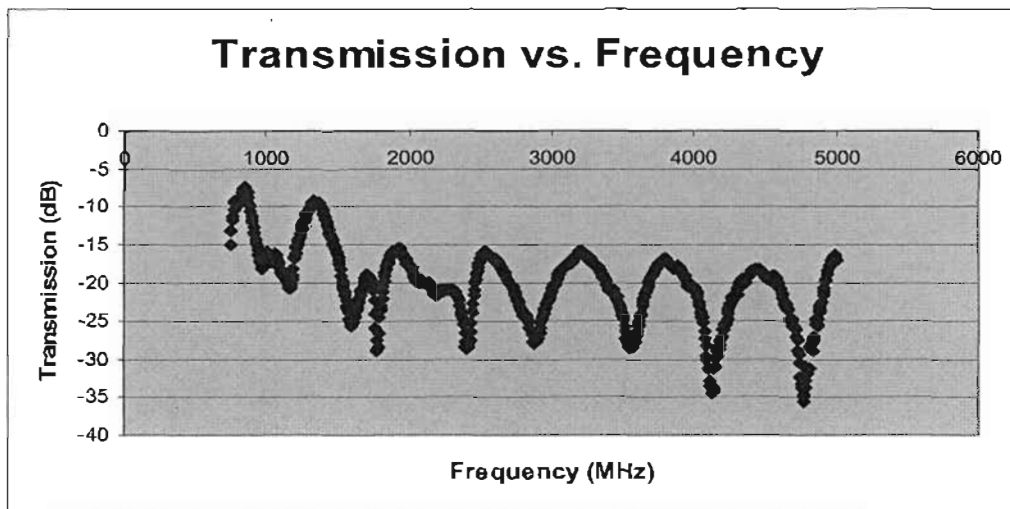
**F23: 15% Copper-doped Unidirectional Specimens**



**F24: 7.5% Hybrid Powder-doped Unidirectional Specimens**

**F25: 15% Hybrid Powder-doped Unidirectional Specimens**

**F26: 1 Ply Mesh/Unidirectional Carbon Specimens**

**F27: 2 Ply Mesh/ Unidirectional Specimens**

## APPENDIX G: MECHANICAL FAILURE IMAGES

### Tensile test images:

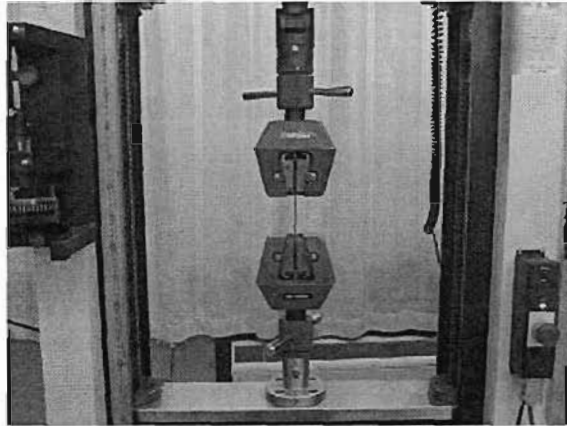


Figure G1: Test in progress

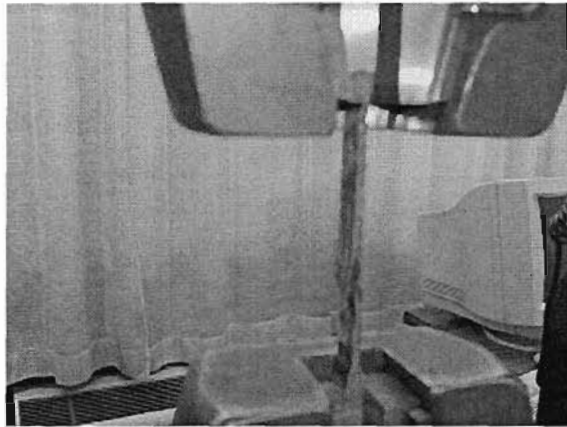


Figure G2: Failure in test

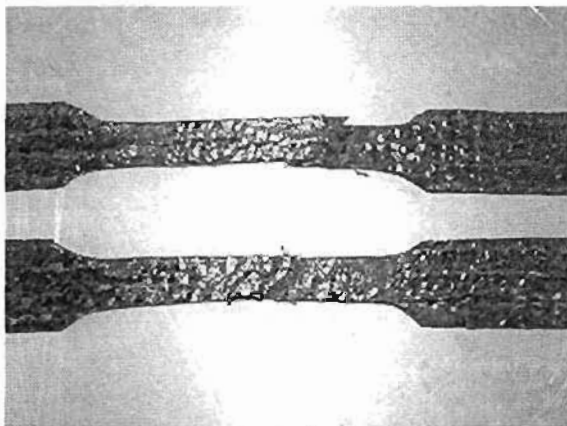


Figure G3: Failed stitched carbon samples

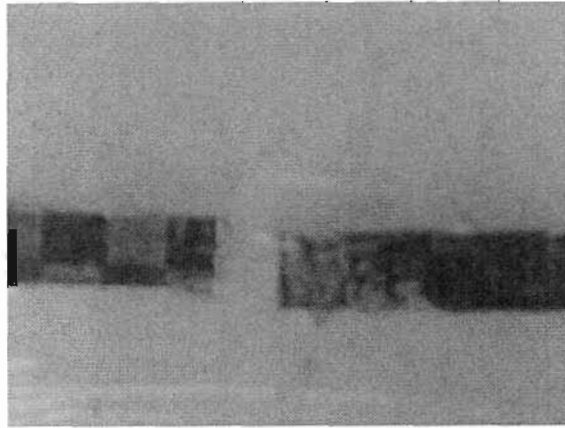


Figure G4: Failed woven carbon sample

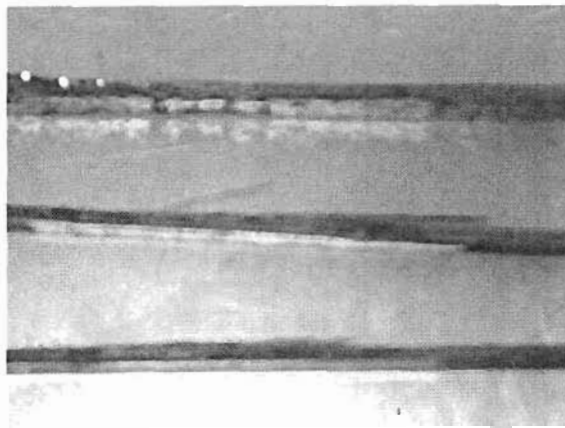


Figure G5: Failed unidirectional carbon samples

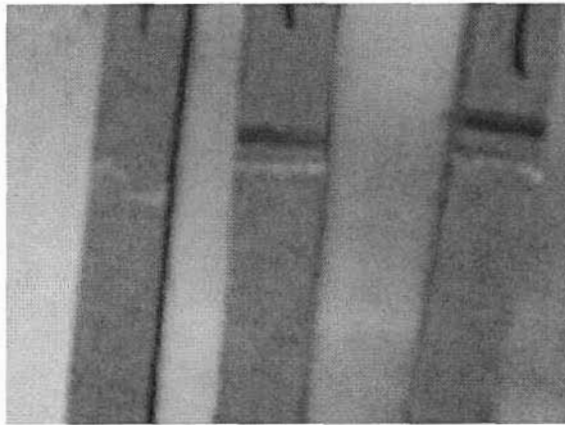


Figure G6: Failure in specimens containing Alumesb fabric

Flexural test images:

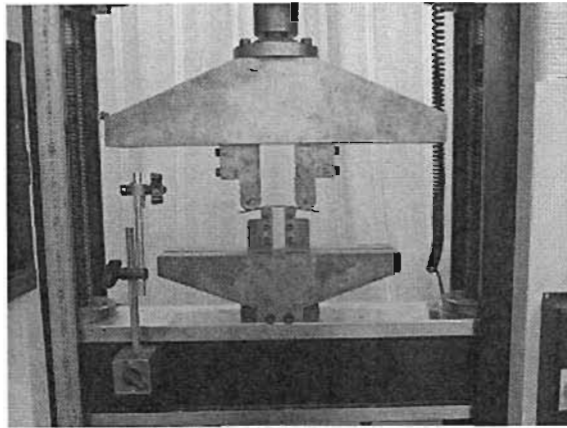


Figure G6: Test in progress

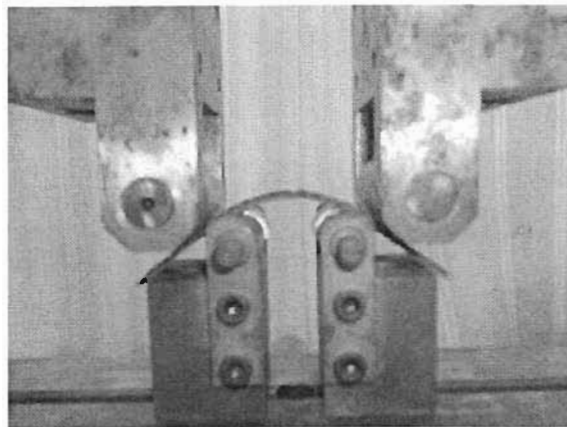


Figure G7: Excessive deflection when testing stitched carbon samples

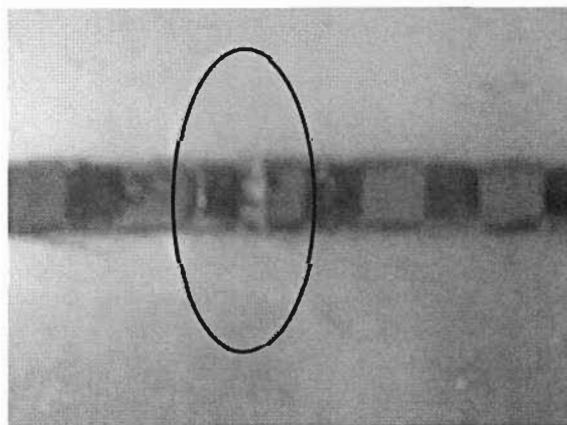


Figure G8: Failure in woven carbon sample

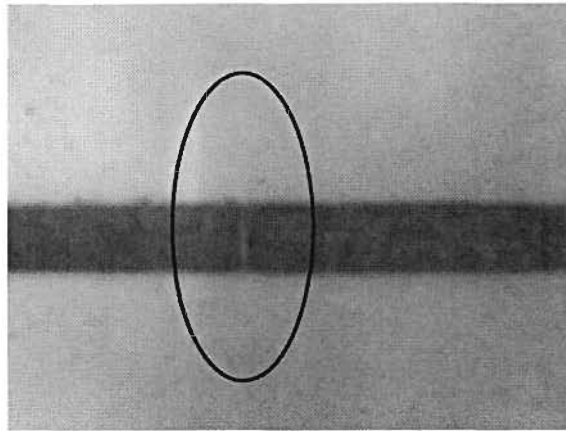


Figure G9: Failure in unidirectional carbon sample

**Compressive test images:**

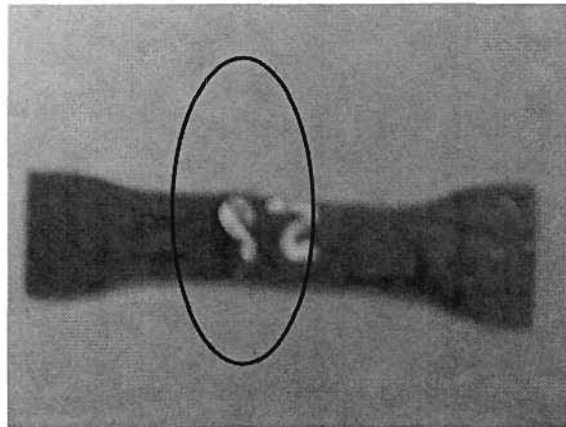


Figure G10: Failure in stitched carbon samples

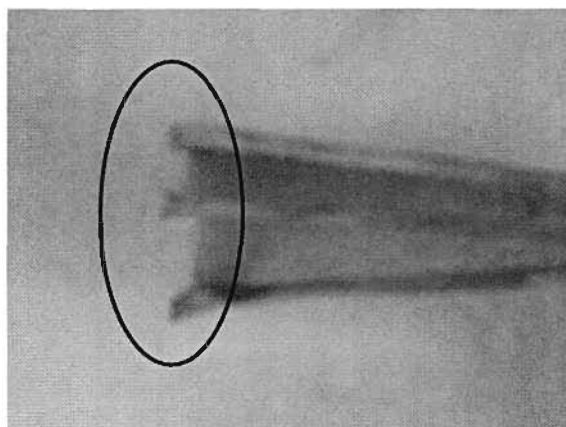
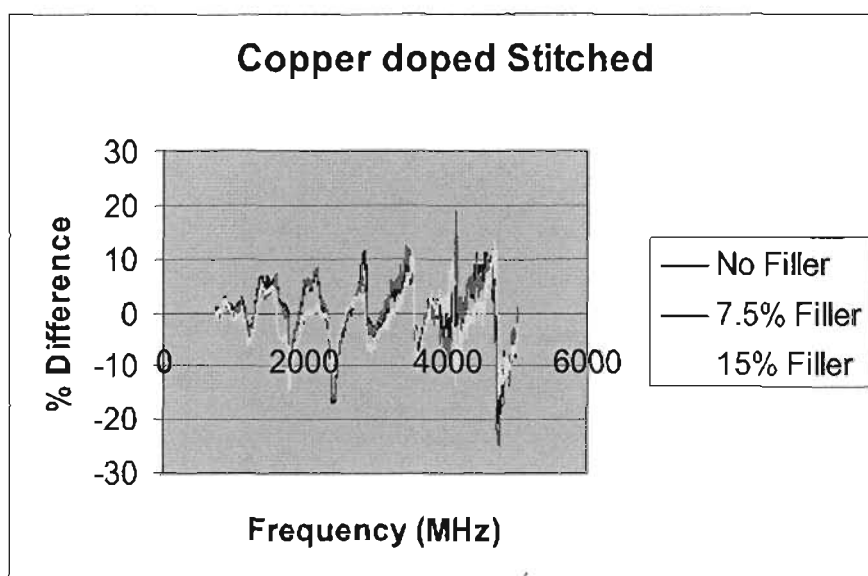
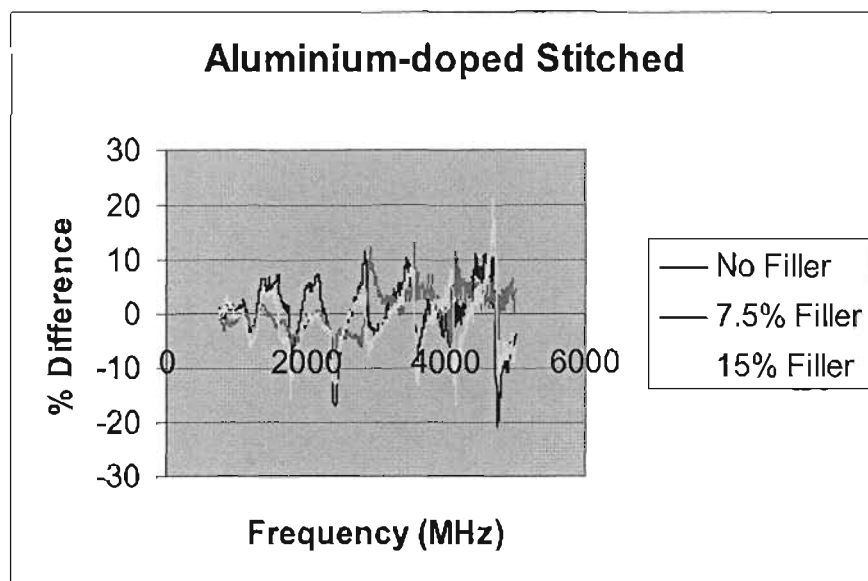


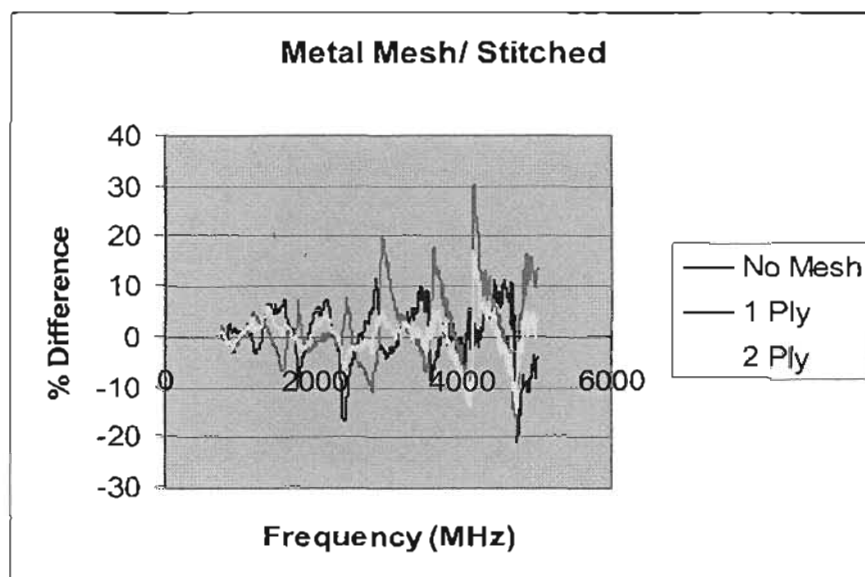
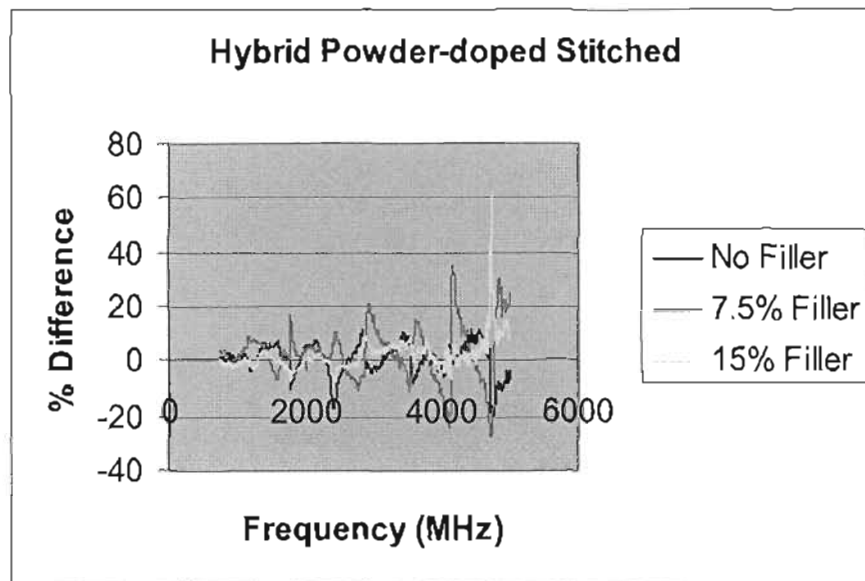
Figure G11: Failure due to crushing in other samples



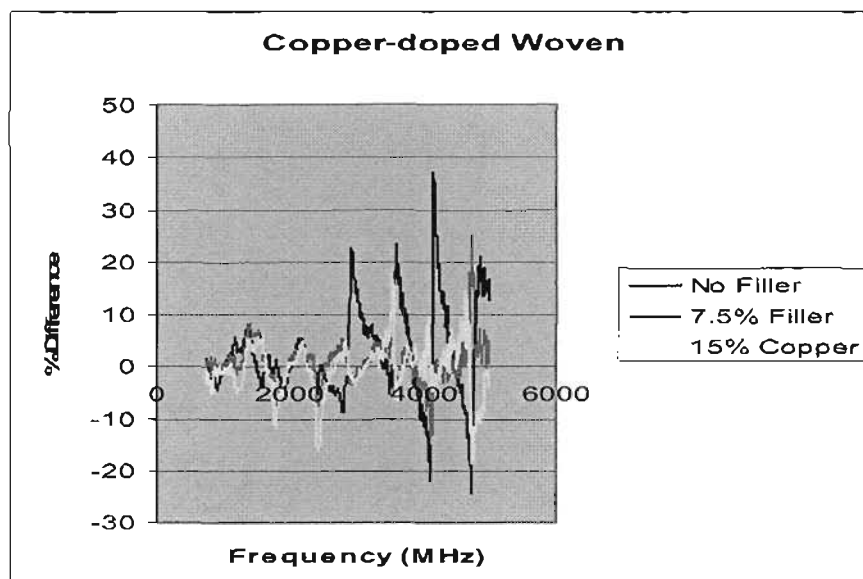
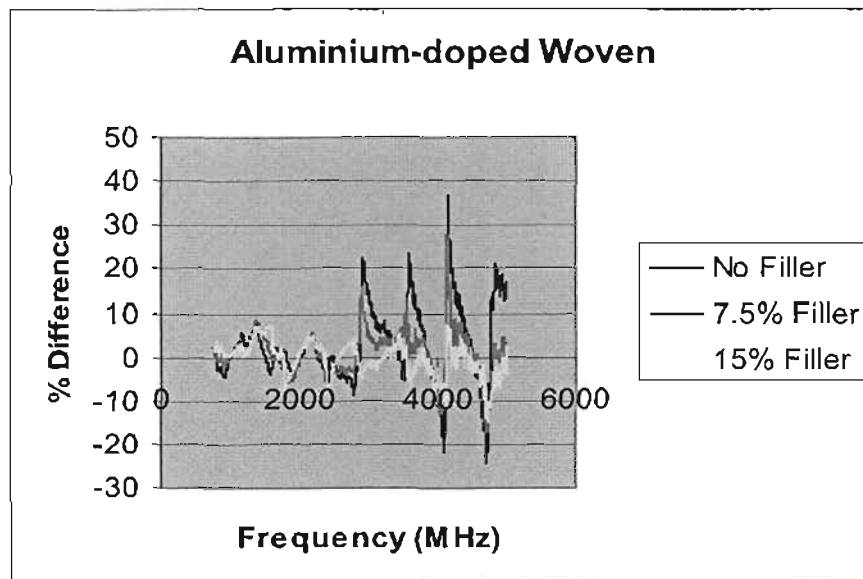
## **APPENDIX H: % DIFFERENCE IN SHIELDING RELATIVE TO ALUMINIUM ANALYTICAL DATA**

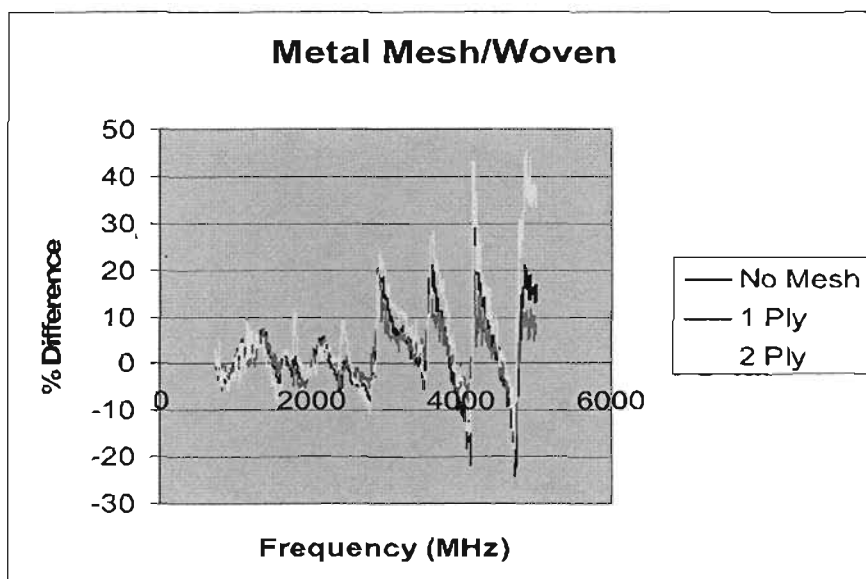
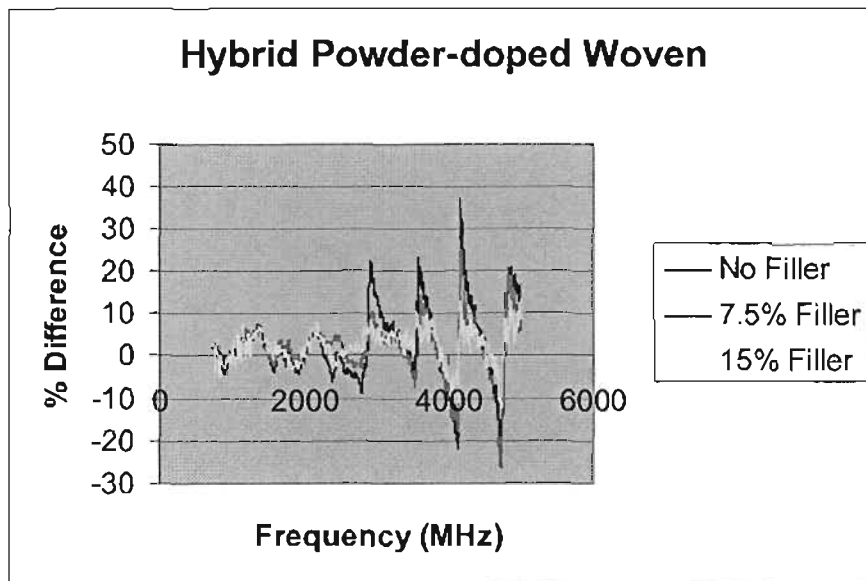
### **Stitched Carbon Specimens**



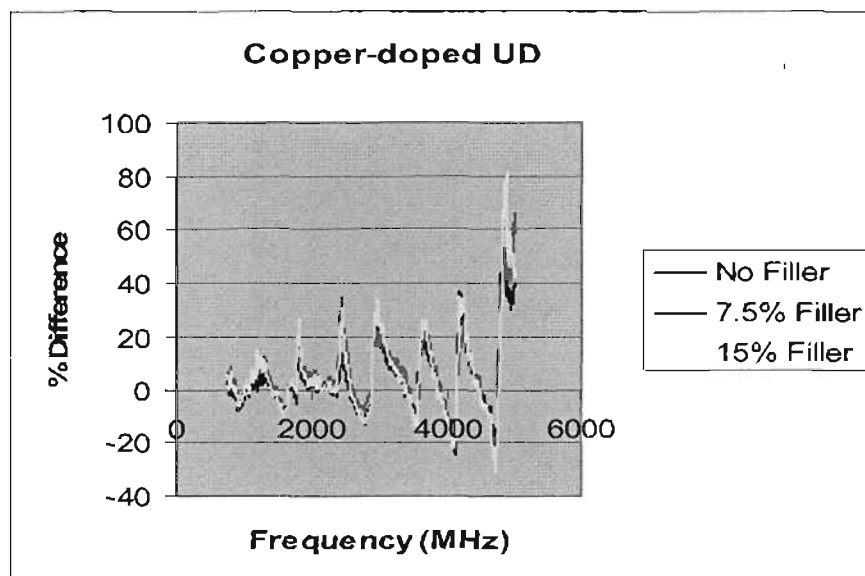
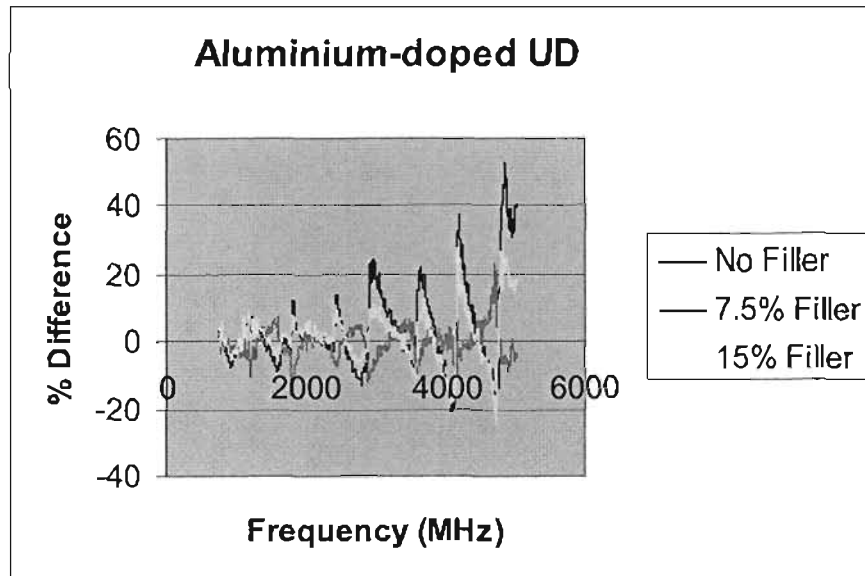


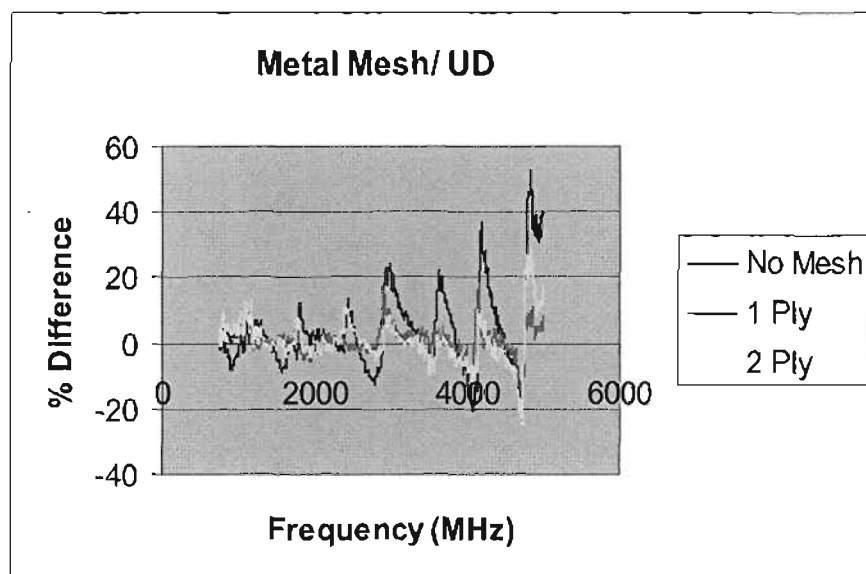
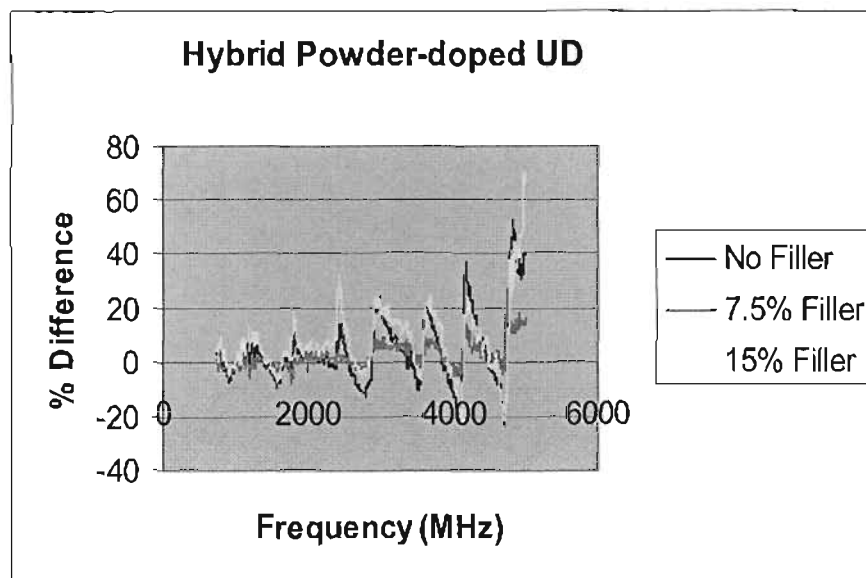
### Woven Carbon Specimens





### Unidirectional Carbon Specimens



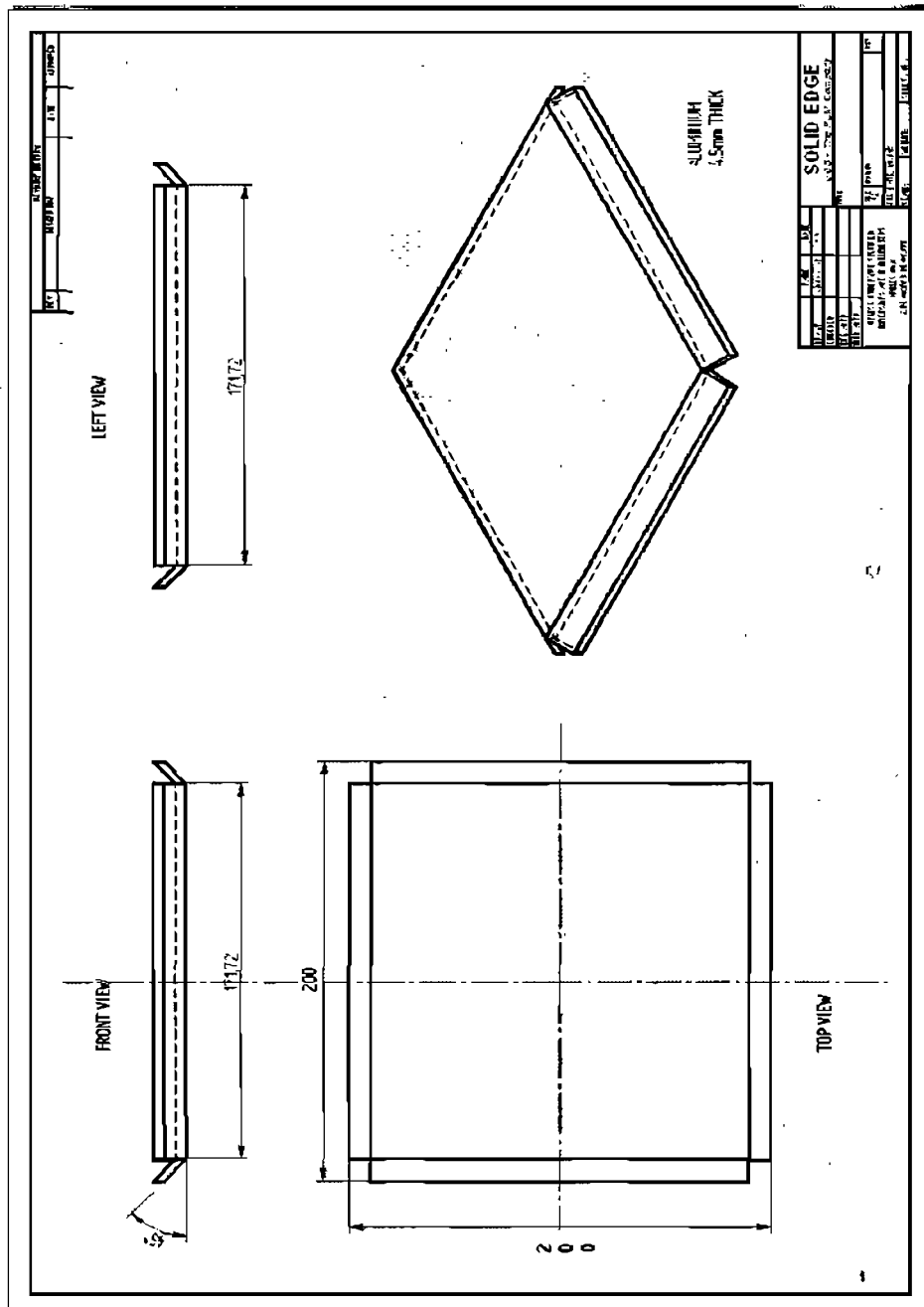


## APPENDIX I: COST ANALYSIS

<u>Material</u>	<u>Material Price</u>	<u>Resin Price</u>	<u>Hardener Price</u>	<u>Filler Price</u>	<u>Mesh Price</u>	<u>Glass Price</u>	<u>Total/300mm<sup>2</sup> Specimens</u>	<u>Total/m<sup>2</sup> Specimens</u>	<u>PRICE ALUMINIUM</u>	<u>Comparative Cost %</u>
Undoped Stitched CF	87.84	7.88	5.63				101.35	1126.06	277.78	-305.38
Undoped Woven CF	207.00	10.00	7.14				224.14	2490.40		-796.54
Undoped UD CF	163.80	10.47	7.48				181.75	2019.48		-627.01
7.5% Al Stitched	87.84	8.82	6.30	0.33			103.29	1147.64		-313.15
7.5% Al Woven	207.00	11.78	8.41	0.33			227.52	2528.00		-810.07
7.5% Al UD	163.80	11.79	8.42	0.33			184.34	2048.24		-637.36
7.5% Cu Stitched	87.84	9.44	6.75	0.47			104.50	1161.12		-318.00
7.5% Cu Woven	207.00	11.58	8.27	0.47			227.32	2525.78		-809.27
7.5% Cu UD	163.80	10.83	7.73	0.47			182.83	2031.49		-631.33
7.5% Hybrid Stitched	87.84	9.01	6.44	0.40			103.69	1152.09		-314.75
7.5% Hybrid Woven	207.00	11.69	8.35	0.40			227.45	2527.20		-809.79
7.5% Hybrid UD	163.80	11.46	8.19	0.40			183.85	2042.77		-635.39
15% Al Stitched	87.84	9.62	6.87	0.66			104.99	1166.51		-319.94
15% Al Woven	207.00	12.47	8.91	0.66			229.03	2544.83		-816.13
15% Al UD	163.80	11.91	8.51	0.66			184.88	2054.27		-639.53
15% Cu Stitched	87.84	10.21	7.29	0.95			106.29	1181.02		-325.16
15% Cu Woven	207.00	12.18	8.70	0.95			228.82	2542.43		-815.27
15% Cu UD	163.80	11.17	7.98	0.95			183.90	2043.35		-635.60
15% Hybrid Stitched	87.84	9.98	7.13	0.80			105.76	1175.10		-323.03
15% Hybrid Woven	207.00	11.90	8.50	0.80			228.19	2535.50		-812.77
15% Hybrid UD	163.80	11.48	8.20	0.80			184.28	2047.54		-637.11
1 Ply Stitched	87.84	9.26	6.61		82.80	3.96	190.47	2116.35		-661.88
1 Ply Woven	207.00	11.21	8.01		82.80	3.96	312.97	3477.49		-1151.89
1 Ply UD	163.80	10.76	7.69		82.80	3.96	269.01	2989.00		-976.03
2 Ply Stitched	87.84	9.66	6.90		165.60	3.96	273.96	3043.96		-995.82
2 Ply Woven	207.00	11.58	8.27		165.60	3.96	396.42	4404.63		-1485.66
2 Ply UD	163.80	10.96	7.83		165.60	3.96	352.14	3912.70		-1308.56

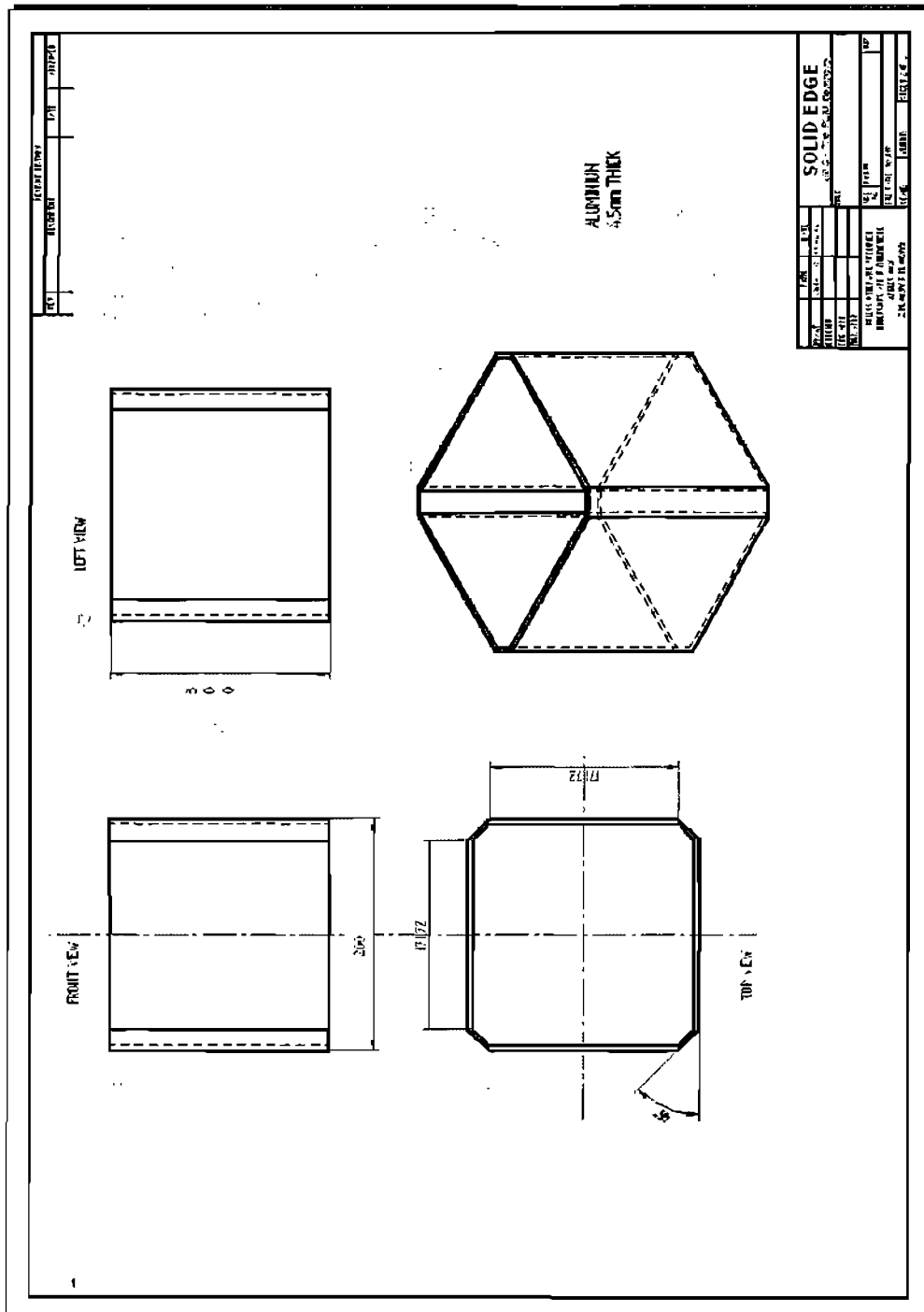
## **APPENDIX J: BOX DESIGNS**

**BOX BASE**



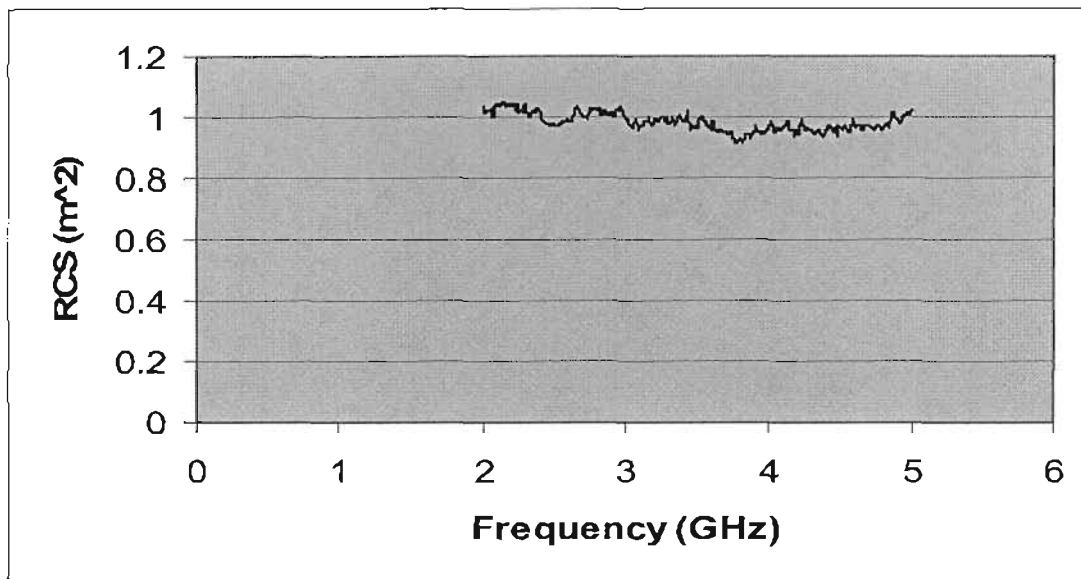


# **BOX SIDES**

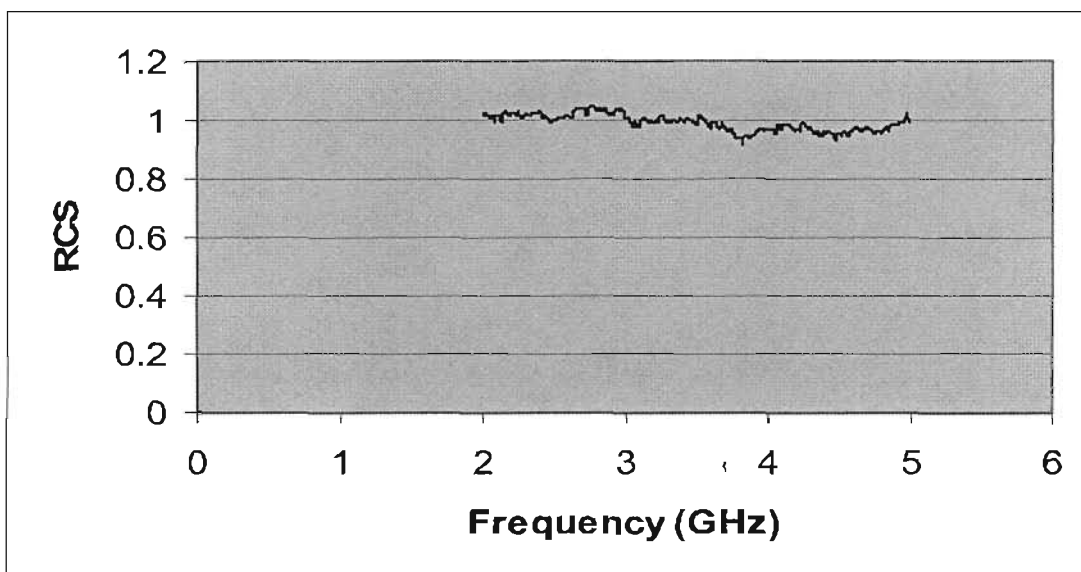


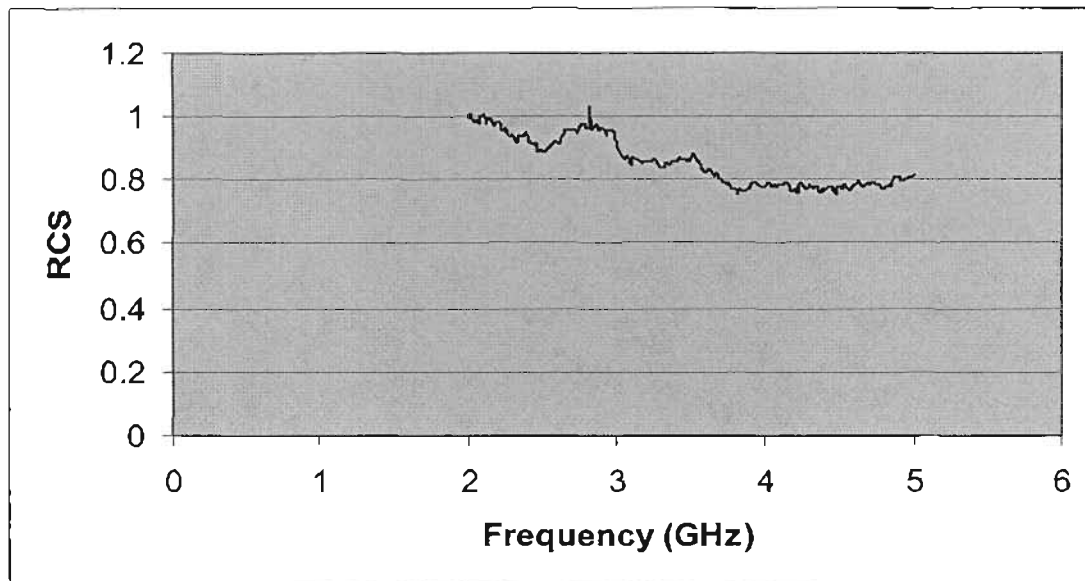
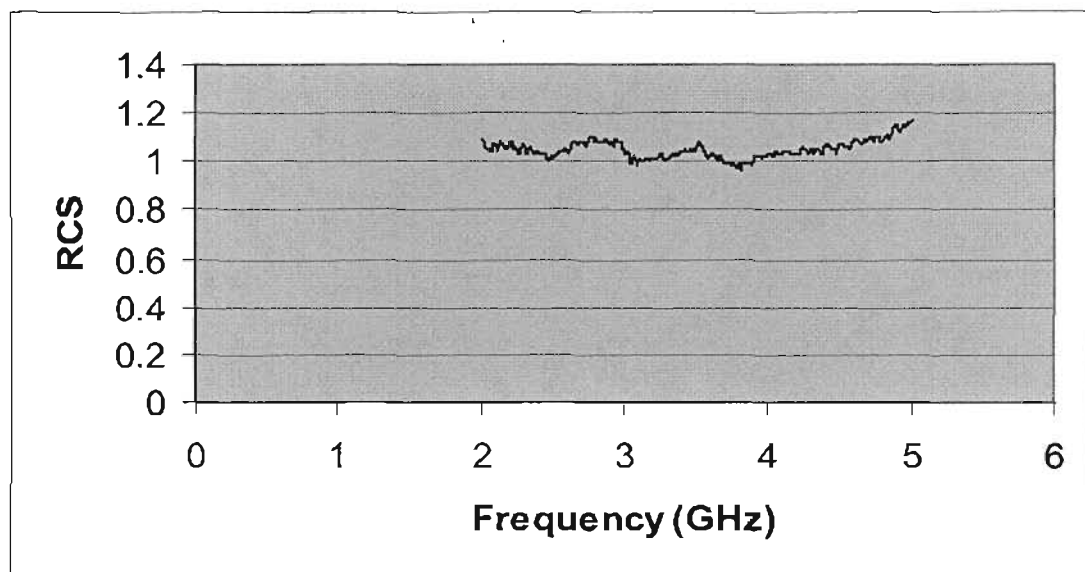
## APPENDIX K: RCS MEASUREMENT RESULTS

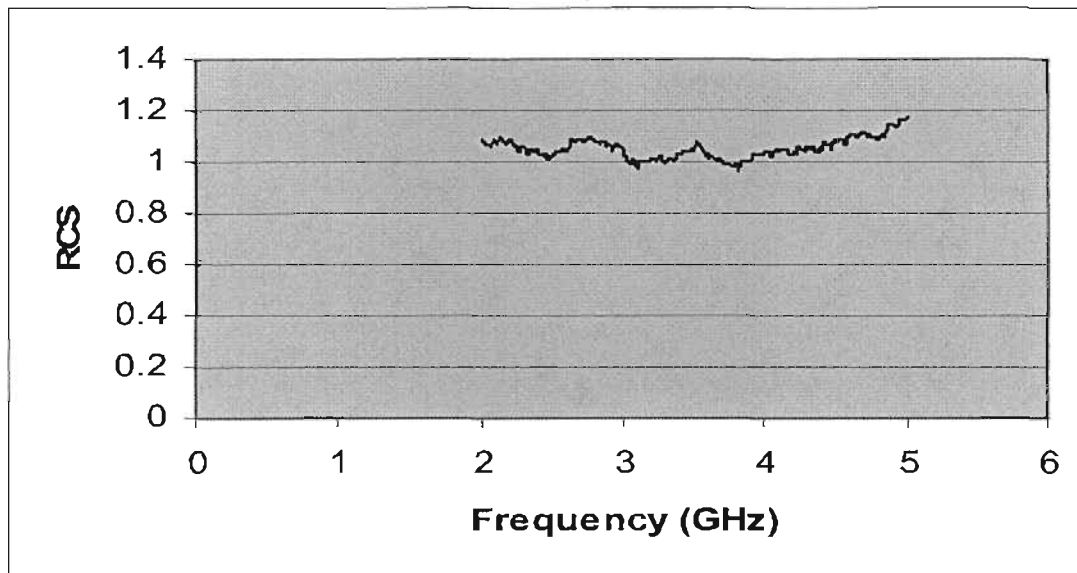
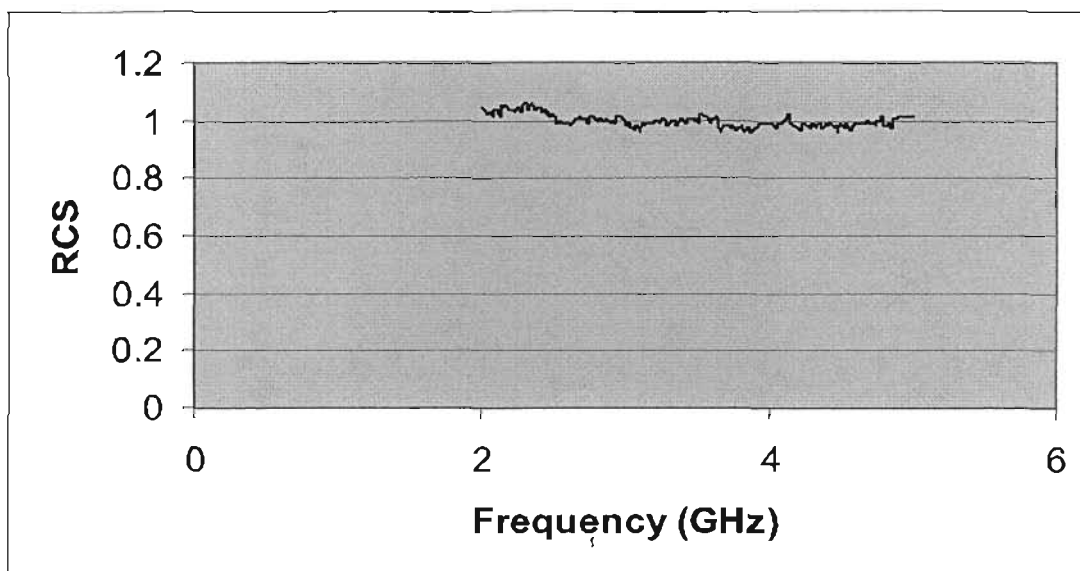
### **K1: Undoped Stitched Carbon Fibre Specimens:**

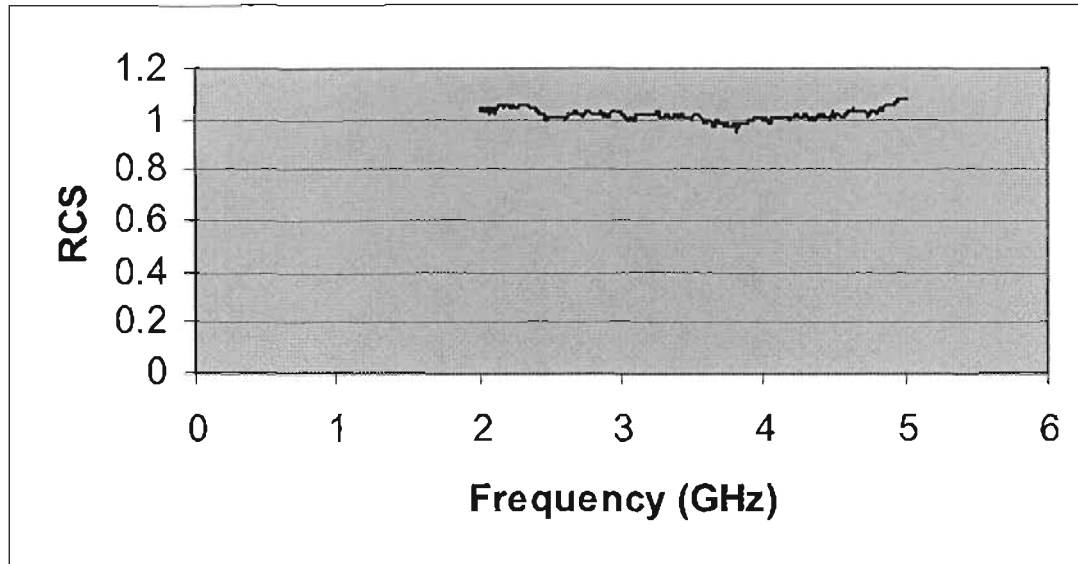
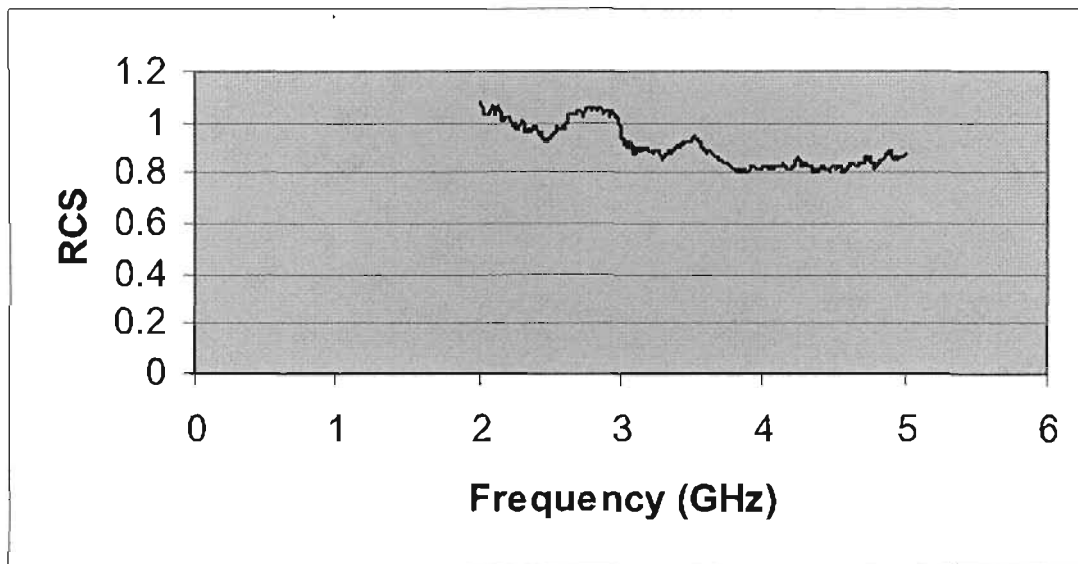


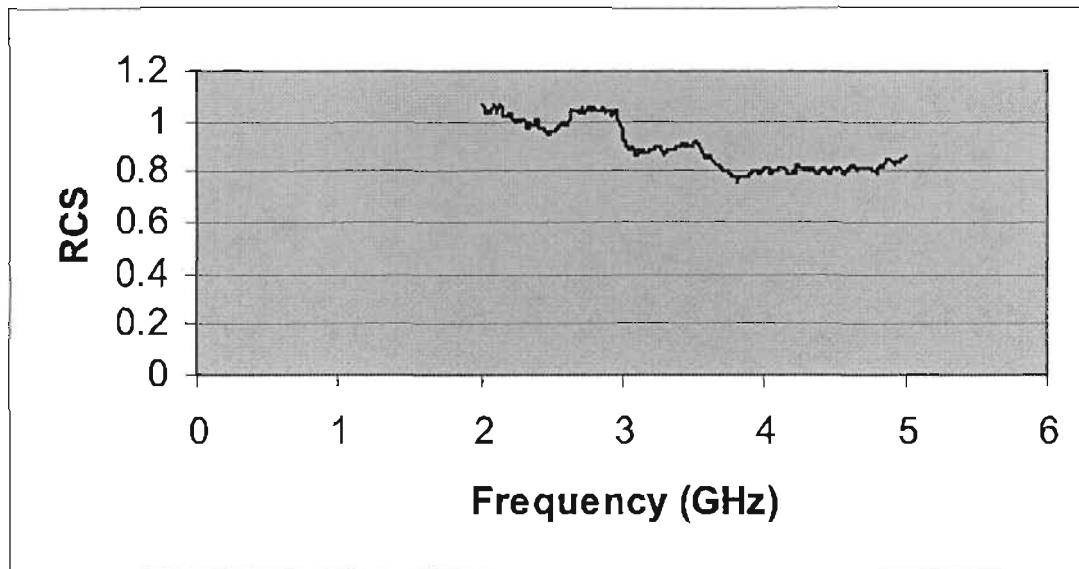
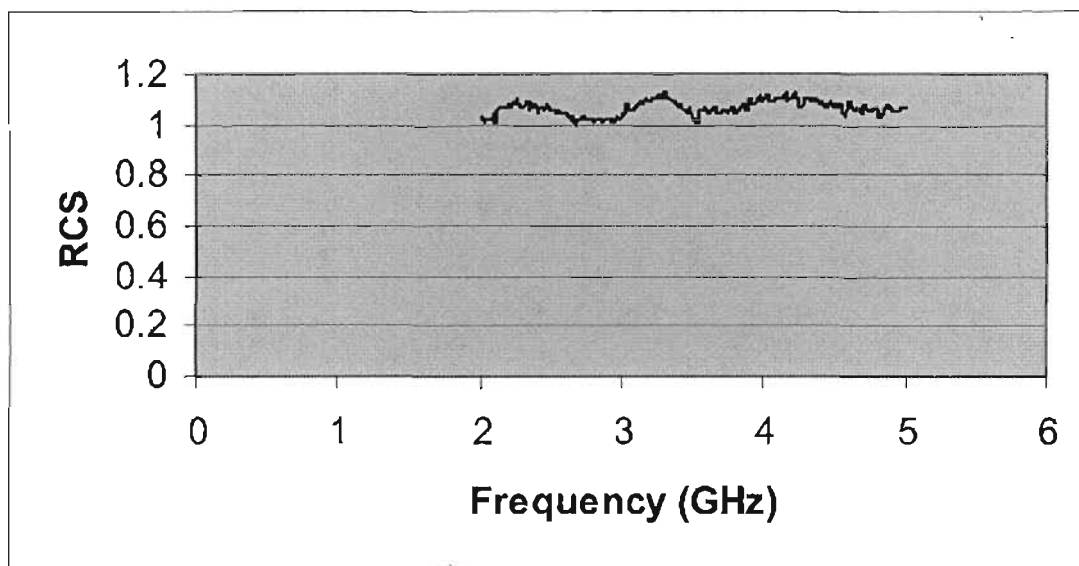
### **K2: 7.5% Aluminium-doped Stitched Carbon Fibre Specimens:**

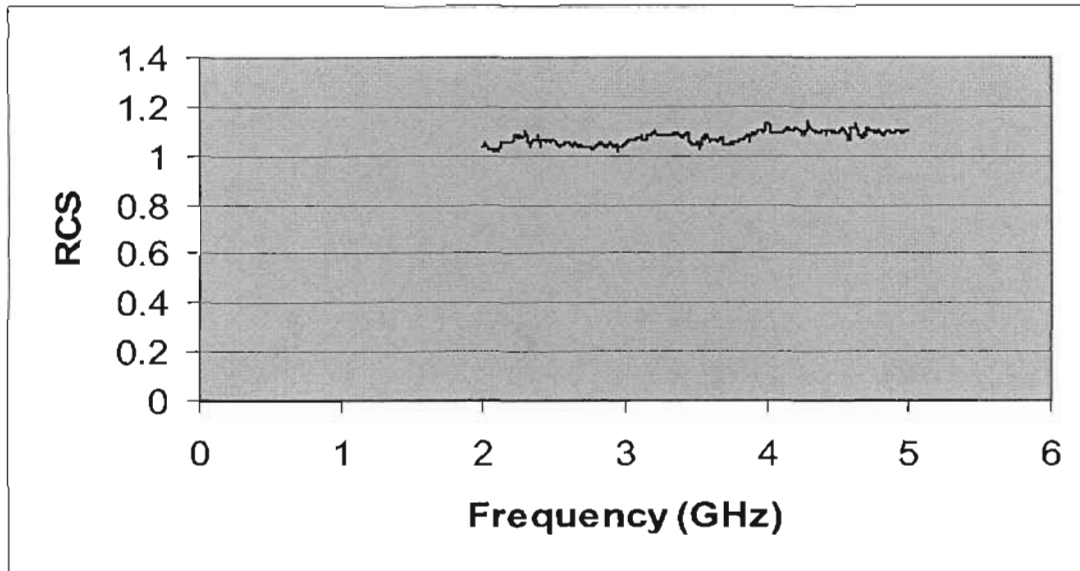
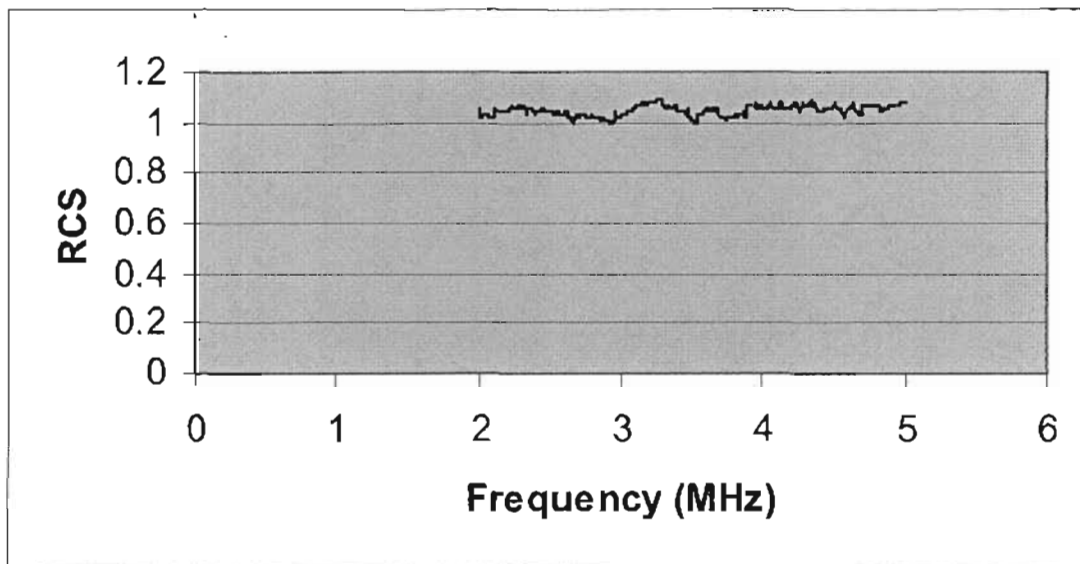


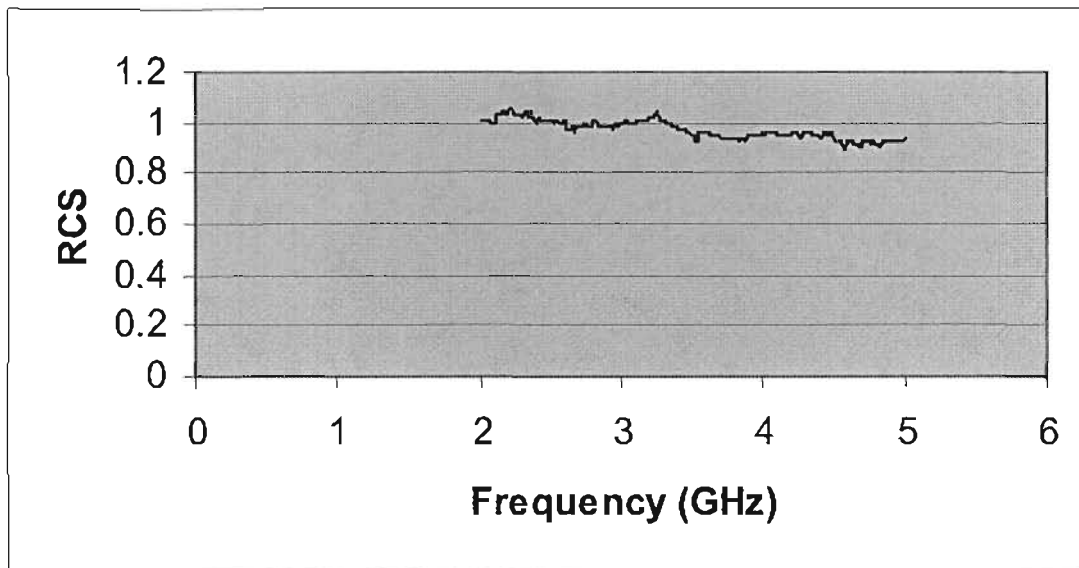
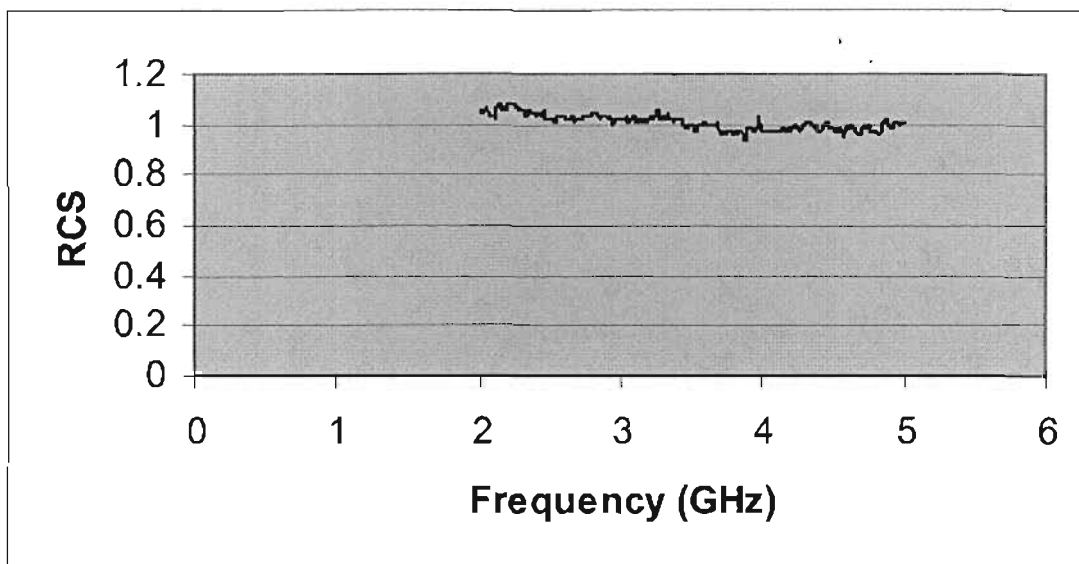
**K3: 15% Aluminium-doped Stitched Carbon Fibre Specimens:****K4: 7.5% Copper-doped Aluminium Stitched Carbon Fibre Specimens:**

**K5: 15% Copper-doped Stitched Carbon Fibre Specimens:****K6 7.5% Hybrid Powder-doped Stitched Carbon Fibre Specimens:**

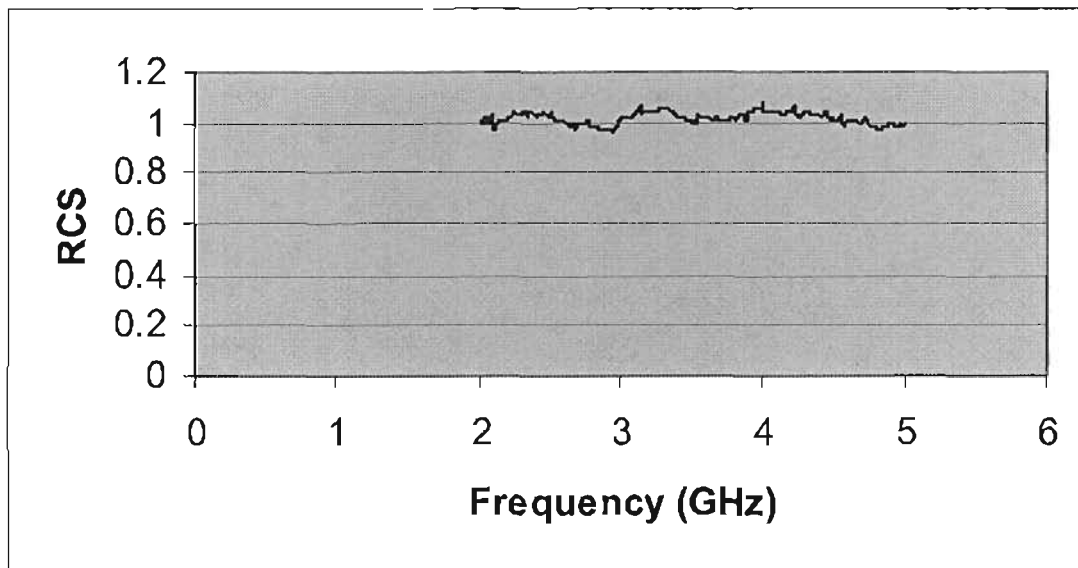
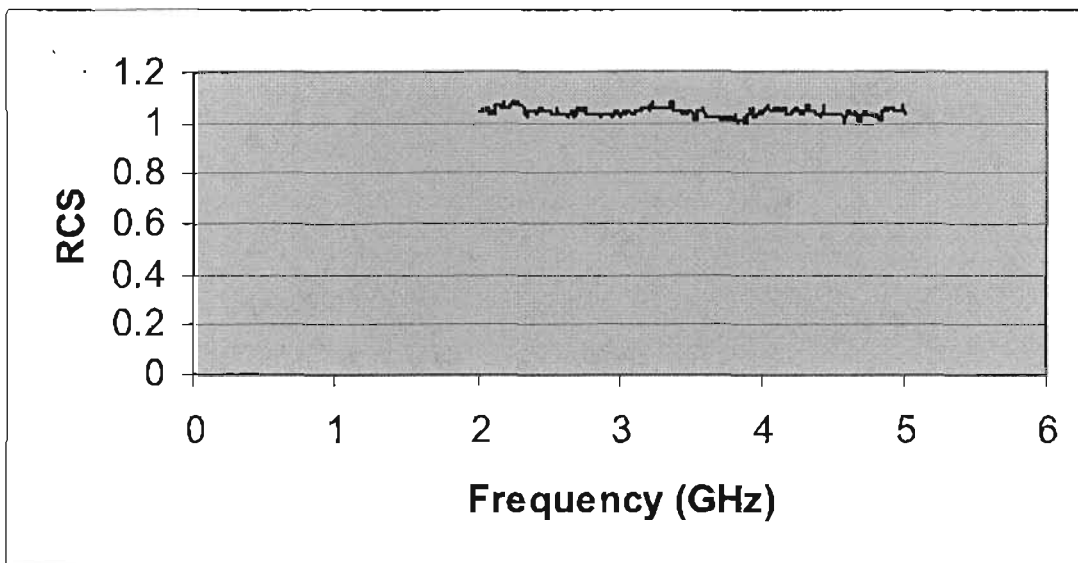
**K7: 15% Hybrid powder-doped Stitched Carbon Fibre Specimens:****K8: 1 Ply Mesh/Stitched Carbon Fibre Specimens:**

**K9: 2 Ply/Mesh Stitched Carbon Fibre Specimens:****K10: Undoped Woven Carbon Fibre Specimens:**

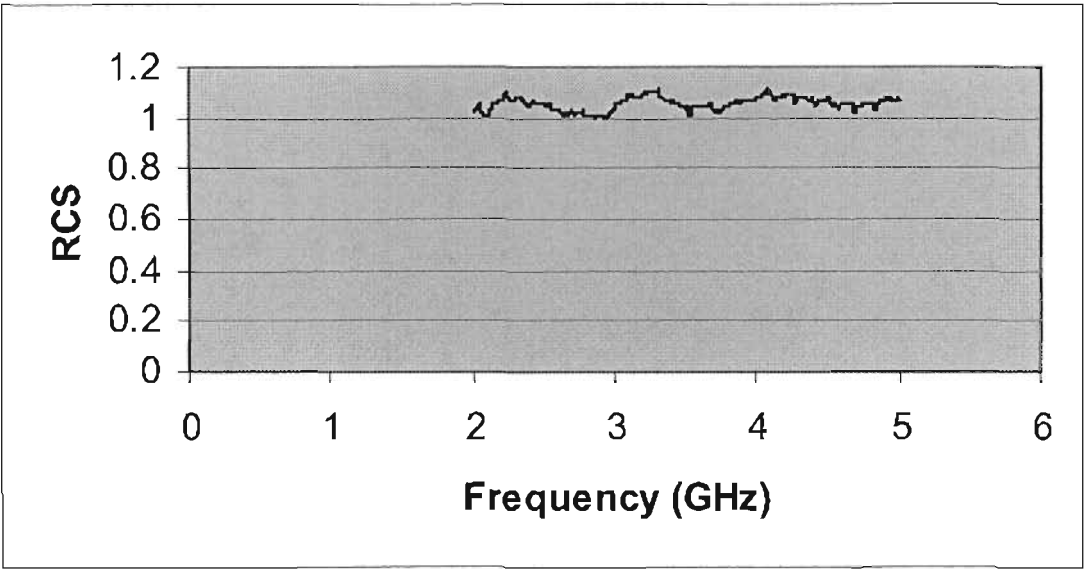
**K11: 7.5% Aluminium-doped Woven Carbon Specimens:****K12: 15% Aluminium-doped Woven Carbon Specimens:**

**K13: 7.5% Copper-doped Woven Carbon Specimens:****K14: 15% Copper-doped Woven Carbon Specimens:**

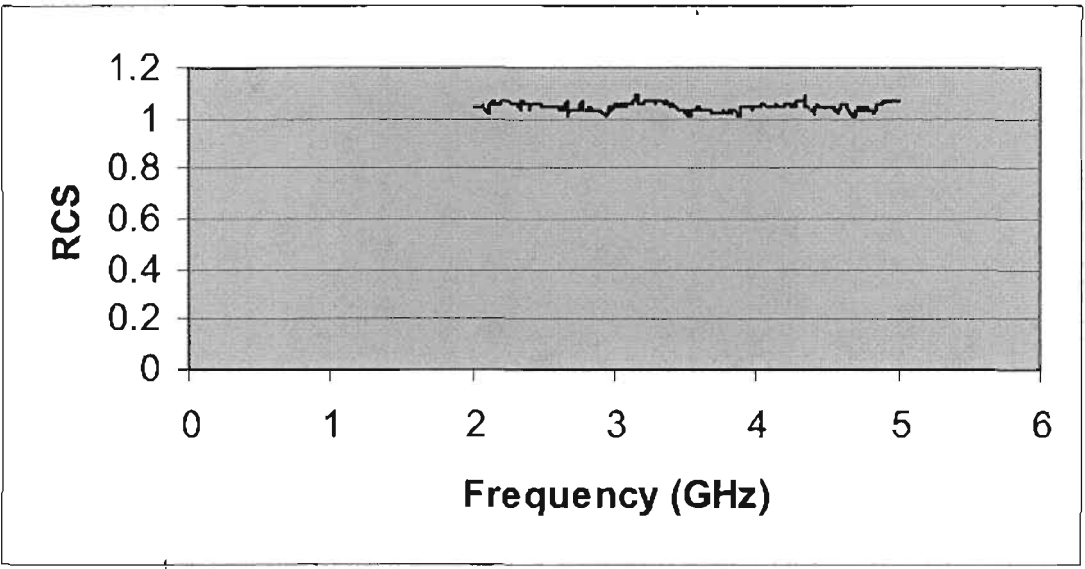


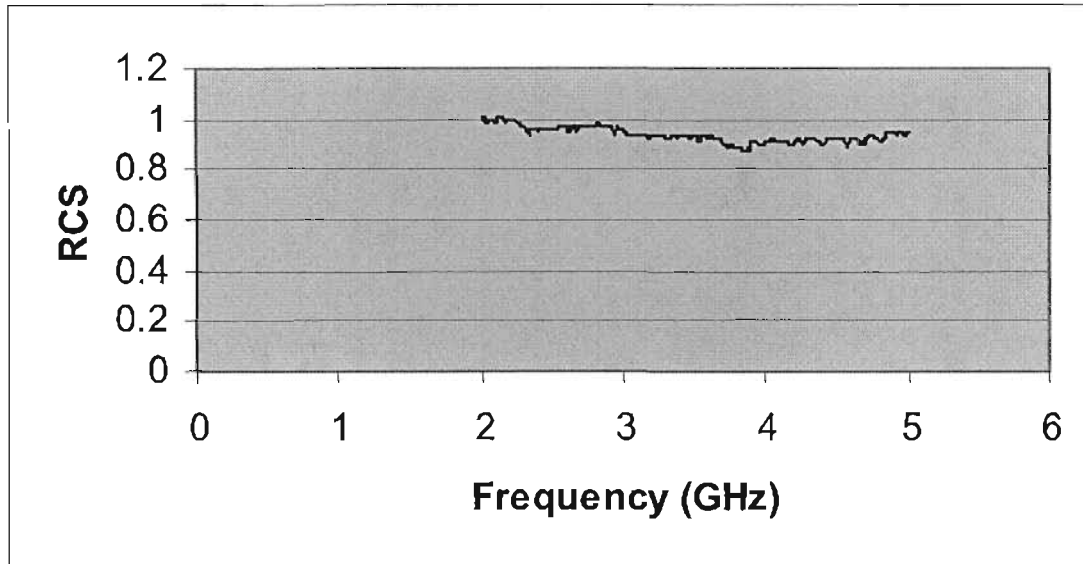
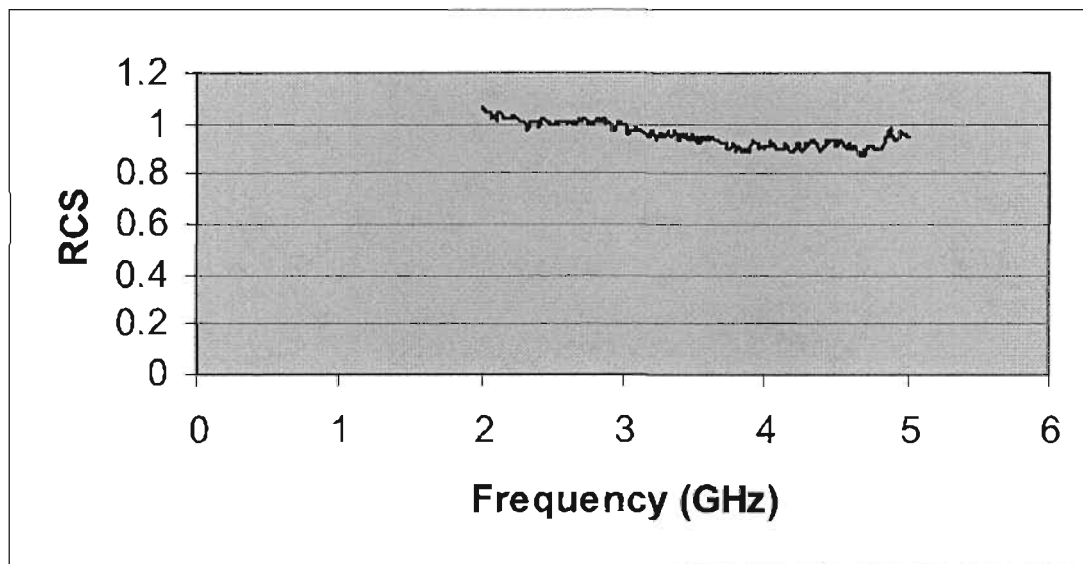
**K15: 7.5% Hybrid powder-doped Woven Carbon Specimens:****K16: 15% Hybrid Powder-doped Woven Carbon Specimens:**

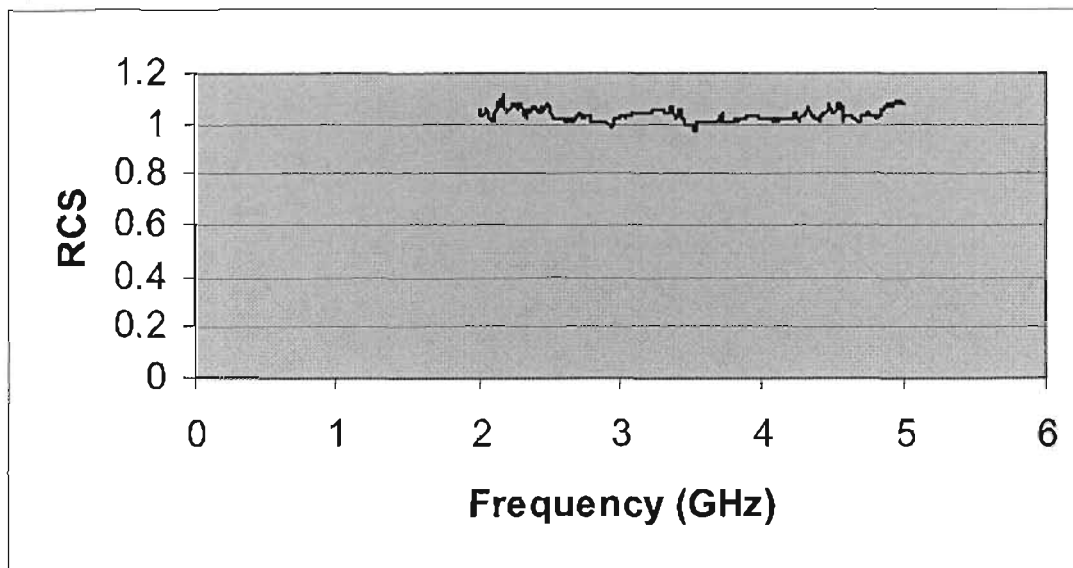
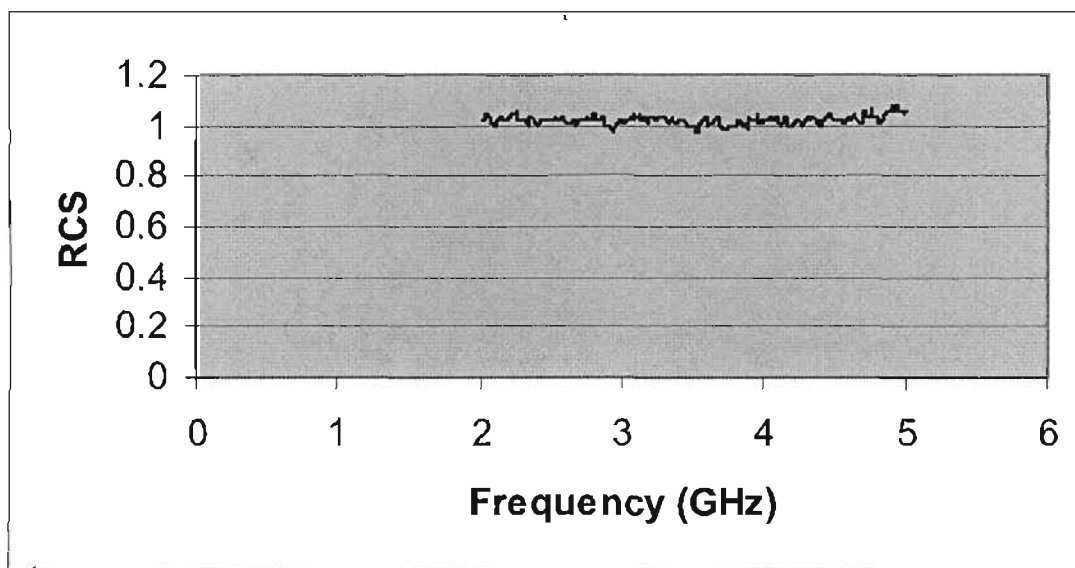
**K17: 1 Ply Mesh/Woven Carbon Specimens:**

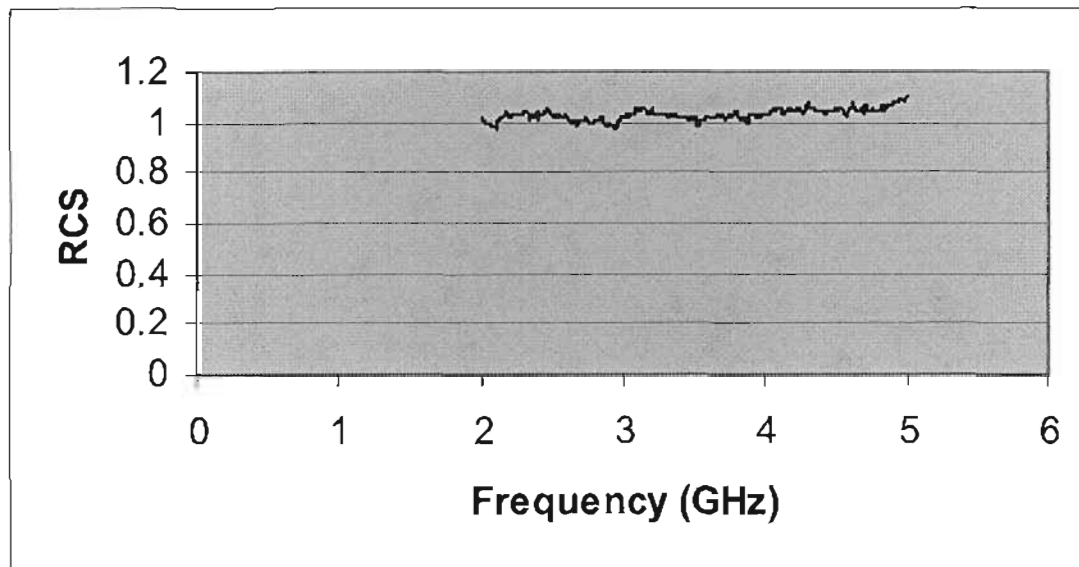
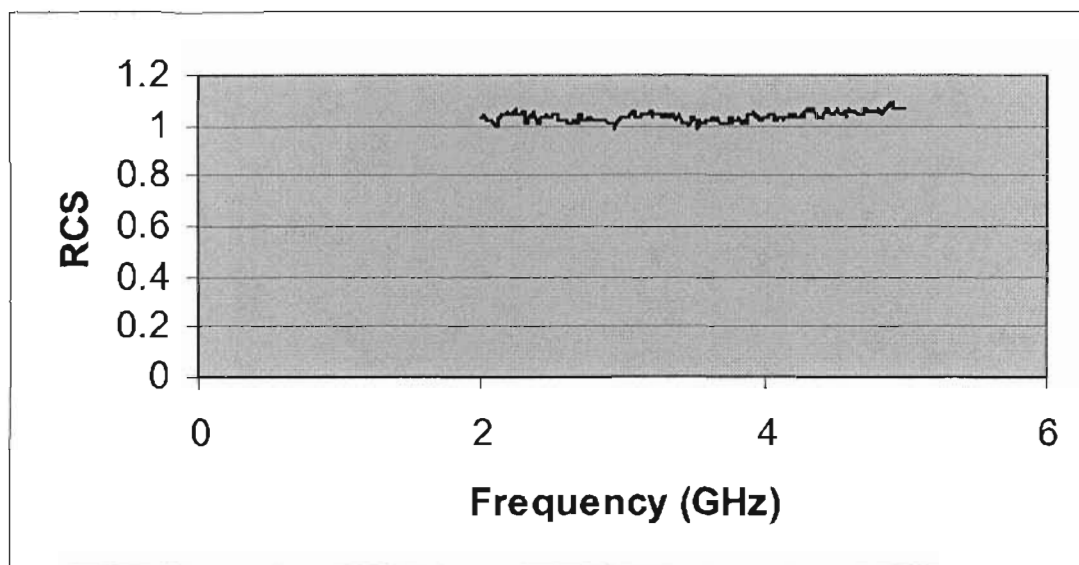


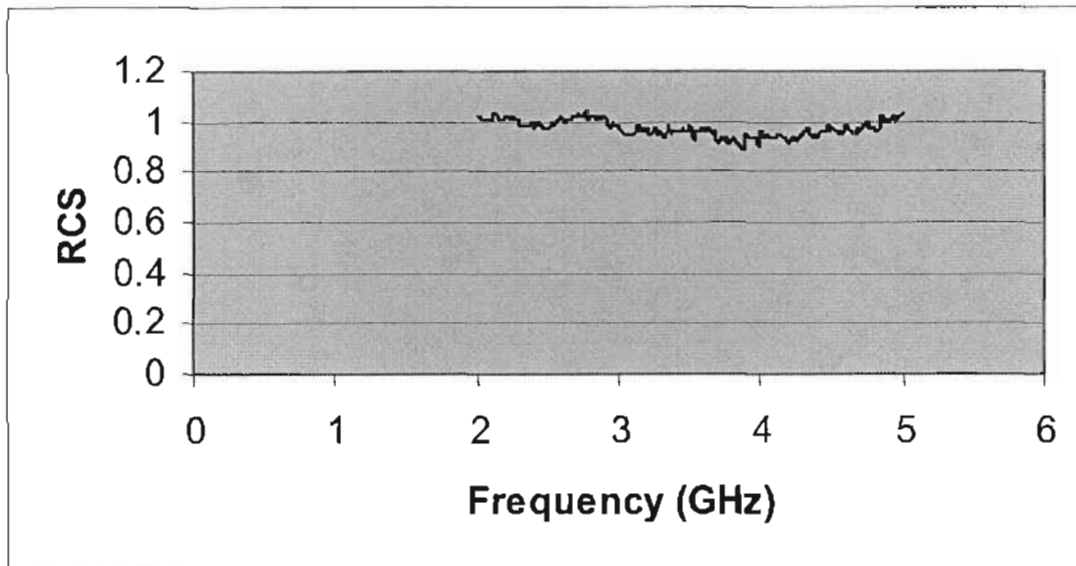
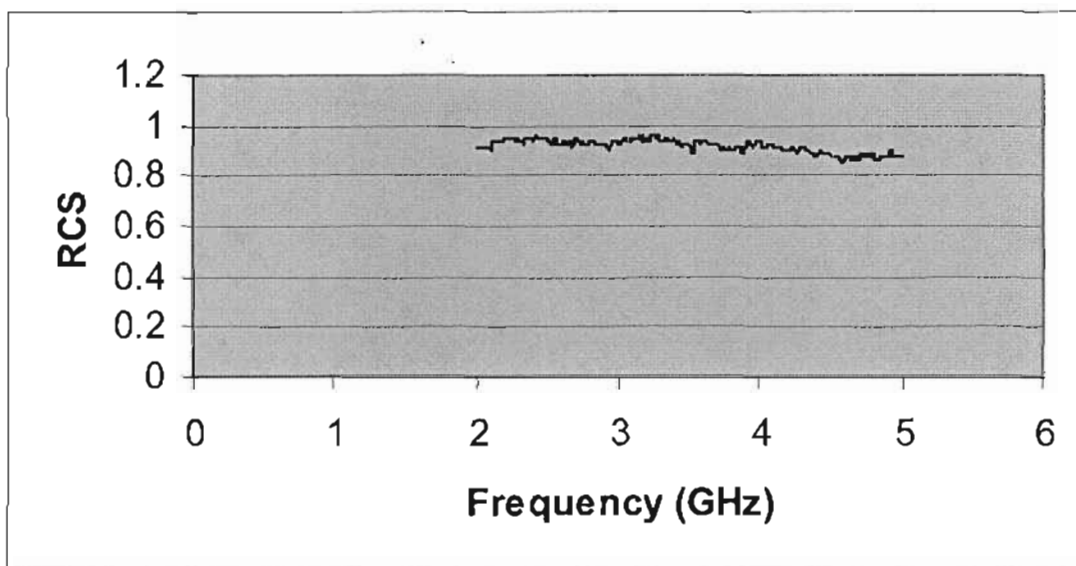
**K18: 2 Ply Mesh/Woven Carbon Specimens:**

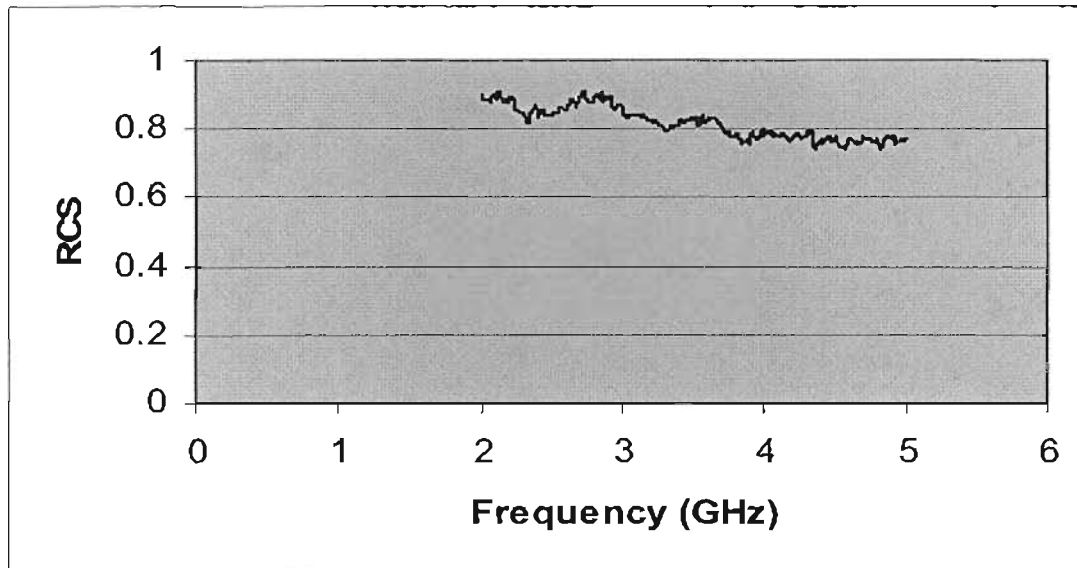


**K19: Undoped Unidirectional Carbon Specimens:****K20: 7.5% Aluminium-doped Unidirectional Carbon Specimens:**

**K21: 15% Aluminium-doped Unidirectional Carbon Specimens:****K22: 7.5% Copper-doped Unidirectional Specimens:**

**K23: 15% Copper-doped Unidirectional Specimens:****K24: 7.5% Hybrid Powder-doped Unidirectional Specimens:**

**K25: 15% Hybrid Powder-doped Unidirectional Specimens:****K26: 1 Ply Mesh/Unidirectional Carbon Specimens:**

**K27: 2 Ply Mesh/ Unidirectional Specimens:**

## **APPENDIX L: Technical Papers**

### **L1: Composites Africa 2006 – Conference Proceedings (17-18 May 2006)**

#### **NEW ELECTROMAGNETIC SHIELDING MATERIALS FOR USE IN THE AEROSPACE INDUSTRY**

**Maharaj D.**<sup>\*</sup>, von Klemperer, C. J. and Sookay, N. K.

School of Mechanical Engineering, University of KwaZulu-Natal,  
Durban, 4041, South Africa

<sup>\*</sup>Corresponding author: Tel +27 31 260 1225 Fax +27 31 260 3217  
E-mail [maharajd2@ukzn.ac.za](mailto:maharajd2@ukzn.ac.za)

#### **ABSTRACT**

Damage caused by electromagnetic interference (EMI) on aerospace vehicles can be catastrophic. Phenomena that fall under the broad EMI definition include the indirect effects of lightning strike, precipitation static (p-static) and electrostatic discharge (ESD). In addition to this, military aircraft also face the additional threat of attack from opposing vehicles. Despite the apparent threat that EMI presents, there has been little new development in the field since the early 1990's [1]. In many aircraft, metals serve as shielding materials, but there are many disadvantages such as weight and cost associated with these materials [2]. The study undertaken involves the research of improved composite alternatives that will be adequate for the purpose of EMI shielding.

#### **1. INTRODUCTION**

Prior to the 1980's, aircraft were manufactured predominantly from metals, most notably steel and aluminium alloys [3]. Due to the inherent strength and electrical conductivity these materials possess, it was deemed sufficient protection against the effects of lightning strike. However, investigation of air disasters at that time found that lightning was the most probable cause of fuel tank explosions [4]. For some time thereafter, this was thought to be the only effect of lightning that required attention.

The 1980's saw demand for high performance aircraft grow at a phenomenal rate [3]. This consequently led to a demand for new materials in the aerospace industry. This led to research of fibre composite materials as possible substitute materials for orthodox metals that were being used. The benefits that composites provide, such as weight reduction and corrosion resistance, made the substitution seem likely. However, there were obstacles preventing this at the time, such as high costs and inadequate information on composite materials.



The 1990's saw a drastic increase in production of sensitive electronic equipment and an increase in electronic control (fly-by-wire) systems in airborne vehicles [1, 5]. In terms of global composite advancement in the aerospace industry, the military have accepted much of the financial expense, as well as the associated risks with developing the new technologies [6]. Coupled with the increasing use of composite materials, there is now a need for more effective electromagnetic interference (EMI) shielding structures in aircraft.

However, despite the apparent threat EMI presents, there has been little advancement in EMI shielding made in the last decade [1]. This is possibly due to EMI shielding providing no value other than protection to the devices they shield. This has been fast changing in recent years, and further demand for improved shielding options is expected to increase drastically in the next few years [1].

## **2. ELECTROMAGNETIC WAVE THEORY**

Before reviewing material selection, an understanding of the fundamental concepts behind lightning strike and EMI protection is required. The term 'electromagnetism' refers to the interaction between electric (E) and magnetic (H) field strengths. This phenomenon is best described by 'Maxwell's equations'. It is well understood that these equations form the basis of fundamental electromagnetic theory.

$$\oint \vec{E} \cdot d\vec{A} = \frac{Q_{encl}}{\epsilon_0} \quad \text{(Gauss's law for Electricity)} \quad (1) \quad [7]$$

$$\oint \vec{B} \cdot d\vec{A} = 0 \quad \text{(Gauss's law for Magnetism)} \quad (2) \quad [7]$$

$$\oint \vec{B} \cdot d\vec{l} = \mu_0 \left( i_c + \epsilon_0 \frac{d\Phi_E}{dt} \right)_{encl} \quad \text{(Ampere's law)} \quad (3) \quad [7]$$

$$\oint \vec{E} \cdot d\vec{l} = -\frac{d\Phi_B}{dt} \quad \text{(Faraday's law)} \quad (4) \quad [7]$$

Faraday's law of electromagnetic induction shows that a changing magnetic flux or magnetic field causes an electromotive force (emf). An emf is defined as the influence that causes a current to travel from a lower to higher potential. The current that results from the induced emf is referred to the induced current:

$$\mathcal{E} = -\frac{d\Phi_B}{dt} \quad \text{Faraday's Law of Electromagnetic Induction} \quad (5) \quad [7]$$

Electromagnetic waves (or electromagnetic radiation) consist of these two fields. The fields travel perpendicularly to each other and at right angles to the plane containing them.

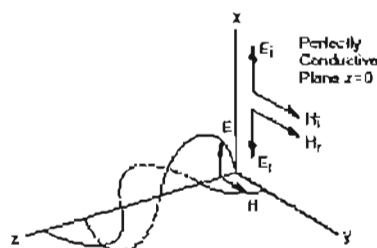


Figure 1: The orientation of E and H fields in a perfect conductor [8]

The relative size between the E and H field depend on the generating source of the wave, and the distance of the wave from the source. The ratio between E and H is referred to as wave impedance, denoted by  $Z_w$ . This relationship is described in the figure below:

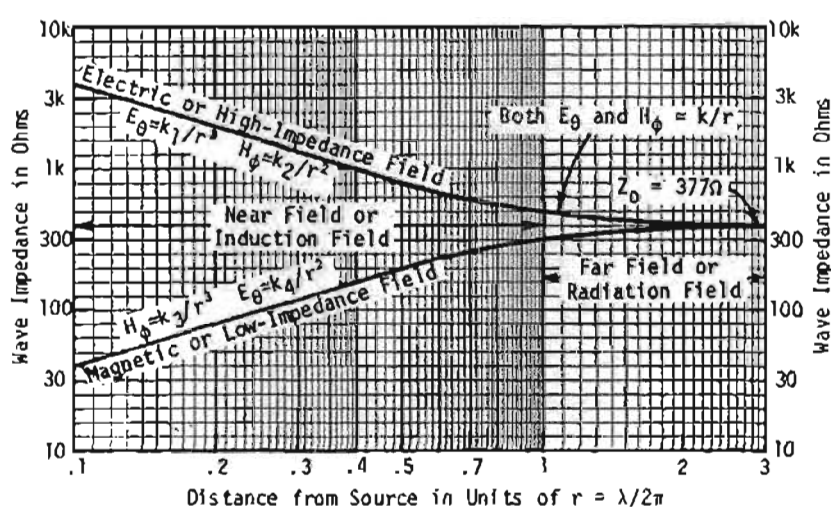


Figure 2: Wave Impedance as a Function of Source Distance [9]

In airborne vehicles, sources of electromagnetic waves include lightning strike, direct electric/magnetic field coupling “AC Hum”, electrostatic discharge (ESD) and external sources of radiated emissions. The effects of EMI range from minor radio static, to a complete shut-down of on-board avionics [10].

Despite the current induced, shielding materials need not necessarily display high electrical conductivity [11]. However, in addition to EMI, the EMI shields on aircraft must also withstand the direct effects of a lightning strike. Lightning strikes can contain current exceeding 200kA. As expected, there will be a drastic increase in temperature at the location of the current strike. Due to the cumulative effects of EMI and direct lightning strike, the shielding material should also display excellent electrical and thermal conduction.

### 3. ELECTROMAGNETIC SHIELDING MECHANISMS

In order for electromagnetic disturbances to occur, there needs to be a source, a coupling path, and victim. The basis for EMI shielding comes from a structure referred to as a Faraday cage. This structure, which contains a conductive outer layer, provides fundamental protection for electronic equipment that is to be protected from electric

fields. The external electric field of the structure redistributes electrons such that the total electric field within the enclosure is zero [7]. In real terms, the Faraday cage effect can be seen in a typical automobile – it is long understood that one of the safest places to be in the event of lightning strike is inside an automobile.

The primary mechanism for shielding in these structures is reflection. Reflection relies on mobile charge carriers, such as electrons, being present within the material. It is therefore essential that the material be conductive. Reflection loss is a function of  $\frac{\sigma_r}{\mu_r}$ , and reflection loss decreases with increasing frequency [2, 11]. ( $\sigma_r$  refers to the conductivity of a material relative to copper, and  $\mu_r$  refers to the permeability of a material relative to copper.)

The secondary mechanism for shielding is absorption. Significant absorption of the waves by the shield requires electric and/or magnetic dipoles within the shield material. Absorption loss is a function of  $\sigma_r \mu_r$ , and absorption increases with increasing frequency. Absorption loss is proportional to shield thickness [2, 11]. As expected, shield thickness is only a factor when dealing with low frequencies. At high frequencies, even metal foils can be effective shields when considering skin depth [8].

The third mechanism for shielding is multiple reflections. Multiple wave reflections take place at surfaces or interfaces within the shield. This mechanism requires the presence of large surface areas or interfaces within the shield [2, 11]. Electromagnetic waves can interact with a surface in a combination of following mechanisms:

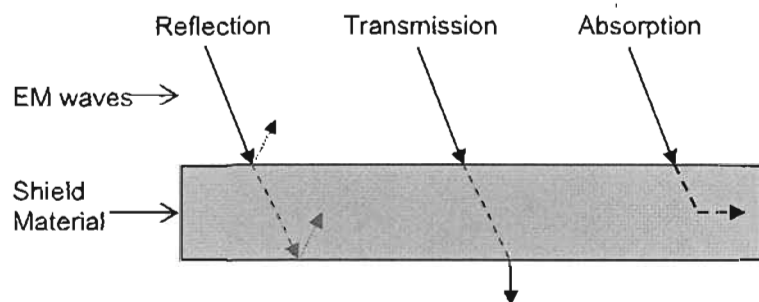


Figure 3: Electromagnetic waves can interact with a surface in a combination of the described mechanisms

It is apparent that the shielding material displays a high degree of conductivity, not only to promote conduction of the lightning current, but also to ensure that reflection is the primary shielding mechanism. Magnetic materials will promote absorption as the primary shielding mechanism. It is imperative that the shield material prevents transmission of the wave into the enclosure.

The industry-favoured approach to determine the degree of shielding is referred to as the 'field theory method'. This method relies on a form of Maxwell's equations to compute a variable referred to as electromagnetic shielding effectiveness (EMSE) which is the degree

of shielding of the material in units of decibel (dB) [9]. The final variable, EMSE is obtained from the following equation:

$$EMSE_{dB} = 10 \log_{10} \left( \frac{P_i}{P_t} \right) \quad (6) \quad [9, 12]$$

Here,  $P_i$  and  $P_t$  refers to the power of the incident and transmitted waves respectively. When the plan wave is incident upon the shielding material, the mechanisms viz. reflection, absorption and multiple reflections are observed. EMSE may be written in terms of these mechanisms:

$$SE_{dB} = SE_R + SE_A + SE_M \quad (7) \quad [2, 13]$$

Where  $SE_R$ ,  $SE_A$  and  $SE_M$  refer to shielding effectiveness associated with reflection, absorption and multiple reflections respectively. It will be imperative for aircraft shielding material to contain a large reflection loss. This will ensure that reflection is the primary shielding mechanism, and will thus promote conduction.

EMI shields do not follow generic designs in the sense that they are specific for the environment in which aircraft operates in. To protect the interests of a nation, the high intensity radiated field (HIRF) environment is usually deemed classified by local government. However, it has been suggested that a good design is one that encompasses the entire electromagnetic spectrum [11].

#### **4. COMPOSITE EMI SHIELDING MATERIALS**

The phenomena causing EMI has been established. It is apparent that materials which display electrical and thermal conductivity be used for external aircraft structures. These materials provide an adequate channel for current flow and promote reflection of electromagnetic waves. A study on the properties of various materials is now required, to establish a benchmark for the design process.

##### **4.1 Materials**

Carbon fibre is long understood as being one of the few conductive reinforcement fabrics available. For this reason, military aircraft, such as the Harrier AV-8B/GR5, began to include carbon fibre epoxy composites in their designs during the 1980's. Extensive studies were undertaken on the material to ensure they displayed adequate EMI shielding. Results obtained indicated that this material contained inherent shielding properties similar to that of the metals that were typically used [14]. Specifically, the pitch-based carbon fibre type has a suitably low electrical resistivity, making it an excellent choice for EMI shielding structures [15, 16]. The following table outlines some of the advantages and disadvantages associated with carbon fibre in aircraft designs:

**Table 1: A comparison between the advantages and disadvantages of using carbon fibre in aircraft (circa 1990) [Amended from 15]**

Advantages	Disadvantages
1. Weight saving over aluminium alloys through high specific stiffness and specific strengths	1. Susceptibility to operational damage and Impact
2. Tailored directional mechanical properties	2. Restricted environmental stability in terms of temperature and moisture absorbency
3. Reduced part counter over metallic equivalents	3. Excessive localised damage though lightning strikes
4. Modified radar response compared to metals	4. Uncertainties on repair techniques
5. Non-corroding in salt environments	5. Cost
6. Excellent fatigue resistance	
7. Dimensional stability	

Table 1 provides some insight into the benefits and limitations of carbon fibre. However, development over the last decade has resulted in improvements in some limitations such as cost reduction and new repair techniques.

The Beechcraft Starship, which is widely regarded as being the world's first all-composite production aircraft, utilised carbon fibre in its airframe. The studies performed on this aircraft displayed that carbon fibre epoxy is approximately 1000 times more resistive than aluminium [17]. The resistance required to adequately provide a channel for lightning current flow is less than  $1\Omega$  [17, 18]. It is unlikely that carbon fibre can provide this resistance [18]. For this reason, meshes or conductive paints are typically used to provide the required conduction channels.

Carbon fibre does, however, possess many of the inherent properties required for masking black boxes, and scattering radar signals at radar frequencies. This was confirmed in South Africa in tests performed on the Seeker II aircraft [18].

From research findings in recent years, there appears to be conflicting results regarding the conductive properties of carbon fibre. It is known that pure carbon is a semi-conductive material, rather than fully conductive [7]. This explains a great dealing when considering the high resistance of carbon fibre material. It is best assumed that carbon

fibre epoxy is not on its own adequate for the application at hand. Rather, different matrix and filler materials which could possibly aid in electrical conduction need to be reviewed.

Research undertaken by Luo and Chung [19], culminated with interesting results regarding possible matrix materials for use with carbon fibre. The study compared epoxy and carbon matrix materials, using carbon fibre filler materials.

The study found composites having continuous carbon fibres to provide better shielding effectiveness than those with discontinuous carbon fibres. Composites with discontinuous fillers were also found to be inadequate for structural application. It was found that small discontinuous carbon fibre filaments (diameter less than  $1\mu\text{m}$ ) caused degradation of shielding effectiveness within the continuous carbon fibre composite.

## 4.2 Filler Materials

It has been established that continuous carbon fillers are adequate for the application. However, there are other filler materials that can serve this purpose as well.

### 4.2.1 Carbon Black

Carbon black consists of tiny spheroids of carbon typically in the order of 20-50 nm in size, and is produced by the burning of carbonaceous materials [20, 21]. It is therefore inexpensive and is widely used in applications that require tensile strength, stiffness, wear resistance and toughness [20, 21].

Most notably, carbon black is used in the automotive industry for use in vehicle tires, but recent years have seen its use in more diverse applications [22, 23]. Such applications include EMI shielding; ESD protective; and radar-absorptive materials. Generally, when exploiting the properties carbon black can provide, trade-offs in material properties are expected. When maximising the electrical conductivity of materials, reductions in flexural modulus and impact strength are seen [24]. This will not be suitable in the event of high current lightning strike and electromagnetic shockwaves.

Properties of carbon black have been manipulated such that very high conductivity is achieved, but again, this resulted in low strength and stiffness. Carbon black in glass/epoxy composites (7%wt (0.6mm thickness) and 5% wt (1.9mm thickness)) has displayed good radar absorptive properties [23]. As reflection is not the primary shielding mechanism, laminates of this type will be unsuitable for lightning strike or EMI protection.

Due to the attractive low cost of carbon black, different loadings of the filler using a variety of fabrics may be explored. However, it appears unlikely that a balance between strength and conductivity will be achieved however, but this may be investigated further.

### 4.2.2 Nanotubes

Since the discovery of fullerene fibres (nanotubes) in the 1980's, a widespread interest in the properties the materials possess has been generated. They are 30-100 times stronger than steels, but weigh less than 20% of steels' mass [20]. Since the discovery, researchers have been exploiting the excellent strength, thermal, electrical and magnetic properties found in nanotubes, and new materials using nanotubes are in constant development [25]. This is seen by the amount of U.S patents for materials using nanotubes filed in the last decade [26-30].

Nanotubes are many thousands of times longer than their diameter, meaning they have a very high aspect ratio [20]. The high aspect ratio of nanotubes means that they can impart the same electrical conductivity at a lower loading than other fillers such as carbon black and chopped carbon fibre, and the composite material containing this filler will be extremely strong [25, 31]. A high aspect ratio also indicates less flaws being present in the laminate [21].

In recent years, the term 'nanotubes' is used interchangeably with 'carbon nanotubes', as these are the type that excite the most interest and have arguably the most potential from a commercial point of view [32]. Nanotubes come in various types, notably single-walled nanotubes (SWNTs) and multi-walled nanotubes (MWNTs).

SWNTs are typically 1-2 nm in diameter and are single molecules. MWNTs are formed out of a collection of SWNTs, in which weak Van der Waals forces hold the tubes together resembling a 'Russian doll' structure [25, 32]. MWNTs are significantly easier to produce, and are consequently cheaper to purchase [31].

Nanotubes are sharp, thin structures that resemble a lightning rod [33]. Electrical conductivity of the nanotube is proportional to its chirality (degree of twist), and it is known that nanotubes have a resistivity less than that of metals [20, 33]. This determines whether the nanotube behaves like a metal (conductor) or a semi-conductor. Summarizing, the physical and mechanical properties of the nanotube are determined by the chirality and aspect ratio.

Industry prices of nanotubes are dependant on the level of purity of the nanotube and range from being 40% pure to >95% pure, which is the most expensive type. Current prices range from US\$ 2.00/g for MWNT (>50nm diameter, 50  $\mu$ m long), to US\$ 2000.00/g for super purified SWNT [32-34]. Also available are special grade nanotubes, which are designed for the specific purpose of EMI shielding [34].

Due to the high cost of nanotubes, much of the development has been restricted to research only. Mass production and commercialisation of nanotubes has not been achieved yet. This is expected to change drastically by 2010 as depicted in the figure below:

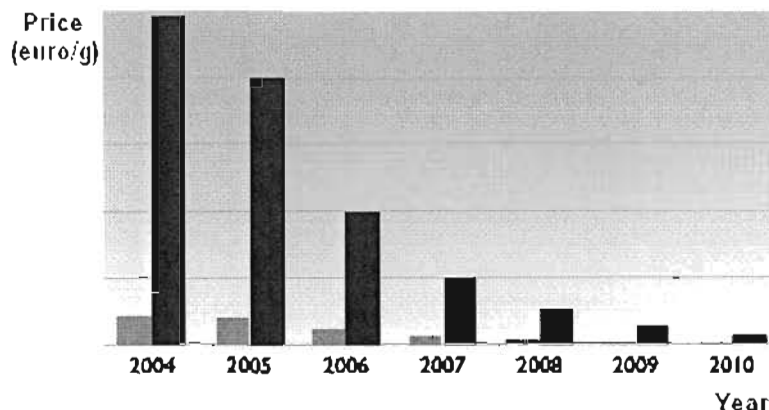


Figure 4: The projected decrease in price of nanotubes by 2010 [Amended from 35]  
 Researchers have found that using nanotubes instead of carbon fibres as filler materials have resulted in up to 90% reduction in loading [21]. However, the limited supply and high cost of nanotubes prevent the integration of nanotubes into current designs.

With the drastic cost reduction coupled with the production increase, it appears that long term possibilities using nanotubes are very promising. The use of this material will be explored further.

#### 4.2.3 Vapour Grown Carbon Nanofibre

In recent years, tests have been performed on materials using vapour-grown carbon fibre (VGCF) as the filler material. VGCFs are similar to MWNTs, but are much larger, and have aspect ratios in the 100-500 range [25].

VGCF is much cheaper, and readily available, making them an attractive option. However, the disadvantage is that there is larger microstructural defects present compared with carbon nanotubes. Research has been undertaken on this filler material in recent years to determine its properties, and also to build a knowledge base that may be transferable to nanotubes [11, 25].

It was found that VGCFs possess excellent strength, electrical and thermal properties. One study using VGCFs in a liquid crystal polymer (LCP) matrix has found electromagnetic SE to be 41 db [11]. However, these results were obtained at a frequency of 15 MHz and using 15 wt% of VGCF. It was determined that the percolation threshold of VGCF in the LCP matrix is 5 wt%. At this point, the resistivity dropped 11 orders of magnitude [11]. The bulk resistivity of the 15 wt% sample was the lowest, at  $7 \times 10^{-2} \Omega.m$ . This value appears too high for lightning conduction. Therefore, research may be carried out using this filler material with epoxy composites, rather than LCP based ones.

Studies performed using vinyl ester composites again displayed percolation behaviour, but at a lower loading of 2 – 3 wt%. Although the samples still contained a high resistivity, it must be noted that the addition of VGCF resulted in a resistivity drop from



the order of  $10^{10}$  to  $10^2$ . Also of interest is the sample displayed two percolation threshold points [36]. This displays the excellent conductive properties found in VGCF. The relatively high resistivity value after the second percolation threshold is a result of the vinyl ester matrix, which is insulating. It is assumed that a material with suitable resistivity will be obtained if non-insulative matrix materials are used.

Due to the low cost and excellent properties, this material will, however, be researched further. However, at this time, VGCF is only available from one supplier in the U.S.A.

#### 4.2.4 Metal Fillers

It is known that metal fillers can be used with composites to form excellent shielding materials. This is to be expected, as metals are known to be some of the best electrical conductors. However, there are a number of disadvantages when working with metals. Metal material is typically expensive, heavy in mass and susceptible to corrosion damage [2, 37-39].

However, due to some metals being intrinsically good conductors and possessing excellent strength properties, the use of metals in applications such as EMI shielding is justly expected. Material availability and the inherent isotropic nature of metals also present benefits.

Chung [40] states that metal particles are more desirable opposed to carbon as filler materials, due to their higher conductivity of metals. The disadvantages of metals as fillers are poor oxidation resistance and thermal instability. However, metal particles are larger in size than carbon particles, and cannot be smaller than  $2\mu\text{m}$  [40]. With this in mind, it appears that even the use of metal particles can lead to excessive weight increase depending on the amount used.

Chung has found that submicron metal particles can be attained by electroplating submicron carbon particles. Such particles can be attained by electroplating carbon particles with a diameter of  $0.1\mu\text{m}$  with nickel to result in  $0.4\mu\text{m}$  diameter nickel filaments. Nickel was selected based on the fact that it is less susceptible to oxidation damage.

The use of 7 vol% of these filaments with a polymer matrix composite resulted in 87 dB shielding effectiveness at 1 GHz. This amount is far greater than that displayed by the same volume of carbon filaments in the same matrix [40].

However, it must be noted that as nickel is ferromagnetic in nature. This implies that nickel will be conducive for absorption, rather than reflectivity. It is evident that a larger absorption loss will result with use of ferromagnetic materials, implying that a low reflectivity value will result.

Metals that are noted for good electrical conductivity are silver, gold, copper and aluminium. Silver and gold are two of the most conductive metals, but seemingly cost

and strength are the prohibiting factors for implementing them into design. Copper will not be a good choice as it is susceptible to oxidation damage. Aluminium filler materials such as powder may therefore be used as the primary metal fillers in test samples.

#### 4.3 Metal Meshes

Metal meshes have long been used to provide electrical conduction in traditionally non-conductive materials. In aircraft such as the Boeing 787, meshes are used to provide a conductive channel for shielding [41]. In recent years, researchers have been trying to find methods of obtaining conductive fabrics by knitting metal wires into glass fabrics.

Cheng et al [39] have developed a feasible method of fabricating conductive knitted fabrics. This was done by knitting copper wires and glass fibres using the uncommingled yarn technique. The results, as expected, showed that the conductivity of this fabric varied with copper content. That is, a better EMSE was obtained as the amount of copper increased.

Chen et al [38], have developed a method of fabricating hybrid conductive fabrics using stainless steel and copper wires. The reinforcement material used was polyamide filaments, and the matrix material was polypropylene. Again, the results show that EMSE is dependant on the metal content in the fabric.

Cheng et al [37, 42], have successfully developed a hybrid fabric by knitting stainless steel and copper wires with carbon fibre using the uncommingled yarn technique. The previous experiments used glass fibre, which is typically insulative and is not typically used for structural applications. The improvement in this fabric comes from the use a carbon fibre, which has excellent conductive and strength properties. However, as explained earlier, carbon fibre is semi-conductive, and as expected, EMSE is dependant on the metal content.

All of these studies were performed in the frequency range of 300 kHz to 3 GHz. This range is perhaps more suitable for shielding home electronic equipment, rather than aircraft electronics/ avionics. Nonetheless, as expected, EMSE is directly proportional to the amount of conductive material used in the hybrid fabrics. Sometimes, however, the optimal shielding point requires over 50% of wire in the fabric [37]. This may be an unnecessary weight inclusion, but as this method is seemingly more cost effective opposed to the use of new filler materials, additional research may be undertaken on hybrid fabrics.

#### 5. CONCLUSION

The phenomena responsible for EMI in airborne vehicles have been established. It has been established that the properties of carbon fibre can be used to form excellent shielding structures. Composites with metal filler materials have been found to be an excellent choice in terms of strength and conduction, but have associated disadvantages such as weight and corrosion. Further investigation using carbon black may be

undertaken to determine whether composites with this filler material can provide both the conductivity and structural strength that is required. It has been determined that VGCF may be adequate for this purpose.

### **ACKNOWLEDGEMENTS**

The continued research of this project is supported by Armscor through a project with Denel Aerospace Systems, South Africa.

### **REFERENCES**

1. Schlechter, M; EMI: Materials and Technologies; Research Report extract – [www.electronics.ca](http://www.electronics.ca); Accessed: December 2005
2. Yuping, D *et al*; Investigation of electrical and electromagnetic shielding effectiveness of polyaniline composite; Science and technology of advanced materials vol. 6 (2005); 513-518
3. Bailey, J.E; Origins of Composite Materials; Composite Materials in Aircraft Structures, 1-8; Longman Scientific and Technical; 1990; UK
4. Thorogood, L; Bolt from the blue; Flight Safety Australia, July-August 2005; [www.casa.gov.au](http://www.casa.gov.au); 48-50.pdf; accessed: February 2006
5. Krohto, E.G; Lightning Strike Evaluations of Reinforced Conductive Airframe Seals; [www.parker.com](http://www.parker.com); lightning strike evals.pdf; accessed: January 2006
6. Bashford, D.P; The Potential of Composite Materials; Composite Materials in Aircraft Structures, 9-16; Longman Scientific and Technical; 1990; UK
7. Young, H.D and Freedman, R.A; Sears and Zemansky's University Physics; tenth international edition; Addison-Wesley Publishing Company, 2000, USA
8. EMI Shielding Theory; [www.chromerics.com](http://www.chromerics.com); pg192theory\_of\_emi.pdf; accessed: February 2006
9. White, D.R.J; Electromagnetic Shielding Materials and Performance; Don White Consultants, Inc.; 1980; USA
10. Turn off your radio; QwikConnect vol. 6, no. 2, April 1999; [glenair.com](http://glenair.com); accessed: February 2006
11. Lozano, K *et al*; Electromagnetic interference shielding effectiveness of carbon nanofiber/LCP composites; Composites Part A: Applied science and manufacturing vol. 36 (2005); 691-697
12. Hong, Y.K *et al*; Electromagnetic interference shielding characteristics of fabric complexes coated with conductive polypyrrole and thermally evaporated Ag; Current Applied Physics vol. 1 (2001); 439-442
13. Lee, C.Y; Electromagnetic interference shielding efficiency of polyaniline mixtures and multilayer films; Synthetic Materials vol.102 (1999); 1346-1349
14. Case Histories; The Potential of Composite Materials; Composite Materials in Aircraft Structures, 228-390; Longman Scientific and Technical; 1990; UK
15. Bashford, D.P; The Potential of Composite Materials; Composite Materials in Aircraft Structures, 9-16; Longman Scientific and Technical; 1990; UK

16. Lovell, D.R; Types of Materials; The Potential of Composite Materials; Composite Materials in Aircraft Structures, 17-38; Longman Scientific and Technical; 1990; UK.
17. Bleck, M.E; Beech Aircraft Corporation; Beechcraft Starship; [www.aviatorservices.com](http://www.aviatorservices.com); accessed: February 2006
18. Lutz, G.W; Notes of the earthing and screening requirements for composite airframes; Obtained: December 2005
19. Luo, X and Chung, D.D.L; Electromagnetic interference shielding using continuous carbon-fiber carbon-matrix and polymer-matrix composites; Composites Part B: Engineering vol. 30 (1999); 227-231
20. Jacobs, J.A and Kilduff, T.F; Engineering Materials and Technology: Structures, Processing, Properties, and Selection 4<sup>th</sup> edition; Prentice Hall; 2001; USA
21. Askeland, D.R; The Science and Engineering of Materials 3<sup>rd</sup> edition; PWS Publishing Company; 1994; USA
22. Das, N.C *et al*; Electromagnetic interference shielding effectiveness of carbon black and carbon filled EVA and NR based composites; Composites Part A: Applied science and manufacturing vol. 31 (2000); 1069-1081
23. Oh, J-H *et al*; Design of radar absorbing structures using glass/epoxy composite containing carbon black in X-band frequency ranges; Composites part B: Engineering vol. 35 (2004); 49-56
24. Carbon Black; [www.azom.com](http://www.azom.com); accessed: January 2006
25. Breuer, O and Sundararaj, U; Big Returns from Small Fibers: A Review of Polymer/Carbon Nanotube Composites; Polymer Composites vol. 25, no.6; December 2004; 630-645
26. J. G. Gerard and H. V. Samuelson, U.S. Patent 6,426,134 (2002)
27. P. Glatkowski, P. Mack, J. L. Conroy, J. W. Piche, and P. Winsor, U.S. Patent 6,265,466 (2001)
28. S. H. Foulger, U.S. Patent 6,417,235 (2002)
29. M. Dupire and J. Michel, U.S. Patent 6,331,265 (2001)
30. A. Fisher, R. Hoch, D. Moy, C. Niu, N. Ogata, H. Tennent, and T. McCarthy, U.S. Patent 6,203,814 (2001)
31. Holister, P *et al*; Nanotubes White Paper; CMP Cientifica; January 2003; Spain
32. Price list; [www.cheaptubesinc.com](http://www.cheaptubesinc.com); accessed: February 2006
33. Applications and Properties of Carbon Nanotubes; [www.cheaptubesinc.com](http://www.cheaptubesinc.com); accessed: January 2006
34. Price list; [www.cnanotech.com](http://www.cnanotech.com); accessed: March 2006
35. Nanotubes for the Composite Market – abstract; [www.cientifica.com](http://www.cientifica.com); accessed: February 2006
36. Xu, J *et al*; Preparation, electrical and mechanical properties of vapor grown carbon fiber (VGCF)/vinyl ester composites; Composites Part A: applied science and manufacturing vol. 35 (2004); 693-701
37. Cheng, K.B *et al*; Effects of yarn constituents and fabric specifications on electrical properties of hybrid woven fabrics; Composites Part A: Applied science and manufacturing vol. 34 (2003); 971-978
38. Chen, H-C *et al*; Electromagnetic and electrostatic shielding properties of co-weaving-knitting fabrics reinforced composites; Composites Part A: applied

- science and manufacturing vol. 35 (2004); 1249-1756
39. Cheng, K.B *et al*; Electromagnetic shielding effectiveness of copper/glass fiber knitted fabric reinforced polypropylene composites; Composites Part A: applied science and manufacturing vol. 31 (2001); 1039-1045
  40. Chung, D.D.L; Electromagnetic interference shielding effectiveness of carbon materials; Carbon vol. 39 (2001); 279-285
  41. Gates, D; Building the 787 – When lightning strikes; Seattle Times article; 5 March 2006
  42. Cheng, K.B *et al*; Electrical and impact properties of the hybrid knitted inlaid fabric reinforced polypropylene composites; Composites Part A: applied science and manufacturing vol. 33 (2002); 1219-1226

**COMPOSITE ELECTROMAGNETIC INTERFERENCE  
SHIELDING MATERIALS FOR AEROSPACE APPLICATIONS**

Denver Maharaj<sup>\*</sup>, Christopher J von Klemperer

*School of Mechanical Engineering, University of KwaZulu-Natal, Howard College  
Campus, Durban, 4041, South Africa*

<sup>\*</sup>Corresponding author: Tel +27 31 260 1225 Fax +27 31 260 3217

E-mail [maharajd2@ukzn.ac.za](mailto:maharajd2@ukzn.ac.za)

**ABSTRACT**

Electromagnetic interference (EMI) occurs when electronic devices are subject to electromagnetic radiation at the same frequency ranges that these devices operate from unwanted sources. Metals typically serve as excellent EMI shielding agents, but their heavy weight, high cost and susceptibility to environmental degradation make them an undesired choice for current electronic devices. Conversely fibre composite materials are typically light weight, flexible and cheaper to produce, but typically lack the inherent EMI shielding capabilities that may be required. This research work addresses the viability of fibre composite materials for use as EMI shielding structures, specifically for aerospace applications. It was found that carbon fibre could suffice this purpose, but likely required filler materials to enhance electrical conductivity and shielding effectiveness (SE).

**Keywords:** Electromagnetic interference, Electrical conductivity, Carbon fibre laminates, Shielding effectiveness

**1. INTRODUCTION**

Aircraft of today are essentially 'fly-by-wire' systems, which refers to the use of digital control systems opposed to the use of analogue control systems of older aircraft. Additional to this, aircraft contain cockpit automation and digital navigation systems [1]. Due to the high amount of on-board digital equipment, the concern regarding prevention of electromagnetic disturbances is not unfounded.

Despite the aerospace industry continually striving for higher-performance vehicles, comparatively little research has been undertaken regarding new electromagnetic shielding options in the past ten years [2]. Fibre composite materials have, however, been identified in recent years as being the desired choice for the replacement of orthodox metals and alloys in this regard. The chief obstacle preventing the substitution is the general inherent lack of electromagnetic shielding capabilities possessed in fibrous composite materials.

EMI in aircraft may be classified into three sub-classes, which are: on-board systems, passenger carry-on devices, and externally generated EMI [1]. When on-board systems interfere with each other, it is referred to as electromagnetic compatibility [1]. Passenger carry-on devices include portable electronic devices that can transmit and receive frequencies, compact disc players and computers. Anyone who has flown on-board an aircraft has been cautioned against use of these devices during flight. Externally-generated EMI refers to disturbances caused by external sources such as lightning strike, HIRF and electromagnetic pulses (EMPs) [1].

There are three shielding mechanisms that could result in attenuation of EMI viz. reflection (R), absorption (A), and multiple reflections (B). The primary mechanism for shielding in highly electrically conductive structures, such as metals, is reflection. Reflection relies on mobile charge carriers, such as electrons, being present within the material. Therefore, the shielding material tends to be electrically conductive, although this is not an essential requirement for shielding [3]. Electrical conduction requires connectivity in the conduction path, whereas shielding does not [3]. Thus, high electrical conductivity is not typically a requirement for shielding, but shielding was found to be enhanced by connectivity [4]. In addition, the exact application for the shielding materials in this work was unknown, and the material could likely be used on exterior surfaces of aircraft and thus be exposed to lightning strike. It was therefore essential that materials that display high conductivity be investigated as well. Reflection loss is a function of  $\sigma_r/\mu_r$ , and reflection loss decreases with increasing frequency [3,4]. ( $\sigma_r$  refers to the conductivity of a material relative to copper, and  $\mu_r$  refers to the permeability of a material relative to copper). The secondary mechanism for shielding in these structures is absorption. Significant absorption of the waves by the shield requires electric and/or magnetic dipoles within the shield material. Absorption loss is a function of  $\sigma_r\mu_r$ , and absorption increases with increasing frequency. Absorption loss is proportional to shield thickness [3,4]. The third mechanism for shielding is multiple reflections. Multiple wave reflections take place at surfaces or interfaces within the shield. This mechanism requires the presence of large surface areas or interfaces within the shield [3,4].

When defining the performance of a shielding material, the term often quoted is shielding effectiveness (SE). The value, obtained in decibels, provides an indication of the quality of shielding a material possesses. The frequency range in this work ranged from 800MHz to 5GHz, and is referred to as being 'far-field', or 'plane waves', measurements [5]. The criteria for these measurements are  $Z_w = 377\Omega$  and  $r > \lambda/2\pi$ , where  $Z_w$  is the free-space impedance,  $r$  = distance from the source (m),  $\lambda$  = wavelength (m). Total SE can be obtained by summing the individual contributions of R, A and B in dB [5].

$$SE_{dB} = R_{dB} + A_{dB} + B_{dB} \quad (1)$$

$$\text{Where: } R_{dB} = 108.1 - 10 \log_{10}(\mu_r f_{MHz} / \sigma_r) \quad (2)$$

$$A_{dB} = 1314.3 t_{cm} \sqrt{f_{MHz} \sigma_r \mu_r} \quad (3)$$

$$B_{dB} = 20 \log_{10}(1 - e^{-2t\sqrt{\pi f \mu \sigma}} e^{-j2t\sqrt{\pi f \mu \sigma}}) \quad (4)$$

Equations (1)-(4) were originally used for computations of metal shielding materials, but researchers have used them for composite materials as well. However, inspection of equation (3) shows that a high  $A_{dB}$  value will result, as it is dependant on frequency. This was found to be doubtful, as highly conductive materials such as aluminium sheet material should display a very low  $A_{dB}$  value. However, Das *et al.* [6] have used a form of equation (3), but the result was reduced by a factor of  $10^3$ , which appears to be more likely. Thus the equation is:

$$A_{dB} = 1.32t \sqrt{f\sigma_r\mu_r} \quad (5)$$

Researchers have used other approximations for composite material SE in recent years. Colaneri and Shaklette [7] have developed an equation for electrically thin samples (thickness < skin depth) for far-field calculations:

$$SE = 20 \log \left( 1 + \frac{Z_0 \sigma d}{2} \right) \quad (6)$$

Where:  $Z_0 = 377 \Omega$

$\sigma$  = electrical conductivity ( $\Omega/m$ )

$d$  = shielding material thickness (m)

Yang *et al.* [3] have used the 'Simon Formalism', and the 'classical good conductor approximation' for their SE calculations. The respective formulas are:

$$SE = 50 + 10 \log_{10}(\rho f)^{-1} + 1.7t(f/\rho)^{\frac{1}{2}} \quad (7)$$

$$\text{Where: } \rho = \text{volume resistivity } \frac{RA}{l} \text{ (}\Omega \text{ cm)} \quad (8)$$

$R$  = volume resistance ( $\Omega$ )

$A$  = Area ( $\text{cm}^2$ )

$l$  = length (cm)

$f$  = frequency (MHz)

$t$  = shielding material thickness (cm)

$$SE = 10 \log \left( \frac{\sigma}{32\pi f \epsilon_0} \right) + 20 \frac{d}{\delta} \log(e) \quad (9)$$

Where:  $\sigma$  = bulk conductivity ( $\Omega/\text{cm}$ )

$f$  = frequency (MHz)

$\epsilon_0 = 8.854 \times 10^{-14} \text{ F/cm}$

$d$  = shielding material thickness (cm)



$$\delta = \text{skin depth} \sqrt{\frac{1}{\mu_0 \pi f \sigma}} \text{ (cm)}$$

$$\mu = 4\pi \times 10^{-9} \text{ H/cm}$$

$$e = 2.718281828$$

However, it was found that there are large discrepancies between the results obtained from use of the various analytical equations and this has been well-documented by previous researchers as well [8,9,10]. These discrepancies have been reported as being quite substantial, and in some cases have been greater than 100dB, especially around jointed surfaces [8]. The computation of SE by use of theoretical equations is thus well-regarded as being a problem in the industry.

## **2. EXPERIMENTAL**

### **2.1 Materials**

Unidirectional carbon; 12K woven carbon;  $\pm 45^\circ$  stitched carbon; and 80/20 unidirectional E-glass fabrics were obtained for use as structural materials. LR20 resin, with LH281 hardener, and Prime 27 resin, with Prime 20 slow hardener, was obtained for use as matrix materials. Aluminium and copper powders, and Alumesh 401 metal fabrics was obtained for use as filler materials. It was initially hoped that materials such as nanotubes could be used for this work, but project budgets and import restrictions prevented its use.

### **2.2 Composite Manufacture**

Initial tests were performed on 80/20 unidirectional E-glass fabric. This material was not considered as an option for actual shielding material, but was used to develop repeatable manufacturing processes for the carbon fabrics. Hand lay-up and vacuum-assisted resin infusion were used as the manufacturing processes in this work. Tests were later performed on the carbon fabrics as well, and it was found that hand lay-up manufacture using the materials with LR20, with LH281 hardener, yielded the most promising results. This manufacturing process and matrix material was thus used for the production of the shielding materials in this work.

It was decided that composite designs consisting of increasing quantities of powders, and designs consisting of increasing quantities of metal mesh should be fabricated and investigated to determine the influence that metal has on shielding materials. The focus was not to determine the exact percolation threshold of the powder in the composite, but rather to ascertain if a general trend with increasing filler loading was observed in mechanical and electrical properties in the composites.

It was decided that the aluminium powder; copper powder; and a mixture of both powders in equal quantities by weight; should be introduced into the matrix materials in 7.5% and 15% filler loadings. It was decided that 15% would be the maximum upper limit for these discontinuous fillers. It was decided that one and two layers of metal

fabrics would be investigated, to determine if increasing the metal content in this way has an influence on SE. The samples with the metal mesh contained a layer of unidirectional E-glass at the carbon interface to prevent possible corrosion damage.

The composites were manufactured in sheets between 2-3mm in thickness, cured for 16hrs at 65° C, and were machined to the dimensions of the test specimens.

## 2.3 Testing

### 2.3.1 Mechanical Testing

Tensile and flexural testing was undertaken using an Instron 5500R universal testing machine. The tests were performed in accordance with ASTM 638-02a and ASTM 69272-02 respectively. Compressive testing was outsourced and performed using a Lloyds universal testing machine. The test was performed in accordance with ASTM 695-02a.

### 2.3.2 Electrical Resistance Testing

Bulk electrical resistance measurements were made using a Philips PM6303 RCL universal bridge circuit. The method was in accordance with ASTM B 193-02, and similar work has been done by Xu *et al.* [11]. The value obtained was in  $\Omega$ , and equation (8) was used to obtain bulk resistivity. The electrical conductivities were obtained by use of:

$$\sigma = \frac{1}{\rho} \quad (10)$$

A copper plate of the same size was measured on the instrument and relative conductivity was obtained by use of:

$$\sigma_r = \frac{\sigma}{\sigma_c} \quad (11)$$

Where:  $\sigma_c$  = electrical conductivity of copper ( $\Omega/\text{cm}$ )

### 2.3.3 Shielding Effectiveness Testing

Far-field SE measurements were obtained by use of a Scientific Atlanta compact range, which contains a Hewlett Packer 8510C network analyzer. Testing equipment of this type is referred to as a 'two-port network system', and variables referred to as 'scattering parameters' (*S*-parameters) are obtained from testing [12]. The test method was suggested by Odendaal [13], as the frequency range in question in this work was above that described in ASTM 4935-99. The sample sizes were 300mm<sup>2</sup> and were measured relative to an aluminum plate.

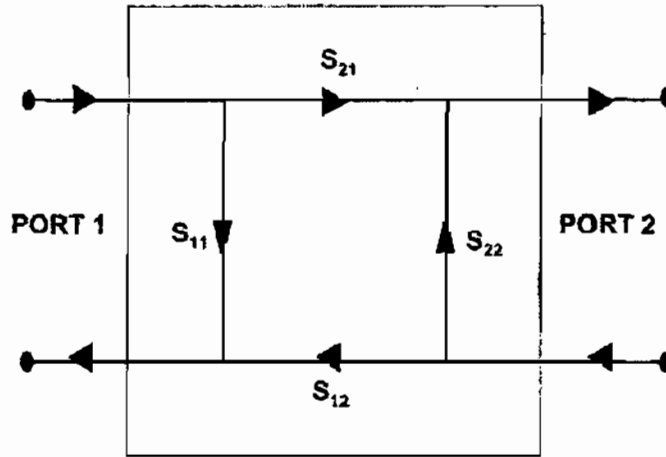


Figure 1: Schematic diagram of S-parameters of a two-ports network system [12]

The  $S_{12}$  ( $S_{21}$ ) and  $S_{11}$  ( $S_{22}$ ) parameters refer to the transmission and reflection coefficients respectively [12]. The analysis of S-parameters yield:

$$T = \left| \frac{E_T}{E_I} \right| = |S_{12}|^2 = |S_{21}|^2 \quad (12)$$

$$R = \left| \frac{E'_I}{E_I} \right|^2 = |S_{11}|^2 = |S_{22}|^2 \quad (13)$$

$$A + R + T = 1 \quad (14)$$

The test for  $S_{12}$  ( $S_{21}$ ) parameters yield a transmission value in dB, which can be used to determine EMSE by use of the following equations [12]:

$$T_R = 10^{\frac{T_{dB}}{20}} \quad (15)$$

$$SE = \log \frac{1}{T_R} \quad (16)$$

Where:  $T_R$  = linear transmission value

Percentage penetration through the shielding material is given by [13]:

$$\% \text{ Penetration} = 10^{\frac{T_{dB}}{20}} \times 100 \quad (17)$$

### **3. RESULTS AND DISCUSSION**

#### **3.1 Mechanical Results**

Tensile testing showed that the stitched carbon fibre laminates possessed surprisingly low strength and elongation properties. The range of strength was between 54 MPa for samples with 7.5% of aluminium and copper powder to 82 MPa for samples two metal mesh layers. Failure was characterised by separation of the fibres at the midsection of the gauge length. All of these samples deflected excessively during flexural testing, and thus the bending strength was indeterminate. The samples had elastic moduli between 7 GPa for samples with 15% copper powder to 14 GPa for samples without filler, which is unsurprising given the level of flexibility they displayed. The compressive strength ranged from 63-96 MPa for samples with 7.5% aluminium and copper powder to that which had 7.5% copper powder. Failure was characterised by separation of the fibres at the midsection of the gauge length. The poor properties displayed by these composites were thus indicative of the stitched carbon itself, as the results were all in accordance.

The results for the woven and unidirectional samples were far more promising. The tensile strength of the woven samples ranged between 820 MPa for samples without filler to 595 MPa for samples with 15% aluminium and copper powder. Failure was characterised by complete fracture of the material at the gauge length. The bending strength of the woven samples was found to increase with increasing filler loading. The samples without filler thus displayed the lowest strength. However, the elastic modulus was found to decrease quite significantly, from 73 GPa without filler to as low as 45 GPa with 7.5% copper powder. Failure was characterised by snapping of the outer fibres at the midsection of the gauge length. The compressive strength results were dubious, as there was evidence of crushing on the end surfaces. There was no visible failure on the gauge length of the specimens, and the results surprisingly indicate far lower compressive stresses than tensile stresses. This could be due to test conditions at the test location where these tests were conducted, as there are known to be discrepancies with results obtained from different sources. However, there was no evidence of failure on the specimen, and the results appear doubtful.

The tensile strength displayed by the unidirectional samples was the highest, with the sample without filler having a strength of 841 MPa. However, tensile strength increased with increasing loadings of copper and aluminium powder mixture, and was 904 MPa at 15% loading. Strength generally decreased with inclusion of the other fillers. Failure was generally characterised by snapping of the fibres across the outer width of gauge length. Bending strength did not significantly change in the samples with discontinuous fillers, and was in the range of 1 GPa. However, bending stress decreased greatly with increasing mesh content, and was 326 MPa in the samples with two metal mesh layers. The samples without filler displayed a high elastic modulus of 180 GPa, and it generally decreased with increasing filler loading. Failure in these samples was characterised by a loud noise, but only slight fracture across the width of the gauge length was visible. Compressive strength was also dubious in these samples, as deformation of the end surfaces was

visible, and there was no visible damage on the specimen length. Again, these values indicate compressive strength was far less than tensile strength.

### 3.2 Electrical Resistance Results

The results from electrical resistance testing are shown in Table 1. Note that copper and aluminium both displayed higher resistances than expected and thus it is likely that the composite specimens had lower resistances as well.

**Table 1: Electrical Properties of the Materials**

<b>Material *</b>	<b>Measured Resistance (<math>\Omega</math>)</b>	<b>Calculated Resistivity (<math>\Omega \cdot \text{cm}</math>)</b>	<b>Calculated Conductivity (<math>\Omega/\text{cm}</math>)</b>	<b>Relative Conductivity</b>
Copper Plate	0.09	0.01	141.10	1.00000
Aluminium Plate	0.10	0.02	61.16	0.43345
Stitched CF NF	8.10	1.85	0.54	0.00383
Stitched CF 7.5%Al	7.20	1.45	0.69	0.00490
Stitched CF 15%Al	13.90	2.79	0.36	0.00254
Stitched CF 7.5%Cu	21.03	4.29	0.23	0.00165
Stitched CF 15%Cu	23.20	4.88	0.21	0.00145
Stitched CF 7.5%H	26.30	6.17	0.16	0.00115
Stitched CF 15%H	42.20	9.70	0.10	0.00073
Stitched CF 1ply	0.59	0.14	7.36	0.05216
Stitched CF 2ply	0.75	0.20	5.06	0.03588
Woven CF NF	23.20	4.80	0.21	0.00147
Woven CF 7.5%Al	50.00	13.42	0.07	0.00053
Woven CF 15%Al	16.64	4.48	0.22	0.00158
Woven CF 7.5%Cu	28.00	7.18	0.14	0.00099
Woven CF 15%Cu	64.00	16.49	0.06	0.00043
Woven CF 7.5%H	64.00	16.21	0.06	0.00044
Woven CF 15%H	46.00	10.90	0.09	0.00065
Woven CF 1ply	0.48	0.10	9.96	0.07055
Woven CF 2ply	0.69	0.16	6.43	0.04557
UD CF NF	5.93	1.24	0.81	0.00571
UD CF 7.5%Al	10.74	2.72	0.37	0.00261
UD CF 15%Al	11.02	2.76	0.36	0.00257
UD CF 7.5%Cu	11.32	2.64	0.38	0.00268
UD CF 15%Cu	14.37	3.25	0.31	0.00218
UD CF 7.5%H	25.80	6.67	0.15	0.00106
UD CF 15%H	31.00	7.13	0.14	0.00099
UD CF 1ply	0.73	0.19	5.38	0.03814
UD CF 2ply	0.29	0.07	13.65	0.09674

\* Note: CF refers to carbon fibre, UD refers to unidirectional, NF refers to materials with no filler, Al refers to aluminium, Cu refers to copper, and H refers to the mixture of aluminum and copper powder

It can be seen that electrical resistance increased with inclusion of fillers in some cases. As the fillers are discontinuous, they were disordered within the matrix material. The electrical properties of composite materials, such as unidirectional carbon laminates are highly dependant on their fibre orientation. The electrical resistances of these laminates were measured perpendicular to the fibre direction, and the results unsurprisingly showed that resistance was higher in the order of 10. Thus, the disordered arrangement of conductive particles, which were lower in resistance to the fibres themselves, could have led to discrepancies in the bulk resistance measurements.

However, the unidirectional carbon laminates were found to display the best results from the carbon materials tested in this work. From the results obtained, it can be seen that these materials will suffice shielding application in practice, as good shielding materials require resistivities of  $10\ \Omega\cdot\text{cm}$  and less [14]. Dhawan *et al.* [15] also report that materials with resistivities less than  $10^2\ \Omega\cdot\text{cm}$  will adequately suffice the purpose of electromagnetic shielding. From the obtained electrical data, SE was analytically obtained from use of the SE equations (1), (6), (7) and (9) presented earlier. The SE results obtained by use of equations (6), (7) and (9) are in accordance, but the results obtained by use of equation (1) do not correlate with those SE results.

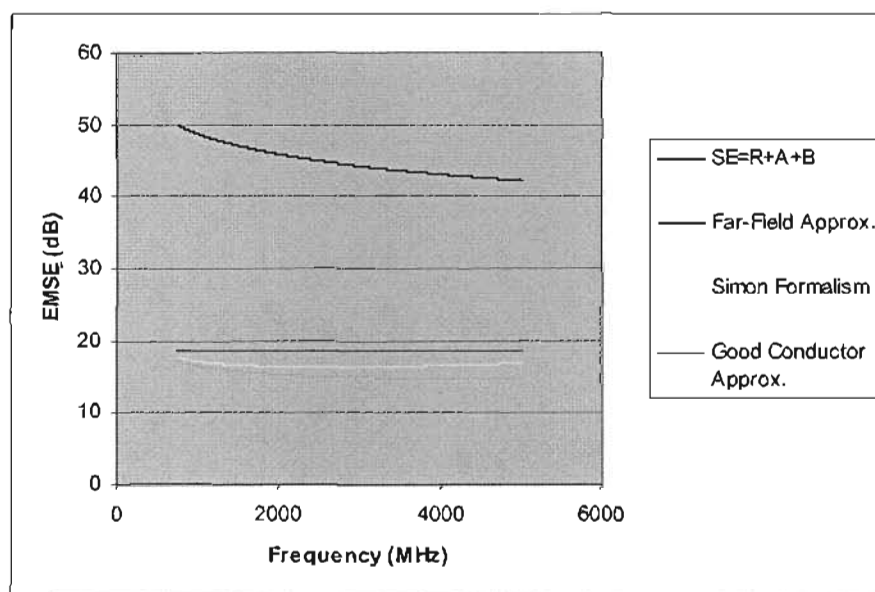


Figure 2: EMSE (analytical) vs. Frequency for unidirectional carbon fibre specimens containing 7.5% aluminium and copper powder

However, equations (7) and (9) were in greater accordance for the samples which contained metal mesh layers. The results obtained by use of equations (1) and (6) were in some accordance as well. However, it has been mentioned that results obtained via use of theoretical equations are known to contain discrepancies when compared with actual results, and thus use of the equations is suitable for approximation only. The results from the analytical computations of the unidirectional samples with two layers of metal mesh are presented in Figure 3 on page 10 of this paper.

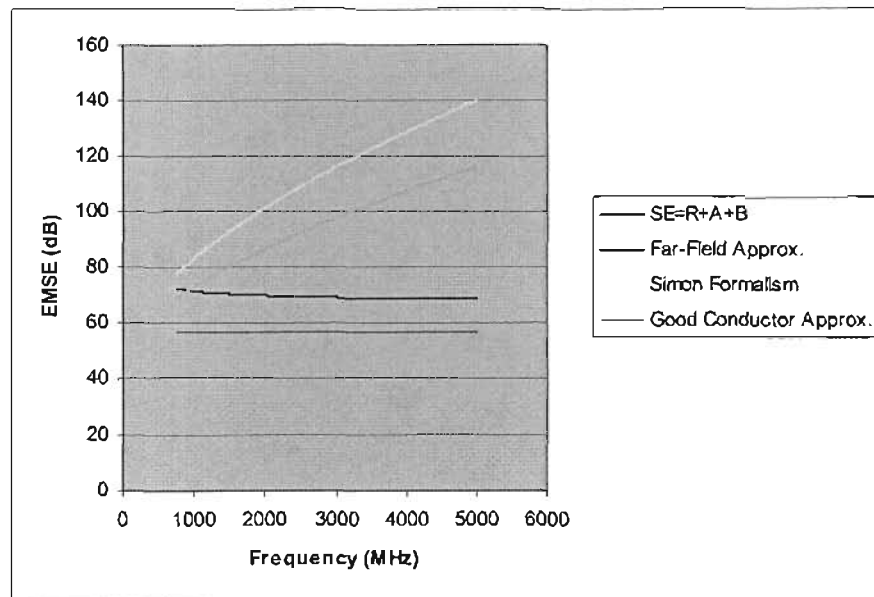


Figure 3: EMSE (analytical) vs. Frequency for unidirectional carbon fibre specimens with two layers of metal mesh.

### 3.3 Shielding Effectiveness results

The results obtained from actual SE testing show that these carbon fibre laminates are suitable for shielding purposes. The  $S_{12}$  ( $S_{21}$ ) were obtained by testing, and SE was obtained by use of equations (15) and (16). The laminates without filler displayed excellent inherent capabilities, and inclusion of fillers enhanced this further. In some tests, the composite samples were found to display better shielding quality than the aluminium plate itself. However, this could be due to diffraction at some frequencies.

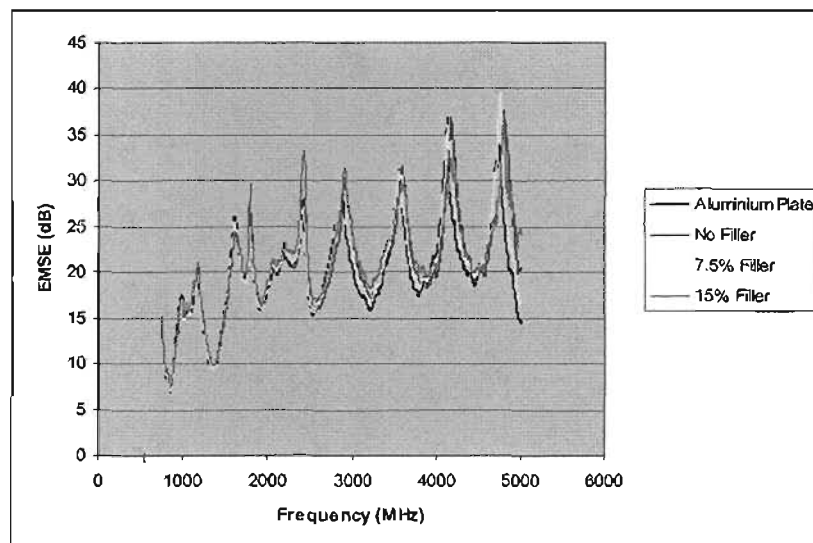


Figure 4: EMSE (actual) vs. Frequency for unidirectional carbon fibre specimens with copper and aluminium powder

However, there were no significant improvements in SE when two metal layers were used instead of one. There was an increase in SE, though not significant to incur the cost of using two layers in practice.

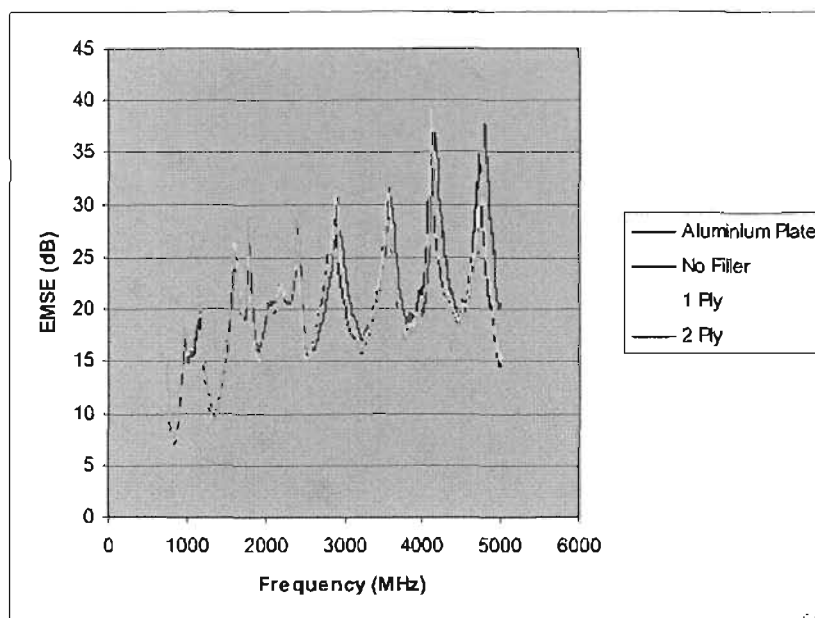


Figure 5: EMSE (actual) vs. Frequency for unidirectional carbon fibre specimens with metal mesh layers

### 3.4 Discussion

There is initially a higher cost when using carbon fibre laminates rather than orthodox metals in aircraft. Such costs are further compounded when the recent restrictions placed on sale of carbon fibre is taken into account. However, the long-term cost saving can in actuality provide a far greater return when increasing fuel cost and material life-cycles are considered. Metals are far heavier, and many of the laminates produced in this work were 50% lighter. The stitched carbon samples, however, will be of no use for structural support. The woven material displayed high strength and good shielding properties, but were also the heaviest of the laminates, being 30% lighter than aluminium on average. The unidirectional carbon fibre was on average 45% lighter than aluminium, and displayed far superior strength properties as well. The cost of including metal powders in matrix materials is less than US\$0.01/g, and even with 15% powder included by weight, only about 30g is required to enhance SE in laminates of the size fabricated in this work. The cost of including metal mesh is significantly greater, at about \$140.00/m<sup>2</sup>, but is evidently required in regions prone to lightning strike for the dissipation of higher currents. Samples with discontinuous fillers were viewed under a microscope and it was seen that connectivity between particles is greatly improved between 7.5% filler loading and 15% filler loading. However, there were fewer particles, and thus lesser connectivity between the copper particles opposed to aluminium particles, due to the comparatively heavy weight and small size of them. Greater connectivity was found in aluminium



powder and the mixture of aluminium and copper powders in all of the samples. However, this did not adversely affect SE of the copper samples, and many of the samples with copper powder displayed greater SE than the aluminium plate in the frequency range tested.

#### **4. CONCLUSION**

It has therefore been shown in this work that SE is dependant on electrical conductivity, although not significantly. This was possibly due to reflection loss decreasing with increasing frequency. There was an improvement in SE between materials with metal mesh compared with materials with the discontinuous fillers, however, not significantly as to justify the use composites with metal meshes on surfaces not exposed to high current.

#### **5. REFERENCES**

1. Shooman, ML; *A study of occurrence rates of electromagnetic interference (EMI) to aircraft with a focus on HIRF (external) high intensity radiated fields*; NASA Contractor Report 194895; National Aeronautics and Space Administration Langley Research Center, Hampton, Virginia; 1994
2. Schlechter, M; *EMI: Materials and Technologies* - abstract; www.electronics.ca
3. Yang, S *et al*; *Electromagnetic interference shielding effectiveness of carbon nanofiber/LCP composites*; Composites Part A: Applied science and manufacturing vol. 36 (2005); 691-697
4. Chung, DDL; *Electromagnetic interference shielding effectiveness of carbon materials*; Carbon vol. 39 (2001); 279-285
5. White, DRJ; *Electromagnetic Shielding Materials and Performance*; Don White Consultants, Inc.; USA; 1980
6. Das, N.C *et al*; *Electromagnetic interference shielding effectiveness of carbon black and carbon filled EVA and NR based composites*; Composites Part A: Applied science and manufacturing vol. 31 (2000); 1069-1081
7. Pomposo, JA *et al*.; *Polypyrrole-based conducting hot melt adhesives for EMI shielding applications*; Synthetic Metals vol.104 (1999); 107-111
8. Kunkel, G; *EMI Shielding Theory*; Equipment Protection Magazine, fall 2003; Webcom Publishing; USA; 2003
9. Wojkiewicz, JL *et al*.; *Electromagnetic shielding properties of polyaniline composites*; Synthetic Metals vol.135-136 (2003); 127-128
10. Colaneri, NF and Shacklette, LW; *IEEE Transactions on Instrumentation and Measurement*; 41 (1992); 2
11. Xu, J *et al*; *Preparation, electrical and mechanical properties of vapor grown carbon fiber (VGCF)/vinyl ester composites*; Composites Part A: applied science and manufacturing vol. 35 (2004); 693-701
12. Hong, YK *et al*; *Electromagnetic interference shielding characteristics of fabric complexes coated with conductive polypyrrole and thermally evaporated Ag*; Current Applied Physics vol.1 (2001); 439-442

13. Private Communication - Prof. JW Odendaal; University of Pretoria; SA; September 2006
14. Satheesh Kumar, K.K *et al*; *Freestanding polyaniline film for the control of electromagnetic radiations*; Current Applied Physics vol.5 (2005); 603-608
15. Dhawan, S.K *et al*; *Shielding behaviour of conducting polymer-coated fabrics in X-band, W-band and radio frequency range*; Synthetic Metals vol. 129 (2002); 261-267

## **REFERENCES**

1. Mobile phones; [http://en.wikipedia.org/wiki/Mobile\\_phone](http://en.wikipedia.org/wiki/Mobile_phone); Date Accessed: December 2005
2. Hong YK, Lee CY, Jeong CK, Sim JH, Kim K, Joo J, Kim MS, Lee JY, Jeong SH and Byun SW; Electromagnetic interference shielding characteristics of fabric complexes coated with conductive polypyrrole and thermally evaporated Ag; *Current Applied Physics* vol.1 (2001); 439-442
3. Turn off your radio; *QwikConnect* vol. 6, no. 2, April 1999; [www.glenair.com/qwikconnect/vol6num2/coverstory.htm](http://www.glenair.com/qwikconnect/vol6num2/coverstory.htm); Date Accessed: February 2006
4. Shooman ML; A study of occurrence rates of electromagnetic interference (EMI) to aircraft with a focus on HIRF (external) high intensity radiated fields; NASA Contractor Report 194895; National Aeronautics and Space Administration Langley Research Center, Hampton, Virginia; 1994
5. Chung DDL; Electromagnetic interference shielding effectiveness of carbon materials; *Carbon* vol. 39 (2001); 279-285
6. Das NC, Khastgir D, Chaki TK and Chakraborty A.; Electromagnetic interference shielding effectiveness of carbon black and carbon filled EVA and NR based composites; *Composites Part A: Applied Science and Manufacturing* vol. 31 (2000); 1069-1081
7. Cheng KB, Ramakrishna S and Lee KS; Electromagnetic shielding effectiveness of copper/glass fiber knitted fabric reinforced polypropylene composites; *Composites Part A: Applied Science and Manufacturing* vol. 31 (2001); 1039-1045
8. Schlechter M; EMI: Materials and Technologies - abstract; <http://www.electronics.ca/reports/materials/GB066Y.html>; Date Accessed: December 2005
9. Cheng KB, Lee KC, Uieng TH and Mou KJ; Electrical and impact properties of the hybrid knitted inlaid fabric reinforced polypropylene composites; *Composites Part A: Applied Science and Manufacturing* vol. 33 (2002); 1219-1226
10. Young HD and Freedman RA; *Sears and Zemansky's University Physics*; tenth international edition; Addison-Wesley Publishing Company, 2000, USA
11. Shuying Yang, Karen Lozano, Azalia Lomeli, Heinrich D. Foltz and Robert Jones; Electromagnetic interference shielding effectiveness of carbon nanofiber/LCP

- composites; *Composites Part A: Applied Science and Manufacturing* vol. 36 (2005); 691-697
12. Satheesh Kumar KK, Geetha S and Trivedi DC; Freestanding polyaniline film for the control of electromagnetic radiations; *Current Applied Physics* vol.5 (2005); 603-608
  13. Dhawan SK, Singh N and Venkatachalam S; Shielding behaviour of conducting polymer-coated fabrics in X-band, W-band and radio frequency range; *Synthetic Metals* vol. 129 (2002); 261-267
  14. Lee CY, Song HG, Jang KS, Oh EJ, Epstein AJ, and Joo J; Electromagnetic shielding efficiency of polyaniline mixtures and multilayer films; *Synthetic Metals* vol.102 (1999); 1346-1349
  15. Dhawan SK; Shielding effectiveness of conducting polyaniline coated fabrics at 101 GHz; *Synthetic Metals* vol.125 (2002); 389-393
  16. EMI Shielding Theory; [www.chomerics.com/products/documents/emicat/pg192theory\\_of\\_emi.pdf](http://www.chomerics.com/products/documents/emicat/pg192theory_of_emi.pdf); Date Accessed: February 2006
  17. White DRJ; *Electromagnetic Shielding Materials and Performance*; Don White Consultants, Inc.; 1980; USA
  18. Walen D; *Lightning and HIRF Protection – An interactive video and teletraining self-study video course*; FAA; 1998; [www.keybridgeti.com/videotraining/manualdl/25808\\_Lightning\\_and\\_HIRF\\_Protection.PDF](http://www.keybridgeti.com/videotraining/manualdl/25808_Lightning_and_HIRF_Protection.PDF); Date Accessed: January 2006
  19. United States Marine Corps lesson guide number: G-13; *Electrostatic Discharge (ESD) and Electromagnetic Interference (EMI)*; Aviation Training Branch, Training Command, Marine Corps Combat Development Command; Quantico, Virginia, 22134-5050
  20. Uman MA; *Lightning*; McGraw-Hill Inc.; 1969; USA
  21. Thorogood L; Bolt from the blue; *Flight Safety Australia*, July-August 2005; [www.casa.gov.au/fsa/2005/aug/48-50.pdf](http://www.casa.gov.au/fsa/2005/aug/48-50.pdf); Date Accessed: February 2006
  22. Parmantier JP; First realistic simulation of effects of electromagnetic coupling in commercial aircraft wiring; *Aircraft Engineering and Aerospace Technology* vol.70, no.1 (1998); 24-28
  23. Uman MA and Rakov VA; The interaction of lightning with airborne vehicles; *Progress in Aerospace Sciences* vol.39 (2003); 61-81
  24. Gates D; Building the 787 – When lightning strikes; *Seattle Times newspaper article*; 5 March 2006
  25. *Electromagnetic Interference Test Procedures (EMITP)*; [www.tscm.com/DI-EMCS-80201B.PDF](http://www.tscm.com/DI-EMCS-80201B.PDF); Date Accessed: February 2006

26. Ms. T Gill; South African Weather Services; September 2006
27. SAE ARP 5414A: Aircraft Lightning Zoning; Federal Aviation Administration; 2005
28. Newman, M.M and Robb, J.D; Protection of Aircraft; Lightning vol. 2; 659-693; 1977; Great Britain
29. Delmonte J; Technology of Carbon and Graphite Fiber Composites; Van Nostrand Reinhold Company; 1981; USA
30. Bleck ME; Beech Aircraft Corporation; Beechcraft Starship;  
[www.aviatorservices.com/starship\\_history\\_1.htm](http://www.aviatorservices.com/starship_history_1.htm); Date Accessed: February 2006
31. Radome network homepage for dielectric radomes; [www.radome.net](http://www.radome.net); Date Accessed: March 2006
32. Kopp C; A doctrine for the use of electromagnetic pulse bombs (Revised draft of RAAF APSC working paper #15; July 1993;  
[www.csse.monash.edu.au/~carlo/archive/MILITARY/APSC/wp15-draft.pdf](http://www.csse.monash.edu.au/~carlo/archive/MILITARY/APSC/wp15-draft.pdf); Date Accessed: January 2006
33. MIL-STD-464; Department of Defense Interface Standard – Electromagnetic Environmental Effects Requirements for Systems; 18 March 1997
34. Majkner, R; Overview – Lightning protection of aircraft and avionics; Sikorsky; 14 October 2003; [www.ieee.li/pdf/viewgraphs\\_lightning.pdf](http://www.ieee.li/pdf/viewgraphs_lightning.pdf) ; Date Accessed: January 2006
35. Pierce, E.T; Atmospherics and Radio Noise; Lightning vol. 1 – Physics of Lightning; 351-381; Great Britain; 1977
36. Norton ME; Static discharger wicks cut precipitation static noise; [www.repeater-builder.com/pdf/staticbusterarticlecomplete.pdf](http://www.repeater-builder.com/pdf/staticbusterarticlecomplete.pdf); Date Accessed: March 2006
37. Electrostatic Discharge Association; [www.esda.org](http://www.esda.org); Date Accessed: March 2006
38. Electromagnetic spectrum; [ewhdbks.mugu.navy.mil](http://ewhdbks.mugu.navy.mil); Date Accessed: March 2006
39. RTP Co. Engineering Plastics; [www.rtpcompany.com](http://www.rtpcompany.com); Date Accessed: December 2005
40. Kunkel G; EMI Shielding Theory; Equipment Protection Magazine, fall 2003; Webcom Publishing, 2003, USA
41. Skin Effect; [en.wikipedia.org/wiki/Skin\\_effect](http://en.wikipedia.org/wiki/Skin_effect); Date Accessed: February 2006
42. Wojkiewicz JL *et al.*; Electromagnetic shielding properties of polyaniline composites; Synthetic Metals vol.135-136 (2003); 127-128
43. Colaneri NF and Shacklette LW; IEEE Transactions on Instrumentation and Measurement; 41 (1992); 2
44. Private communication: Prof. JW Odendaal – professor of electromagnetism; University of Pretoria; September 2006

45. Pomposo J A, Rodriguez J and Grande H; Polypyrrole-based conducting hot melt adhesives for EMI shielding applications; *Synthetic Metals* vol. 104 (1999); 107-111
46. MIL-STD-285; Military standard attenuation measurements for enclosures, electromagnetic shielding, for electronic test purposes, method of.; Department of Defense Interface Standard; 25 June 1956;
47. Luo X and Chung DDL; Electromagnetic interference shielding using continuous carbon-fiber carbon-matrix and polymer-matrix composites; *Composites Part B: Engineering* vol. 30 (1999); 227-231
48. Middleton DH; *Composite Materials in Aircraft Structures*, Longman Scientific and Technical, 1990, Singapore
49. Dastin SJ; *Aircraft Composite Materials and Structures – Seminar notes*; Grumman Corp. – Aircraft Systems Division; Mail Stop B10-25, Bethpage, New York, 11714
50. Duan Yuping, Liu Shunhua and Guan Hongtao; Investigation of electrical and electromagnetic shielding effectiveness of polyaniline composite; *Science and Technology of Advanced Materials* vol. 6 (2005); 513-518
51. Cheng, KB, Uieng TH and Hsing WH; Effects of yarn constituents and fabric specifications on electrical properties of hybrid woven fabrics; *Composites Part A: Applied Science and Manufacturing* vol. 34 (2003); 971-978
52. Chen, HC, Lee KC and Lin JA; Electromagnetic and electrostatic shielding properties of co-weaving-knitting fabrics reinforced composites; *Composites Part A: Applied Science and Manufacturing* vol. 35 (2004); 1249-1256
53. Schlechter M; EMI: Materials and Technologies - abstract;  
<http://www.electronics.ca/reports/materials/GB066Y.html>; Date Accessed: December 2005
54. Huang C and Wu C; The EMI shielding effectiveness of PC/ABS/nickel-coated-carbon-fibre composites; *European Polymer Journal* vol.36 (2000); 2729-2737
55. Krupa I, Novak I and Chodak I; Electrically and thermally conductive polyethylene/graphite composites and their mechanical properties; *Synthetic Materials* vol.145 (2004); 245-252
56. Private communication: Dr. CJ von Klemperer – senior lecturer and project supervisor ; School of Mechanical Engineering UKZN; August 2006
57. Chandrasekhar P and Naishadham K; Broadband microwave absorption and shielding properties of a poly(aniline); *Synthetic Metals* vol.105 (1999); 115-120

58. Carbon Black - <http://www.azom.com/details.asp?ArticleID=2084#>; Date Accessed: January 2006
59. Oh JH, Oh KS, Kim KG and Hong CS; Design of radar absorbing structures using glass/epoxy composite containing carbon black in X-band frequency ranges; *Composites Part B: Engineering* vol. 35 (2004); 49-56
60. Sandler JKW, Kirk JE, Kinloch IA and Shaffer MSP; Ultra-low electrical percolation threshold in carbon-nanotube-epoxy composites; *Polymer* vol.44 (2003); 5893-5899
61. Jia W, Tchoudakov R, Segal E, Narkis M, Siegmann A; Electrically conductive composites based on epoxy resin with polyaniline-DBSA fillers; *Synthetic Metals* vol.132 (2003); 269-278
62. Haynes KK and Clark M; Lightning strike protection: novel nonwoven technology; *JEC Composites* no.24 April 2006; 32-33
63. Gardiner G; Lightning strike protection for composite structures; *Composites World* July 2006; Ray Publishing; 44-50
64. Composite Trends Aerospace from Hexcel; [www.hexcel.com/NR/rdonlyres/7181CA0F-27EC-4D03-A3B4-5DE9AA8F454C/0/compositetrends-aerospace05.pdf](http://www.hexcel.com/NR/rdonlyres/7181CA0F-27EC-4D03-A3B4-5DE9AA8F454C/0/compositetrends-aerospace05.pdf); Date Accessed: July 2006
65. Kelly A; *Handbook of Composites vol.4: Fabrication of Composites*; 2<sup>nd</sup> printing; Elsevier Science Publishers B.V; 1986; Netherlands
66. Grayson M; *Encyclopedia of Composite Materials and Components – Encyclopedia Reprint Series*, John Wiley and Sons, Inc, 1983, USA
67. [www.auf.asn.au/scratchbuilder/composites.html](http://www.auf.asn.au/scratchbuilder/composites.html); Date Accessed: July 2006
68. [composite.about.com/library/weekly/aa980323.htm](http://composite.about.com/library/weekly/aa980323.htm); Date Accessed: July 2006
69. [www.vetrotexasiapacific.com](http://www.vetrotexasiapacific.com); Date Accessed: July 2006
70. Best JR; Glass fiber may be key to business – recycled automobile components; *Ward's Auto World*; Primedia Business Magazines and Media Inc.; June 1994
71. Glass Fibre - [en.wikipedia.org/wiki/Fiberglass](http://en.wikipedia.org/wiki/Fiberglass) ; Date Accessed: June 2006
72. Glass Fibre - <http://composite.about.com/library/weekly/aa980323.htm>; Date Accessed: July 2006
73. Hancox NL; *Fibre Composite Hybrid Materials*; Applied Science Publisher Ltd.; 1981; Great Britain
74. Department of Defense Handbook – *Composite Materials Handbook vol.3: Polymer Matrix Composites Materials Usage, Design and Analysis*; US Department of Defense; 17 June 2002

75. [composite.about.com/od/aboutcompositesplastics/l/aa050597.htm](http://composite.about.com/od/aboutcompositesplastics/l/aa050597.htm); Date Accessed: August 2006
76. Bleck ME; Beech Aircraft Corporation; Beechcraft Starship; [www.aviatorservices.com/starship\\_history\\_2.htm](http://www.aviatorservices.com/starship_history_2.htm); Date Accessed: February 2006
77. Lutz G.W; Notes of the earthing and screening requirements for composite airframes; Obtained: December 2005
78. [www.geocities.com/CapeCanaveral/1320/](http://www.geocities.com/CapeCanaveral/1320/) ; Date Accessed: June 2006
79. [www.carbonfiber.gr.jp](http://www.carbonfiber.gr.jp); Date Accessed: May 2006
80. "In the composites race, jets may beat out bikes" - article; The Wall Street Journal: 24 January 2006
81. Boyce Components LLC; [www.netcomposites.com](http://www.netcomposites.com); Date Accessed: August 2006
82. LR20/LH281 Laminating epoxy resin system; Product data sheet; AMT Composites, Durban; 2006
83. Prime 27 Epoxy Infusion System; Product data sheet; SP Systems, United Kingdom; 2006
84. Askeland DR; The Science and Engineering of Materials; 3<sup>rd</sup> Edition; PWS Publishing Company; 1994; USA
85. Jacobs JA and Kilduff TF; Engineering Materials and Technology: Structures, Processing, Properties, and Selection 4<sup>th</sup> edition; Prentice Hall; 2001; USA
86. Carbon Black - <http://www.azom.com/details.asp?ArticleID=2084#>; Date Accessed: January 2006
87. Breuer O and Sundararaj U; Big Returns from Small Fibers: A Review of Polymer/Carbon Nanotube Composites; Polymer Composites vol. 25, no.6; December 2004; 630-645
88. JG Gerard and H V. Samuelson, U.S. Patent 6,426,134 (2002)
89. P Glatkowski, P Mack, J L Conroy, J. W. Piche, and P. Winsor, U.S. Patent 6,265,466 (2001)
90. S H Foulger, U.S. Patent 6,417,235 (2002)
91. M Dupire and J Michel, U.S. Patent 6,331,265 (2001)
92. A Fisher, R Hoch, D Moy, C Niu, N Ogata, H Tennent, and T McCarthy, U.S. Patent 6,203,814 (2001)
93. Holister P, Harper TE and Vas CR; Nanotubes White Paper; CMP Cientifica; January 2003; Spain
94. Applications and Properties of Carbon Nanotubes; [www.cheaptubesinc.com](http://www.cheaptubesinc.com);



Date Accessed: January 2006

95. Price list; [www.cheaptubesinc.com](http://www.cheaptubesinc.com); Date Accessed: February 2006
96. Price list; [www.cnanotech.com](http://www.cnanotech.com); Date Accessed: March 2006
97. Nanotubes for the Composite Market – abstract; [www.cientifica.com](http://www.cientifica.com); Date Accessed: February 2006
98. Private communication: Ms. L Brelsford – sales representative; Carbon Nanotechnologies; June 2006
99. Jun Xu, John P Donohoe and Charles U. Pittman Jr.; Preparation, electrical and mechanical properties of vapor grown carbon fiber (VGCF)/vinyl ester composites; Composites Part A: applied science and manufacturing vol. 35 (2004); 693-701
100. [www.mdatechnology.net](http://www.mdatechnology.net); Date Accessed: June 2006
101. Private communication: Customer representative - Applied Sciences, Inc.; July 2006
102. Materials for Lightning Protection of Aircraft Components and Systems; Alumesh 401 Product data sheet; Brochier SA; 1998; France
103. [www.designinsite.dk](http://www.designinsite.dk); Date Accessed: August 2006
104. Prentice N; Vacuum infusion for polymer composites: Tooling and Parts ; AMT Composites, Johannesburg, SA; April 2005
105. Tarnopol'ski YM; Static test methods for composites; Van Nostrand Reinhold Company Inc.; 1985; USA
106. ASTM Designation: 638-02a; 'Standard test method for Tensile properties of plastics'; 2003
107. ASTM Designation: 3039/D 3039M-00; 'Standard test method for Tensile properties of polymer matrix composite materials'; 2003
108. Private communication: Mr. NK Sookay – lecturer; School of Mechanical Engineering UKZN: August 2006
109. ASTM Designation: 695-02a; 'Standard test method for Compressive properties of rigid plastics'; 2003
110. ASTM Designation: 3410; 'Standard test method for the compressive properties of polymer matrix composite materials'; 2003
111. ASTM Designation: 790-02; 'Standard test methods for Flexural properties of unreinforced and reinforced plastics and electrical insulating materials'; 2003
112. ASTM Designation: 6272-02; 'Standard test methods for Flexural properties of unreinforced and reinforced plastics and electrical insulating materials by four-point bending'; 2003

113. Staab GH; Laminar composites; Butterworth-Heinemann; 1999; USA
114. Summerscales J; Composites Design and Manufacture (BEng) – MATS 324 university course notes; University of Plymouth; United Kingdom
115. Private communication: Dr. DA Hoch – senior lecturer; School of Electrical, Electronic and Computer Engineering UKZN; July 2006
116. Private communication: Dr. S Mneney – senior lecturer; School of Electrical, Electronic and Computer Engineering UKZN; July 2006
117. ASTM Designation: 4935-99; ‘Standard test method for measuring the electromagnetic shielding effectiveness of planar materials’; 2003
118. Private communication: Dr. R Anandjiwala – staff member; CSIR Pretoria; September 2006
119. Private communication: Mr. M Arnold – proprietor; Miketronics, Durban; September 2006
120. Private communication: Ms. L Robertson – staff member; HKK Earthing and Lightning Protection Systems; September 2006
121. Private communication: Ms. SJ Smith – staff member; Afridek, KZN; September 2006
122. Private communication: Mr. R Lippiatt – staff member; Earthwise, Durban; September 2006
123. Private communication: Mr. D Govender – staff member; MG Electrical, Durban; September 2006
124. Private communication: Mr. L Erwee – staff member; CPE, KZN; September 2006
125. Private communication: Customer relations representative; MW Pontin, KZN; September 2006
126. Private communication: Customer relations representative; Clearline; KZN; September 2006
127. Private communication: Mr. G Mashinini – electrical resistivity tester; SABS, Johannesburg
128. South African Journal of Science; [www.nrf.ac.za](http://www.nrf.ac.za); Date Accessed: August 2006
129. Private communication: Prof. JW Odendaal; professor of electromagnetism; University of Pretoria ; August 2006
130. Equipment photo: Prof. JW Odendaal; professor of electromagnetism; University of Pretoria; October 2006
131. Fordham JA; An introduction to antenna test ranges, measurements and instrumentation;

132. ASTM Designation 257-99; 'Standard test method for dc resistance or conductance of insulating materials'; 2005
133. ASTM Designation: 'Standard test method for Resistivity of electrical conductor materials'; 2003
134. Tsotra P and Friedrich K; Electrical and mechanical properties of functionally graded epoxy-resin/carbon fibre composites; Composites Part A vol.34 (2003); 75-82
135. Private communication: Mr. B Burton – senior lecturer School of Electrical, Electronic and Computer Engineering UKZN; October 2006
136. Private communication: Ms. K Hall – company director AMT Composites Durban; August 2006
137. Private communication: Dr. CJ von Klemperer – senior lecturer and project supervisor; School of Mechanical Engineering UKZN; August 2006
138. "Doping" – [www.answers.com/topic/doping-semiconductor](http://www.answers.com/topic/doping-semiconductor); Date Accessed: January 2006
139. Private communication: Prof. S Adali – professor; School of Mechanical Engineering UKZN; November 2006
140. Sookay N; Environmental degradation of composite materials final Hystou report; UKZN; January 2005
141. Piggot MR; Compressive strength of composites: How to measure it and how to improve it; [stinet.dtic.mil](http://stinet.dtic.mil); 1993; 1-9
142. Gere JM; Mechanics of materials 5<sup>th</sup> edition; Brooks/Cole; 2001; USA
143. Kunkel G; Lightning induced electromagnetic fields into aerospace vehicles; Evaluation Engineering Magazine; August 1990; 1-6
144. "Radar cross section" – [www.aerospaceweb.org/question/electronics/q0168.shtml](http://www.aerospaceweb.org/question/electronics/q0168.shtml); Date Accessed: September 2006
145. Private communication: Prof. JW Odendaal; professor of electromagnetism; University of Pretoria; October 2006